

**Fachhochschule Aachen  
Campus Jülich**

**Transients in the Operation of a Small Modular Reactor**

Master's Thesis  
Eduardo Roberto Rodrigues de Brito Junior  
Matr. No.: 3259527

Department of  
Chemistry and Biotechnology  
Master of Science in Nuclear Applications.

Jülich, August 2021

# Statement

This master thesis is my own independent work and is the result of my sole efforts. No other sources or references have been used in its production apart from the ones quoted.

---

Eduardo Roberto Rodrigues de Brito Junior

This work has been supervised by:

1. Examiner: Prof. Dr. rer. nat. Boris Neubauer (FH-Aachen)
2. Examiner: Prof. Dr. phil. nat. Christoph Langer (FH-Aachen)

# Acknowledgement

Gratitude to God, creator of the entire universe and the only one capable of providing wisdom, knowledge, and happiness to men; without Him, nothing would be possible. God has guided and provided me days to expand my abilities and build a beautiful family built on the rock that is Jesus Christ. God graciously gifted me with this excellent opportunity to be among capable and talented people from FH-Aachen University of Applied Sciences and to finalize this excellent qualification in the nuclear area amidst much effort, daytime studies, difficult days for humanity due to the pandemic; however, with health, enthusiasm, willpower, determination and loved ones cheering for another academic success – my family.

I thank my wife Simone Greicy Cruz Moura and my daughter Alice Ayres Moura Rodrigues for their support, patience, understanding, incessant prayers, and resignations during this challenging work period. They are the loves of my life.

I thank my parents, Eduardo and Sandra Brito, for the education provided and for the effort made to give me a good creation in the face of a world full of challenges and many adversities. They are essential to me. I also thank all the people in my family, my wife's family, and brothers in Christ who have supported us with prayers that were and continue to be precious to us.

I thank Prof. Dr. rer. nat. Boris Neubauer for his supervision and valuable advice, which were of fundamental importance in the development of this work.

I thank all the professors for the effort made during this period of the pandemic to continue promoting quality classes. In particular, I thank Prof. Dr. rer. nat. Elisabeth Paulßen, Prof. Dr. phil. nat. Christoph Langer and Prof. Dr. rer. nat. Karl Ziemons for organizing the Master's program.

I thank the Brazilian Navy for the financial support provided to my family and me during our time in Germany. Furthermore, I thank the CC(EN) Rodrigo Renan Baroni, who always helped me during my journey to the university. I also thank 1SG-MA Guilherme Dias Souza Lima for his help in accessing the iPWR simulator used in this work.

I am grateful for the support of the FH-Aachen University of Applied Sciences during this period as a student. I am always available to contribute to this exceptional institution.

Finally, I thank all the people, directly and indirectly, related to this work and are not mentioned here because I certainly would not remember them all.

# List of abbreviations

<b>AC</b>	Alternating Current
<b>ADS</b>	Automatic Depressurization System
<b>AFWS</b>	Auxiliary Feedwater System
<b>AGR</b>	Advanced Gas-cooled Reactors
<b>BOL</b>	Beginning of Core Life
<b>BOP</b>	Balance of Plant
<b>BP</b>	Burnable Poison
<b>BWR</b>	Boiling Water Reactor
<b>CBS</b>	Containment Building System
<b>CCS</b>	Containment Cooling System
<b>CCWS</b>	Component Cooling Water System
<b>CMT</b>	Core Makeup Tank
<b>CNR</b>	Condenser System
<b>CPRSS</b>	Containment Pressure and Radioactive Suppression System
<b>CRDM</b>	Control Rod Drive Mechanism
<b>CST</b>	Coolant Storage Tank
<b>CVCS</b>	Chemical and Volume Control System
<b>CWS</b>	Circulating Water System
<b>DC</b>	Direct Current
<b>DHR</b>	Decay Heat Removal
<b>DHRS</b>	Decay Heat Removal System
<b>DNB</b>	Departure from Nucleate Boiling
<b>DPM</b>	Decades per Minute
<b>DRW</b>	Differential Rod Worth
<b>ECCS</b>	Emergency Core Cooling System
<b>ECT</b>	Emergency Cooldown Tank
<b>EDG</b>	Emergency Diesel Generator
<b>EFPD</b>	Effective Full Power Day
<b>EOL</b>	End of Core Life
<b>FNR</b>	Fast Neutron Reactors
<b>FTC</b>	Fuel Temperature Coefficient
<b>FWS</b>	Feed Water System
<b>GEN</b>	Generator System
<b>GHG</b>	Greenhouse Gas
<b>GIS</b>	Gravity Driven Water Injection System
<b>HTGR</b>	High-Temperature Gas-cooled Reactors
<b>HWR</b>	Heavy Water Reactors
<b>IAEA</b>	International Atomic Energy Agency

**iPWR** Integrated Pressurized Water Reactor  
**IRWST** In-containment Refueling Water Storage Tank  
**LOCA** Loss of Coolant Accident  
**LWGR** Light Water Graphite-moderated Reactors  
**MSIV** Main Steam Isolation Valve  
**MSS** Main Steam System  
**MTC** Moderator Temperature Coefficient  
**NPP** Nuclear Power Plant  
**NSSS** Nuclear Steam Supply System  
**PCCS** Passive Core Cooling System  
**PCM** Per Cent Mille  
**PCMWS** Passive Core Makeup Water System  
**PCS** Protection and Control System  
**PDHR** Primary Decay Heat Removal System  
**PIS** Pressure Injection System  
**PORV** Power-Operated Relief Valve  
**PPM** Parts Per Million  
**PRHRS** Passive Residual Heat Removal System  
**PSIS** Passive Safety Injection System  
**PTS** Pressurized Thermal Shock  
**PWR** Pressurized Water Reactor  
**PZR** Pressurizer  
**RCP** Reactor Coolant Pump  
**RCS** Reactor Coolant System  
**RHRS** Residual Heat Removal System  
**RPV** Reactor Pressure Vessel  
**RWST** Refueling Water Storage Tank  
**SCS** Shutdown Cooling System  
**SDHR** Secondary Decay Heat Removal System  
**SG** Steam Generator  
**SGTF** Steam Generator Tube Failure  
**SIT** Safety Injection Tank  
**SMR** Small Modular Reactor  
**SUR** Start-up Rate  
**TUR** Turbine System  
**WNA** World Nuclear Association

# Abstract

There is a significant worldwide effort to limit global warming. Among the main sectors that have contributed to the warming is the energy sector. In that sense, means of generating energy with low emissions of GHGs have been sought. The use of renewables power such as solar and wind has been steadily increasing. However, only nuclear power and hydropower can generate electricity continuously and reliably and are the only options with low emission of GHGs capable of replacing the power produced by fossil fuels. Therefore, NPPs can be essential allies in combating the emission of GHGs and then reducing global warming to the desired level. Although the new designs of NPPs have sought to reduce costs and construction time, these plants continue to be huge facilities and still costly. At the same time that the design of high-power NPPs has evolved, there have also been advances in small-power plants. In the wake of cost reduction and increasing safety, the SMRs appeared. The term SMRs refers to reactors with modular manufacture and with power generation in the range between 25 MWe to 300 MWe. Thus, SMRs provide low carbon energy as large NPPs but with more flexibility and affordability. Due to its importance, this work discusses the new designs of NPPs, focusing on PWR SMRs. Additionally, the use of a PC-based SMR simulator to study transients originated in normal operation conditions and in accident conditions of NPPs is demonstrated.

**Keywords:** Small modular reactors (SMRs); iPWR simulator; SMR transients.

# Contents

<b>Statement</b>	<b>1</b>
<b>Acknowledgement</b>	<b>2</b>
<b>List of Abbreviations</b>	<b>3</b>
<b>Abstract</b>	<b>5</b>
<b>1 Introduction</b>	<b>14</b>
1.1 Overview . . . . .	14
1.2 Purpose of the Research . . . . .	16
1.3 Organization of the Work . . . . .	17
<b>2 Pressurized Water Reactors</b>	<b>18</b>
2.1 Overview . . . . .	18
2.2 Main PWR Components and Systems . . . . .	20
2.2.1 Reactor pressure vessel (RPV) . . . . .	20
2.2.2 Steam generators (SGs) . . . . .	20
2.2.3 Reactor coolant pump (RCP) . . . . .	21
2.2.4 Pressurizer (PZR) . . . . .	24
2.2.5 Chemical and volume control system (CVCS) . . . . .	26
2.2.6 Auxiliary feedwater system (AFWS) . . . . .	27
2.2.7 Residual heat removal system (RHRS) . . . . .	28
2.2.8 Emergency core cooling system (ECCS) . . . . .	28
2.2.9 Containment building system (CBS) . . . . .	30
<b>3 Reactor Operating Parameters</b>	<b>32</b>
3.1 Reactor Kinetics . . . . .	32
3.1.1 The role of prompt and delayed neutrons . . . . .	32
3.1.2 Criticality . . . . .	33
3.1.3 Reactivity . . . . .	33
3.1.4 Installed neutron sources . . . . .	34
3.1.5 Subcritical multiplication . . . . .	34
3.1.6 Neutron flux and power . . . . .	35
3.1.7 Reactor period . . . . .	36
3.1.7.1 Prompt critical reactor period . . . . .	37
3.1.7.2 Delayed critical reactor period . . . . .	37
3.1.7.3 Prompt neutron response . . . . .	38
3.1.7.4 Delayed neutron response . . . . .	39

3.1.7.5	Reactor start up rate (SUR) . . . . .	39
3.2	Control Rod Worth . . . . .	40
3.2.1	Differential and integral control rod worth . . . . .	40
3.2.2	Control rod shadowing . . . . .	41
3.3	Reactivity Coefficients . . . . .	42
3.3.1	Moderator temperature and moderator density coefficients . . . . .	42
3.3.1.1	Change in MTC with boron concentration . . . . .	45
3.3.1.2	Change in MTC with core age . . . . .	45
3.3.2	The void coefficient of reactivity . . . . .	45
3.3.3	Fuel temperature coefficient of reactivity . . . . .	45
3.3.3.1	Changes in FTC with changes in fuel temperature . . . . .	47
3.3.3.2	Changes in FTC with changes in moderator density . . . . .	47
3.3.3.3	Changes in FTC with changes in core age . . . . .	47
3.4	Neutron Poisons . . . . .	48
3.4.1	Xenon concentration . . . . .	48
3.4.2	Samarium concentration . . . . .	51
3.4.3	Control poisons . . . . .	53
3.5	Core Lifetime . . . . .	54
3.5.1	Core excess reactivity . . . . .	54
3.5.2	Neutron flux profiles . . . . .	55
3.5.2.1	Heterogenous core flux . . . . .	55
3.5.2.2	Core lifetime neutron flux profile . . . . .	55
3.5.2.3	Neutron reflectors . . . . .	57
3.5.2.4	Fuel loading patterns . . . . .	57
3.5.2.5	Coolant temperature . . . . .	57
3.6	Transients . . . . .	58
3.6.1	Power maneuvering . . . . .	59
3.6.2	Reactor scram . . . . .	60
3.6.3	Loss of coolant flow . . . . .	61
<b>4</b>	<b>Small Modular Reactors (SMRs)</b>	<b>62</b>
4.1	Core and Fuel Technologies in iPWRs . . . . .	62
4.1.1	Safety design criteria . . . . .	63
4.1.1.1	Fuel burnup . . . . .	63
4.1.1.2	Reactivity coefficients . . . . .	64
4.1.1.3	Power distribution . . . . .	64
4.1.1.4	Shutdown margin . . . . .	65
4.1.1.5	Maximum reactivity insertion rate . . . . .	65
4.1.1.6	Power stability . . . . .	65
4.1.2	Design features to achieve the criteria . . . . .	66
4.1.2.1	Setting the enrichment of the fissile material . . . . .	66
4.1.2.2	Burnable poisons (BPs) . . . . .	66
4.1.2.3	In-core fuel management . . . . .	68
4.1.3	iPWR design specifics . . . . .	69
4.1.3.1	Fuel designs in the smaller cores . . . . .	69
4.1.3.2	Use of control rods and burnable poisons to control reactivity . . . . .	70
4.1.3.3	Core loading . . . . .	72
4.1.3.4	Other design considerations . . . . .	72



4.2	Essential Reactor Systems Components in iPWRs . . . . .	73
4.2.1	Integral components . . . . .	73
4.2.1.1	Pressure vessel and flange . . . . .	73
4.2.1.2	RCS piping . . . . .	76
4.2.1.3	Pressurizer, heaters, spray valve, pressurizer relief tank, and baffle plate . . . . .	76
4.2.1.4	Pumps . . . . .	78
4.2.1.5	Riser . . . . .	78
4.2.1.6	Steam generators and tube sheets . . . . .	78
4.2.1.7	Control rods and reactivity control . . . . .	80
4.2.1.8	Control rod drive mechanisms . . . . .	80
4.2.1.9	Automatic depressurization system valves . . . . .	80
4.2.1.10	Relief valves . . . . .	81
4.2.1.11	Core basket, core barrel, core baffle . . . . .	81
4.2.1.12	Instrumentation . . . . .	81
4.2.2	Connected system components . . . . .	81
4.2.2.1	Chemical and volume control system (CVCS) . . . . .	81
4.2.2.2	Residual heat removal and auxiliary feedwater systems . . . . .	82
4.2.2.3	Emergency core cooling system and refueling water storage tank . . . . .	82
4.2.2.4	External pool . . . . .	83
4.2.2.5	Control room habitability equipment . . . . .	83
4.2.2.6	Diesel generators and electrical distribution . . . . .	83
4.3	Some Small Modular Reactors Today . . . . .	84
4.3.1	CAREM . . . . .	84
4.3.2	ACP-100 . . . . .	86
4.3.3	System-Integrated Modular Advanced Reactor (SMART) . . . . .	88
4.3.4	KLT-40S . . . . .	90
4.3.5	SMR-160 . . . . .	91
4.3.6	NuScale . . . . .	93
4.3.7	EPR . . . . .	97

**5 iPWR Simulator 101**

5.1	Systems Simulated . . . . .	101
5.1.1	Reactor core and reactor coolant system (RCS) . . . . .	101
5.1.2	Main steam system (MSS) . . . . .	103
5.1.3	Feedwater system (FWS) . . . . .	104
5.1.4	Turbine system (TUR) . . . . .	105
5.1.5	Generator system (GEN) . . . . .	105
5.1.6	Condenser system (CNR) . . . . .	106
5.1.7	Circulating water system (CWS) . . . . .	106
5.1.8	Containment building system (CBS) . . . . .	106
5.1.9	Automatic depressurization system (ADS) . . . . .	107
5.1.10	Containment cooling system (CCS) . . . . .	108
5.1.11	Gravity driven water injection system (GIS) . . . . .	108
5.1.12	Pressure injection system (PIS) . . . . .	108
5.1.13	Passive decay heat removal system (PDHR) . . . . .	109
5.1.14	Protection and control system (PCS) . . . . .	109
5.2	Systems Not Simulated . . . . .	110

5.2.1	Shutdown cooling system (SCS)	110
5.2.2	Containment venting	110
5.2.3	Generator auxiliaries	110
5.2.4	Turbine auxiliaries	111
5.2.5	Off-site power, diesel, and battery lights	111
<b>6</b>	<b>Transients</b>	<b>112</b>
6.1	Power Maneuvering	112
6.2	Reactor Scram	118
6.3	Loss of Coolant Flow	122
6.4	Steam Generator Tube Failure (SGTF)	126
<b>7</b>	<b>Conclusion</b>	<b>138</b>

# List of Figures

1.1	Nuclear electricity production [2]. . . . .	15
2.1	Simplified schematic of a PWR [14]. . . . .	19
2.2	Typical PWR RPV layout [16]. . . . .	21
2.3	U-tube steam generator [16]. . . . .	22
2.4	Once-through steam generator [16]. . . . .	23
2.5	RCP cutaway [16]. . . . .	24
2.6	PZR cutaway view [16]. . . . .	25
2.7	PZR and PZR relief tank [16]. . . . .	26
2.8	CVCS scheme [16]. . . . .	27
2.9	AFWS scheme [16]. . . . .	28
2.10	RHRS scheme [16]. . . . .	29
2.11	Typical PWR ECCS components [16]. . . . .	30
2.12	Containment spray system [16]. . . . .	31
3.1	Prompt jump and prompt drop [17]. . . . .	38
3.2	Negative reactivity insertion [17]. . . . .	40
3.3	Dependency of axial neutron flux with the control rod position [17]. . . . .	41
3.4	Position dependency of the differential control rod worth [17]. . . . .	41
3.5	Integral rod worth curves referenced to bottom and top of core [17]. . . . .	42
3.6	Effects of rod shadowing [17]. . . . .	43
3.7	Relative moderator density changes for equal temperature changes [17]. . . . .	44
3.8	Effect of moderator-to-fuel ratio on reactivity in under-moderated and over-moderated reactors [18]. . . . .	44
3.9	Doppler effect in uranium-238 capture reaction [17]. . . . .	46
3.10	Doppler broadening of resonance peak in microscopic cross-section for absorption [17]. . . . .	47
3.11	Xe-135 reactivity for different power levels [17]. . . . .	49
3.12	Xe-135 reactivity for start up to 100% power followed by shutdown [17]. . . . .	50
3.13	Xenon-135 concentration changes during power variations [17]. . . . .	51
3.14	Xenon-135 concentration for a shutdown followed by reactor startup [17]. . . . .	52
3.15	Samarium-149 reactivity for different power levels [17]. . . . .	52
3.16	Samarium-149 reactivity for clean core startup [17]. . . . .	53
3.17	$k_{excess}$ change over operating fuel cycle [17]. . . . .	55
3.18	Distortion of radial neutron flux in heterogeneous core [17]. . . . .	56
3.19	Radial neutron flux profile at BOL and EOL [17]. . . . .	56
3.20	Effect of reflection on neutron flux profiles [17]. . . . .	57
3.21	Simplified two-stage burn fuel loading to flatten the neutron flux profile [17]. . . . .	58
3.22	The bottom-top coolant flow temperature profile in PWRs [17]. . . . .	58

4.1	Examples of BP distribution designs [19]. . . . .	67
4.2	Comparing the core size of some iPWRs and a large modern PWR [19]. . . . .	69
4.3	Relative heights of $17 \times 17$ fuel designs considered in iPWRs today [19]. . . . .	71
4.4	Generic iPWR components [19]. . . . .	74
4.5	Typical two-loop PWR piping and component configuration [19]. . . . .	76
4.6	SGs simplified diagram in NuScale design [20]. . . . .	79
4.7	CAREM reactor pressure vessel and internals [19]. . . . .	85
4.8	ACP-100 reactor with other main equipment connected [7]. . . . .	87
4.9	Simplified scheme of the SMART RPV [19]. . . . .	88
4.10	Layout of the KLT-40S reactor [19]. . . . .	90
4.11	SMR-160 major components of the RCS [19]. . . . .	92
4.12	Cutaway view of NuScale SMR and reactor module [19]. . . . .	94
4.13	NuScale boron concentration variation with fuel cycle [20]. . . . .	96
4.14	EPR cutaway [21]. . . . .	98
4.15	EPR boron concentration variation with fuel cycle [21]. . . . .	99
5.1	Main screen of the iPWR simulator. . . . .	102
5.2	RCS, CBS, SCS, ADS, CCS, GIS, PDHR, and PIS. . . . .	103
5.3	MSS, FWS, TUR, GEN, and CNR. . . . .	104
5.4	Circulating water system. . . . .	107
6.1	Steps to load initial condition number 1 in iPWR simulator. . . . .	113
6.2	Selecting turbine leading control, load demand and load rate. . . . .	113
6.3	Nuclear power in power maneuvering transient. . . . .	113
6.4	Electric power in power maneuvering transient. . . . .	114
6.5	Steam flow to the turbine and to the condenser in power maneuvering transient. . . . .	114
6.6	Steam and feedwater flow in helical-coil tube 1 of the SG in power maneuvering transient. . . . .	115
6.7	Steam and feedwater flow in helical-coil tube 2 of the SG in power maneuvering transient. . . . .	115
6.8	RCS average temperature and core inlet and core outlet temperatures in power maneuvering transient. . . . .	115
6.9	PZR level control setpoint and PZR level in power maneuvering transient. . . . .	116
6.10	CVCS charge and discharge flows in power maneuvering transient. . . . .	116
6.11	MTC, FTC, and control rods reactivities in power maneuvering transient. . . . .	117
6.12	Startup rate during the transient in power maneuvering transient. . . . .	117
6.13	Xenon-135 reactivity in power maneuvering transient. . . . .	118
6.14	PZR pressure in power maneuvering transient. . . . .	118
6.15	Starting the scram transient in the simulator. . . . .	119
6.16	Core reactivity in reactor scram transient. . . . .	119
6.17	Nuclear and thermal powers in reactor scram transient. . . . .	120
6.18	Moderator and fuel temperatures in reactor scram transient. . . . .	120
6.19	Moderator and fuel reactivities in reactor scram transient. . . . .	121
6.20	The -80 seconds stable period of the nuclear power in reactor scram transient. . . . .	121
6.21	Increase in the negative reactivity inserted by xenon-135 after the scram in reactor scram transient. . . . .	122
6.22	Inserting a failure in the reactor stepbacks. . . . .	123
6.23	Generic Malfunction page showing the failed pumps. . . . .	123
6.24	Coolant flow in the core in loss of coolant flow transient. . . . .	124

6.25	Average coolant temperature in loss of coolant flow transient. . . . .	124
6.26	Core, MTC, and FTC reactivities in loss of coolant flow transient. . . . .	125
6.27	Nuclear power in loss of coolant flow transient. . . . .	125
6.28	Average fuel temperature in loss of coolant flow transient. . . . .	125
6.29	Xenon-135 negative reactivity in loss of coolant flow transient. . . . .	126
6.30	Inserting a SG tube failure with 16% severity. . . . .	127
6.31	N-16 alarm indicating high radiation level in main steam line 1 in SGTF transient.	127
6.32	PZR level in SGTF transient. . . . .	128
6.33	PZR and RPV pressures in SGTF transient. . . . .	128
6.34	Core inlet and outlet temperatures and average coolant temperature in SGTF transient. . . . .	128
6.35	Subcooling margin in SGTF transient. . . . .	129
6.36	Steam flow and feedwater flow in the faulted helical-coil tube in SGTF transient.	129
6.37	Steam flow and feedwater flow in the non-faulted helical-coil tube in SGTF transient. . . . .	130
6.38	Steam pressure in the steam lines 1 and 2 and in the steam header in SGTF transient. . . . .	130
6.39	CVCS charge and discharge flow in SGTF transient. . . . .	130
6.40	Trips page showing the reactor trip, the turbine trip, and the generator breaker opening in SGTF transient. . . . .	131
6.41	Steam flow to the turbine and to the condenser in SGTF transient. . . . .	131
6.42	Core reactivity in SGTF transient. . . . .	132
6.43	Nuclear power and thermal power in SGTF transient. . . . .	132
6.44	Flow through ADS valves in SGTF transient. . . . .	133
6.45	Increase in the suppression pool temperature due to the ADS actuation in SGTF transient. . . . .	133
6.46	PIS flow into the RCS in SGTF transient. . . . .	134
6.47	Flow in the PDHR in SGTF transient. . . . .	134
6.48	DHR pool temperatures in SGTF transient. . . . .	134
6.49	GIS flow in SGTF transient. . . . .	135
6.50	RCS boron concentration in SGTF transient. . . . .	135
6.51	RPV level in SGTF transient. . . . .	136
6.52	RCS coolant flow rate in SGTF transient. . . . .	136
6.53	Fuel temperature in SGTF transient. . . . .	136

# List of Tables

4.1	Summary of key nuclear design parameters for large PWR and range of iPWRs [19].	70
4.2	Summary of key reactor parameters of the NuScale [7]. . . . .	94
4.3	Summary of some important NuScale reactor core design parameters [20]. . . . .	95
4.4	Summary of some important NuScale reactor control rod assembly parameters [20].	95
4.5	Summary of NuScale reactivity coefficients and boron worth coefficient [20]. . . . .	96
4.6	Summary of reactivity worths in NuScale [20]. . . . .	97
4.7	Summary of key reactor parameters of the EPR [21]. . . . .	97
4.8	Summary of some EPR reactor core design parameters [21]. . . . .	98
4.9	Summary of some important EPR reactor control rod assembly parameters [21].	99
4.10	Summary of EPR reactivity coefficients and boron worth coefficient [21]. . . . .	99
4.11	Summary of reactivity worths in EPR [21]. . . . .	100

# Chapter 1

## Introduction

### 1.1 Overview

Global warming and climate changes are essential questions facing the world in the present days. The production and use of energy account for approximately two-thirds of greenhouse gases (GHGs) emissions, making them vital issues to address climate change [1]. The international community has identified the need to limit the temperature increase to 1.5 °C above pre-industrial levels. In that sense, low carbon electricity generation becomes a valuable tool to aid in reaching this level. Among the most important technologies for clean energy production are nuclear power, hydropower, wind, and solar. Wind and solar technologies cannot provide energy continuously, while hydropower can cause considerable environmental consequences due to the necessity of dumping the water, changing the water flow, droughts, among others. In this scenario, nuclear power generation appears as a reliable, steady, and clean supply of power where its use can reduce GHGs emissions and meet the necessity of the increasing world population.

According to [2], around 10% of the world's electricity is produced by 440 nuclear power plants (NPPs), and 50 more reactors are under construction. In 2019, NPPs supplied 2657 TWh of electricity, and in 2018 this value was 2563 TWh which represents the seventh consecutive year of rising in global nuclear generation (Figure 1.1 [2]). From 1971 until 2018, hydropower and nuclear power supplied the majority of low carbon generation. Over this period, the electricity supplied by NPPs is estimated to have avoided a total of 74 gigatonnes of carbon dioxide [1]. Besides, NPPs are now being designed to provide non-electric services such as heating for homes and businesses, heating and cooling for industrial purposes, desalination of seawater, and hydrogen production. These services can also contribute to the process of reducing GHGs emissions [3].

Another important factor that contributes positively to NPPs is their resilience and safety in the face of extreme events [3]. As discussed above, climate change mitigation requires that the energy sector employ low carbon energy generation. Nevertheless, energy generation also needs to withstand and adapt to extreme events and changes in the environment. A recent demonstration of this resilience was observed during the COVID-19 pandemic. The pandemic has imposed several restrictions and has negatively affected the economy in the entire world. Despite the worldwide constraints, the NPPs continued to operate and generate energy safely. Climate changes also pose a challenge to NPPs. Global warming has been causing periods of heavy rainfall, extremes temperatures, high winds, and significant sea level rises. However, robustness in NPPs designs has proven to be effective against these events. Besides, after the

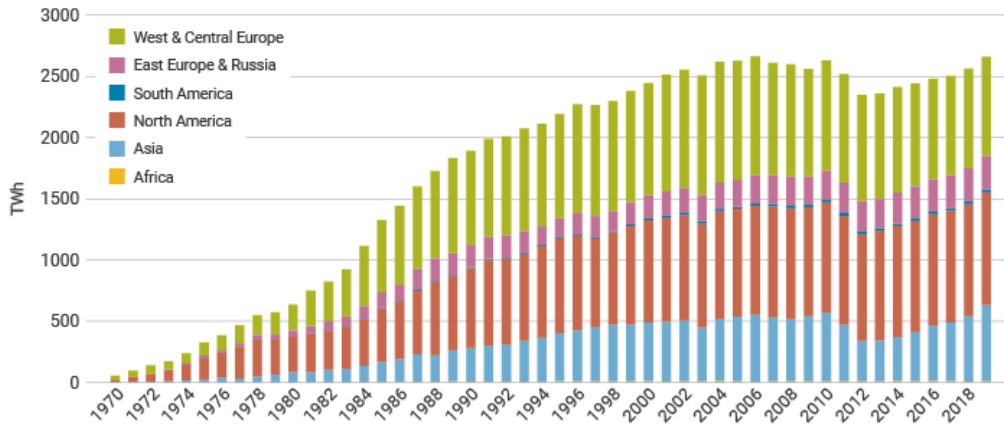


Figure 1.1: Nuclear electricity production [2].

Fukushima accident, further measures have been adopted to enhance the safety of existing NPPs and improve designs of new plants against extreme events.

The operation life of NPPs is another crucial issue. NPPs were built to have an operation life between 30 and 40 years. Though, the advance in materials science and technology are helping to extend the operation life of NPPs. The cost of refurbishing NPPs for a long operation period is much lower than building new plants [3]. After the refurbishment, the NPPs can safely continue the operation for an additional 20 to 40 years. The degradation is one of the significant challenges that must be dealt with in the aging of NPPs. During the operation, the components and structures are exposed to high temperatures, intense conditions, and continuous operation, resulting in wearing. The development of new techniques that provide a better corrosion resistance of the NPPs components and structures makes those elements more economically feasible for a life-extended operation of NPPs. Additionally, the use and analysis of the complexes and massive data collected during the operation of the NPPs also contribute to the extension of their operation life. With these data, researchers can predict how the NPPs components age under different conditions, and then they can determine what needs to be replaced and when the replacement is necessary. These actions not only help the extension of the operation life of NPPs but also improve their performance.

It has been discussed how NPPs can be essential allies in combating the emissions of GHGs and then reducing global warming to the desired level. However, to fulfill their role, NPPs must be economically viable. In that sense, advanced reactors have contributed to cost reduction, greater public acceptance, and streamlined licensing. These factors are helping countries to consider NPPs as an option to achieve their climate goals. The design of NPPs has evolved over six decades due to research, development, and lessons learned in nuclear power [3]. Some features present in advanced reactors are their enhanced thermal efficiency, optimized use of natural resources, waste minimization, modular construction, longer operation life, higher availability, further reduced possibility of core melt accidents, greater use of burnable absorbers to extend fuel life, and ability to address both electricity production and non-electric application of nuclear power [4]. At present, there are 15 advanced reactors in operation. Among the new designs, one may cite the South Korean APR-1400 (1400 MWe), the Russian VVER-1200 (1200 MWe), the French EPR-1750 (1750 MWe), and the North American AP-1000 (1250 MWe) [5]. The standardized design and modular construction of these new NPPs reduce their capital cost and construction time, which are fundamental features.

As previously discussed, the new designs of NPPs have sought to reduce costs and construction time. However, these plants continue to be huge facilities and still costly. At the same time



that the design of high-power NPPs has evolved, there have also been advances in small-power plants. Several reactors of this type were built to be used for naval propulsion and as neutron source, yielding enormous expertise in designing this type of facility [6]. The International Atomic Energy Agency (IAEA) describes small modular reactors (SMRs) as newer generation reactors designed to generate electric power typically up to 300 MWe, whose components and systems can be produced and then transported as modules to the sites for installation as demanded [7]. The SMRs provide low carbon energy as large NPPs but with more flexibility and affordability. Thus, they can be used on smaller power grids and be built in places where large reactors would not be practical. In 2020 the world's first SMR started its commercial operation. The Akademik Lomonosov floating nuclear power plant has two KLT-40S (35 MWe each) that are now generating energy to power a city of around 100 000 people [3]. At present, there are more than seventy SMR designs under development for different applications. Among them, one may cite the Argentinian CAREM (27 MWe), the South Korean SMART (107 MWe), and the North American NuScale (60 MWe) [7].

The employment of NPPs requires extensive training of the involved personnel. Well-trained personnel minimizes the risks associated with human failures, maintaining the safety standards offered by advanced designs of NPPs. Thus, in support of developing the human resource in the Member States, the IAEA has established education and training programs on active learning about nuclear technologies using PC-based basic principle simulators [8]. In this program, the IAEA provides the development and distribution of PC-based basic principle simulators, including manual and related documentation, sponsors education and training courses, and workshops on physics and technology of advanced reactors. These simulators offer efficient hands-on learning of physics and engineering designs of various reactor types. Currently, IAEA provides NPP simulation software that simulates the behavior of pressurized water reactors (including SMRs), pressurized heavy water reactors, boiling water reactors, and a part-task simulator. Additionally, high-temperature gas-cooled reactor and sodium-cooled fast reactor are under development. Together with associated documentation, these simulators are distributed at no cost to interested parties in the IAEA Member States.

## 1.2 Purpose of the Research

As discussed, there is a significant worldwide effort to limit the global temperature increase to 1.5 °C above pre-industrial levels. Among the main sectors that have contributed to global warming is the energy sector. In that sense, means of generating energy with low emissions of GHGs have been sought. The use of renewables power such as solar and wind has been steadily increasing. However, only nuclear power and hydropower can generate electricity continuously and reliably and are the only options with low emission of GHGs capable of replacing the power produced by fossil fuels.

Due to its importance, this work discusses the new designs of NPPs, focusing on SMRs. Additional comparisons with more conventional NPPs are also presented. Remarkably there are a vast number of types of nuclear reactors such as advanced gas-cooled reactors (AGRs), pressurized water reactors (PWRs), boiling water reactors (BWRs), light water graphite-moderated reactors (LWGRs), fast neutron reactors (FNRs), heavy water reactors (HWRs), and high-temperature gas-cooled reactors (HTGRs). However, this work focuses on the PWR as it is the most common type, with about 300 reactors operable for power generation and several others employed for naval propulsion [9]. Further information about the other types of reactors can be found in the References [4], [6], [7], [9], and [10].

Contributing to the safety of NPPs, simulators play an essential role in training NPP personnel. Most NPPs employ simulators for training and retraining their personnel once it is impossible to do this on the operating plants. The need for simulator training increased sharply due to the identification of operator errors in the Three Mile Islands and Chernobyl accidents [11]. In that sense, this work demonstrates the use of a PC-based simulator to study transients originated in normal operation conditions and in accident conditions of NPPs. The selected simulator is the IAEA Integral Pressurized Water Reactor Simulator (SMR), which simulates a generic design of an integral pressurized water reactor.

## 1.3 Organization of the Work

This work is organized as follows:

- Chapter 2 discusses basic principles of PWR reactors.
- Chapter 3 presents important parameters and definitions related to the operation of NPPs. This chapter also includes a description of some NPPs transients.
- Chapter 4 discusses the features of SMR designs. This chapter also compares SMR designs with large PWR designs. A more detailed discussion of some SMR designs is also included.
- Chapter 5 describes the IAEA Integral Pressurized Water Reactor Simulator (SMR).
- Chapter 6 includes the results and the discussions of the transients simulated in the IAEA Integral Pressurized Water Reactor Simulator (SMR).
- Chapter 7 presents the conclusions followed by the bibliography employed.

# Chapter 2

## Pressurized Water Reactors

### 2.1 Overview

The PWR is the most common type of nuclear reactors, with about 300 reactors operable for power generation and several others employed for naval propulsion [9]. The design of PWRs originated from research into submarines with nuclear propulsion after the Second World War. The first submarine prototype was built at Idaho National Laboratory in the United States in 1953, and the first submarine with nuclear propulsion, USS Nautilus, was launched in 1955. The first PWR power station was the Shippingport Atomic Power Station, also in the United States. The unit started up in 1957 and generated 60 MWe. However, it is considered a PWR demonstration instead of the first commercial power station due to its unusual design. This honor is then credited to the Yankee Rowe power station, which started in 1960. This plant had the capacity of generating 185 MWe [12].

PWRs use light water as moderator and coolant. The typical PWR design is divided into three circuits named primary, secondary, and tertiary. The main components of the primary are the reactor core, reactor pressure vessel (RPV), and the primary loops. Depending on the design, the primary can have one or more loops connected to the RPV. The following main parts compose each loop: reactor coolant pumps (RCPs), steam generator (internal tubes), and the pressurizer (PZR) connected to only one loop. The main components of the secondary circuit include the steam generator (hull), steam turbine, main condenser (hull), condensate pumps, and feedwater pumps. Among the main components of the tertiary circuit are the main condenser (tubes side), circulation pumps, and heat sink (atmosphere, river water, seawater).

In the primary circuit, the heat is produced by fission in the reactor core. The RCPs pump the water in the primary loops through the reactor to remove the thermal energy produced by the core. The primary circuit is kept at high pressure to prevent water from boiling. The hot pressurized water then flows through the tubes of the steam generator (hot leg), where it is cooled by the water from the secondary circuit, and then it is pumped back to the reactor vessel (cold leg), closing the cycle. In a typical PWR, water enters the pressure vessel at a temperature of about 290 °C and exits at about 325 °C [13]. The primary pressure is maintained at approximately 15 MPa by the PZR, connected by a surge line to the hot leg of only one loop. The PZR is kept at saturation (steam and water together). When a pressure increase is required, heaters in the PZR boil the water into steam, and when a pressure decrease is required, steam is condensed into water. The pressure control in one loop works in all loops due to the principle of communicating vessels.

In the steam generator (SG), the primary high-pressure hot water circulates inside the tubes

while the outer surface of these tubes is in contact with the low pressure and cooler feedwater returning from the main condenser. The heat transferred from the primary circuit to the secondary circuit in the SG makes the feedwater boil resulting in steam. Steam flows from the SG and is used to drive the turbine that drives the electric generator to produce electricity. This steam expands through the turbine and, after leaving the turbine, it is condensed in the main condenser. The condensate is extracted from the condenser hot well by the condensate pumps, and it is pumped back to the SG secondary side by the feedwater pumps. In a typical PWR, the steam is produced at about 293 °C and 5 MPa [13].

In the condenser, the steam used in the turbine is condensed in the main condenser hull by rejecting heat to the water circulating inside the condenser tubes. The water flowing inside these tubes, from the tertiary circuit, is pumped by the circulation pumps from the heat sink, which can be river water, seawater, or water from cooling towers. In PWRs, the SGs are the boundary between the primary and the secondary circuit, and there is no communication between the water in both circuits. The same occurs with the secondary and the tertiary circuit where the condenser is the boundary. The overall efficiency of a PWR is between 32% and 33% [13]. A simplified schematic of a PWR is presented in Figure 2.1 [14].

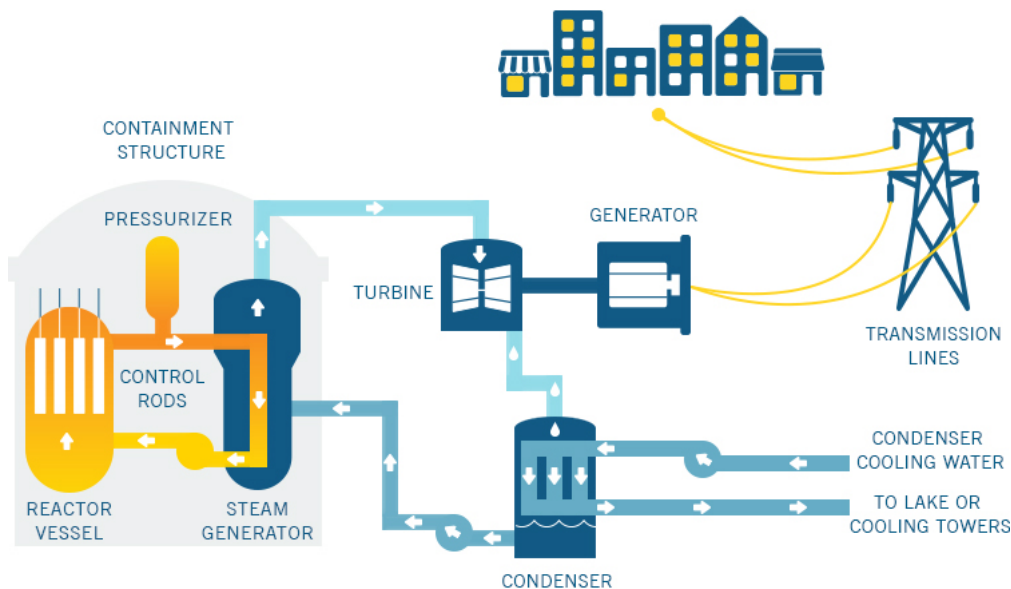


Figure 2.1: Simplified schematic of a PWR [14].

The PWR uses as fuel slightly enriched uranium dioxide ( $\text{UO}_2$ ). The enrichment varies between 2% to 5%. The  $\text{UO}_2$  is a black ceramic material used in small cylindrical pellets with 1 cm diameter and 2 cm long, which are typically concave on the ends. The pellets are arranged into sealed stainless steel or zircaloy tubes (cladding) about 4 m long to form a fuel rod. Zircaloy is an alloy of zirconium (small neutron absorption cross section) with small amounts of iron, tin, chromium, and nickel. During the reactor operation, the pellets expand axially and fill the gaps between the pellets. The zircaloy fuel tubes also prevent the release of fission products to the coolant. On some occasions, it is observed that some fuel pellets, although expanding initially when the operating temperature is reached, later contract due to a gradual increase in the density of the  $\text{UO}_2$  (densification). The densification leaves void spaces within the fuel tubes, and because of the high pressure of the moderator coolant, it increases the stresses in the fuel tube, increasing the probability of cladding rupture. For that reason, the fuel tubes are pressurized with helium at approximately 3.4 MPa. The accumulation of

fission products increases the pressure gradually up to 14 MPa near the end of core life [13]. The fuel rods are then arranged in a square lattice structure called a fuel assembly. A typical fuel assembly contains  $17 \times 17$  fuel rods [15].

The control of the PWR is accomplished by the control rods made of neutron absorbing material such as boron, hafnium, and cadmium [9]. These rods usually enter the core from the top and are inserted or withdrawn from the core to decrease or increase power. In some PWRs, together with control rods, it is also used boric acid diluted in the coolant water to control the reactor (chemical shim). The power increase is achieved by boron dilution and the power decrease by boration. Typical PWR has a generating capacity of 1000 MWe, although early plants were much smaller. Advanced PWR designs range from 1100 to 1700 MWe, while SMRs generate up to 300 MWe [12].

## 2.2 Main PWR Components and Systems

### 2.2.1 Reactor pressure vessel (RPV)

The RPV houses the reactor core and all associated support and alignment devices. The most important components are the reactor vessel, the reactor core, the core barrel, and the upper internals package. Figure 2.2 [16] shows a typical PWR RPV layout.

The RPV is a cylindrical vessel with a hemispherical bottom head and a removable hemispherical top head, which allows for the refueling of the reactor. There is one inlet nozzle (cold leg) and one outlet nozzle (hot leg) for each RCS loop. Typically, the RPV is constructed of low-alloy carbon steel clad, and all the surfaces that come into contact with reactor coolant are covered with austenitic stainless steel in order to increase corrosion resistance.

The core barrel is inside of the RPV and houses the fuel. Toward the core barrel bottom, there is a lower core support plate where the fuel assemblies are sit. The core barrel and all the lower internals hang inside the RPV from the internals support ledge. Outside of the core barrel, there are irradiation specimen holders where samples of material used to manufacture the vessel are placed. Periodically, some of these samples are removed and tested to observe how the radiation from the fuel has affected the material strength.

The upper internals packages sit on top of the fuel. It contains the guide columns (guide tubes) that guide the control rods when they are moved in the core. The upper internals package inhibits the core from moving up during operation due to the force from the coolant flowing through the assemblies.

When the reactor coolant flows through the RPV, it enters the RPV at the inlet nozzle and hits against the core barrel, which forces the water to flow downward in the space between the RPV wall and the core barrel. After reaching the bottom of the RPV, the flow turns upward to pass through the fuel assemblies to remove the heat generated by the fission process. The heated water enters the upper internals region, where it is directed to the outlet nozzle and goes to the SG.

### 2.2.2 Steam generators (SGs)

The reactor coolant flows from the reactor into the SG. Inside the SG, the hot reactor coolant flows inside several tubes. The feedwater from the secondary circuit flows around outside the tubes, where it removes heat from the primary. After absorbing enough heat, the feedwater starts to boil and form steam.

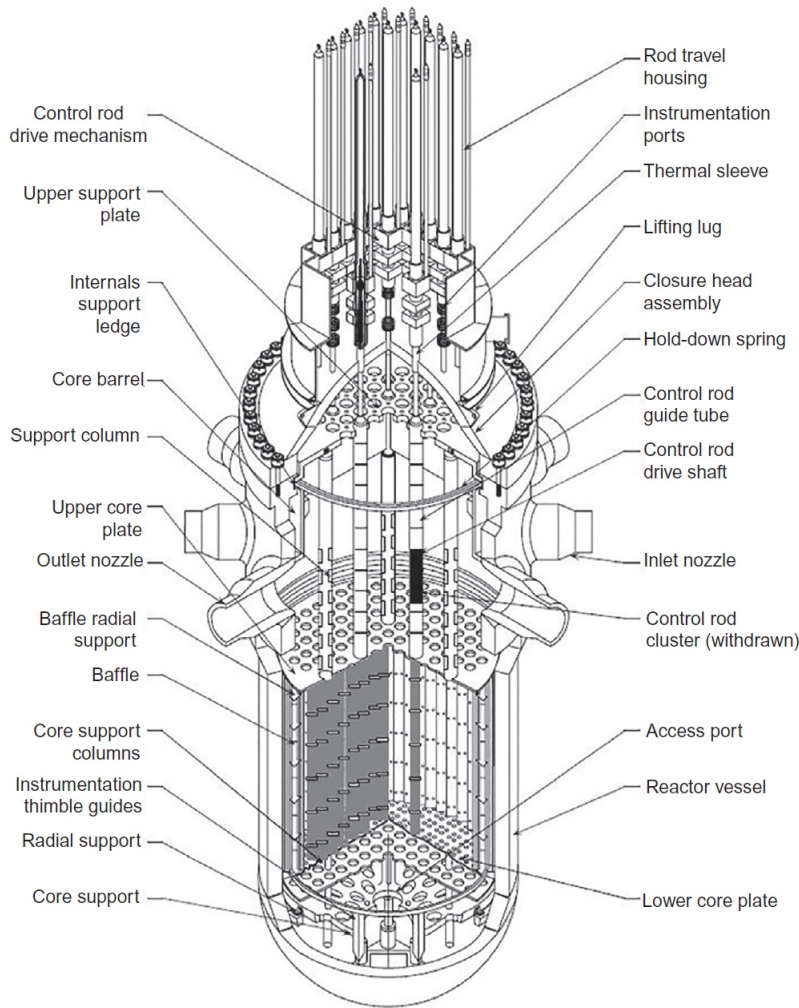


Figure 2.2: Typical PWR RPV layout [16].

Depending on the model, the SG operations differ slightly. In the U-tube design (Figure 2.3 [16]), the steam and water mixture passes through multiple stages of moisture separations. One stage causes the mixture to spin, forcing the water to the outside. Then, the water is drained and used to produce more steam. The drier steam is directed to the second stage of separation, where the mixture is forced to make rapid changes in direction. Due to the ability of steam to change direction compared to the water, the steam exits the SG, and the water is drained for reuse.

In the once-through SG design (Figure 2.4 [16]), the primary coolant flow is from the top to the bottom of the SG. Due to the heat transfer achieved by this design, the steam that exits this SG contains no moisture.

In both designs, the steam is then directed to the main turbine, and the coolant is directed to the suction of the RCPs.

### 2.2.3 Reactor coolant pump (RCP)

The RCP provides forced primary coolant flow to remove the amount of heat generated by the fission process in the reactor core. Without a pump, there is natural circulation flow through the reactor. However, this flow is not enough to remove the heat when the reactor

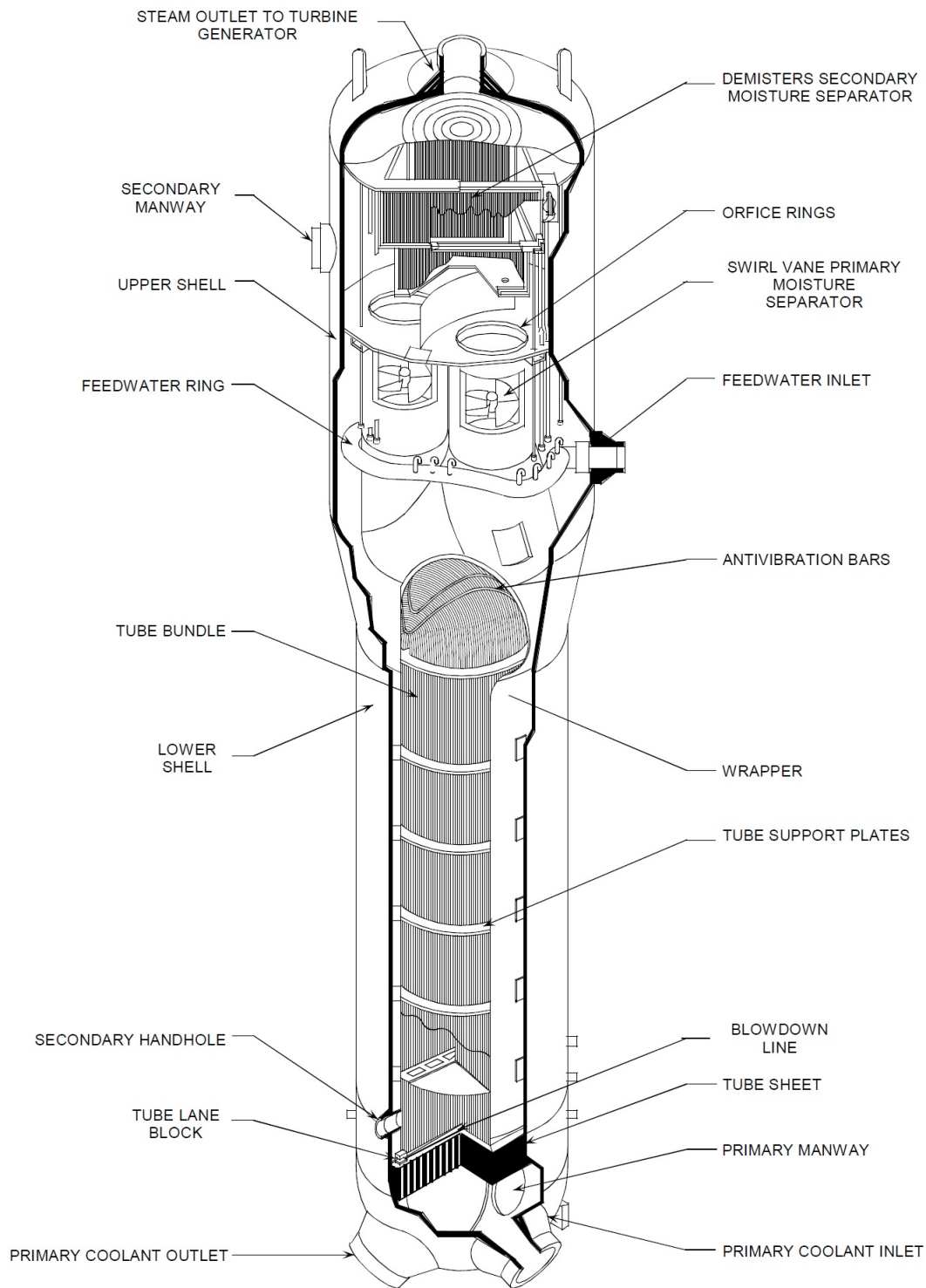


Figure 2.3: U-tube steam generator [16].

operates at power. The natural circulation is enough only when the plant is shut down.

The reactor coolant coming from the SG enters the suction side of the pump. The pump impeller increases the water velocity. The velocity increase is converted to pressure in the discharge volute. In a typical RCP, the increase in pressure is approximately 0.6 MPa [16]. The coolant from the pump discharge side enters the cold leg side of the RPV. Inside the core, the coolant removes heat from the fuel and is sent back to the SGs.

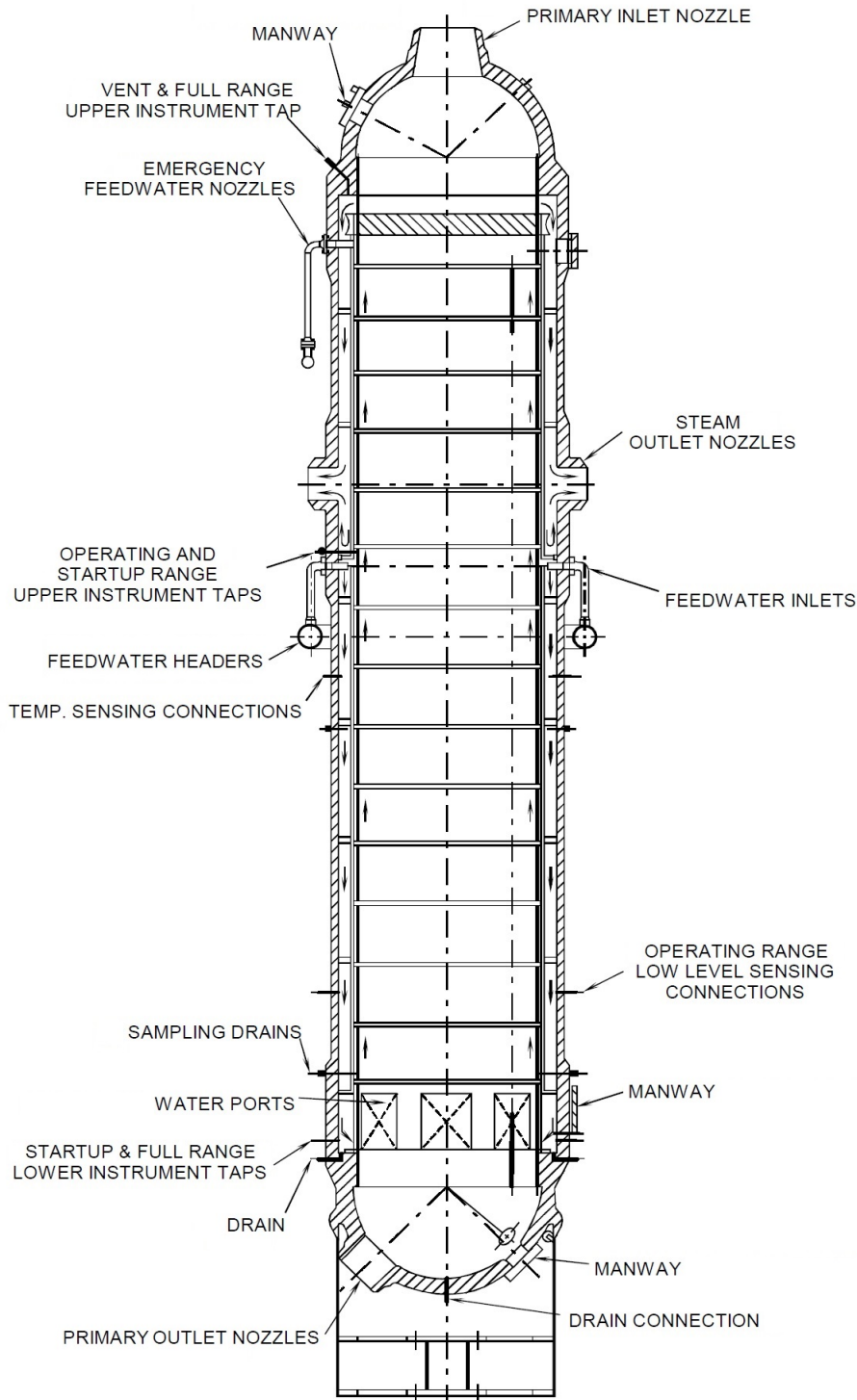


Figure 2.4: Once-through steam generator [16].

The RCP major components are the motor, the hydraulic section, and the seal package. Figure 2.5 [16] shows an RCP cutaway. The motor consists of a large air-cooled electric motor. The motor power ranges from 4500 to 7500 kW and provides a flow of approximately 400 m<sup>3</sup>/min.

The hydraulic section of the pump consists of the impeller and the discharge volute. The impeller is attached to the pump motor by a long shaft. The seal package, located between the motor and the hydraulic section, prevents any water from leaking up the shaft into the



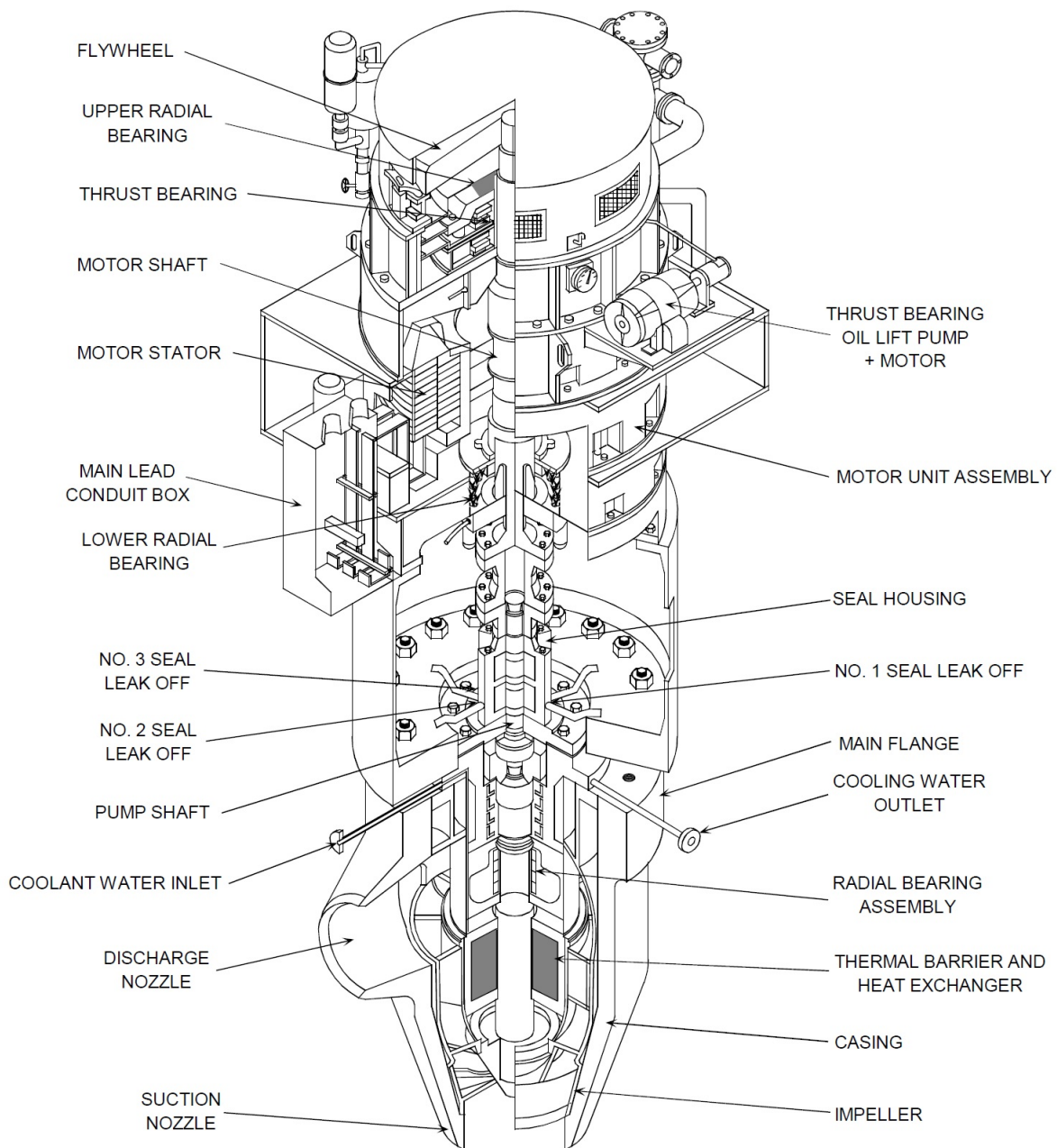


Figure 2.5: RCP cutaway [16].

containment atmosphere.

## 2.2.4 Pressurizer (PZR)

The PZR controls the RCS pressure. The pressure is controlled by using electrical heaters, PZR spray, power-operated relief valves (PORVs), and safety valves. Figure 2.6 [16] presents a cutaway view of a PZR.

The PZR operates with an equilibrium mixture of steam and water. In case of pressure changes, the components actuate to bring the pressure back to the normal operating pressure. Normally, the pressure deviation is associated with the change in the RCS temperature. When the RCS temperature increases, the density of the reactor coolant decreases, and the water

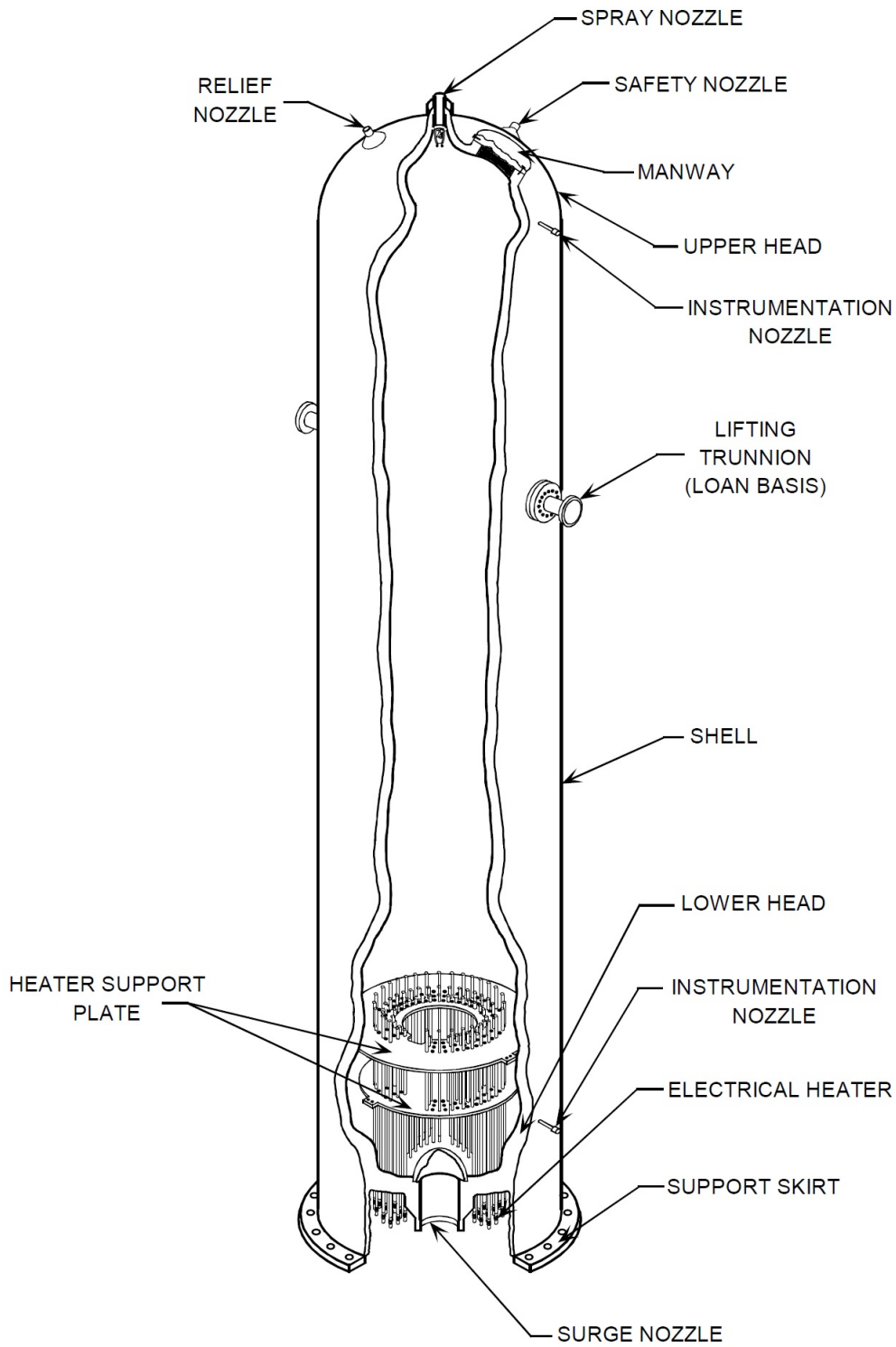


Figure 2.6: PZR cutaway view [16].

expands. As the PZR is connected to the RCS via the surge line, the water expands into the PZR. Thus, the steam at the top of the PZR is compressed, and the pressure increases. The opposite effect happens when the RCS temperature decreases. The water becomes denser, occupying less space. Then, the PZR level decreases, causing the pressure to decrease.

If the pressure increases above the desired setpoint, the spray line allows relatively cold water from the RCP discharge to be sprayed into the steam space. The cold water condenses

the steam into water, resulting in pressure reduction. If the pressure continues to increase, the PZR relief valves open and dump steam to the PZR relief tank. If the operation of the relief valves is not enough to reduce the pressure, the safety valves open also discharging to the PZR relief tank. If the pressure decreases, the electrical heaters energize to boil more water into steam, increasing the pressure. If the pressure continues to decrease, the reactor protection system actuates and trips the reactor due to low pressure in the RCS.

The PZR relief tank is a large tank containing water with a nitrogen atmosphere. The water in the tank condenses any steam discharged by the safety or relief valves. As the RCS contains hydrogen, the nitrogen atmosphere prevents the hydrogen from accumulating in a potentially explosive environment. Figure 2.7 [16] shows the PZR and PZR relief tank.

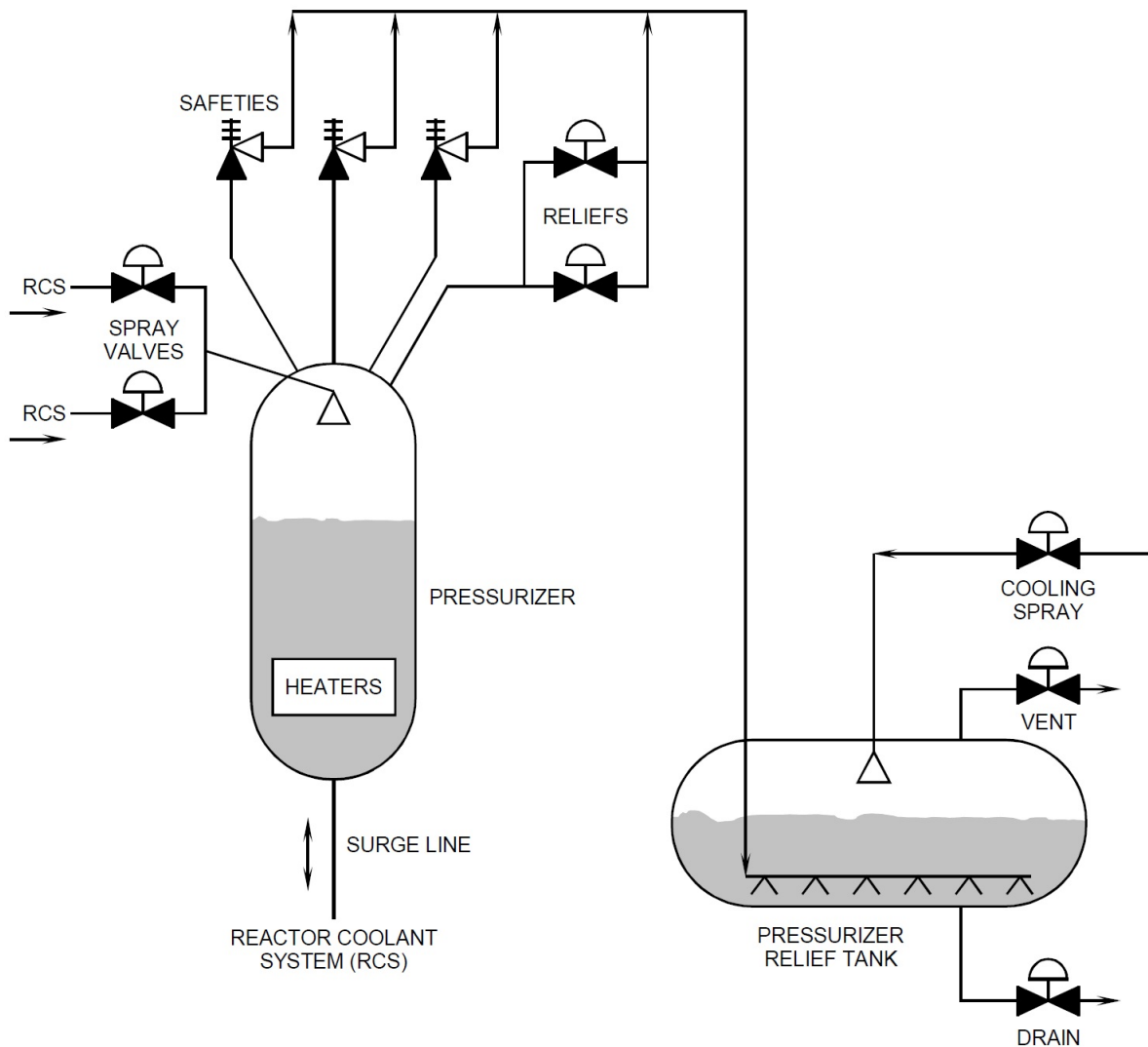


Figure 2.7: PZR and PZR relief tank [16].

## 2.2.5 Chemical and volume control system (CVCS)

The CVCS is a major support system for the RCS. It purifies the RCS using filters and demineralizers, adds and removes boron as necessary, and maintains the level of the PZR at

the desired setpoint. A small amount of water, approximately  $0.28 \text{ m}^3/\text{min}$ , is continuously routed through the CVCS (letdown). The letdown provides a continuous cleanup of the RCS, maintaining the coolant purity and helping to decrease the amount of radioactive material in the coolant.

The RCP seals prevent the leakage of primary coolant to the containment atmosphere. The CVCS provides seal injection to cool and lubricate the seals. The water in CVCS is cooled by heat exchangers and cleaned by the filters and demineralizers. Figure 2.8 [16] presents an example of a CVCS scheme. A flow patch also routs the letdown flow to the radioactive waste system for processing or disposal (not shown in Figure 2.8 [16]).

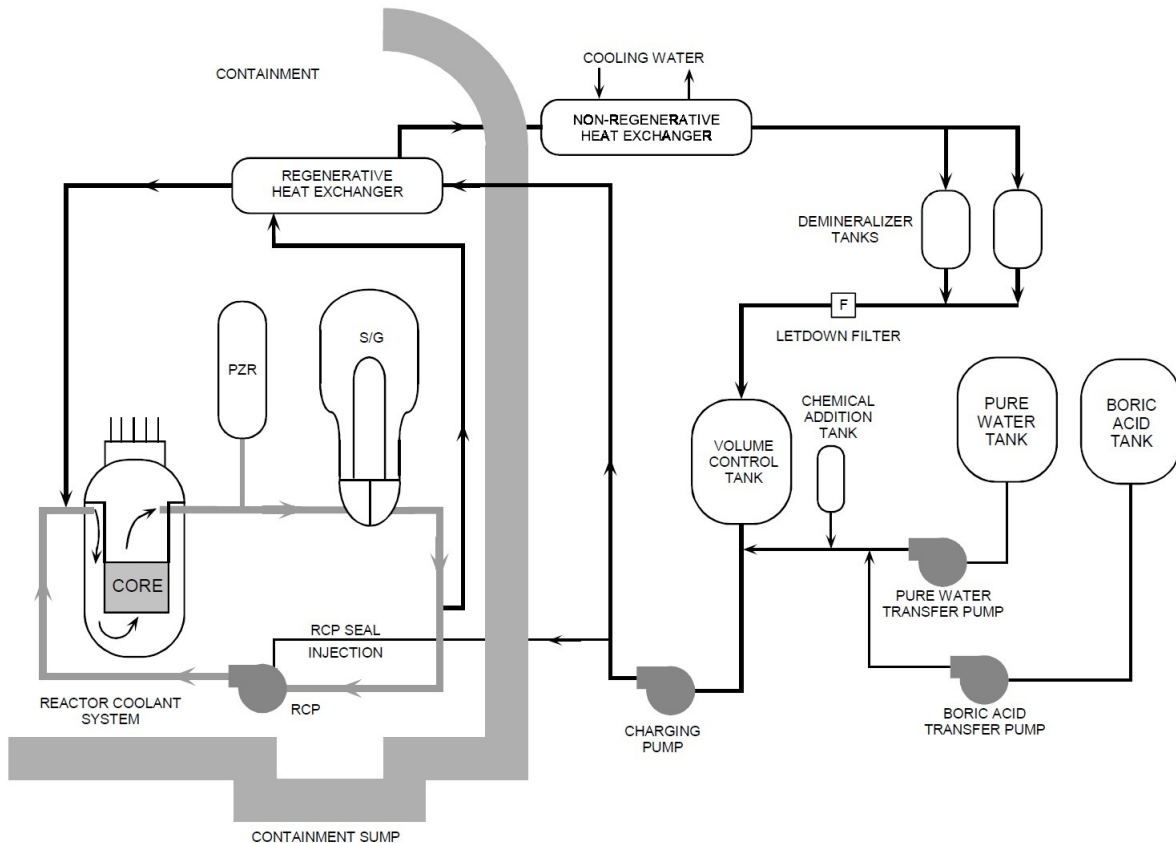


Figure 2.8: CVCS scheme [16].

## 2.2.6 Auxiliary feedwater system (AFWS)

Even after the reactor shutdown, a significant amount of heat continues to be produced by the decay of fission products (decay heat). The decay heat is enough to cause fuel damage if not properly removed. In that sense, systems must be designed and installed in the plant to remove the heat from the core and transfer it to the environment, even in shutdown conditions. When the maintenance on RCS components is required, the temperature and pressure of the RCS have to be reduced low enough to allow personnel access to the equipment.

The AFWS and turbine bypass valves (steam dump valves) work together to allow the operator to remove decay heat from the reactor. Figure 2.9 [16] presents an AFWS scheme. The AFWS pumps water from the condensate storage tank to the SGs, where the water boils to make steam. The steam can be dumped into the main condenser through the steam dump

valves. The circulating water condenses the steam and takes the heat to the environment. When the steam dump is not available, the steam can be dumped directly into the atmosphere through the atmospheric relief valves.

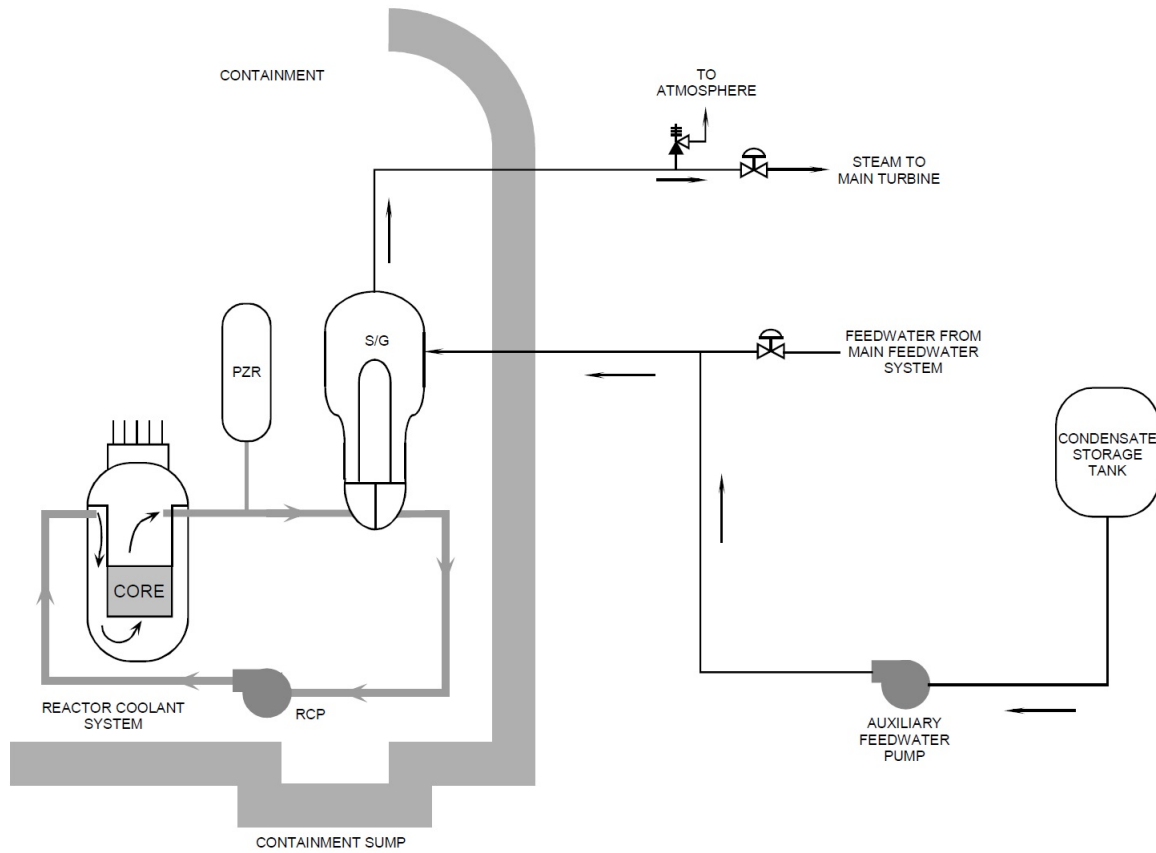


Figure 2.9: AFWS scheme [16].

### 2.2.7 Residual heat removal system (RHRS)

At some point, the decay heat is not enough to generate sufficient steam in the SGs to continue the cooldown. When the RCS temperature and pressure are reduced within operational limits, the RHRS is used to continue the cooling by removing heat from the core and transferring it to the environment.

The cooldown is performed by routing part of the reactor coolant through the RHRS heat exchanger, which is then cooled by the component cooling water system (CCWS). The heat removed by the CCWS is transferred to the service water system in the CCWS heat exchanger. The heat removed by the service water system is transferred directly to the environment. The RHRS can cool the plant to a temperature level low enough to perform maintenance functions and refueling. Figure 2.10 [16] presents an RHRS scheme.

### 2.2.8 Emergency core cooling system (ECCS)

The ECCS provides core cooling to minimize fuel damage after a loss of coolant accident (LOCA), which is accomplished by injecting a large amount of cool borated water into the RCS.

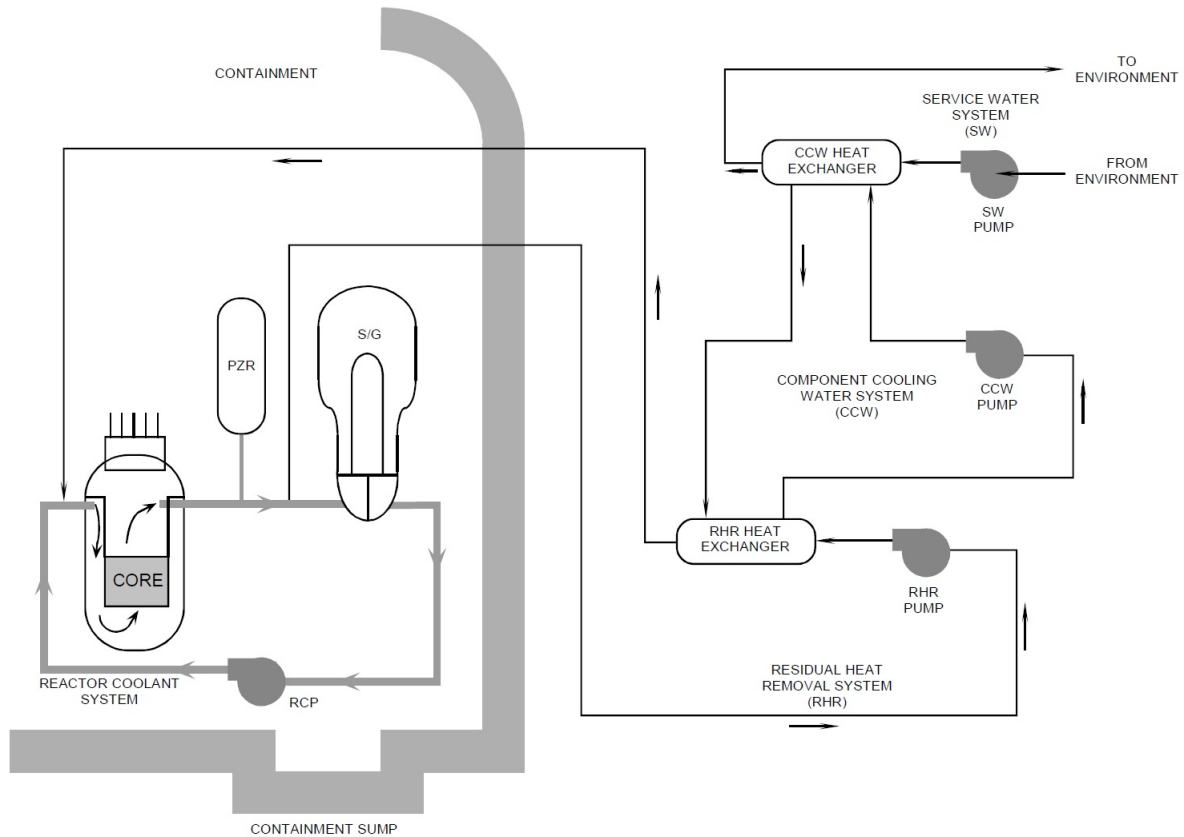


Figure 2.10: RHR scheme [16].

Additionally, this system provides extra neutron poisons to guarantee the reactor remains shut down following the cooldown due to a main steam line rupture. The water source of the ECCS is the refueling water storage tank (RWST).

To inject large quantities of borated water, the ECCS consists of four separated systems, as presented in Figure 2.11 [16]. These systems are the high-pressure injection system, intermediate pressure injection system, cold leg accumulators, and the low-pressure injection system (residual heat removal). Each system has two pumps, each of which can provide sufficient flow (Figure 2.11 [16] shows only one pump for each system). These systems must operate when the plant's normal supply power is lost. Thus, the systems are powered by the plant emergency power system.

The high-pressure injection system uses the pumps located in the CVCS. When an emergency actuation signal is received, the system is automatically realigned to take water from the RWST and pump it into the RCS. This system is designed to provide water to the core during emergencies where the RCS pressure remains relatively high, such as small breaks in RCS, steam break accidents, and steam generator tube failure.

The intermediate pressure injection system also operates in emergencies where the RCS pressure remains relatively high, for example, after small to intermediate size primary breaks. Following an emergency start signal, the pumps take water from the RWST and pump it into the RCS.

The cold leg accumulators are passive elements; they do not require electrical power to operate. These tanks contain large quantities of borated water and are pressurized with nitrogen. When the RCS pressure drops below the pressure of the tanks, the nitrogen forces borated water out of the tanks into the RCS. These tanks provide water to the RCS during emergencies

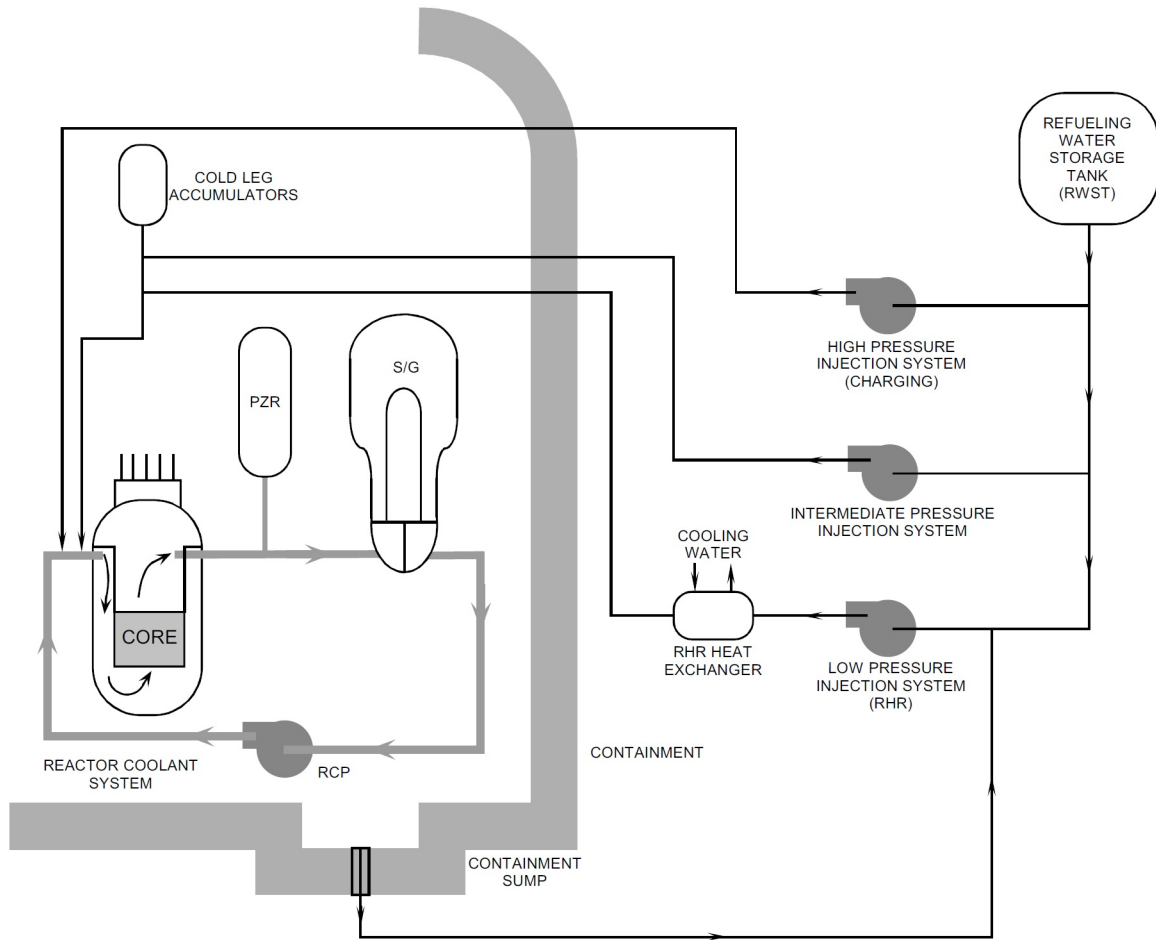


Figure 2.11: Typical PWR ECCS components [16].

where the primary pressure drops very rapidly, such as large breaks in the primary.

The low-pressure injection system injects water from the RWST into the RCS during large breaks, which causes a very low RCS pressure. Additionally, this system can take water from the containment sump, pump it through the RHR heat exchanger for cooling, and then send it back to the reactor for core cooling. This cooling method is used when the RWST empties after a large primary system break. This operation is called long-term core cooling or recirculation mode.

### 2.2.9 Containment building system (CBS)

Containments are designed to withstand pressures and temperatures accompanying a high energy fluid (primary coolant, feedwater, or steam) release inside the building. However, exposure to high temperature and pressure over a long period of time tends to degrade the concrete. When a break occurs in the primary system, the coolant released into the containment building contains fission products (radioactive material). If the concrete develops any cracks, the high pressure in the containment tends to force radioactive material from the containment into the environment. To limit these leakages after an accident, a steel liner is used to cover the inside surface of the containment building. This liner acts as a vapor-proof membrane to prevent any gas from escaping through any cracks that may develop in the concrete.

Additionally, two systems are designed to reduce the containment temperature and pressure after an accident inside the containment building. The fan-cooler system circulates air through heat exchangers to accomplish cooling. The other system is the containment spray system. Figure 2.12 [16] shows the containment spray system.

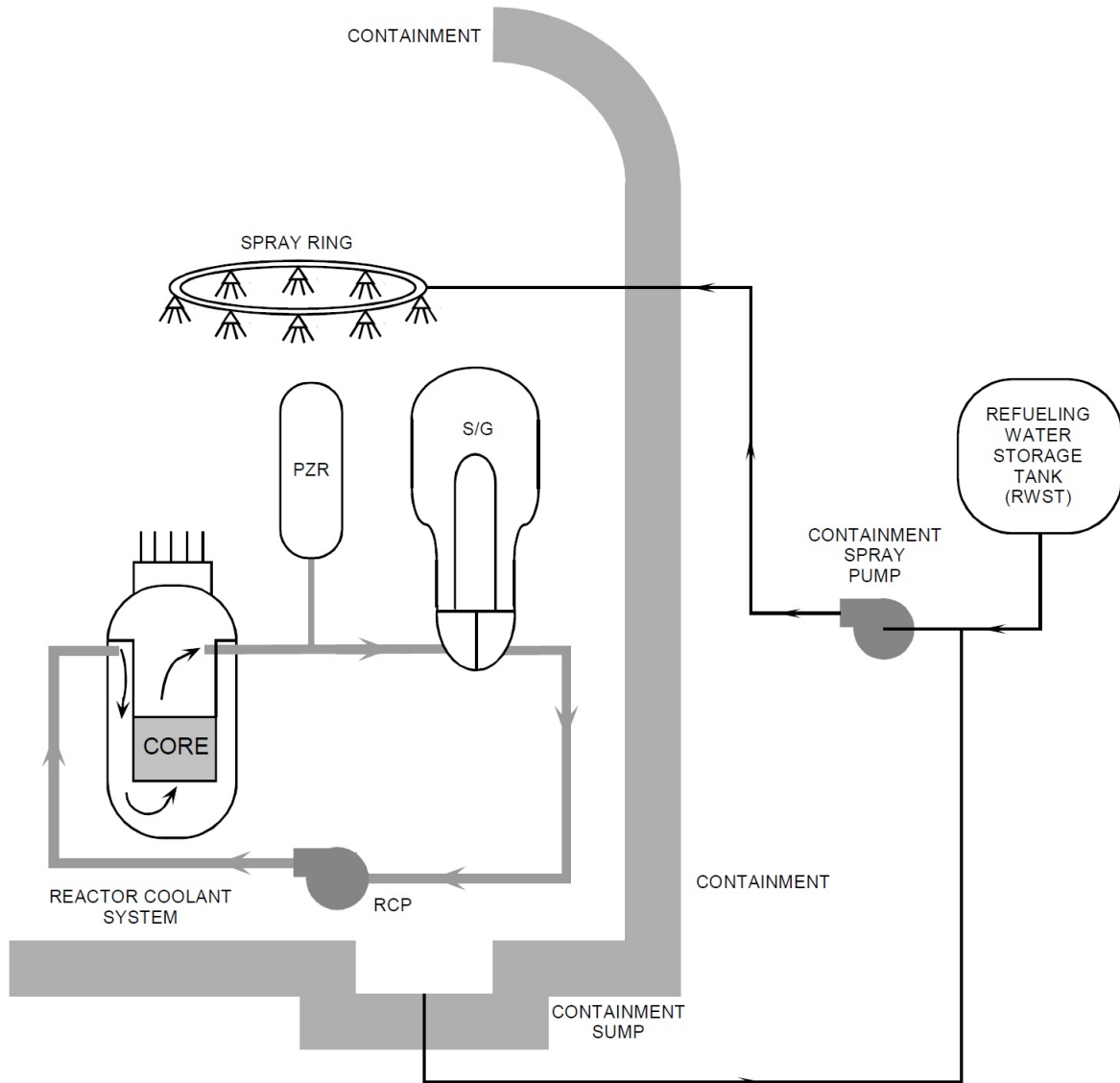


Figure 2.12: Containment spray system [16].

Following a primary or a secondary system break inside the containment building, the containment atmosphere becomes filled with steam. To reduce the pressure and temperature inside the building, the containment spray starts automatically. The containment spray pump takes suction from the RWST and pumps the water into spray rings in the upper part of the containment. The water droplets, cooler than steam, remove heat from the steam, causing the steam to condense. The steam condensation reduces the pressure and the temperature of the containment atmosphere, similarly to the PZR operation. Like the RHRS, the containment spray system can take water from the containment sump if the RWST goes empty.



# Chapter 3

## Reactor Operating Parameters

The operation of nuclear reactors requires operators to monitor important parameters of the reactor. During the operation, some of these parameters can be controlled directly by the operator, while others cannot. This section aims to present a brief description of the main operating parameters of reactors.

### 3.1 Reactor Kinetics

Reactor kinetics describes how the neutron flux, and consequently the power, depends on time. The discussions presented in this section are simplified. A more detailed discussion can be found in [13].

#### 3.1.1 The role of prompt and delayed neutrons

Fission neutrons can be emitted as prompt or delayed neutrons. Prompt neutrons are emitted at the time of the fission event, typically on the order of  $10^{-14}$  seconds after the fission of the nucleus. Delayed neutrons are emitted from the decay of several different fission products, which are called delayed neutron precursors. They are generated on average approximately 12.58 seconds after the initial fission event [17]. This huge difference is important in reactor operation.

The prompt neutron lifetime begins when a prompt neutron is released and ends when it is absorbed in another nucleus. The delayed neutron lifetime begins when the delayed neutron is released by the decay of the fission products and ends when it is absorbed in another nucleus. In both cases, the lifetime is found by adding the slowing down time and the diffusion time. Delayed and prompt neutrons are generated as fast neutrons. In that sense, both have a similar lifetime of thermalization and reabsorption in approximately  $10^{-4}$  seconds timespan [17].

The prompt and delayed neutrons generation time is the time required for a neutron, delayed or prompt, from one generation to cause the fissions that produce the next generation of neutrons. The prompt neutron generation time ( $l^*$ ) includes the time for its creation ( $10^{-14}$  seconds) and its lifetime ( $10^{-4}$  seconds). Thus, the prompt neutron generation time is:

$$l^* = 10^{-14} \text{ s} + 10^{-4} \text{ s} \approx 10^{-4} \text{ s} \quad (3.1)$$

The delayed neutron generation time ( $l_d$ ) includes the time for its creation (12.58 seconds) and its lifetime ( $10^{-4}$  seconds). Thus, the delayed neutron generation time is:

$$l_d = 12.58 \text{ s} + 10^{-4} \text{ s} \approx 12.58 \text{ s} \quad (3.2)$$

As can be observed, the prompt neutron generation time is very short, which would make the reactor hard to control. For that reason, reactors typically operate in a way that delayed neutrons are essential to maintain the fission chain reaction.

### 3.1.2 Criticality

One way to quantify the changing number of neutrons is to compare the neutrons produced in one generation with the neutrons produced in the previous generation considering the different ways neutrons can be produced or lost. The factor that is used in this comparison is the effective multiplication factor ( $k_{eff}$ ) which is defined by [17]:

$$k_{eff} = \frac{\text{number of neutrons in a generation}}{\text{number of neutrons in the previous generation}} \quad (3.3)$$

$$k_{eff} = \epsilon L_f p L_{th} f \eta \quad (3.4)$$

The fast fission factor ( $\epsilon$ ) is given by the ratio between the number of fast neutrons produced by all fissions and the number of fast neutrons produced by thermal fissions. The fast non-leakage probability ( $L_f$ ) is the probability that a fast neutron does not escape from the reactor. The resonance escape probability ( $p$ ) is the probability that neutrons are not absorbed in the resonance during the thermalization. The thermal non-leakage probability ( $L_{th}$ ) is the probability that a thermal neutron does not escape the reactor. The thermal utilization factor ( $f$ ) is the ratio of neutrons absorbed in the fuel to the neutrons absorbed in all material in the core, including the fuel. The thermal fission factor ( $\eta$ ) is the average number of fast neutrons produced for each thermal neutron absorbed in the fuel. These neutrons are then present in the next generation.

The formula presented in Equation 3.4 is known as the six factors formula, which results in the effective multiplication factor ( $k_{eff}$ ). When this factor is equal to 1, the number of neutrons in each generation is constant, and the reactor is critical. When  $k_{eff}$  is above 1, more neutrons are produced in each generation, and the reactor is supercritical. When  $k_{eff}$  is below 1, fewer neutrons are produced in each generation, and the reactor is subcritical. Among the six factors, fast non-leakage factor, resonance escape probability, thermal non-leakage factor, and thermal utilization factor reduce the number of neutrons in the generation, while the fast and thermal fission factors increase the number of neutrons. To control the reactor, the operator needs to control the number of neutrons in the core, which can be done by varying the factors in the six factors formula.

### 3.1.3 Reactivity

The reactivity gives a measure of the departure of the reactor from the criticality. The reactivity ( $\rho$ ) is defined by [17]:

$$\rho = \frac{k_{eff} - 1}{k_{eff}} \quad (3.5)$$

The reactivity is a dimensionless number. However, artificial units are used to make this value easier to express. By definition, the value of the reactivity that results from the Equa-

tion 3.5 is in units of  $\Delta k/k$ . Other units are the  $\% \Delta k/k$  and pcm (per cent mille). The relation among these units is given by [17]:

$$1 \frac{\Delta k}{k} = 100 \% \frac{\Delta k}{k} = 10^5 \text{ pcm} \quad (3.6)$$

The effective multiplication factor can be obtained by rearranging the Equation 3.5:

$$k_{eff} = \frac{1}{1 - \rho} \quad (3.7)$$

The reactivity also describes the states of the reactor. When the reactivity is zero, the reactor is critical. When the reactivity is negative, the reactor is subcritical. When the reactivity is positive, the reactor is supercritical.

The reactivity is also used to describe operator actions or component effects. The operator can insert “negative reactivity” to lower the overall core reactivity, which can be done by inserting the control rods in the core or by boration. On the other hand, the operator can insert “positive reactivity” to increase overall core reactivity, which can be done by withdrawing the control rods from the core or by boron dilution. The same idea can be used with the reactor fuel, which may have a “reactivity worth,” contributing to the overall core reactivity.

Observing the Equation 3.7, when negative reactivity is inserted, the denominator increases, reducing the effective multiplication factor. Conversely, when positive reactivity is inserted, the denominator in Equation 3.7 decreases, and the effective multiplication factor increases. During the reactor operation, fuel consumption inserts negative reactivity in the core, reducing overall core reactivity in case the operator does not take any action. On the other hand, refueling increases the overall core reactivity. These effects are described in more detail in the following sections.

### 3.1.4 Installed neutron sources

Artificial neutron sources are installed in reactors to ensure that the neutron population remains high enough to allow visible indication of neutron level on the monitoring instruments while the reactor is shut down or during the startup process. The use of neutron sources gives an accurate picture of the reactor conditions and any changes in them. The neutron source is placed near the reactor core with the only purpose of producing neutrons. These sources are generally neutron emitters like californium-252 or a mixture of an alpha-emitter and a material that undergoes alpha-neutron reactions like americium-beryllium [18]. The neutrons produced in the neutron source are called source neutrons.

### 3.1.5 Subcritical multiplication

Subcritical multiplication is the phenomenon that accounts for the changes in neutron flux due to reactivity changes when the reactor is subcritical. This phenomenon takes place during the reactor startup. During the startup, reactivity insertions are performed to bring the reactor to the supercritical state and to increase the neutron flux in the core. In the early stages, even though the reactor is still subcritical, the neutron flux increases. This increase in the neutron flux is the subcritical multiplication, and it occurs because, in addition to fission neutrons, source neutrons are added. The subcritical multiplication only takes place when the source neutrons are enough to compensate for the neutron loss. The relationship is given by [17]:

$$S_0 = N(1 - k_{eff}) \quad (3.8)$$

where  $S_0$  is the number of source neutrons (source strength), and  $N$  is the total number of neutrons, including fission and source neutrons. The term  $1 - k_{eff}$  represents the relative loss of neutrons in each generation. Equation 3.8 can be rearranged as:

$$N = \frac{S_0}{1 - k_{eff}} \quad (3.9)$$

The Equation 3.9 is the value at which the neutron counts stabilize due to the subcritical multiplication. This equation shows that the neutrons count rises as the effective multiplication factor approaches unity, despite the reactor being subcritical. As the source neutron level is constant ( $S_0$  is constant), the Equation 3.8 can be set equal to itself for different neutron counts and multiplication factors, resulting in:

$$N_1(1 - k_{eff,1}) = N_2(1 - k_{eff,2}) \quad (3.10)$$

The Equation 3.10 gives the changes in effective multiplication factor based on changes in the neutron counts. During shutdown operations, this equation can be used to predict the effect that a reactivity addition has on the neutron level.

### 3.1.6 Neutron flux and power

The reactor power measures the rate at which the reactor produces energy. It can be thermal power (heat production rate) or electrical power (electrical power generated from the thermal energy). Thermal energy is produced by the mechanisms resulting from nuclear fission, such as the decay of fission products or the loss of kinetic energy by fission neutrons and fission products.

The neutron flux is the rate at which neutrons pass through a unit area. It can describe the neutron population and, consequently, the rate of fission and other reactions. The reaction rate per volume for each type of neutron interaction can be calculated from the neutron flux and neutron cross-section by [17]:

$$R = N\sigma\phi = \Sigma\phi \quad (3.11)$$

where  $R$  is reaction rate per volume,  $N$  is the number density of target nuclei,  $\sigma$  is the microscopic cross-section of the reaction,  $\phi$  is the neutron flux, and  $\Sigma$  is the macroscopic cross-section of the reaction. Knowing the energy released by fission, it is possible to use the Equation 3.11 to relate the neutron flux in the reactor and the reactor power.

As discussed, the reactor power is closely related to the fission rate and the neutron flux. It means that the reactor power is related to the number of neutrons in the reactor core and consequently is affected by the reactivity. When the reactor is critical, its power is stable, while the power increases or decreases if the reactor is supercritical or subcritical, respectively. The effective multiplication factor compares the number of neutrons produced in one generation to the number of neutrons produced in the previous generation. In that sense, the number of neutrons produced in the  $n$ -th generation, from a initial number of neutrons  $N_0$ , is given by [17]:

$$N_n = N_0 k_{eff}^n \quad (3.12)$$

As the reactor power is, within a reasonable approximation, related to the neutron population, the power after  $n$  generations can be described as:

$$P = P_0 k_{eff}^n \quad (3.13)$$

where  $P_0$  is the initial power before an increase or decrease to the power  $P$  after  $n$  generations. A similar equation can be found where the power is dependent on the time instead of the generation number and effective multiplication factor.

### 3.1.7 Reactor period

In order to find the time-dependent equation of the reactor power for given conditions, the generation number ( $n$ ) can be found by the number of mean neutron generation times,  $\bar{l}$ , that have passed at some time,  $t$  [17]:

$$n = \frac{t}{\bar{l}} \quad (3.14)$$

From Equation 3.14, the effective multiplication factor can be set to a time-dependent exponential introducing a new term  $\tau$ , the reactor period [17]:

$$e^{\frac{t}{\tau}} = k_{eff}^{\frac{t}{\bar{l}}} \quad (3.15)$$

$$\frac{t}{\tau} = \frac{t}{\bar{l}} \ln(k_{eff}) \quad (3.16)$$

$$\ln(k_{eff}) = \frac{\bar{l}}{\tau} \quad (3.17)$$

For reactors,  $k_{eff}$  is generally close to the unity, then the natural logarithmic term in Equation 3.17 can be approximated by [17]:

$$\ln(k_{eff}) \approx \frac{k_{eff} - 1}{k_{eff}} = \rho \quad (3.18)$$

Using Equation 3.18 in Equation 3.17, the reactor period is given by:

$$\tau = \frac{\bar{l}}{\rho} \quad (3.19)$$

Replacing the term  $k_{eff}^n$  in Equation 3.13 by the Equation 3.15, the reactor power can be expressed as a function of time:

$$P = P_0 e^{\frac{t}{\tau}} \quad (3.20)$$

From the Equation 3.20, it is observed that the reactor period is the amount of time it would take for the reactor power to increase by a factor of e.

The reactor period depends on the mean neutron generation time and the reactivity. In order to find the mean generation time, the effect of prompt and delayed neutrons must be considered. The effective delayed neutron fraction ( $\bar{\beta}_{eff}$ ) is used in this consideration. Generally, delayed neutrons are produced at lower energy than prompt neutrons. For that reason, delayed neutrons need less thermalization before thermal fission, and they are less likely to be

absorbed or lost. However, they are less likely to induce fast fission. The effective delayed neutron fraction considers the relative number of delayed neutrons to total neutrons which produce fission. It does not account for those lost during thermalization or leaked from the reactor core. Additionally, the neutron release time for delayed neutrons results in a delayed increase in neutron population and power. This effect can be considered using  $\bar{\beta}_{eff}$  as delayed neutron fraction and  $1 - \bar{\beta}_{eff}$  as the prompt neutron fraction.

### 3.1.7.1 Prompt critical reactor period

Prompt criticality occurs when the reactor is critical by prompt neutrons alone. In this state, the following is true [17]:

$$(1 - \bar{\beta}_{eff})k_{eff} = 1 \quad (3.21)$$

Substituting Equation 3.7 in Equation 3.21 and rearranging results in:

$$\rho = \bar{\beta}_{eff} \quad (3.22)$$

From Equation 3.22, one may conclude that the prompt criticality occurs when the reactor is supercritical by a positive reactivity insertion equal to or greater than the effective delayed neutron fraction.

In a prompt critical reactor, where there is no dependence on delayed neutrons, the mean neutron generation time is the prompt neutron generation time ( $l^*$ ). From Equation 3.19, the reactor period becomes:

$$\tau = \frac{l^*}{\rho} \quad (3.23)$$

As the prompt neutron generation time is on the order of  $10^{-4}$  seconds, even small reactivity changes could result in a short reactor period and consequently a rapid rise in power. This situation is unstable and difficult to control.

### 3.1.7.2 Delayed critical reactor period

Power reactors typically maintain the criticality and combine the delayed and prompt neutrons during the operation, the delayed critical condition. In this situation, the mean neutron generation ( $\bar{l}$ ) can be calculated using the prompt neutron generation time ( $l^*$ ), the delayed neutron generation time ( $l_d$ ), and the effective delayed neutron fraction ( $\bar{\beta}_{eff}$ ) [17]:

$$\bar{l} = (1 - \bar{\beta}_{eff})l^* + \bar{\beta}_{eff}l_d \quad (3.24)$$

For reactivity changes, the response of prompt neutrons occurs faster than the delayed neutrons because delayed neutrons have a longer generation time. This effect can be considered by adding the reactivity to the prompt neutron fraction and subtracting reactivity from the delayed neutron fraction in Equation 3.24 [17]:

$$\bar{l} = (1 - \bar{\beta}_{eff} + \rho)l^* + (\bar{\beta}_{eff} - \rho)l_d \quad (3.25)$$

In the case of a reactor operating in the delayed critical condition, thus [17]:

$$(1 - \bar{\beta}_{eff} + \rho) \approx 1 \quad (3.26)$$

$$\bar{l} \approx l^* + (\bar{\beta}_{eff} - \rho)l_d \quad (3.27)$$

Using Equation 3.27 and replacing the delayed neutron generation time by the inverse of  $\lambda_{eff}$  (the effective neutron precursor decay constant) in Equation 3.19, it is possible to determine the reactor period for a delayed critical reactor [17]:

$$\tau = \frac{l^*}{\rho} + \frac{\bar{\beta}_{eff} - \rho}{\rho\lambda_{eff}} \quad (3.28)$$

The effective neutron precursor decay constant ( $\lambda_{eff}$ ) is approximately equal to  $0.1 \text{ s}^{-1}$  (supercritical condition),  $0.08 \text{ s}^{-1}$  (critical condition), and  $0.05 \text{ s}^{-1}$  (subcritical condition) [17].

Equation 3.28 is just an approximation to calculate reactor periods dependent on reactivity. A more rigorous relation, where the reactivity addition rate ( $\dot{\rho}$ ) is considered, can be used to determine reactor transient periods [17]:

$$\tau = \frac{l^*}{\rho} + \frac{\bar{\beta}_{eff} - \rho}{\rho\lambda_{eff} + \dot{\rho}} \quad (3.29)$$

Equation 3.29 can be used to predict the reactor period during the time period reactivity is being inserted, during control rods withdrawn or boron dilution, for example.

### 3.1.7.3 Prompt neutron response

Equation 3.28 gives a useful method for relating reactivity in the core of a nuclear reactor and the reactor period. The first term is the prompt term; it is a function of the prompt neutron generation time and reactivity. This term is generally much smaller than the second term and would have only a minor contribution to the reactor period. The second term is the delayed term; it is a function of the existing delayed neutron parameters in the core and reactivity. The second term has a delayed response because the delayed neutrons are not generated immediately. Following a reactivity change, the first term dominates in the early stages. Thus, it is observed a short period and rapid power response. These rapid responses are called prompt jump in positive reactivity insertion and prompt drop in negative reactivity insertion. These effects are presented in Figure 3.1.

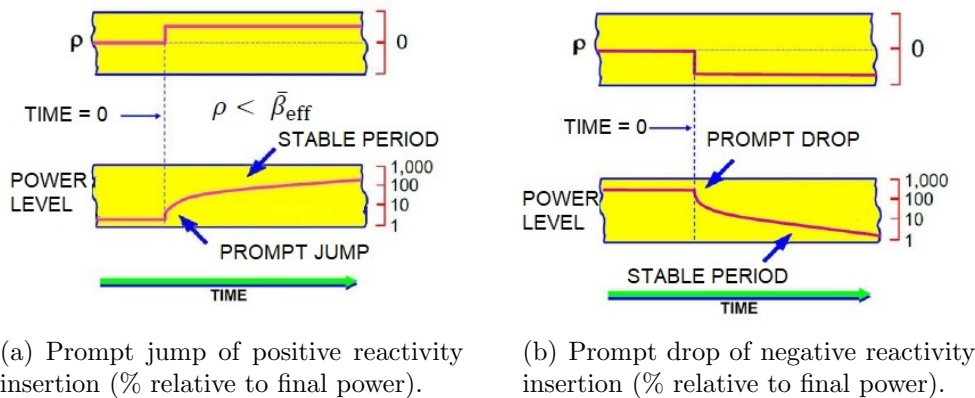


Figure 3.1: Prompt jump and prompt drop [17].

The prompt responses of power can be described as follows [17]:

$$P_f = P_i \frac{\bar{\beta}_{eff}}{\bar{\beta}_{eff} - \rho} \quad (3.30)$$

where  $P_i$  is the reactor power before the prompt response and  $P_f$  is the reactor power after the prompt response.

#### 3.1.7.4 Delayed neutron response

The delayed neutron term contributes to the building up of a stable reactor period following small reactivity changes, as can be observed in Figure 3.1. Additionally, this term has a notable effect following large negative reactivity insertions. It can set a temporary minimum reactor period or maximum power reduction rate by delaying the response to a negative reactivity insertion.

Following the insertion of a large negative reactivity, the prompt neutron level falls very quickly. After few seconds, the delayed neutron level drops because of fission products decaying away. However, some of these delayed neutron precursors have a substantial half-life, which results in more time to decay and continuing neutron production. The reactor period then is dominated by the decay constant of the longest-lived delayed neutron precursors.

Considering that the negative reactivity is sufficient to approximate the removal of the effective delayed neutron fraction, the Equation 3.28 can be reduced as [17]:

$$\tau = \frac{l^*}{\rho} + \frac{\bar{\beta}_{eff} - \rho}{\rho \lambda_{eff}} \approx -\frac{\rho}{\rho \lambda_{longest}} \approx -\frac{1}{\lambda_{longest}} \quad (3.31)$$

where  $\lambda_{longest}$  is the decay constant of the longest-lived neutron precursors. One of these longest-lived neutron precursors is the Br-87 that has a half-life of 55.9 seconds, resulting in a decay constant of approximately  $0.0124 \text{ s}^{-1}$  [17]. Using this value in Equation 3.31, the reactor period results in:

$$\tau = -\frac{1}{\lambda_{longest}} = -\frac{1}{0.0124 \text{ s}^{-1}} \approx -80 \text{ s} \quad (3.32)$$

This negative period is observed after large negative reactivity insertions and limits the power reduction rate, regardless of the amount of negative reactivity inserted. The approach to the -80 s reactor period for negative reactivity insertions can be observed in Figure 3.2(a) [17].

After the longest-lived delayed neutron precursors decay away, the reactor returns to the stable subcritical state. The different reactor period stages following a reactor trip, which consists of a large insertion of negative reactivity, are presented in Figure 3.2(b) [17].

#### 3.1.7.5 Reactor start up rate (SUR)

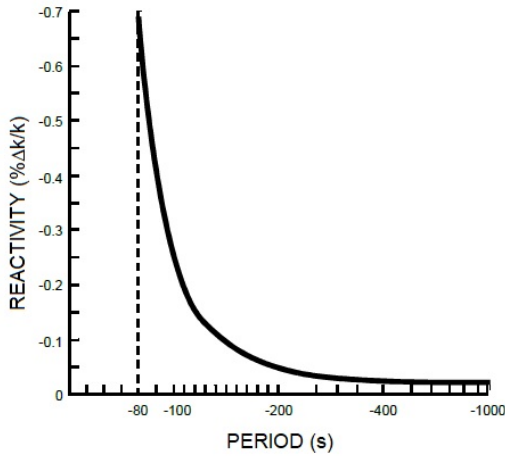
The reactor start-up rate (SUR) is defined as the number of factors of ten that a power changes in one minute. The unity of SUR is decades per minute (DPM). The relation between start-up rate and reactor power is given by:

$$P = P_0 \cdot 10^{t \cdot \text{SUR}} \quad (3.33)$$

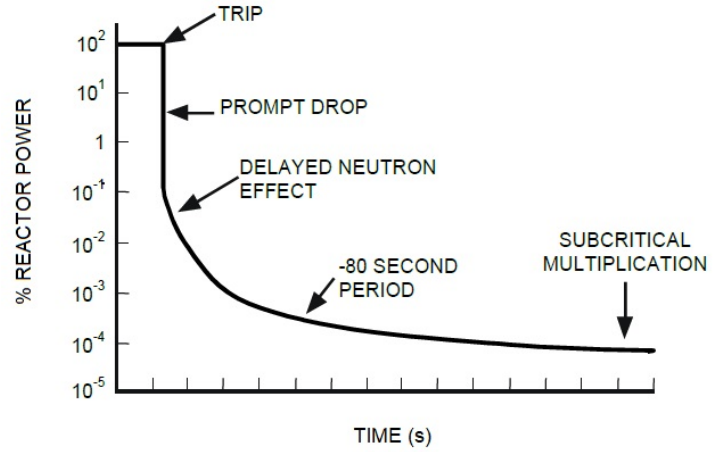
The relationship between SUR (in DPM) and reactor period ( $\tau$  in seconds) is given by:

$$\text{SUR} = \frac{26.06}{\tau} \quad (3.34)$$





(a) Negative 80 s reactor period.



(b) Reactor power changes stages after a trip.

Figure 3.2: Negative reactivity insertion [17].

## 3.2 Control Rod Worth

Control rods are made of neutron-absorbing materials (high neutron absorption cross-section) used to adjust the reactivity of the core by reducing the number of neutrons allowed to produce fission in the fuel. The control rods can be used for coarse control, fine control, or fast shutdowns. Control rods are generally employed to compensate for short-term reactivities effects like fission product poisoning, for example. On the other hand, the boron concentration in the coolant/moderator is used to compensate for long-term reactivity changes such as fuel depletion. The effectiveness of a control rod (ability to add positive or negative reactivity to the core) depends on the neutron flux distribution and core geometry.

### 3.2.1 Differential and integral control rod worth

The effectiveness of a specific control rod to absorb neutrons is referred to as control rod worth (reactivity inserted by the control rod). The neutron flux in a reactor is not uniform, and the control rods are inserted in the core starting from the top in the PWRs. As inserted, the control rods experience different neutron flux depending on the position and impact the neutron flux in a non-uniform way. These effects can be observed in Figure 3.3 [17]. In that sense, the control rod worth depends on the height and position where the control rod is inserted in the core. The control rod worth can be described in two ways: differential control rod worth and integral control rod worth.

The differential control rod worth is the reactivity change per unit movement of a control rod. The differential control rod worth accounts for how the change in reactivity depends on the position. Since the control rods move vertically, the control rod position is referred to as rod height. Differential rod worth (DRW) is given by [17]:

$$\text{DRW} = \frac{\Delta\rho}{\Delta h} \quad (3.35)$$

where  $\Delta\rho$  is reactivity change and  $\Delta h$  is the change in height in units of length. The differential control rod worth units can be pcm/cm,  $\Delta k/k/\text{cm}$  or other measures of reactivity per unit of length. An example of differential control rod worth is presented in Figure 3.4 [17].

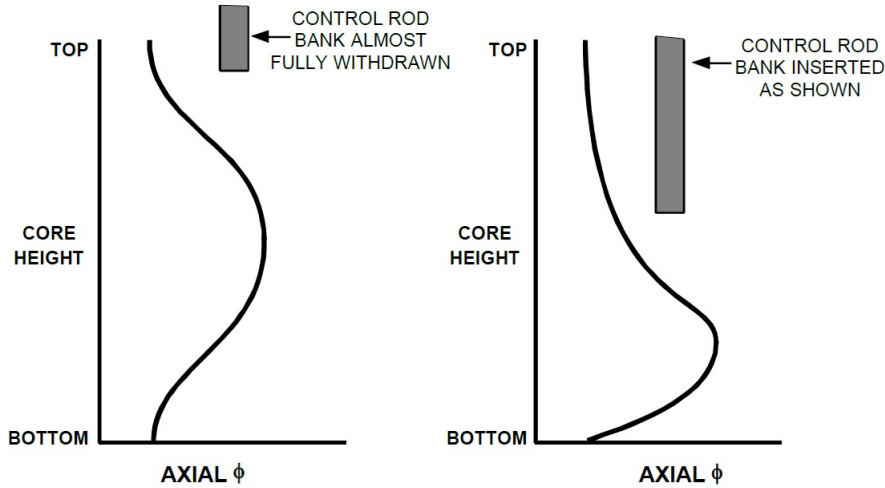


Figure 3.3: Dependency of axial neutron flux with the control rod position [17].

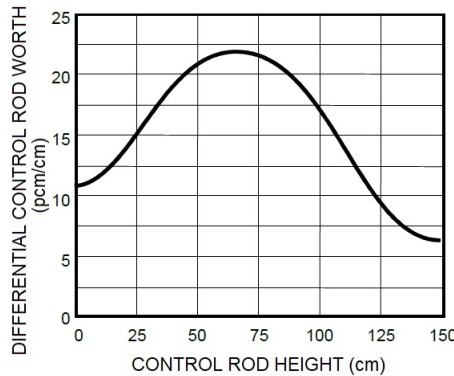


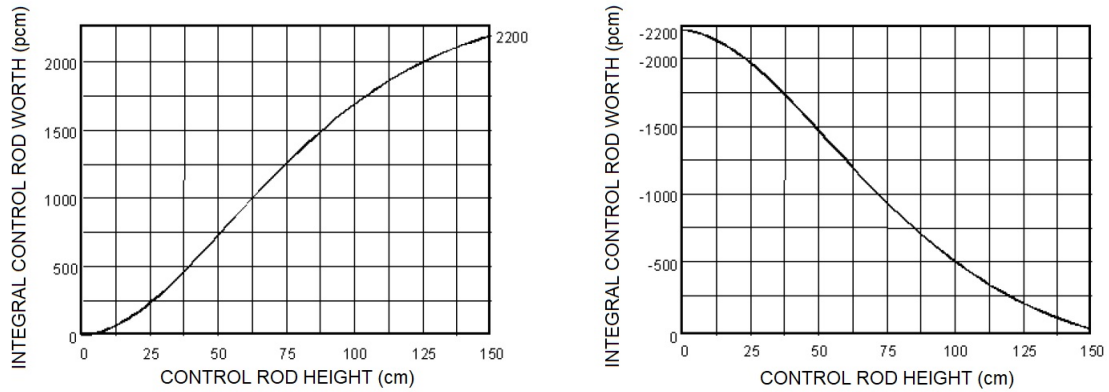
Figure 3.4: Position dependency of the differential control rod worth [17].

The total reactivity inserted to the core by moving a control rod from a reference position to any other rod height is called the integral control rod worth. The integral control rod worth can be obtained by integrating the differential control rod worth over some distance of control rod insertion. An example of integral control rod worth is presented in Figure 3.5 [17].

### 3.2.2 Control rod shadowing

The control rod shadowing occurs when the presence of one control rod influences the control rod worth of the other control rod. When a control rod is inserted into the reactor core, the neutron flux in the vicinity is depressed. To keep consistent reactor power, despite the control rod insertion, the neutron flux needs to be compensated elsewhere in the core; this results in a rise in the flux away from the control rod. Therefore, in addition to reducing the neutron flux in an area around the control rod, neutron flux rises a distance from it. This effect can be observed in Figure 3.6(a) [17]. In that sense, there are three regions of neutron flux response: the area near the control rod with decreased flux (point A in Figure 3.6 [17]), an area far from the control rod where neutron flux is increased (point B in Figure 3.6 [17]), and a single point between the two areas in which the neutron flux is not affected (point C in Figure 3.6 [17]).

These changes in the neutron flux in the core make a second control rod be submitted to a different neutron flux than it would without the presence of the first, resulting in it having a



(a) Positive reactivity inserted in the core as rod is withdrawn. (b) Negative reactivity removed from the core as rod is withdrawn.

Figure 3.5: Integral rod worth curves referenced to bottom and top of core [17].

different effect on overall reactivity and therefore having a different worth. If the second control rod is inserted in the region near the first control rod, the worth of the second control rod is reduced from the worth it would be if the first were not there (Figure 3.6(b) [17]). When the rod is inserted in the region far from the first, the rod worth is increased (Figure 3.6(c) [17]). The worth remains the same if the control rod is placed at the exact point where the neutron flux is not affected by the first control rod (Figure 3.6(d) [17]).

### 3.3 Reactivity Coefficients

Changes in physical properties of the materials in the reactor result in changes in reactivity. The reactivity depends strongly on the thermodynamic state of the reactor system. Reactivity coefficients are useful to describe parameters that affect reactivity. Such parameters include moderator temperature and density coefficient, void coefficient, and fuel temperature coefficient. These parameters can be quantified in terms of reactivity coefficient ( $\alpha_x$ ), which describes the reactivity changes per unity in the parameter [17]:

$$\alpha_x = \frac{\Delta\rho}{\Delta x} \quad (3.36)$$

Equation 3.36 states that for an adjustment in some parameter  $x$ , a corresponding change in reactivity is observed. The value of this reactivity is equal to the reactivity coefficient multiplied by the change in  $x$ . From the operational perspective, the operator needs to know how the change in any plant parameter affects the reactor power. This knowledge allows the operator to predict the reactor response during transients that involve changes in plant operating parameters.

#### 3.3.1 Moderator temperature and moderator density coefficients

In the discussion of moderators, the moderator-to-fuel ratio ( $N^m/N^U$ ) is very important. This ratio compares the amount of moderator in the core with the amount of fuel. Increasing the amount of moderator in the core increases the moderator-to-fuel ratio while reducing the amount of moderator reduces the moderator-to-fuel ratio.

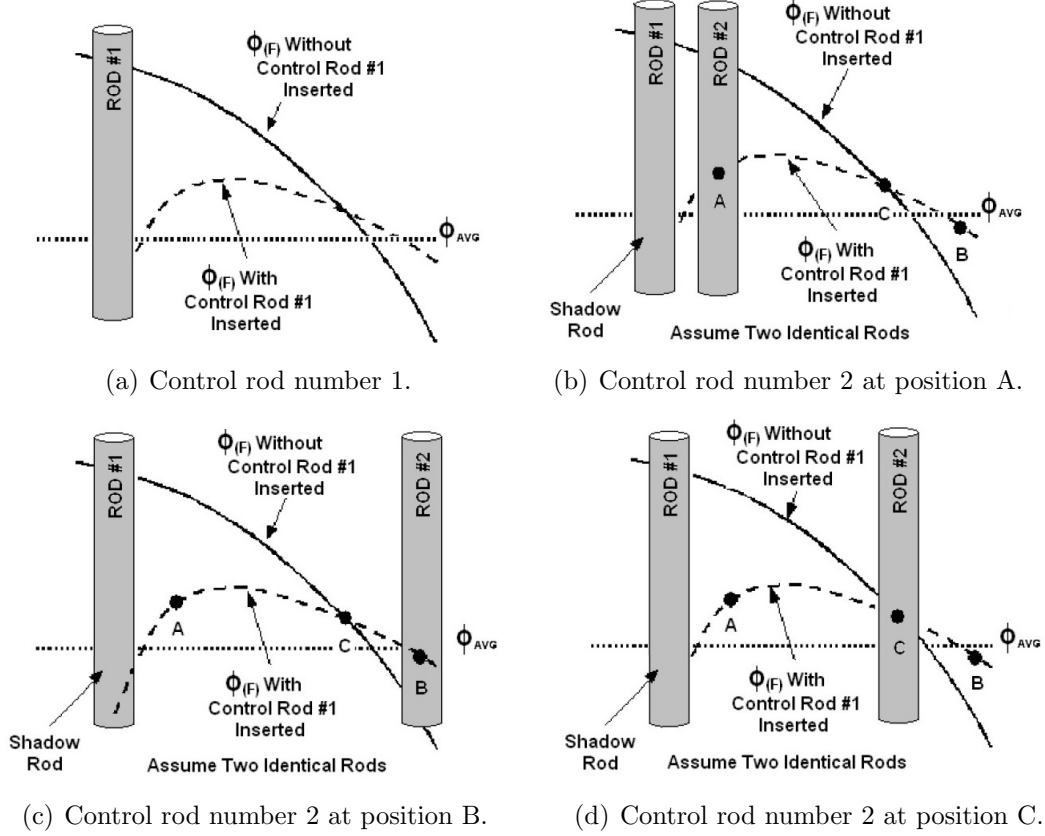


Figure 3.6: Effects of rod shadowing [17].

The moderator temperature affects the reactivity due to the thermal expansion of the moderator, which reduces the moderator density. Depending on the moderator-to-fuel ratio, the effect on reactivity can be either positive or negative. The moderator temperature reactivity coefficient (MTC) is represented by [17]:

$$\alpha_{T, \text{moderator}} = \frac{\Delta\rho}{\Delta T_{\text{moderator}}} \quad (3.37)$$

where  $\alpha_{T, \text{moderator}}$  is the moderator temperature reactivity coefficient, and  $\Delta T_{\text{moderator}}$  is the change in temperature of the moderator. The units of this reactivity coefficient are then a measure of reactivity per degree of moderator temperature.

When the moderator temperature increases, the moderator expands, and consequently, its density decreases. This decrease in density is important because moderation becomes less effective (less thermalization). The change in density due to a temperature change is not uniform. As the temperature increases, the magnitude of the density change for a given temperature change gets larger. This effect can be observed in Figure 3.7 [17].

Increasing the moderator density, more atoms of the moderator are present between the fuel rods. This increase results in more neutron moderation in the region between fuel elements, increasing the chances of neutrons being thermalized without experiencing resonance absorption (mostly occurs in fuel materials). This effect increases the resonance escape probability for increased moderator density.

On the other hand, the decrease in moderator density due to an increase in moderator temperature results in less moderation in the core. In that sense, the path traveled by the neutrons in the core is extended, which increases the likelihood neutrons interact with non-fuel

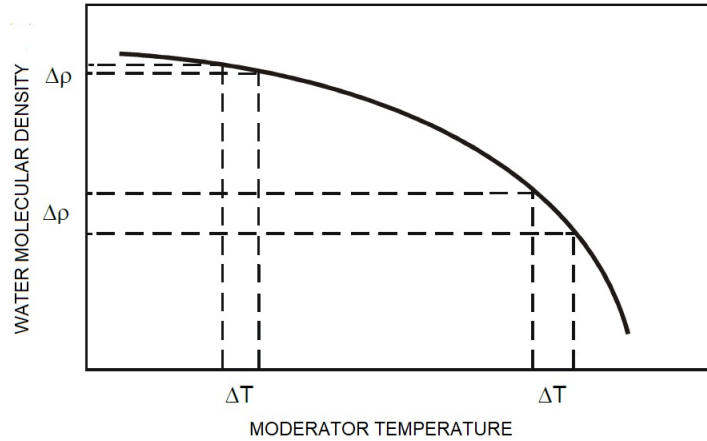


Figure 3.7: Relative moderator density changes for equal temperature changes [17].

materials such as control rods. This effect increases the control rod worth, which contributes to an overall decrease in the thermal utilization.

As described, varying the moderator density due to moderator temperature changes affects the thermal utilization factor and the resonance escape probability. In that sense, it is useful to describe moderator density in terms of under-moderated and over-moderator states based on the moderator-to-fuel ratio. These states describe whether a moderator density change causes a net positive or net negative reactivity when considering the effects in the resonance escape probability and the thermal utilization factor. In an under-moderated state, the density decrease results in a net decrease in reactivity (negative MTC), where a density decrease in an over-moderated state results in a net increase in reactivity (positive MTC). These effects are shown in Figure 3.8 [18]. For safety reasons, reactors are designed to have a MTC negative; this means that a power excursion increases the moderator temperature, which adds a negative reactivity to the core that counterbalances the power excursion. Thus, reactors are projected to operate in an under-moderated state.

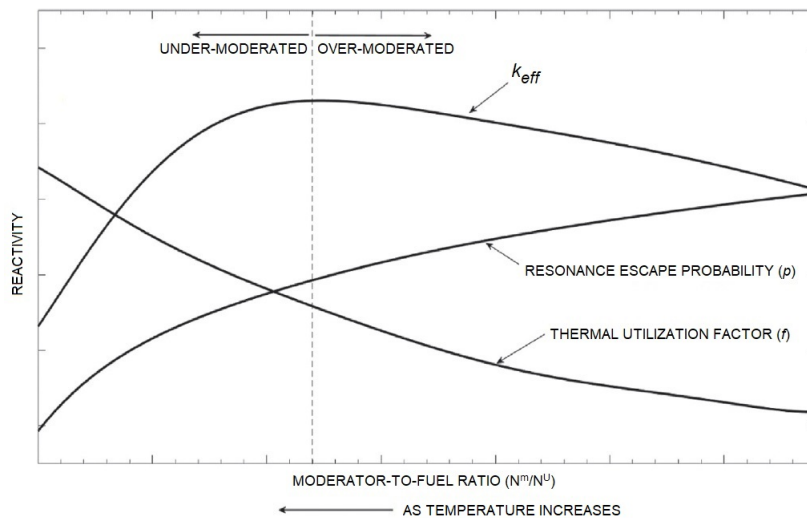


Figure 3.8: Effect of moderator-to-fuel ratio on reactivity in under-moderated and over-moderated reactors [18].

The moderator parameters enable another mode of operation, which depends on the heat removal from fuel. Reducing the moderator flow rate by changing the speed of the reactor

coolant pump, the water stays in the core for a longer period of time. The moderator is then heated to a higher level in the core, which results in a decrease in moderator density. In an under-moderated state, this decrease in moderation adds negative reactivity to the core resulting in power reduction.

### 3.3.1.1 Change in MTC with boron concentration

The presence of boron in the coolant changes the value of the moderator temperature coefficient. The magnitude of the impact on this coefficient depends on the boron concentration in the coolant. This impact can be explained as follows. When the temperature of the moderator increases, three effects take place. The first effect is the decrease in boron concentration (decreasing density), resulting in a positive reactivity insertion. Secondly, the thermal utilization factor increases slightly, resulting in a positive reactivity insertion because there are fewer water molecules and boron per cubic centimeter available for absorption reaction within the core. The last effect is the reduction of the resonance escape probability due to fewer moderator molecules per cubic centimeter, which results in an insertion of negative reactivity. These effects are competing effects that take place after each increase in the moderator temperature. For high boron concentrations, the MTC tends to be less negative. As boron concentration approaches zero, the coefficient tends to be more negative. Thus, at the beginning of core life (BOL), the MTC is less negative (more boron in the moderator), while at the end of core life (EOL), the coefficient is more negative (less boron in the moderator).

### 3.3.1.2 Change in MTC with core age

As discussed previously, the boron concentration is reduced during the core life, which results in a more negative MTC as the nuclear reactor core ages.

## 3.3.2 The void coefficient of reactivity

The void coefficient of reactivity is more important in systems with boiling conditions like BWRs; thus, this effect has less importance in PWRs. The void coefficient of reactivity is caused by the formation of steam voids in the moderator. The void coefficient of reactivity ( $\alpha_{\text{void}}$ ) is defined as the change in reactivity ( $\Delta\rho$ ) per percent change in the void volume ( $\Delta\text{void}$ ). As steam voids start to form, voids displace the moderator from the coolant channels within the core, which reduces the moderator effectiveness and increases the neutron path length, resulting in a negative reactivity insertion. The void coefficient of reactivity can be calculated by (in the unity of reactivity per %void) [17]:

$$\alpha_{\text{void}} = \frac{\Delta\rho}{\Delta\text{void}} \quad (3.38)$$

## 3.3.3 Fuel temperature coefficient of reactivity

The fuel temperature coefficient of reactivity (FTC) has a greater effect on reactivity in the core than the moderator temperature coefficient for some reactors. This coefficient is called prompt temperature coefficient because an increase in reactor power causes an immediate change in the fuel temperature. The FTC ( $\alpha_{T,\text{fuel}}$ ) is defined as the change in reactivity ( $\Delta\rho$ ) per degree change in fuel temperature ( $\Delta T_{\text{fuel}}$ ). The FTC is given by (in units of measure of reactivity per degree of moderator temperature) [17]:

$$\alpha_{T,\text{fuel}} = \frac{\Delta\rho}{\Delta T_{\text{fuel}}} \quad (3.39)$$

The FTC is also known as the fuel Doppler reactivity coefficient. This name is used because the FTC results from the Doppler effect, also called Doppler broadening. The Doppler broadening describes an increase in the chance for neutrons to be resonantly absorbed due to the higher temperature of the material in the core. This effect is related to nuclei vibration as temperature increases, which causes an apparent broadening of the resonance peaks for absorption. By vibrating, depending on the direction of movement at a particular time, the relative energy of an incident neutron may appear different. Thus, a single neutron appears to be a few energies at once. In that sense, these neutrons are more readily absorbed in the resonance region during the thermalization process since they may appear to have an energy corresponding to a resonance peak for absorption of nuclei in the core. This phenomenon is illustrated in Figure 3.9 [17].

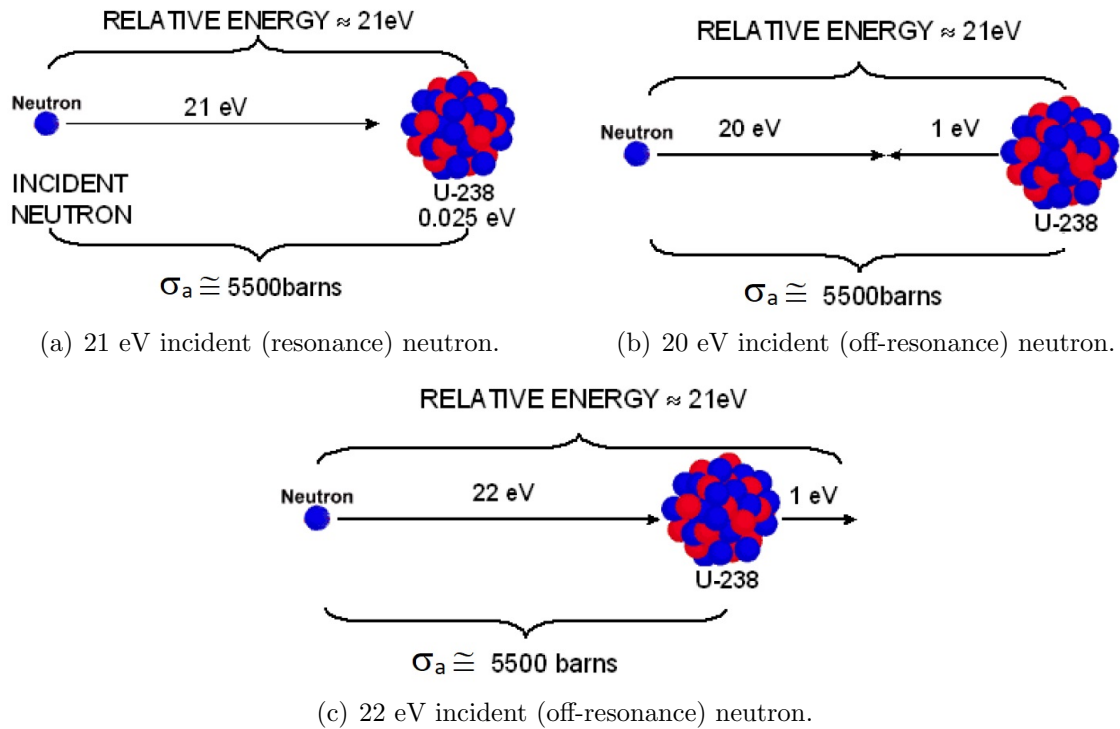


Figure 3.9: Doppler effect in uranium-238 capture reaction [17].

The Doppler phenomenon can be described as a broadening of the resonance peaks once the capture cross-section is spread from their typical values. The result is a relative lower cross-section where the resonance peak is located and an increased cross-section at nearby energies. Therefore, it is possible that neutrons with energies outside a resonance peak can be absorbed. In U-235 fueled reactors with low enrichment, the U-238 is responsible for a large amount of resonance absorption occurring in the fuel. In thermal reactors, the Doppler effect has a negative effect on reactivity due to the fuel composition. The broadening of a resonance peak is presented in Figure 3.10 [17].

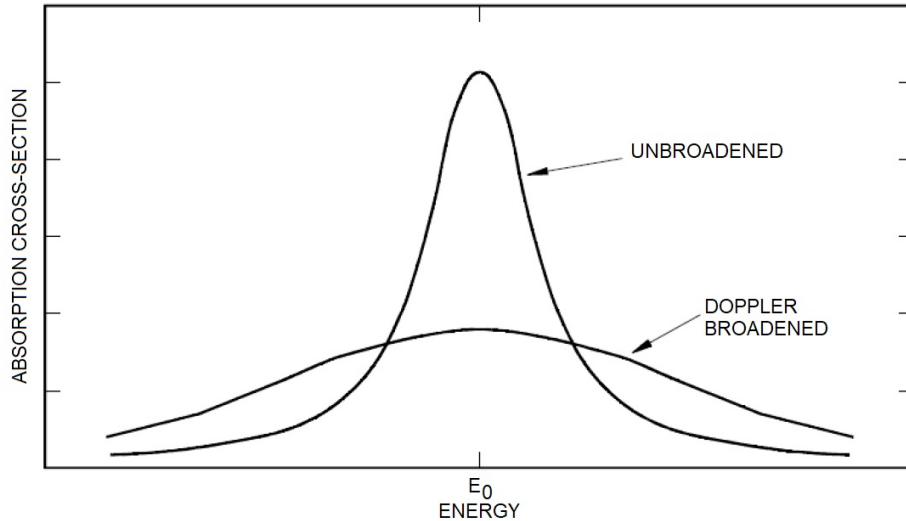


Figure 3.10: Doppler broadening of resonance peak in microscopic cross-section for absorption [17].

### 3.3.3.1 Changes in FTC with changes in fuel temperature

As it was discussed, when the fuel temperature increases in a nuclear reactor, the resonance peaks for capture broaden, which allows the fuel to capture neutrons in resonance over a large range of energy levels. This effect results in an insertion of a negative reactivity when the temperature of the fuel is increased.

At low fuel temperature, the resonance absorption peaks are very narrow, and only a small fraction of neutrons passing through the resonance energy spectrum are absorbed. A slight increase in the fuel temperature causes a significant fractional increase in the number of neutrons resonantly absorbed. However, at high fuel temperature, the resonance absorption peaks are already broad, then a small increase in the fuel temperature results in a small fractional increase in the number of neutrons resonantly absorbed.

For the same temperature increase, the broadening of the resonant peaks is more significant at low fuel temperatures than at high fuel temperatures. Thus, the magnitude of the FTC is higher at low fuel temperature than at high fuel temperature.

### 3.3.3.2 Changes in FTC with changes in moderator density

The moderator density also affects the FTC. When the moderator density is high, the slowing down time and slowing down length of the neutrons are very short. Thus, changes in resonant absorption peaks cause a relatively smaller effect on the FTC than at low moderator density. When the moderator density is low, slowing down time and slowing down length of the neutrons are longer. Therefore, any change in resonance absorption peaks is more significant at low moderator density than at high moderator density since the neutrons spend relatively more prolonged time in the resonance energy region. Thus, the FTC is more negative at lower moderator density.

### 3.3.3.3 Changes in FTC with changes in core age

At BOL, the fuel consists mainly of uranium-238 and uranium-235. These fuels cause a reasonable amount of resonance absorption. At EOL, approximately the same amount of



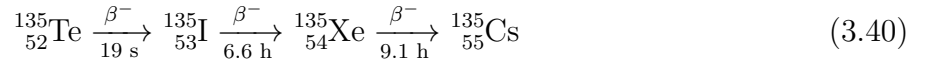
uranium-238 is still present. However, the amount of uranium-235 is reduced considerably, and plutonium-239 and plutonium-240 are produced. The broadening effect is stronger in plutonium-240 than in uranium-238 [18]. Therefore, as plutonium-240 builds up in the reactor, the FTC becomes more negative. Additionally, at EOL, fission products are present in the core that were not present at the BOL, which resonantly capture a considered number of neutrons. These two effects cause the FTC to be more negative at EOL than at the BOL.

## 3.4 Neutron Poisons

During the reactor operation, fission products are generated from the fission in the fuel. Together with the delayed neutron precursors, these fission products influence the core reactivity by interacting with neutrons. The fission products with significantly high neutron absorption cross-sections, which have a more significant effect on the core reactivity, are known as neutron poisons. Among the several fission products with considerable high absorption cross-sections, xenon-135 and the samarium-149 are the most significant to the reactor operation. The reactivity contribution of these poisons is closely related to their concentration in the reactor. Additionally, control poisons can also be intentionally introduced to affect reactivity for extended periods of time.

### 3.4.1 Xenon concentration

Xenon-135 is produced in a reactor in two ways. The first way is through direct production from fission, and the second way is by the radioactive decay of other fission products. The decay chain which results in xenon-135 production is [17]:



Observing Equation 3.40, the half-life of tellurium-135 is so short that the production of xenon-135 can be described as the decay of iodine-135. Thus, the total production rate of xenon-135, including both directly from fission and from the decay of iodine-135, is given by [17]:

$$\left( \frac{dN_{\text{Xe-135}}}{dt} \right)^+ = \gamma_{\text{Xe-135}} \phi \Sigma_f^{\text{fuel}} + \lambda_{\text{I-135}} N_{\text{I-135}} \quad (3.41)$$

where the left side of the Equation 3.41 is the rate of xenon-135 production,  $\gamma_{\text{Xe-135}}$  is the fission product yield of xenon-135 directly from fission of fuel materials,  $\phi$  is the neutron flux,  $\Sigma_f^{\text{fuel}}$  is the macroscopic cross-section for fission in the fuel materials,  $\lambda_{\text{I-135}}$  is the decay constant of iodine-135 and  $N_{\text{I-135}}$  is the number density of iodine-135 nuclei. During stable reactor power, the production from fuel fission accounts for only 5% of xenon-135 production, while iodine-135 radioactive decay produces 95%.

Xenon-135 is a strong neutron poison that is depleted when it absorbs a neutron. Additionally, it is a radioactive nuclide itself and undergoes radioactive decay, as shown in Equation 3.40. The removal of xenon-135 from the reactor is given by [17]:

$$\left( \frac{dN_{\text{Xe-135}}}{dt} \right)^- = \phi \sigma_a^{\text{Xe-135}} N_{\text{Xe-135}} + \lambda_{\text{Xe-135}} N_{\text{Xe-135}} \quad (3.42)$$

where the left side of the Equation 3.42 is the rate of xenon-135 removal,  $\sigma_a^{\text{Xe-135}}$  is the microscopic cross-section for absorption of xenon-135,  $N_{\text{Xe-135}}$  is the number density of xenon-135 nuclei, and  $\lambda_{\text{Xe-135}}$  is the decay constant of xenon-135. The xenon-135 absorption cross-section is approximately  $2.6 \cdot 10^6$  barns for thermal energy neutrons and it has a half-life of 9.1 hours [17]; at stable reactor power, 80% of the xenon-135 depletion is caused by neutron absorption and 20% is caused by xenon-135 decay.

The amount of iodine-135 in the reactor stabilizes when the production from fission and decay of iodine-135 are equal. Thus:

$$\gamma_{\text{I-135}}\phi\Sigma_f^{\text{fuel}} = \lambda_{\text{I-135}}N_{\text{I-135}} \quad (3.43)$$

where the term  $\gamma_{\text{I-135}}$  is the fission product yield of iodine-135 directly from fission. From Equation 3.43, the stable number density of iodine-135 nuclei is given by:

$$N_{\text{I-135}} = \frac{\gamma_{\text{I-135}}\phi\Sigma_f^{\text{fuel}}}{\lambda_{\text{I-135}}} \quad (3.44)$$

In Equation 3.44, the production yield of iodine-135 includes the production of tellurium-135. When the condition in Equation 3.44 is met, and the neutron flux is stabilized, the amount of xenon-135 in the reactor also begins to stabilize. This effect can be described by setting the production and loss of xenon-135 equal [17]:

$$\gamma_{\text{Xe-135}}\phi\Sigma_f^{\text{fuel}} + \lambda_{\text{I-135}}N_{\text{I-135}} = \phi\sigma_a^{\text{Xe-135}}N_{\text{Xe-135}} + \lambda_{\text{Xe-135}}N_{\text{Xe-135}} \quad (3.45)$$

Substituting Equation 3.44 into Equation 3.45, the number density of xenon-135 atoms at equilibrium at a stable reactor power is given by [17]:

$$N_{\text{Xe-135}} = \frac{\phi\Sigma_f^{\text{fuel}}(\gamma_{\text{Xe-135}} + \gamma_{\text{I-135}})}{\sigma_a^{\text{Xe-135}}\phi + \lambda_{\text{Xe-135}}} \quad (3.46)$$

From Equation 3.46, the xenon-135 reaches an equilibrium value that depends on the neutron flux and consequently the reactor power. However, the xenon-135 concentration (and corresponding reactivity) is not directly related to the reactor power (doubling the power does not double the negative reactivity contribution). This effect is presented in Figure 3.11 [17].

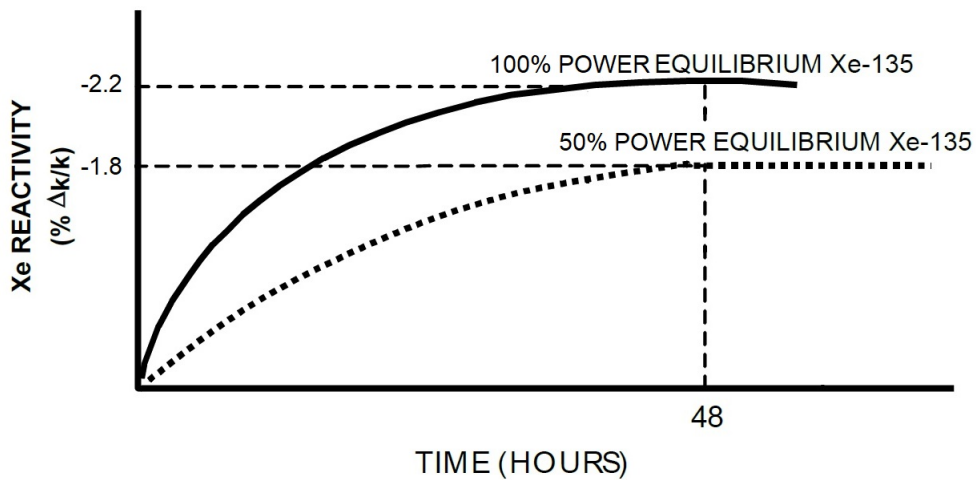


Figure 3.11: Xe-135 reactivity for different power levels [17].

In a power increase, the xenon-135 concentration increases to the equilibrium. However, this

equilibrium is reached after a delay from the power change because iodine-135 must accumulate and decay before the stabilization. During this time, the neutron flux has also increased, resulting in a non-proportional amount of depletion by absorption until reaching the equilibrium value. Similarly, any adjustments to the reactor power immediately change the absorption depletion rate, with the production through decay being delayed.

When the reactor is shut down, the xenon-135 production by fission and depletion by absorption stop immediately; however, there remains an inventory of iodine-135 that continues to decay. Thus, the xenon-135 concentration continues to rise for several hours following the shutdown or any other negative power change. After a significant amount of iodine-135 has depleted, the decay of xenon-135 dominates the balance, and the xenon-135 concentration begins to fall. In Figure 3.12 [17], it is presented the changes happening in xenon-135 reactivity for an initial rise power of 100% power followed by the reactor shutdown.

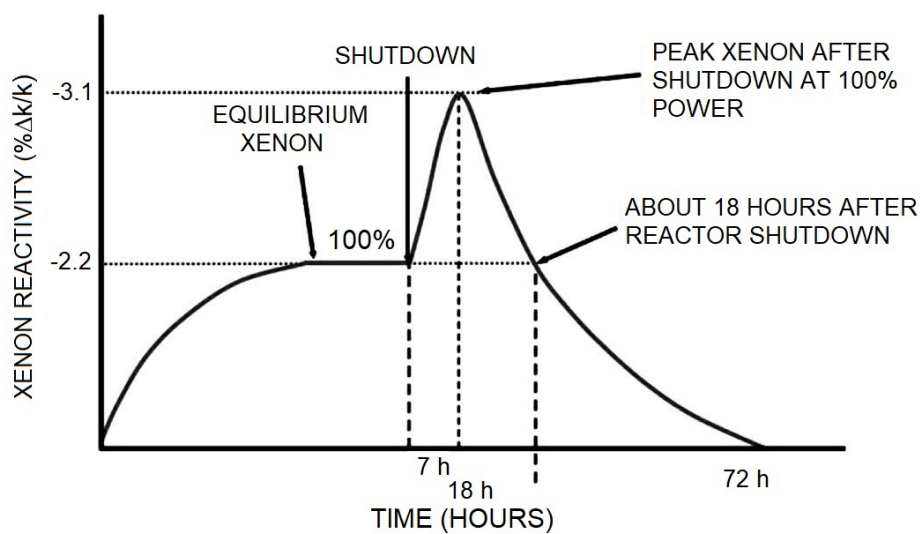


Figure 3.12: Xe-135 reactivity for start up to 100% power followed by shutdown [17].

A positive power change from a stable power level results in the increase of the depletion by absorption, and the concentration of iodine-135 takes time to accumulate and produce xenon-135. This effect results in a temporarily lowered xenon-135 concentration. The Figure 3.13 [17] presents how the xenon concentration changes after a power reduction from 100% power to 50% power and then a return to 100% power. From this graph, it is possible to observe the temporary increase in the xenon concentration after the power reduction before reaching the lower xenon equilibrium concentration for 50% power. After returning the power to 100% power, a temporary power reduction is observed before reaching the higher xenon equilibrium concentration for 100% power.

Fluctuations of xenon-135 concentration in the reactor greatly impact the reactor operation and can cause a phenomenon called xenon precluded startup. This phenomenon happens when the reactor startup is inhibited by xenon-135 remaining in the core after the reactor shutdown. It occurs because, after a shutdown, the xenon-135 concentration remains at a risen level for several hours. If a reactor startup is attempted during this time, the negative reactivity effects caused by the risen of xenon-135 concentration can slow or prevent the reactor startup. This effect is presented in Figure 3.14 [17].

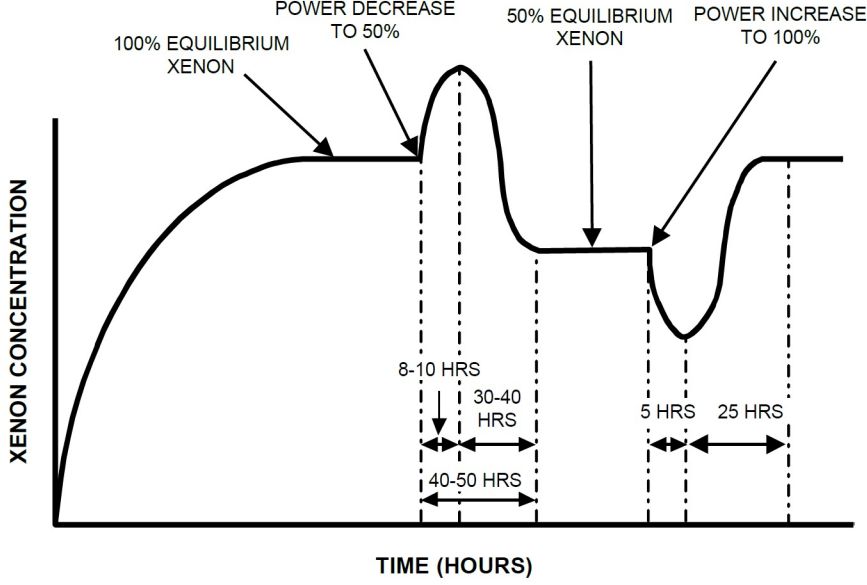


Figure 3.13: Xenon-135 concentration changes during power variations [17].

### 3.4.2 Samarium concentration

The amount of samarium-149 produced directly from fission is negligible. The most significant amount of samarium-149 is produced by radioactive decay of direct fission products. The radioactive decay pathway for samarium-149 production is [17]:



Though, neodymium-149 has a half-life of 1.7 hours; it is short when compared to the promethium-149 half-life. Thus, this decay chain can be collapsed, and the production of samarium-149 can be described by the decay of promethium-149. At stable reactor power, the production and decay of promethium-149 reach a stable value given by [17]:

$$\gamma_{\text{Pm-149}} \phi \Sigma_f^{\text{fuel}} = \lambda_{\text{Pm-149}} N_{\text{Pm-149}} \quad (3.48)$$

$$N_{\text{Pm-149}} = \frac{\gamma_{\text{Pm-149}} \phi \Sigma_f^{\text{fuel}}}{\lambda_{\text{Pm-149}}} \quad (3.49)$$

where  $\gamma_{\text{Pm-149}}$  is the fission product yield of promethium-149 directly from fission of fuel,  $\phi$  is the neutron flux,  $\Sigma_f^{\text{fuel}}$  is the macroscopic cross-section for fission in the fuel,  $\lambda_{\text{Pm-149}}$  is the decay constant of promethium-149 and  $N_{\text{Pm-149}}$  is the number density of promethium-149 nuclei. Compared to xenon-135, samarium-149 has a long half-life of approximately  $2 \cdot 10^{15}$  years [17] and the decay losses are negligible. Therefore, the only significant mode for removal is by neutron absorption. Thus, equilibrium is reached when the production by the decay of promethium-149 and the neutron absorption of samarium-149 are equal [17]:

$$\lambda_{\text{Pm-149}} N_{\text{Pm-149}} = \phi \sigma_a^{\text{Sm-149}} N_{\text{Sm-149}} \quad (3.50)$$

where  $\sigma_a^{\text{Sm-149}}$  is the microscopic cross-section for absorption in samarium-149 and  $N_{\text{Sm-149}}$  is the number density of samarium-149 nuclei. Substituting Equation 3.49 in Equation 3.50, results in the equilibrium number density of samarium-149 atoms [17]:

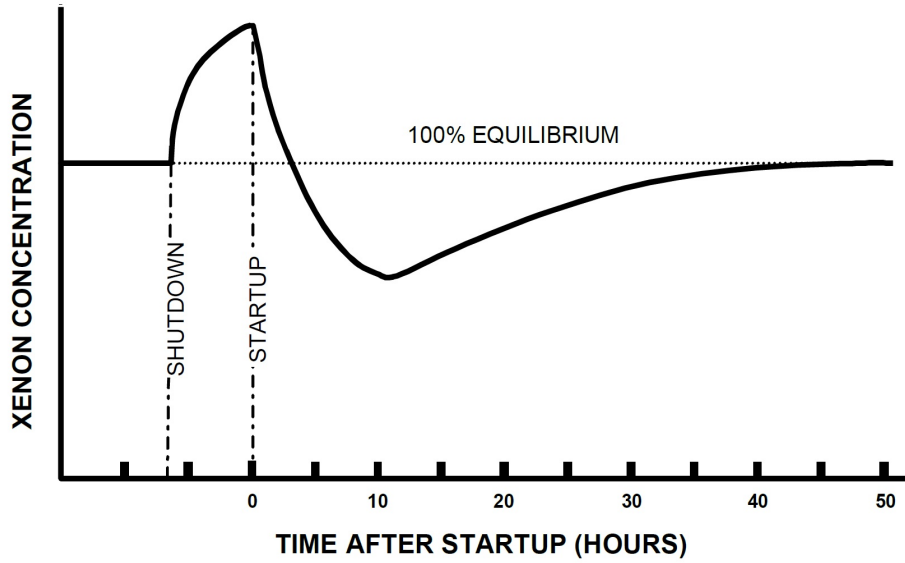


Figure 3.14: Xenon-135 concentration for a shutdown followed by reactor startup [17].

$$\gamma_{\text{Pm-149}} \phi \Sigma_f^{\text{fuel}} = \phi \sigma_a^{\text{Sm-149}} N_{\text{Sm-149}} \quad (3.51)$$

$$N_{\text{Sm-149}} = \frac{\gamma_{\text{Pm-149}} \Sigma_f^{\text{fuel}}}{\sigma_a^{\text{Sm-149}}} \quad (3.52)$$

As samarium-149 has only one significant mode of production and depletion, the concentration behaves differently from xenon-135. As can be observed from Equation 3.52, the equilibrium number density of samarium-149 does not depend on the neutron flux. As a result, samarium-149 reaches a single equilibrium concentration in the reactor regardless of power. This effect is presented in Figure 3.15 [17].

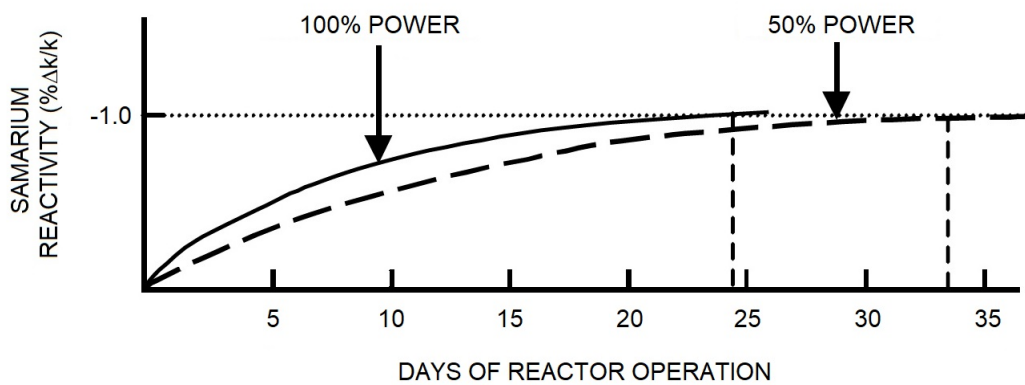


Figure 3.15: Samarium-149 reactivity for different power levels [17].

The removal of samarium-149 from the reactor stops after the reactor shut down because the only significant mode of samarium-149 depletion is neutron absorption. Thus, there is always a concentration of samarium-149 in the core, except in the initial startup from the clean core. After the shutdown, samarium-149 production continues due to an inventory of promethium-149 remaining in the core, which continues to decay. This effect increases samarium-149 concentra-

tion until promethium-149 is depleted. Figure 3.16 [17] presents this behaviour. Because the shutdown equilibrium concentration of samarium-149 is higher than the operating equilibrium concentration, the reactivity effect of samarium-149 is maximum at the startup of the reactor.

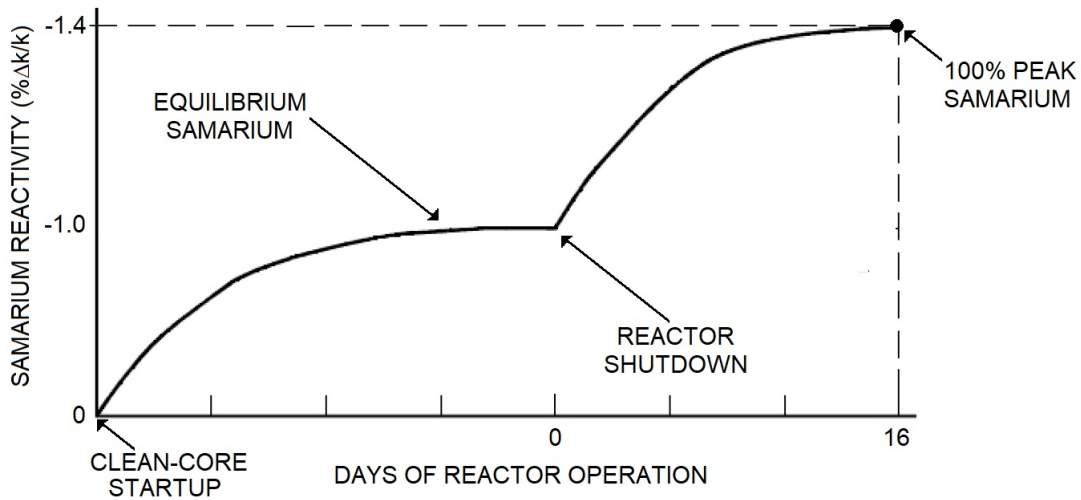


Figure 3.16: Samarium-149 reactivity for clean core startup [17].

### 3.4.3 Control poisons

Together with fission product poisons, other neutron poisons may be introduced to the reactor to control the excess reactivity at BOL and to control the reactivity over the reactor lifetime. Two common examples are burnable absorbers (burnable poisons) and boric acid dissolved in the coolant/moderator of the reactor (chemical shim).

Burnable poisons (BPs) are high neutron absorption cross-section material introduced to the core either in fuel or as separate core components. The main idea of BPs is that, as neutrons are absorbed, the material is converted into a nuclide with a lower cross-section for neutron absorption. Examples of BPs are boron (boron-10) and gadolinium.

The products of interaction between BPs and neutrons have a small cross-section for absorption interactions. Thus, the magnitude of the negative reactivity effect of BPs decreases over time. The purpose of BPs is to decrease reactivity at BOL when there are large amounts of fuel. When the fuel is depleted and the neutron population decreases, the BP is burned away and compensates for the fuel burning.

In PWRs, chemical shim also introduces negative reactivity by reducing the neutron proceeding to fission and lowering the thermal utilization. Unlike other forms of reactivity control, which are localized to inserted rods or stationary components, the chemical shim is homogeneously distributed throughout the core. It also similarly controls the long-term reactivity as BPs. At BOL, the coolant/moderator has high boron concentrations, and over the lifetime, this concentration is reduced. During normal operations, the reactivity influence of chemical shim is relatively slow compared to control rod manipulation. High boron concentrations are also used in several safety systems to inject large negative reactivity to assist in reactor shut down after an accident.

## 3.5 Core Lifetime

During the reactor operation, several changes occur in the reactor core caused by many material changes resulting from neutron interactions over extended periods of time. Fuel is slowly depleted as uranium-235 (or other fuel) undergoes fission and converts to fission products. The long-term fuel depletion process is known as fuel burnup and is measured in units of megawatt-days per metric ton of heavy metal (MWd/ton or MWd/MTHM) or gigawatt-days per metric ton of heavy metal (GWd/ton or GWd/MTHM). The fuel burnup gives the amount of energy produced per unit of fuel material mass.

The fuel burnup is also related to the production of many other isotopes such as plutonium-239 generated by neutron capture in uranium-238 followed by two beta decays, accumulation of fission products, and depletion of absorbing materials. These changes result in differences in the neutron flux profile and subsequently affect the power and temperature distributions within the core.

Several considerations are required in the design and operation of the reactor to account for heterogeneous conditions and changing material composition. These considerations guarantee safe, long-term, and economical operation of the reactor by optimizing the rate of burnup within the reactor core.

### 3.5.1 Core excess reactivity

As discussed, uranium-235 fuelled nuclear reactors deplete as a result of fission interaction. The fission reaction rate per volume is given by [17]:

$$R_f = \phi \Sigma_f^{\text{fuel}} \quad (3.53)$$

The fuel burn rate depends on the neutron flux (or power) and the amount of fuel remaining in the core. Another useful way to describe the amount of fuel remaining, as well as other long-term contributors to reactivity, is in terms of the excess multiplication factor and excess reactivity. The excess neutron multiplication factor is the amount of neutron multiplication available in the core above the neutron multiplication required for the criticality, then [17]:

$$k_{\text{excess}} = k_{\text{eff}(\text{max})} - 1 \quad (3.54)$$

where the maximum effective multiplication factor ( $k_{\text{eff}(\text{max})}$ ) is the  $k_{\text{eff}}$  in the reactor with no control rods inserted. Similarly, the excess reactivity refers to the core reactivity in excess of the absolute minimum to maintain a stable neutron multiplication factor. The excess reactivity is given by [17]:

$$\rho_{\text{excess}} = \frac{k_{\text{eff}(\text{max})} - 1}{k_{\text{eff}(\text{max})}} = \frac{k_{\text{excess}}}{k_{\text{eff}(\text{max})}} \quad (3.55)$$

In addition to the fuel burnup, the core excess terms also account for the influence of fission product poisons and BPs. In Figure 3.17 [17] the variation of  $k_{\text{excess}}$  over operating fuel cycle is presented. The following discussion refers to this figure. In the early stages of operation, fission product poisons accumulate to equilibrium concentrations, decreasing the excess reactivity, as shown by the decrease in  $k_{\text{excess}}$  between points A e B. In the absence of other factors, the fuel depletion would continue to lower the excess reactivity. However, BPs present in the core are depleted faster than fuel, resulting in a temporary increase in  $k_{\text{excess}}$  between points B and C. After enough of the BP is burned away, fuel depletion becomes the dominant effect, and the

excess falls as can be observed in the decrease of  $k_{excess}$  between the points C and D. In the point D, the excess reactivity reaches zero. At this point, the reactor can no longer operate and must be refueled. The goal of the design is to optimize the operating time before refueling by accounting for fission product poisons and introducing BPs to the system to balance the fuel depletion.

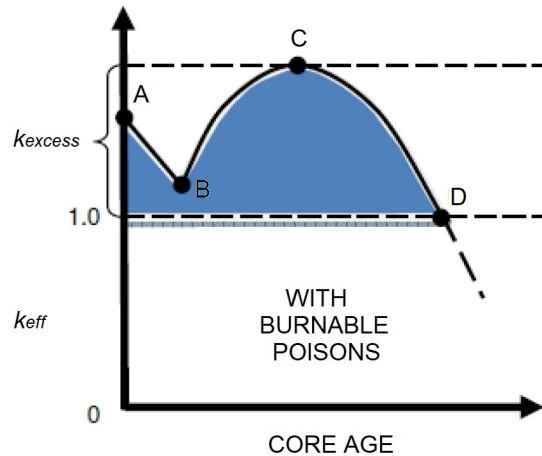


Figure 3.17:  $k_{excess}$  change over operating fuel cycle [17].

## 3.5.2 Neutron flux profiles

Real reactors are not homogeneous; several essential considerations arise from the reality of heterogeneous core and non-uniform flux.

### 3.5.2.1 Heterogeneous core flux

The reactor core consists of a variety of finite components and materials. Thus, the neutron profile does not consistently decrease away from the core center. Instead, the neutron flux consists of a series of local variations corresponding to the different core materials, then flux increases and decreases due to the presence of these different materials. Figure 3.18 [17] provides a simplified view of the neutron radial flux profile where only fuel rods and the moderator are present. The thermal neutron flux in the moderator increases compared to the homogeneous core due to the thermalization of neutrons in this region. On the other hand, thermal neutron flux within the fuel is depressed due to the absorption. In a real core, further complexity is introduced as there are also different materials such as structural components, control rods, and discrete regions of a fuel rod: fuel, gap, and cladding. As a result, there is different neutron flux depending on the radial position in the core, proximity to the fuel, moderator, and absorbers.

### 3.5.2.2 Core lifetime neutron flux profile

Fuel assemblies are typically organized in cylindrical patterns to constitute the reactor core. Thus, neutrons produced in the core center are less likely to escape from the core than those produced in assemblies far from the center. This effect results in an increased neutron flux in the core center that decreases towards the core edges.



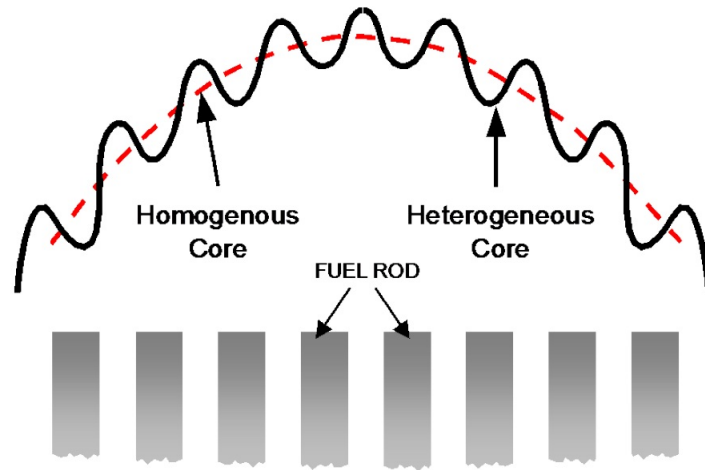


Figure 3.18: Distortion of radial neutron flux in heterogeneous core [17].

However, the increased flux increases the rate of fuel burnup and fuel depletion in the core center over time. At BOL, the neutron flux profile is significantly different from the EOL profile due to differences in the fuel burnup. As the fuel in the core center depletes faster than the fuel in the core edges, the flux profile is depressed in the center during the core life. This effect is presented in Figure 3.19 [17].

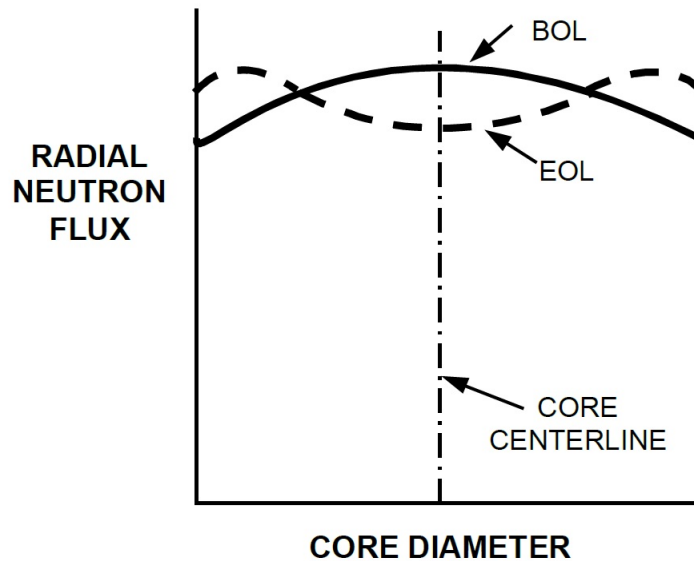


Figure 3.19: Radial neutron flux profile at BOL and EOL [17].

The axial neutron flux profiles at BOL and EOL also present similar behavior, once the axial center of the fuel also has a higher neutron flux than axial ends. The neutron flux profile also corresponds closely to the relative power and temperature profiles of the core once the number of fissions occurring depends on the flux.

### 3.5.2.3 Neutron reflectors

Neutron reflectors are materials with high elastic scattering cross-sections such as water or graphite used to reflect neutrons back to the core. Additionally, reflectors may be used to minimize the BOL and EOL neutron flux discrepancies by flattening the overall neutron flux profile. These materials are placed around outside the core to reflect neutrons that would otherwise leak from the core. These reflected neutrons contribute to fission in the fuel near the core edges, increasing the neutron flux in these regions. The flattened neutron flux profiles reduce the variations in power, burnup, and temperature over the core. The effect of reflection on neutron flux profiles is presented in Figure 3.20 [17].

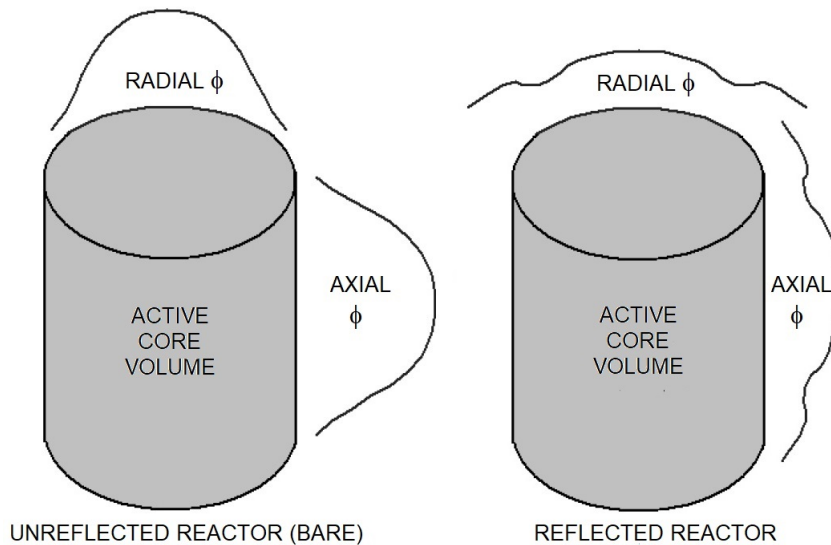


Figure 3.20: Effect of reflection on neutron flux profiles [17].

### 3.5.2.4 Fuel loading patterns

Another method that can be used to flatten the neutron flux profile to burn the fuel efficiently is to load differently burned fuel into the core in specific patterns. As a simple example, when refueling the reactor at the EOL, low burnup fuel can be reused by moving it from the outer region of the core toward the center. The high burnup fuel from the core center is removed, and fresh fuel is placed in the outer regions of the core. The final core at BOL has partially burned fuel in the center of the core and unburned fuel toward the outside, which results in a flattened neutron flux profile over the core life. This concept is presented in Figure 3.21 [17]. Real fuel loading patterns are more complex than the one described previously. For example, more effective loading patterns may use high burnup fuel around outside of the core to reduce neutrons leakage or may have alternating layers of high burnup and low burnup fuel to minimize local neutron flux variations.

### 3.5.2.5 Coolant temperature

The temperature distribution is also not uniform in a reactor. In PWRs, the coolant flows from the bottom to the top of the core, as shown in Figure 3.22 [17]. Thus, cold water enters into the bottom of the core and begins to heat as it removes heat from the core. As the

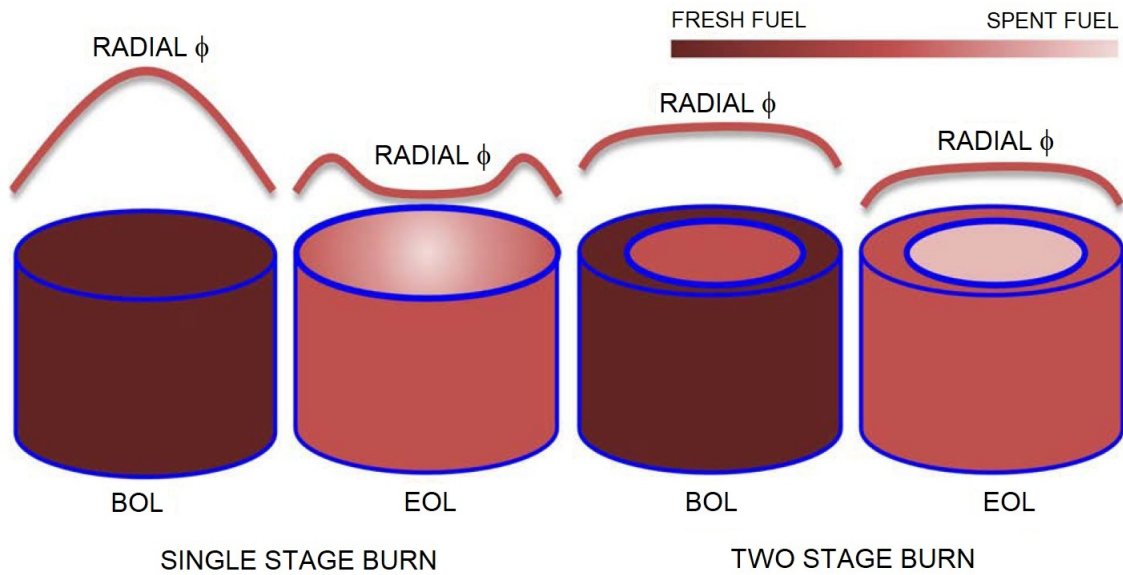


Figure 3.21: Simplified two-stage burn fuel loading to flatten the neutron flux profile [17].

temperature of the coolant increases, it is less effective in removing heat from the core. As a result, cooler regions of the core are toward the coolant entrance and warmer regions toward the coolant exit. This effect leads to variations in the fuel and moderator temperatures, which affects non-uniformly the reactivity coefficients, leading to variations in neutron flux, power, and fuel burnup in the axial direction.

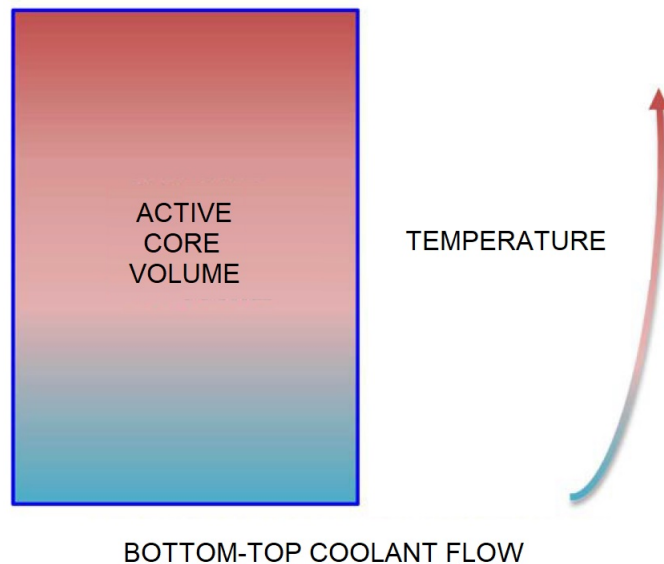


Figure 3.22: The bottom-top coolant flow temperature profile in PWRs [17].

### 3.6 Transients

Transients are characterized by changes in operating parameters, temperature and pressure, in response to operator action or accident conditions. They always present significant and

simultaneous changes to many reactivity contributing parameters. Thus, the explanation of various transients concerning affected parameters is useful for understanding the complexity of reactor system operation and designs and in understanding the functioning principles of reactor systems.

There are a large number of possible transients that can happen in reactors. Thus, some simple and representative transient scenarios are discussed here: power maneuvering, reactor scram, and loss of coolant flow. Power maneuvering represents a simple and basic representation of normal operation. The reactor scram transient is essential because the effects of a scram are part of many accident transients as an important accident prevention and response mechanism. The loss of coolant flow is a symptom of several possible failures, the effects of which may also be seen in a variety of accident transients.

These transients are explained in terms of their effect on each parameter explained in this section. For simplicity, it is assumed that the reactor safety systems remain operational. However, safety system failure or inadequacy may result in extreme and undesired accident conditions. The complex behavior of operating parameters in most severe accidents is sometimes not well known and difficult to model.

### 3.6.1 Power maneuvering

Power maneuvering is a change in reactor power demand. The following analysis considers a power change from 100% power to 50% power. After some days at 50% power, the reactor is returned to 100% power.

The power is reduced by inserting control rods in the core. The rod insertion gives negative reactivity to the core, giving the reactor power a negative period, and power reduces during the time to the 50% power level. This power change results from the increased neutrons absorbance in the control rods. In terms of the six factor formula, the thermal utilization factor (ratio of thermal neutrons absorbed in fuel to those absorbed in all reactor material) is reduced because more neutrons are absorbed in non-fuel nuclei. In general, for power maneuvering, the insertion of control rods is done slowly. Thus, the fast phenomena such as the prompt drop in the neutron level are not significant, and the reactor parameters change slowly. As power is reduced, fewer fissions occur, and the fuel and moderator temperatures both decrease.

Water density changes dominate the MTC. As the moderator temperature decreases, the moderator density increases. Most reactors are designed to be in an under-moderated state to protect the reactor by inserting negative reactivity when the temperature rises, which means this system has a negative MTC. However, the MTC leads to a positive reactivity insertion as the temperature decreases. The FTC is dominated by the Doppler broadening that results in a negative FTC. Thus, positive reactivity is added as fuel temperature decreases.

The positive reactivity insertion caused by the moderator and fuel temperature changes counterbalances the negative reactivity insertion of the control rods. When the control rods are inserted to the 50% power position, temperature decreases so that overall core reactivity is zero and power stabilizes. Additional adjustments in the control rods or chemical shim may be necessary to balance the effect of slow processes (fission products decaying, for example) to equilibrate to the new power.

Xenon-135 and samarium-149 concentrations begin at the equilibrium levels for 100% power. After reducing reactor power to 50% power, these concentrations start to change. Xenon-135 continues to be produced by the decay of iodine-135, and concentration increases for several hours following the power reduction until it reaches a maximum value. When the xenon-135 begins to decrease, it falls over a couple of days to the new equilibrium value corresponding to

50% power. The samarium-149 concentration increases for several days after power reduction due to the continued decay of promethium-149. After an extended period, the samarium-149 concentration falls to reach an equilibrium at the same level as 100% power.

Additionally to xenon-135 and samarium-149, other fission products also decay to new equilibrium values. The decay of these fission products results in the continued production of decay heat at a higher level than the equilibrium for 50% power. The delayed neutron precursor inventory continues to decay and produce delayed neutrons at an increased rate before reaching the 50% power equilibrium concentration. Reaching new equilibriums for decay heat and delayed neutron precursor concentrations is a slow process. Thus, reactivity adjustment may be necessary to compensate for the slight reduction in the production of heat and delayed neutrons.

After stabilizing overall conditions, the control rods are slowly removed to return the reactor to 100% power. A positive reactivity insertion caused by control rod withdrawal results in an increased thermal utilization factor and a positive reactor period. The moderator and fuel temperatures rise due to the increased number of fissions. As MTC and FTC are negative, negative reactivity is inserted as the power rises. This effect slows the power rise, counterbalancing the positive reactivity insertion of the control rod withdrawal. After some time, the reactor stabilizes by balancing reactivity at zero. Some operations may be necessary to account for slow processes. As other fission products accumulate to new equilibrium values, the heat production by the decay of fission products and the production of delayed neutrons by delayed neutron precursors rise.

Returning to 100% power, xenon-135 and samarium-149 are burned faster than they are produced. Xenon-135 concentration falls over few hours due to the increased neutron flux until the decay of iodine-135 for the new power levels is reached. After this, the concentration of xenon-135 begins to rise to the equilibrium value for 100% power. Samarium-149 concentration initially falls due to the increased neutron flux but returns to the original equilibrium value after few weeks.

### 3.6.2 Reactor scram

In accident conditions or when reactor parameter limits are reached, the reactor responds with the insertion of all control rods to prevent or mitigate the effects of an accident. This sudden insertion of all control rods is known as a reactor scram. The following description refers to a manual scram from the reactor at full power.

The control rod insertion creates a large negative reactivity. This results in a rapid decrease in power and neutron flux. Because heat is no longer produced from fission, the moderator and fuel temperatures decrease. Despite the reduced number of fissions and the resulting loss of heat production following the scram, there is still a neutron source and a heat source in the core. Following the shutdown, the initial inventory of radioactive fission products and activated materials continues to undergo radioactive decay for extended periods. This effect is known as decay heat and accounts for the continued production of approximately 6% of the heat at full power. Thus, the loss of heat removal capabilities could lead to rising fuel and moderator temperatures. Additionally, neutrons continue to be generated from the inventory of delayed neutron precursors produced at full power, which results in the negative period of the reactor power to stabilize at approximately  $-80$  seconds after the rapid drop of prompt neutron levels.

Compared to moderator and fuel temperatures that decrease slowly, the prompt neutron responds very fast to the negative reactivity insertion. Thus, the negative reactivity insertion results in a sudden low reactivity followed by the reactivity changes caused by the MTC and

FTC. These two effects result in a slight increase in reactivity following the initial decrease. This increase is caused by the decrease in the fuel and moderator temperatures, which result in positive reactivity insertion.

After the scram, xenon-135 continues to be produced for several hours, thereby inserting negative reactivity during this period. When radioactive decay becomes the dominant term in xenon-135 production/loss, it decays for few days, and the negative reactivity inserted by the xenon-135 gradually decreases. Samarium-149 continues to be produced after the scram and then approaches the shutdown equilibrium concentration resulting in a stable negative reactivity insertion.

### **3.6.3 Loss of coolant flow**

The loss of coolant flow means a lack of flow in the primary coolant loop. Here, it is considered a loss of flow in the primary coolant loop during full power operation. The flow for this example decreases linearly from 100% to 50% over few seconds. As the flow rate decreases, the water remains in the core region for a longer time, which increases the coolant temperature. This effect results in a negative reactivity insertion due to the MTC. The inserted negative reactivity results in decreased reactor power. However, as the reactor power decreases, the fuel temperature also decreases. Due to the FTC, the decrease in fuel temperature inserts positive reactivity.

After the transient, the reactor reaches a stable condition at lower full power once the MTC and FTC balance each other. In the following hours, xenon-135 concentration increases before decreasing to the new equilibrium level. The temperature is slightly adjusted during this time to counter xenon-135 concentration changes.

# Chapter 4

## Small Modular Reactors (SMRs)

World Nuclear Association (WNA) defines SMRs as nuclear reactors generating up to 300 MWe, designed with modular technology using module factory fabrication, pursuing economies of series production and short construction times [6]. The interest in small reactors and modular reactors construction is not new. Early reactors for commercial electricity production were of small size due to the careful engineering process of constructing plants beginning at small ratings to gain the needed construction and operational experience necessary to move confidently to larger ratings. Besides, small units were built to provide electric power for remote military sites, for ocean deployment, for submarine propulsion, naval and commercial ships, and for aircraft propulsion [19].

As a consequence of the high cost of large power reactors to generate energy, there is a move to develop smaller units that may be built independently or as modules in a larger complex, requiring significantly reduced capital investments [6]. An additional premise is that electric generation cost can be made comparable to that of existing large-sized plants by employing the manufacture of multiple identical modules and design simplification [19]. As previously discussed, with this prospect of cost reduction and the possibility of being employed in remote areas, SMRs appear as an essential option for energy generation with low emission of GHGs, thereby being an important tool to reduce global warming to the desired levels.

Due to the growing interest in SMRs, this section presents a description of the integral pressurized-water reactor (iPWR) designs, comparing them with large PWR designs. The section is accompanied by a brief description of some iPWR designs that are being developed nowadays.

### 4.1 Core and Fuel Technologies in iPWRs

Over 60 years ago, nuclear power was introduced into mankind, representing a substantial change that rivals and potentially exceeds those of the combustion engine and electricity. However, nuclear weapons and the nuclear accidents that have happened over time have transformed nuclear power into a more and more controversial issue, resulting in a divided public opinion. Consequently, nuclear power has been unable to fulfill its potential neither to maintain its promises; it will remain so for the near future unless it goes through a drastic change from its current status. The facilitator for this change could be the deployment of SMRs, beginning directly with the iPWR designs whose features and technology are discussed in this section.

SMRs share many of the same design principles as other reactor types. In particular,

iPWRs are designed based on the extensive nuclear design experience of hundreds of large PWRs operating worldwide. Nuclear design involves several major objectives that include [19]:

- **Safety:** the fuel and the core must be designed to withstand all operational demands and anticipated accidents, which means that constraints on the fuel rod power peaking, total reactivity, reactivity coefficients, control rods worths, shutdown margins, and delayed neutron fraction have to be analyzed and demonstrated to be within limits. It means that plant must be licensable.
- **Economics:** the fuel and core must produce the required energy that the utility demands over the established time period, while the fuel costs must be minimized.
- **Reliability:** the fuel and core must operate predictably and reliably.
- **Operations:** the fuel and the core must be projected for relative ease of operation with minimum complexity for the operator.
- **Strategy:** the fuel and the core must achieve strategic requirements of the utility, if and when set, such as plutonium management, load following, and fast ramp-up in power.

In order to meet the objectives listed previously, there are several design features that developers can work with to develop an effective and viable design. Such features include enrichment of the fissile material, burnable poison (BP) types, BP loadings (location, number, and weight percent), location of the fuel (fresh and irradiated) within the core, control rod locations and level of insertion, and frequency and number of fuel assemblies replaced during its maintenance outage [19].

In that sense, the nuclear design of any reactor, including iPWRs, specifically focuses on the core physical characteristics, the safety and operational performance of the fuel and the core, and the reactivity control systems in the fuel and the core [19]. In the following, the design process and features of the PWRs and specifics of iPWRs are described, including the description of important safety design criteria and principles in the nuclear design of reactors, design features used to achieve a viable and economic nuclear design, and how the design principles and features were addressed in iPWR designs.

### **4.1.1 Safety design criteria**

In this section, the major safety design criteria for PWRs are emphasized. The discussion includes fuel burnup, reactivity coefficients, power distribution, shutdown margin, maximum reactivity insertion rate, and power stability.

#### **4.1.1.1 Fuel burnup**

As discussed in Section 3.5, the fuel burnup is defined as the amount of energy extracted per mass of initial fuel loaded. The units are megawatt-days per ton of heavy metal loaded in the core (MWd/ton or MWd/MTHM) or gigawatt-days per ton of heavy metal loaded in the core (GWd/or GWd/MTHM). The burnup requirements are drawn from the utility needs in terms of the energy output of the reactor and the refueling frequency. Achieving the designed burnup requires sufficient excess reactivity in the fuel, and the fuel must be replenished at an appropriate frequency. For a typical iPWR, it can range from 1 to 5 years, although 12 to 24 months are more typical in moderns light water reactors [19].



The excess reactivity must guarantee that the PWR core maintains criticality at full power operating conditions throughout the cycle of operation. It must compensate for effects such as fuel depletion, the buildup of fission products poisons, and loss of reactivity caused by changes in temperature of the moderator and the fuel. There is no limit on the amount of excess reactivity allowed in the core. However, other parameters such as reactivity coefficients and shutdown margin are affected by the excess reactivity; thus, it is essential to control the amount of excess reactivity present in the core.

Limits on burnup are imposed not only by design warranties associated with the fuel but also licensing limits for the maximum fuel rod average burnup. For typical large PWRs, the average fuel rod burnup is 60 to 62 GWd/ton. Thus, since many iPWR designs rely on experience in large PWRs, a similar limit is expected.

#### **4.1.1.2 Reactivity coefficients**

The reactivity coefficients were discussed in detail in Section 3.3. From this section, one may point that there are two main reactivity coefficients: the fuel temperature coefficient (FTC) and the moderator temperature coefficient (MTC). For safety reasons, iPWRs are designed to have a negative temperature coefficient. As discussed, the FTC is known as the prompt temperature coefficient because it acts with little or no delays if power rises. The use of slightly enriched uranium in PWRs and iPWRs ensures that the FTC is negative due to the Doppler effect taking place mainly in the U-238 present in the fuel. In general, the FTC only becomes of concern when the fuel has lower U-238 content caused by a higher enrichment or adding other material such as plutonium. Therefore, there is relatively little nuclear design in the control of FTC for PWRs and iPWRs.

On the other hand, MTC responds more slowly to power rise in PWR and iPWR cores due to the time to transfer heat from the fuel to the moderator. In PWRs and iPWRs, the increase in moderator temperature decreases the moderator-to-fuel ratio and moderator density. These effects generally reduce the core reactivity, resulting in a negative MTC. However, as discussed in Section 3.3, in reactors that contain diluted boron in the moderator, the MTC becomes less negative if the boron concentration in the moderator increases. This effect is caused because as moderator temperature increases, the density of the moderator decreases, resulting in the decrease in the density of the soluble boron that is present, therefore reducing the neutron absorption in the boron. This effect is increased for higher boron concentration. Thus, the nuclear design of the fuel and the core use burnable poison rods to limit the amount of soluble boron necessary in the coolant to control the excess reactivity and ensure a negative MTC in the core throughout the operation cycle.

#### **4.1.1.3 Power distribution**

Many fuel operating limits (performance and safety) for PWRs and iPWRs are directly related to the maximum linear power density of the fuel. As a first approximation, for a given fuel rod geometry, the peak fuel temperature, the surface heat flux, the decay heat generation rate, and the stored thermal energy are proportional to the fuel rod linear power density [19]. Thus, the nuclear designer has to maximize the total power output while minimizing power peaking (consequently the linear power density) for the fuel assembly in the core and for the individual fuel rods.

For the nuclear designer, the power distribution of the core must be such that [19]:

- The fuel does not exceed specified peak linear heat rates under normal operating conditions. This value is determined as part of the safety analysis for the core.
- The fuel does not exceed the design basis set for departure from nucleate boiling (DNB). The DNB is the point at which the heat transfer from a fuel rod quickly reduces as a result of the insulating effect of a steam blanket formed on the rod surface when the temperature continues to increase. This value is obtained by thermal-hydraulic analysis.
- Under normal and abnormal operating conditions, the maximum linear heat rate does not cause the fuel to melt. This value is provided to the nuclear designer.
- The fuel rod power and burnup are consistent with the assumptions and analysis in the fuel rod thermo-mechanical performance analysis.

These requirements must be guaranteed under nominal reactor operating conditions and under a range of extreme power shapes and variations. These extreme shapes reflect the experience at operating reactors (based on large PWRs) and are chosen to be intentionally conservative, such as axial power distorted by control rod insertion/withdrawal and load follow conditions.

#### **4.1.1.4 Shutdown margin**

In iPWRs and large PWRs, there are generally two independent systems to control reactivity, each relying on different operation principles. In large PWRs, the primary reactivity control system uses soluble acid boric in the coolant. However, many iPWRs are designed without the presence of soluble boron in the coolant.

The second reactivity control method consists of the use of control rods. These rods must ensure subcriticality under normal operations, including anticipated operational occurrences, with enough margin to tolerate malfunctions, including stuck rods. The control system must control the rate of reactivity change during normal operational maneuvers such as xenon depletion.

Both systems should be able to ensure that fuel design limits are not exceeded. Additionally, each one of the systems should be able to ensure subcriticality at cold conditions.

#### **4.1.1.5 Maximum reactivity insertion rate**

The amount of reactivity inserted by control rod withdrawal (in normal or accident conditions) or by diluting the boron in the coolant, when present, must be limited to avoid damage to the fuel and the core components. It is required to demonstrate the limits on maximum linear rate and margins to DNB. By analyzing the control rod worth and the allowed speed of movement of the control rods, the reactivity insertion rate can be limited.

#### **4.1.1.6 Power stability**

The reactor core can become unstable to power oscillations for several reasons, such as initiated by instability in the reactivity control systems or turbines. Spatial effects caused by the xenon can also initiate oscillations (xenon oscillations). Instability is mainly an issue in large core sizes, being less significant in small cores. Stability in the control systems for the reactor hardware means that total core power oscillations are not usually possible, and the nuclear design of the control rods and core can guarantee that the xenon effects are self-limiting.

## 4.1.2 Design features to achieve the criteria

### 4.1.2.1 Setting the enrichment of the fissile material

The first stage in the nuclear design of an iPWR or other type of reactor is to determine the enrichment requirements for the fuel to provide the energy output over the time period requested by the utility. For large reactors, the current enrichment design limit is 5% of uranium-235 [19]. In equilibrium conditions, after several operation cycles, the cycle length and operations are more constant, and the enrichment is unlikely to change significantly. However, before reaching the equilibrium, the enrichment varies to adjust the cycle length, the amount of reloaded fuel, and the target burnup. Similarly, if the utility cycle length is changed, the enrichment may also be required to change.

The fuel also needs to have enough enrichment to ensure sufficient reactivity for its designed lifetime, which is typically between one or four cycles of operation depending on the iPWR and the fuel design [19]. The nuclear designer must work closely with the utility to analyze the optimum cycle length of operation for the reactor, considering the electricity demand perspective, duration of the outage, and, in the case of several iPWR units in the same site, the schedule for maintenance and refueling outages throughout the year.

Once the fuel enrichment is governed by the desired operational cycle length and the fuel burnup, the core replenishment fraction must also be considered. Generally, in iPWRs and large PWRs, a fraction of the core (called batch) is replaced after each operational cycle. The remaining fuel is reloaded back in the core but in different locations to their previous location. In some iPWR designs, there is a plan to replace all of the fuel after each fuel cycle. The proportion of core replacement and the frequency of replacement is known as the fuel management scheme. Examples of fuel management include: replace one-fourth of the fuel assemblies every 12 months, replace one-third of the fuel assemblies every 18 months, replace half of the fuel assemblies every 24 months, and replace all fuel assemblies every 48 months [19].

Increasing the number of batches increases the fuel burnup. However, increasing the number of batches decreases the cycle length and results in more frequent refueling, decreasing the time that the reactor is available to produce energy. Yet, even a small number of assemblies in the core that need refueling or reloading can have a significant impact on the economics. In that sense, a compromise of two to four batches is used.

### 4.1.2.2 Burnable poisons (BPs)

After defining the required enrichment and the number of fuel assemblies, the designer evaluates the need for BPs in the fuel assemblies. As sufficient enrichment has to be present for the fuel lifetime, the excess reactivity has to be controlled, particularly during the first cycle. In large PWRs and in iPWRs, the core reactivity during the cycle is controlled by the use of control rods or by diluted boron in the coolant, or both. The use of BPs assists in controlling the power peaking within and between the assemblies, and it assists in reducing the core excess reactivity, thereby lowering the soluble boron concentration and resulting in a negative MTC.

Materials having a high neutron capture cross-section are chosen as BPs. However, upon capture, these materials must become an isotope with a low absorption cross-section, meaning they are burnable upon irradiation. In large PWRs, boron and gadolinium are used, meaning they are the most likely to be used in iPWRs also. The absorbing material can be mixed with the fuel itself during the manufacture of the fuel pallets or can be loaded as separated components in the fuel assemblies.

While boron (boron-10) burns out quickly due to its high absorption cross-section, gadolinium tends to burn out more slowly. Thus, boron BPs are more suitable for short operation cycles, and gadolinium more suitable for longer cycles. Compared to the uranium, the lower thermal conductivity of the gadolinium requires the fissile enrichment of the carrier material for the gadolinium poison to be lowered to avoid power peaking concerns. For iPWRs looking for long cycle lengths or those requiring a much longer time reactivity hold-down, erbia is another option. Compared to boron and gadolinium, erbia has a much lower absorption cross-section, resulting in a slow depletion. Additionally, all the isotopes of erbia have reasonable absorption cross-sections, meaning the isotopes produced by capture also have a reactivity hold-down effect [19].

The designer must consider the magnitude of the reactivity hold-down, the duration, and the depletion rate. Combining the number of BP rods, the weight percent of BP in those rods, and the BP material type gives the designer enough degrees of freedom to achieve the desired result. Figure 4.1 [19] presents examples of BP distribution. BPs are loaded near the water holes (instrument and guide thimbles) as further thermalization of neutrons improves their effectiveness.

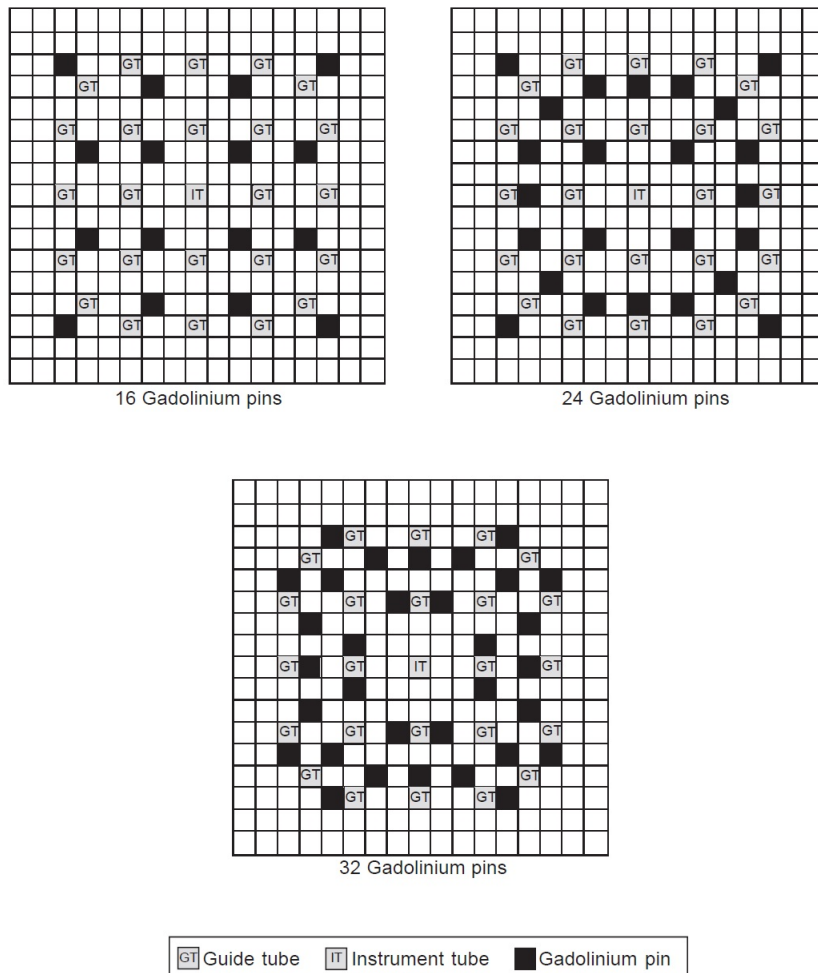


Figure 4.1: Examples of BP distribution designs [19].

### 4.1.2.3 In-core fuel management

After defining the fuel enrichment, the number of fuel assemblies to be loaded in the cycle, and the type of BPs that are most suited for the iPWR being developed, the next step consists of determining how to load the core and which assemblies loaded in the previous cycle of operation are available and suitable to be reloaded. This step is referred to as in-core fuel management, and a major part of the nuclear design effort is concerned with it.

The aim is to load the core to provide a flat and smooth distribution of reactivity throughout the core. This distribution of the assemblies in the core is known as the loading patterns. Too high reactivity results in high assembly powers, resulting in power peaking in the fuel rods being too high. The core is loaded in quarter core symmetry to avoid that power and performance in one quadrant to be higher than the others. Thus, the fuel assemblies are loaded in groups of four, one in each quadrant. In most iPWR and most large PWRs, the fresh fuel is loaded toward the center, and previously irradiated batches of fuel are loaded toward the edge of the core. This loading pattern improves the neutron economy because it reduces the neutron radial leakage out of the core, which is especially important for iPWR due to the smaller cores result in a much higher neutron leakage than large PWRs. Thus, iPWRs are more prone to power peaking with all of the higher reactivity at the center of the core, which requires higher BP loadings.

At the same time the designer assesses the core loading for power peaking, the energy requirements are also checked to guarantee that there is enough enrichment loaded in the fresh fuel assemblies. The number and content of BPs can be changed if sufficiently low peaking cannot be achieved. However, the designer must be aware that once the BPs deplete in the core, the power distribution changes and can lead to higher power peaking during the operation cycle than at the start.

Another key criterion of the design process is the economics of the required fuel. The fuel costs for a given operation cycle are affected mainly by the number of fresh fuel assemblies required and their enrichment. Once fuel is loaded in a quarter core symmetry, an additional new fuel means the need for four assemblies, which increases the fuel price. If the core is designed such that there is too much radial or axial leakage (relevant to iPWRs), then additional fuel enrichment is required to achieve the required cycle length and fuel burnup, which increases the fuel enrichment costs.

Reducing the number of fuel and BP rod types can be used to improve fuel economics. Keeping the number of fissile enrichments to a minimum across the assemblies, rather than having multiple enrichments, is a good practice. Additionally, minimizing the variations for the BP types and enrichment of fissile materials in the BP rods and the BP loading itself is crucial to reduce the fuel costs. Also, the designer must ensure that the BP burns out completely, meaning that there is no residual absorption of the BP in the fuel. This effect is important for highly poisoned cores where the impact would be greater. For iPWRs that require high BP loadings (long cycles or single batch cores), minimizing the residual absorption by using boron rather than gadolinium, or combining the two, would be warranted [19].

The compactness of the iPWR combined with fewer assemblies available makes the loading pattern design process more challenging and the achievement of an optimized core design more complex. For example, iPWRs have the order of one-fifth of the fuel assemblies of a large PWR as shown in Figure 4.2 [19].

Once the cycle length has been achieved with power peaking, fuel rod, and assembly burnup within the allowed constraints, a brief safety analysis is completed before the full set of detailed analyses and reports being completed. The usual checks include power peaking through the cycle, MTC at hot full power and hot zero power, and shutdown margin [19].

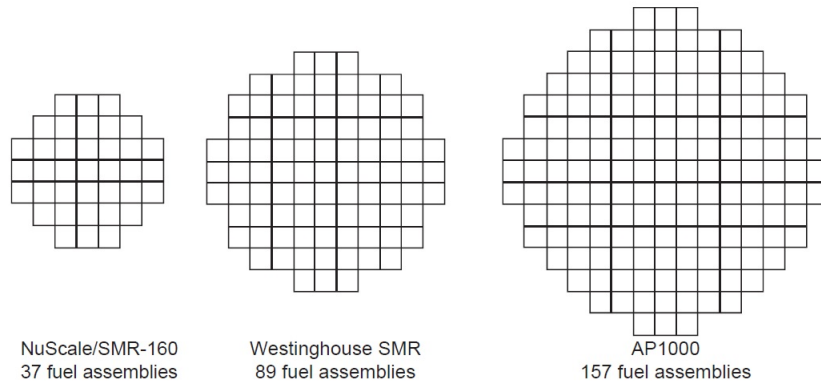


Figure 4.2: Comparing the core size of some iPWRs and a large modern PWR [19].

As observed, establishing an optimized nuclear core design is a rigorous process that typically takes several weeks of man effort and iteration. Additionally, the following steps in the design require interfaces with other elements of the design team, such as transient analysis, thermal hydraulics, mechanical design, and fuel performance, and additional iteration may be required before starting manufacturing the fuel.

### 4.1.3 iPWR design specifics

#### 4.1.3.1 Fuel designs in the smaller cores

The first iPWR design specific to be considered is the compactness of the core compared with large PWRs, in terms of the number of fuel assemblies and, in some cases, the height of the fuel assemblies. Table 4.1 [19] presents a summary of key nuclear design parameters of three SMRs (SMR-160, mPower, and NuScale) and a large PWR (AP-1000). The mPower was suspended in 2014, but it is included for reference; SMR-160 and NuScale are discussed in detail in Section 4.3. It is worth observing that although the fuel heights and overall loading are different in each iPWRs, they have the same  $17 \times 17$  array of fuel pins (see Figure 4.3 [19]). The choice for this configuration relies on the excellent operational performance of these fuel types in large PWRs operating today, which builds on extensive development work that has developed fuel designs toward a large number of thinner fuel pins to allow higher rod powers and improve thermal margins.

A large PWR has 157 to 193 fuel assemblies while iPWRs have between 37 and 89 [19]. The fewer assemblies result in fewer degrees of freedom to optimize the loading pattern and smooth out the reactivity and the resulting power distribution across the core. Thus, the iPWR core design and loading pattern are not so straightforward as they may appear despite the fewer fuel assemblies. These degrees of freedom are not only in terms of fuel design and burnable poisons loading in fresh fuel, but also, after the first cycle, the previously irradiated fuels have a variety of burnups resulting in different reactivities that can be distributed throughout the core to smooth the power distribution and then achieve the power peaking limits.

Another factor that must be considered in smaller cores is the greater radial and axial neutron leakages, which result in a more significant variation in assembly power from the center, more fuel consequently more power is generated, to the limits of the core, where less power is generated. The radial leakage can be reduced by ensuring only fuels with lower reactivities are loaded in the core-periphery or by using radial reflectors, such as stainless steel, instead of the water used in large PWRs. Regarding axial neutron leakage, large PWRs use what is known as

Table 4.1: Summary of key nuclear design parameters for large PWR and range of iPWRs [19].

Model	AP-1000	mPower	SMR-160	NuScale
<b>Power</b>				
Thermal power (MWth)	3400	530	500	160
Electrical power (MWe)	1150	225	160	60
Reactivity control	Rods and boron	Rods	Rods and boron	Rods and boron
<b>Fuel in core</b>				
Fuel assemblies	157	69	57	37
Array	17 × 17	17 × 17	17 × 17	17 × 17
Active fuel height (m)	4.3	2.4	3.7	2.0
Mass in the core (ton)	85	20	15	9
Enrichment	< 5.0% U-235	< 5.0% U-235	< 5.0% U-235	< 5.0% U-235
Cycle length (month)	18	48	48	24
<b>Fuel demand</b>				
Ton fuel per reload	36.6	20	14.7	Unknown
Ton per GW year	21.2	29.3	33.8	Unknown
Linear rating (kW/m)	19	12	14	8

axial reflectors. These reflectors are sections of active fuel height where the usual enrichment is reduced or, in some cases, natural (0.71% U-235) or even tails (approximately 0.3% U-235) uranium is used. Typically, they are located few centimeters at the top and bottom of the fuel stack. These reflectors improve the fuel economy by reducing the neutron leakage from the core and reducing the fuel costs in terms of enrichment needs in an area of the fuel and core where relatively little power is generated and, therefore, little need for fuel enrichment. However, axial enrichment variation in the fuel stack tends to increase the fuel cost because of the complexity of manufacturing a fuel type with more enrichments, zones, and diversity.

#### 4.1.3.2 Use of control rods and burnable poisons to control reactivity

SMRs using control rods and burnable poisons to control excess reactivity instead of soluble boron require increased axial and radial complexity in fuel designs. While in large PWRs, there may be a control rod located in one out of three or four fuel assemblies, iPWRs have a much higher density of control rods, especially in those that do not use soluble boron. When boron is used to control excess reactivity, the control rods usually are fully withdrawn. However, removing the need for boron simplifies the chemical volume control system (CVCS) and results in capital and operational cost savings because there is no need to handle depleted soluble boron. Thus, in iPWRs without soluble boron, the control rods and the sequence in which they are moved allow for compensation in the reduction in excess reactivity (as fuel depletes), for axial power changes, and for xenon variations.

On the other hand, inserting a control rod displaces the power away from its location to somewhere in the core, and excessive movements can thermally cycle the fuel, possibly resulting in fuel failures. It is also necessary to control the rate of rod withdrawal due to fuel performance and reactivity insertion limits. In that sense, there is also a need to develop a control rod sequence for the control rod groupings to ensure appropriate reactivity compensation and, at

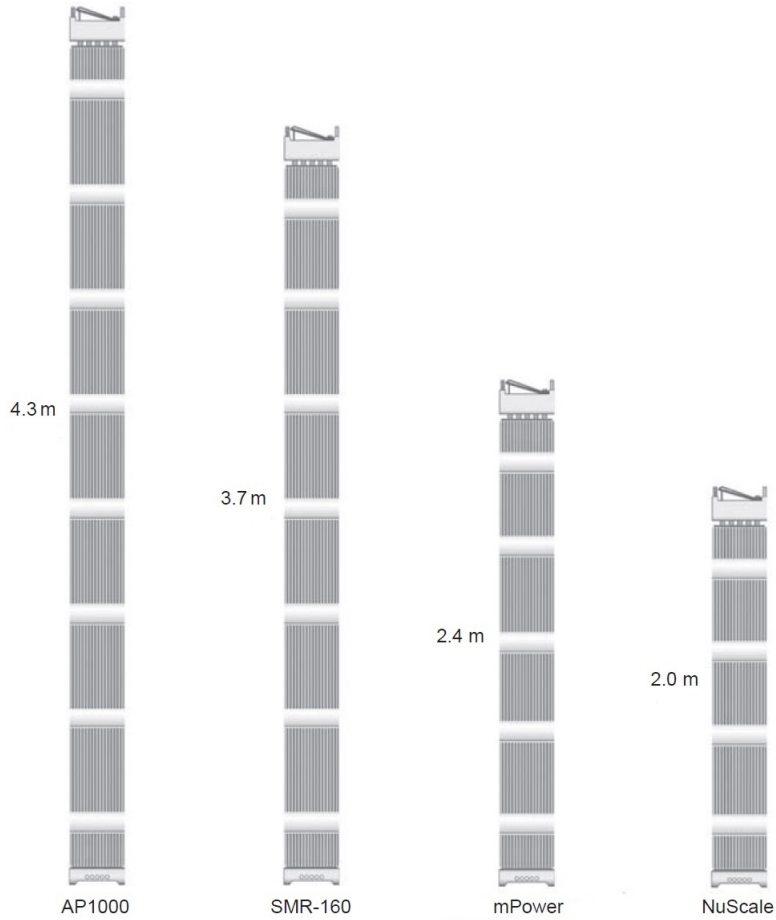


Figure 4.3: Relative heights of  $17 \times 17$  fuel designs considered in iPWRs today [19].

the same time, to ensure that other limits are not exceeded. Even though soluble boron is used, similar challenges regarding excess reactivity control are observed in iPWRs designs looking to achieve a long cycle length once greater fissile loadings are required to extend cycle length.

Inserting control rods during a cycle results in strongly varying axial power shapes. When control rods are inserted in an iPWR, the power skews to the bottom of the core and results in higher peaking factors. This effect can be attenuated by using higher burnable poison loadings in the lower part of the fuel or varying the fissile enrichment axially. Additionally, the assemblies where the control rods are inserted during the cycle have their peak pin power pushed radially away from the inserted control rod locations. Thus, radial burnable poison loadings are also required to reduce the radial peaking factors. These effects tend to lead to a heterogeneous nuclear design in terms of fuel assemblies and areas with significant flux suppression in the fuel pins around the burnable poisons and control rods and results in power peaking around inserted control rods and burnable poison locations. A more heterogeneous core produces a nonuniform radial and axial fuel depletion, which results in inefficient use of the fuel. Furthermore, in iPWRs that use natural circulation, the nonuniformity in power and the resulting moderator density require additional thermal-hydraulic analysis to guarantee sufficient cooling and an accurate prediction and coupling of the neutronic and thermal-hydraulic feedback.

When high gadolinium loads are used, special attention is required to the fissile enrichment of the fuel pins carrying the gadolinium. Gadolinium has a lower thermal conductive than uranium, then the fissile enrichment of the carrier material for the gadolinium poison must be lowered to avoid power peaking concerns. Thus, to offset the lower enrichments in these



burnable poison fuel pins, other pins need to have their enrichment increased. Therefore, the larger the number of gadolinium in the core greater the additional enrichment required in the other fuel pins. Hence, achieving a long operational cycle as long as possible requires average fuel enrichment as high as possible, which may result in conflict if a licensing limit on the enrichment is set (5% of U-235, for example).

#### 4.1.3.3 Core loading

Some iPWRs are designed to replace all the fuel after each operation cycle (once through or single-batch reload), mPower and SMR-160 are examples of this design. As the fuel is all fresh for each reloading, it simplifies the nuclear design because the same fuels with the same features (such as loaded in the same locations with the same enrichment and BP loadings) can be repeated for every operation cycle; therefore, once the nuclear design is optimized, it is purely duplicated for every cycle and for every reactor deployed.

Fresh fuel has a cosine-like power distribution with peaking at the center. Thus, loading all fresh fuel into the core without inserted control rods or axially varying BP distribution may result in peaking limits violations. Irradiated fuel has a much flatter axial power distribution. Thus, in cores with a mix of fresh and depleted fuel, the flattening influence helps to reduce the axial power peaking.

Loading all fresh fuel means that only control rods and BPs can smooth the power distribution across the core, which results in higher control rod and BP use in the designs rather than utilizing the lower excess reactivity that results because some of the fuel has been irradiated. As with fresh cores in large PWRs, the use of asymmetric BPs in certain core locations may be necessary to achieve the power peaking limits, increasing the fuel cost.

Additionally, fresh fuel loaded on the core periphery tends to have lower powers and lower resulting burnups than the power in fuel assemblies in the core center. As the fuel is loaded for only one operation cycle, there is no opportunity to reload the fuel to achieve higher burnups and ensure that all of the fuel within a given batch achieves similar burnups. This effect is an indication of how single-batch cores are not as efficient as multi-batch ones.

As can be observed in Table 4.1 [19], due to the power output required and the fuel management of the iPWRs under development today, there are significant variations in the fuel demands per reload. These examples indicate that iPWRs tend to require more fuel per GW year-electrical basis than a large PWR such as AP-1000. The outage time must be taken into account in the overall economics. For an iPWR with a three-year cycle length compared to an AP-1000 with a one-and-a-half year cycle length, the iPWR has half lesser outages for refueling and maintenance, representing approximately 750 more days generating power. Each iPWR design can operate with a range of fuel management schemes, depending on customer and market needs and overall economics, and further developments of the nuclear design options can continue during the development and demonstration phases.

#### 4.1.3.4 Other design considerations

For designs that do not use boron in the coolant, the MTC is more negative. Thus, for a given temperature variation up the core (core is colder at lower part than at upper part), there is a greater reactivity shift, resulting in power variation, with more reactivity and power at the bottom of the core. The iPWRs, with large temperature gradients from the bottom to the top of the core, have significant axial variations in power, which requires greater control over the reactivity and axial powers.

Additionally, extensive use of control rods and BPs in some iPWRs results in a harder neutron spectrum, which means a greater proportion of the neutrons are at higher energies because the absorbing materials capture thermal neutrons. The hardening of the spectrum has two consequences. Firstly, the harder neutron spectrum generates more plutonium in the irradiated fuel. The resulting plutonium can add more fissile material to the irradiated fuel, which reduces the initial U-235 enrichment requirements for the fuel. Secondly, the harder spectrum impacts the overall vessel, reflector, barrel fluence and may have adverse effects on the lifetime of those components.

From a fuel management perspective, having several iPWRs on the same site and sharing facilities, such as the spent fuel pool, brings advantages. When the fuel is reloaded for several cycles, fuels can be swapped between reactors resulting in a much more extensive selection of fuel to choose from to achieve the most economical and optimized core design, leading to more efficient use of the existing fuels and the potential to purchase less fuel over the lifetime operations of several units.

## 4.2 Essential Reactor Systems Components in iPWRs

The principle iPWR reactor coolant system (RCS) components are typically identical in function to similar components in large PWRs; only the size, the number, and the location of many of these components have been significantly changed.

An iPWR can be described, in the simplest way, compared to current PWR designs as “more water less pipe.” Due to the integral nature of iPWRs designs, the available water volume in an iPWR relative to the thermal power rating of the reactors is significantly increased compared with current PWR designs. Furthermore, the size and length of RCS piping are significantly reduced compared with current PWR designs. This feature reduces the need for many of the active safety components present in large PWRs, which increases the operator response time to plant disturbances.

In the following sections, individual components associated with the integral RCS and external systems and components connected to RCS are discussed. Differences and similarities with current PWR designs are highlighted. The secondary side of iPWRs and PWRs are very similar, except for the option for air cooling present in some iPWR designs. Thus the secondary side is not included in the discussion. A generic iPWR layout and key components are presented in Figure 4.4 [19].

### 4.2.1 Integral components

#### 4.2.1.1 Pressure vessel and flange

The typical PWR reactor pressure vessel (RPV) was described in Section 2.2.1. The RPV holds the individual fuel assemblies, the control rods, and a significant percentage of the reactor coolant. The RPV provides one of several safety barriers to fission product release and supports the control rods and the reactor vessel internals, which support the reactor fuel and direct coolant flow within the vessel. The RPV is usually a cylindrical vessel with a hemispherical bottom head and a removable, flanged, and gasketed, hemispherical top head [19]. The bottom head welds to the cylindrical shell, and the top head is bolted to the cylindrical shell via the flanges. The vessel is manufactured of low-alloy carbon steel clad on the inside with a thin layer of austenitic stainless steel. The RPV cylinder is typically made up of several thick-walled ring

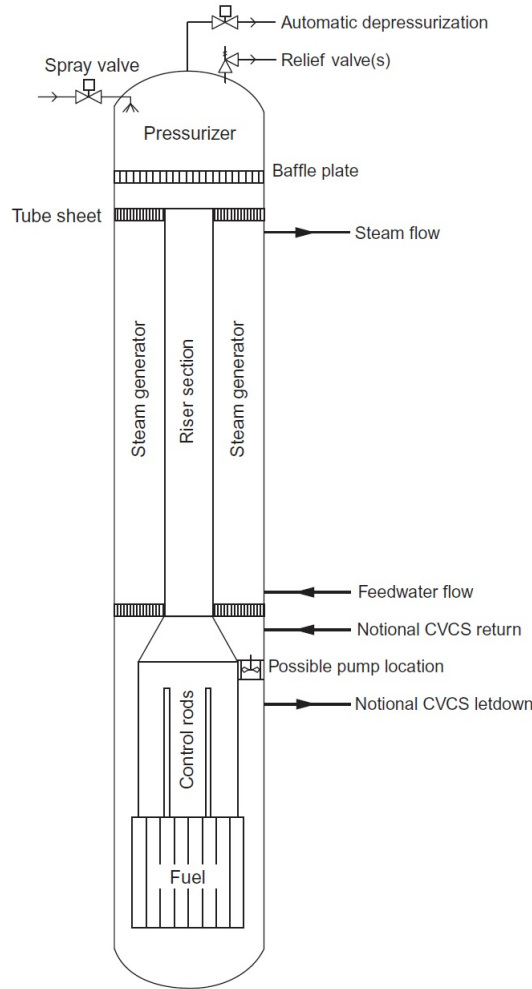


Figure 4.4: Generic iPWR components [19].

forgings that are welded together circumferentially. The circumferential weld closest to the fuel region of the vessel is usually called the beltline region. Figure 2.2 [16] presents a typical PWR RPV.

Currently, large PWR RPV concerns include vessel embrittlement, pressurized thermal shock (PTS), and primary water stress corrosion cracking [19]. Neutron embrittlement occurs over time once the vessel is exposed to the neutron flux. The area of significant concern for embrittlement is the vessel beltline weld. Introducing cold water while the vessel is pressurized may result in PTS, which produces increased thermal stress in the vessel wall. Over time, the vessel becomes brittle, and it can become more susceptible to cracking, especially due to the added stresses induced by PTS [19]. The presence of boric acid aggravates the primary water stress corrosion. Primary water stress corrosion cracking may compromise RPV integrity near the vessel head penetration nozzles and other flow areas. This effect may result in vessel leakage or, in more extreme cases, an increased potential for control rod ejection.

Large PWR RPV size depends on the number of fuel assemblies and excess reactivity necessary to achieve the desired power level and the fuel cycle length. Nevertheless, the ratio of cylindrical height to diameter in a current large PWR RPV ranges from 2 to 2.5, and the coolant pressure design is around 17.2 MPa [19]. The instrumentation vessel penetrations are generally below the fuel region in a PWR. The large inlet and outlet nozzles for providing reactor coolant to and from the vessel are just above the fuel area in the vessel.

Current iPWR RPV holds the pressurizer (PZR), the steam generator (SG), individual fuel assemblies, and control rods. Except for isolable support systems, such as the chemical and volume control system (CVCS), the entire reactor coolant inventory is inside the iPWR pressure vessel. An iPWR RPV performs the same roles as a current large PWR RPV. In an iPWR, the pressure vessel flange is usually located above the top of the fuel and below the integral SG, which is significantly different from the pressure vessel head flange in a large PWR. This arrangement facilitates refueling in the tall iPWR pressure vessels and SG inspection. The SMART iPWR is one exception, which retains the RPV flange at the vessel head. Besides, the SMR-160 uses an offset SG, allowing the RPV flange to remain at the vessel head. The SMR-160 is not a true iPWR because the SG is flanged externally to the RPV and is not internal to the vessel. In this case, the RPV flange remains at the vessel head.

As the fuel in iPWRs usually has half the height of current PWR fuel, the thick-walled ring forgings that constitute the iPWR vessel can be stacked such that no weld exists adjacent to the fuel, reducing the vessel embrittlement concern. Additionally, as can be observed in Figure 4.4 [19], the riser section needs to be sufficiently large in diameter to accommodate the motion of the control rods. Consequently, the internal position of the SGs in an iPWR design forces the RPV wall to be more distant from the reactor fuel than it is in a conventional PWR. Therefore, there is added water shielding in the downcomer region of the iPWR RPV relative to a conventional PWR, consequently reducing the RPV fluence and contributing to diminishing the vessel embrittlement concern. As the iPWR vessel materials are the same as current PWR designs, the PTS remains an operational concern for iPWR vessels. However, lessening the vessel fluence and the beltline weld embrittlement issue in the iPWR vessel likely contributes to the relaxation of the overall iPWR operating window for PTS compared to the current large PWRs. Additionally, some iPWR designs plan to use internal control rod drives, and others are planning to eliminate the use of boron chemical shim in normal operations. Those designs without boron diminish the primary water stress corrosion cracking concerns for iPWR pressure vessels.

Although iPWR RPV has a smaller volume than large PWR, the ratio of cylindrical height to diameter in a iPWR pressure vessel ranges from 4 to 7 [19], which is greater than the current large PWR. This ratio aids in promoting the natural circulation for emergency operations and normal operations in some iPWRs. Once almost the entire reactor coolant inventory is inside the RPV and not distributed in loop piping and other components, as in conventional PWRs, the natural circulation cooling is effective and efficient. Besides, because the pressure vessel includes additional components not included in large PWRs, the water volume relative to core thermal power is increased significantly. The coolant design pressure of an iPWR is equivalent to or slightly lower than current large PWRs.

Vessel penetrations in iPWRs are significantly different from large PWRs. In iPWRs, there are no penetrations below the top of the fuel; the instrumentation access is always above the fuel. Moreover, as there are no external coolant loops, the large PWR inlet and outlet piping penetrations, typically 70 to 79 cm [19], are eliminated in iPWRs, which practically eliminates any chance for large-break LOCA. The maximum vessel penetration in iPWRs is typically 5 cm or less for iPWR reactor support systems [19]. In addition, these penetrations are well above the top of the reactor fuel relative to large PWRs, which allows a significant amount of water to continue available to cool the reactor following a small-break LOCA.

#### 4.2.1.2 RCS piping

In large PWRs, the hot RCS water leaving the top of the reactor fuel is directed into the RCS hot leg piping. This piping, nominally 74 cm piping [19], connects to a U-tube or a once-through SG, where the heat is transferred from the primary circuit to the secondary circuit to generate steam which drives the turbine generator. The colder primary water exits the SG into the intermediate leg piping, nominally 79 cm piping [19], which connects to the suction side of the reactor coolant pump (RCP). The intermediate leg pipe is usually the largest diameter pipe in the RCS and is located below the top of the fuel assemblies, making a leak in this piping section the most problematic of all large-break LOCA. The RCP discharges into the 70 cm [19] RCS cold leg, which directs primary water back into the RPV. Large PWRs typically employ two, three, or four reactor coolant loops. A typical two-loop large PWR RCS is presented in Figure 4.5 [19].

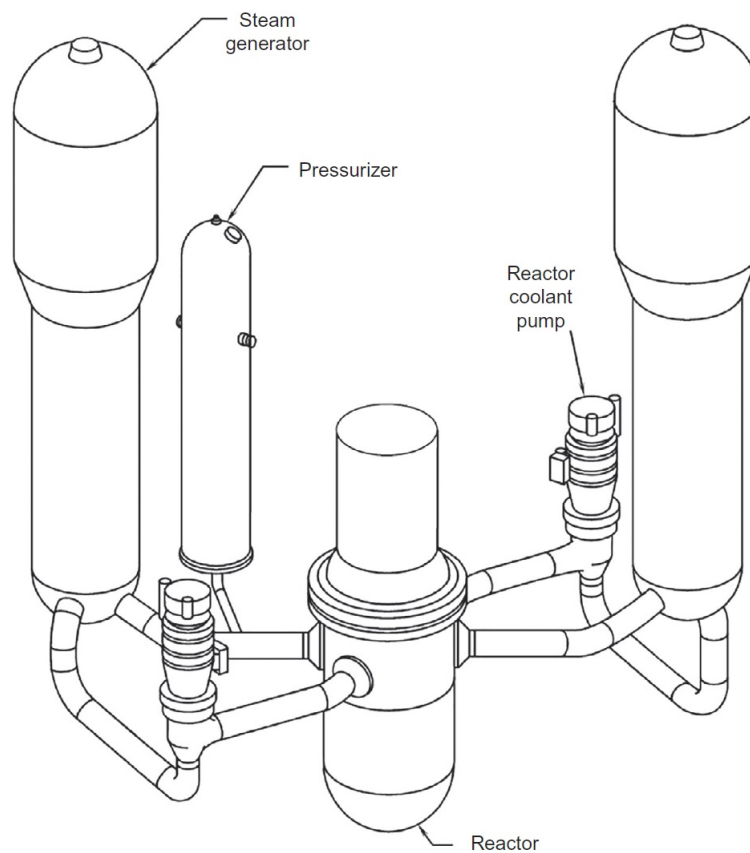


Figure 4.5: Typical two-loop PWR piping and component configuration [19].

As the PZR and SG functions are integrated into the iPWR pressure vessel, all the large diameter piping associated with current large PWRs are eliminated, eliminating any possibility of a large-break LOCA in all iPWRs. Thus, active emergency equipment, such as high-pressure injection pumps to mitigate the consequences of large-break LOCA, are also eliminated in iPWRs.

#### 4.2.1.3 Pressurizer, heaters, spray valve, pressurizer relief tank, and baffle plate

In PWRs, a PZR maintains the pressure of the primary coolant system in a range to avoid boiling occurs in the primary circuit under normal and transient operations. In current large

PWRs, the PZR is a separate cylindrical tank connected to the RCS piping by a surge line, nominally 25 cm [19] in diameter, and a spray line, nominally 10 cm [19] in diameter. Pressure is usually controlled using heaters and a spray valve to maintain the pressure range. A balance of water and steam exists in the PZR space. The water level in the PZR indicates water inventory present in the RCS. Some large PWRs also use a power-operated relief valve (PORV) connected to a PZR relief tank to assist in the pressure control. The PORVs open to reduce the pressure before the system reaches the RCS safety valve relief set point. A PORV stuck open is a potential small-break LOCA initiating event.

The PZR provides the surge volume for the RCS. If RCS temperature water increases, the less dense water surges into the PZR, compressing the steam space and increasing the primary pressure. Steam begins to condensate to lower the pressure, which may be sufficient for small or slow transients associated with a minor RCS temperature change. However, commonly, pressure rises to the spray valve set point. The open spray valve admits colder primary water from the RCS cold leg into the steam space to rapidly condense steam and reduce pressure. The discharge pressure of the RCP drives the spray flow. On the other hand, if RCS temperature water decreases, the denser water causes water to flow out of the PZR into the RCS hot leg, expanding the steam space and decreasing the primary pressure. Thus, PZR heaters heat the PZR water to increase pressure. Large PWR PZR was discussed in Section 2.2.4.

The iPWRs integrate the PZR into the top of the RPV. A baffle plate or a head plate with drilled openings separates the PZR from the RCS and acts as a surge line. Due to the integral nature of the PZR, the surge line is eliminated. The volume of an iPWR PZR is considerably larger than a current large PWR PZR relative to reactor thermal power; for some designs, the PZR volume is about five times larger per unit of power than large PWRs [19]. This larger PZR volume, coupled with larger RCS water inventory overall relative to reactor thermal power, generally provides slower pressure transients. Consequently, an operator has more time to analyze changes in plant operating conditions and respond accordingly. Besides, the need for a fast-acting spray valve is eliminated because, in most cases, the natural steam condensation following a slower in-surge of coolant into the large volume PZR adequately maintains the pressure of the RCS under normal operations and expected transients. The integrated location of the PZR in iPWRs also provides a more direct indication to the operator of the water level directly above the top of the reactor fuel.

In many iPWRs, the normal spray valve is eliminated because it is not essential to fine-tune the system pressure, and in designs without RCP, there is not enough driving head in the RCS to provide adequate spray flow. Even in iPWRs employing smaller RCP, the driving head created in RCS is much lower than that in large PWRs. Larger PWRs also employ an auxiliary spray valve to backup the normal spray valve when the RCP is unavailable or the normal spray valve is inoperable. The auxiliary spray valve is typically driven by the charging pump discharge (from the chemical and volume control system). Some iPWRs are likely to use this approach to include the PZR spray function. Thus, the spray line is not necessarily eliminated in iPWRs but is generally limited to less than the 10 cm diameter employed in large PWRs. PZR heaters in iPWRs function the same as the heaters in large PWRs.

PORVs are not incorporated into iPWR PZR design. A stuck open PORV was the cause of the Three Mile Island accident, which is eliminated in the iPWRs. The safety relief valve discharge is directed to the containment or another storage tank inside the containment. Therefore the PZR relief tank also is not incorporated in iPWRs. Additionally, piping to provide nitrogen cover gas on the PZR relief tank and the need for a drain system and an associated pump are eliminated in iPWRs. In large PWRs, the nitrogen is used to provide an overpressure to the pressure relief tank to help condense steam and keep an inert atmosphere.

#### 4.2.1.4 Pumps

The RCP provides primary coolant flow to remove heat generated by the fission process. Large PWRs utilize one or two RCP per loop to provide the forced coolant flow through the primary system. The natural circulation does not provide sufficient flow to remove the heat generated during power operations. Each 4500 to 7500 kW pump provides a flow of approximately 400 m<sup>3</sup>/min to remove the heat produced by the fuel assemblies for delivery to the SGs. A driving head of approximately 0.6 MPa is generated by the RCP [19]. In current large PWRs, a loss of one or more RCP results in a reactor trip. These large pumps have a seal to limit leakage, and the seals require cooling, which presents a risk of small leaks and intersystem leakage. The newer PWRs generation, like the AP-1000 design, use a canned RCP to eliminate this possibility. Large PWR RCP was discussed in Section 2.2.3.

The integral nature of the iPWR pressure vessel makes the use of RCP more challenging. Several iPWRs plan to incorporate multiple RCP. Due to space limitations in the primary flow path, it is not possible to incorporate the RCP used in current large PWRs. Thus, smaller RCPs are required in these designs to deliver the necessary flow. While specific RCP design detail is not yet available, the resulting driving head is likely to be smaller. A canned type pump is likely to be incorporated. The pumps may be installed in the hot leg at the top of the SGs or in the cold leg beneath the SGs. As an example, the inactivated mPower was intended to use 12 pumps. The Korean SMART iPWR design plans to use four canned RCPs [19]. The NuScale and the SMR-160 design do not plan to use RCPs, but natural circulation cooling. All iPWR designs are capable of removing reactor decay heat by natural circulation cooling following a reactor shutdown. Therefore, dedicated AC backup is not required for the designs using RCPs.

#### 4.2.1.5 Riser

Once SGs are integral to the pressure vessel, it is required an area within the vessel to upward reactor coolant flow from the fuel assemblies to the upper tube sheet at the top of the integral SGs. This area is called the riser section, which is analogous to the RCS hot leg in large PWRs. At the top of the riser section, coolant flow is directed down into the integral SGs. The riser also provides space for the control rod drive mechanisms to operate.

#### 4.2.1.6 Steam generators and tube sheets

Current large PWRs use two to four separate large SGs, one for each coolant loop. These SGs are U-tube or once-through type heat exchangers (see Section 2.2.2). In both cases, the higher pressure primary water flows inside the SG tubes, and the lower pressure secondary fluid is outside the tubes. In U-tube SG designs, dry slightly saturated steam is delivered to the turbine generator, while in once-through SG design, supersaturated steam is delivered [19].

These SGs have up to 22 m in height and contain 3000 to 16 000 tubes welded to a tube sheet. The SG tube sheet and tubes are part of the RCS boundary. An SG tube rupture provides a short circuit path for the primary coolant to escape containment with the secondary fluid. SG tube issues include tube bending, wastage, thinning, corrosion, flow-induced vibration, cracking and deformation of U-tube bend or support plates, tube leakage, and fractures [19].

The most developed iPWR designs plan to use two principle SG heat exchangers designs. The first design is a once-through helical-coil tube SG. The second design is a once-through straight-tube SG. There is no evidence that the U-tube SG design to be used in current iPWRs, eliminating the most significant current SG tube concerns regarding cracking and deformation of

the U-tube bend. The helical-coil tube SGs provide additional heat transfer surface in a limited space, and the helical fluid flow generates less flow-induced vibration. Also, helical-coil tube SGs reduce thermal stress on the feedwater and steam headers generated by thermal expansion of the tubes. Once-through straight-tube SGs also have little flow-induced tube vibration. Therefore, fewer tube supports are required, limiting low fluid flow areas and the associated corrosion concern. However, once-through straight-tube designs generate larger thermal stress on the feedwater and steam headers due to the thermal expansion of the tubes. Helical-coil tube SGs are more costly to manufacture than once-through straight-tube SG due to the complexity of the design, but the cost and complexity are worth the stress reduction on the SG headers and the increase in heat transfer area compared with the once-through straight-tube SG design.

The NuScale iPWR design plans to utilize two separated intertwined helical-coil tube SGs with the high-pressure primary fluid outside the SGs tubes and the lower pressure secondary fluid inside the SG tubes, as shown in Figure 4.6 [20]. The SMART iPWR is designed to use eight separate mini helical-coil tube SGs in the downcomer space around the reactor pressure vessel riser section [19]. The CAREM iPWR is designed for 12 separated mini helical-coil tube SGs in the downcomer space. These three designs produce superheated steam. In the SMR-160, an SG and superheater directly flanged to the top section of the RPV are employed. This design has the advantage of providing more direct access to the reactor fuel during the refueling process. In Section 4.3 these SMR designs are briefly presented.

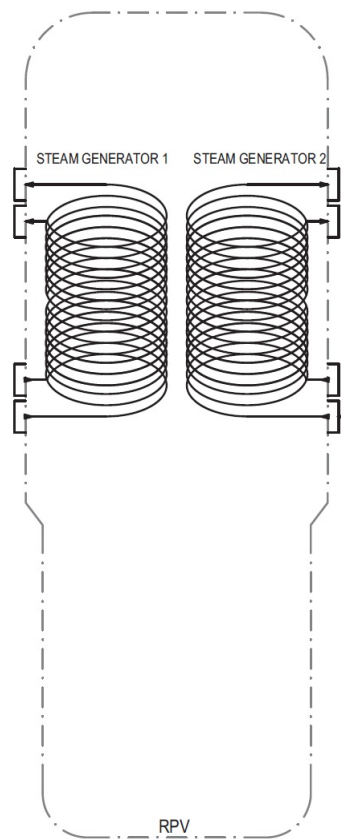


Figure 4.6: SGs simplified diagram in NuScale design [20].



#### 4.2.1.7 Control rods and reactivity control

Control rods act to control the fission rate by inserting or withdrawing neutron absorbing material from the reactor fuel core. Large PWRs typically use  $17 \times 17$  fuel assemblies with guide tubes for 24 control rod fingers, which are operated together using a spider assembly. Even though all fuel assemblies can host a control rod assembly, not all fuel assemblies are fitted with control rod assembly. Control rods usually are split into two groups, control groups, and shutdown groups. The shutdown groups are entirely withdrawn from the core to provide a significant source of negative reactivity to shut down the reactor in case of an accident. Control groups are usually partially inserted into the core and are slowly withdrawn over the fuel cycle to compensate for fuel burnup and keep operating temperature.

Soluble boric acid to the reactor coolant is used as a second method to control reactivity in large PWRs. Boric acid, a strong neutron absorber, is referred to as chemical shim. At the BOL, the RCS is heavily borated and then slowly diluted over the fuel cycle together with control rod movement to compensate for the excess reactivity needed to provide a 12 to 24 months fuel cycle.

Some iPWR designs plan to use a half-height version of the  $17 \times 17$  array fuel assemblies, allowing similar spider assembly rods to be used. The iPWR cores contain fewer fuel assemblies than large PWRs and have a higher percentage of fuel assemblies fitted with a control rod spider assembly to control excess reactivity. Some iPWRs may fit a very high percentage of fuel assemblies with a control rod spider assembly and opt not to use the chemical shim for normal reactor operation. However, most iPWRs use concentrated boron as an emergency backup to shut down the reactor when not all control rods can be inserted into the core. Thus, support systems for boric acid batches production are required in most iPWRs.

#### 4.2.1.8 Control rod drive mechanisms

In large PWRs, control rod drive mechanisms (CRDMs) are external to the reactor vessel above the reactor vessel head. For refueling, the CRDMs are decoupled from the control rod spider apparatus, and the control rods are left in the respective fuel assemblies while the head is removed.

Some iPWRs plan to continue using the CRDMs external to the reactor vessel. However, since RPV is much taller than the current PWR pressure vessel and the iPWR pressure vessel flange is not located at the top of the pressure vessel, some design considerations are necessary on how the shaft of the control rod spider is decoupled from the CRDM and protected when the upper RPV is removed from the lower RPV for refueling. SMART and NuScale designs plan to use external control rods [19].

Other iPWRs intend to use CRDMs internal to the RPV, which requires some materials and reliability testing due to the high temperature and pressure environment inside the RPV. Electrical cabling is necessary to penetrate the RPV flange to operate the CRDMs and provide control rod position indication. Radiation effects on internal CRDMs are mitigated relative to large PWRs by the column of water in the taller SMR vessel.

#### 4.2.1.9 Automatic depressurization system valves

The most recent large PWR designs, such as the AP-1000, use automatic depressurization systems (ADS) to allow primary pressure to be rapidly reduced, following a LOCA, to allow low-pressure injection systems or gravity-fed water sources to supply water to the reactor to keep the core covered.

The iPWR designs also include an ADS into the protection systems. This system has the same function as in large PWRs. Generally, the ADS is initiated by opening valves connected to the PZR steam space. The steam is typically directed into a water-filled storage tank inside the containment or collected directly within the containment for recycling back into the core to keep the fuel covered. The water from the containment storage tank located in a high place in the containment can be injected into the reactor vessel by the gravity after the pressure has been reduced to the atmospheric pressure.

#### **4.2.1.10 Relief valves**

Safety relief valves are included in large PWR reactors to protect the RCS from exceeding the design pressure (see Section 2.2.4). The valves relieve steam to PZR relief tank and are connected to this tank via 15 cm pipelines [19].

The iPWR designs also require safety relief valves. The valves are connected to the PZR steam space at the top of the integrated RPV. However, the connecting pipes are smaller than the 15 cm lines employed in large PWRs. As with ADS valves, the steam relieved from an iPWR relief valve is directed into a water-filled storage tank inside the containment or released directly into the containment environment. PZR relief tank is not used in iPWRs.

#### **4.2.1.11 Core basket, core barrel, core baffle**

Core basket assembly is used in large PWRs to support the RPV internal assemblies (see Section 2.2.1). These assemblies usually include a cylindrical core barrel to separate and preheat the incoming cold leg reactor coolant from the fuel assemblies. A thermal shield surrounds the core barrel. The core barrel directs the cold leg coolant to the bottom of the core. The fuel assemblies are supported inside the core barrel. A core baffle is used to adapt the square fuel assemblies to the shape of the cylindrical core barrel. The iPWR designs have the same arrangement [19].

#### **4.2.1.12 Instrumentation**

The ability to monitor core conditions is fundamental in iPWR designs and differs in implementation from the large PWRs. Measurements obtained from PWR operating loops, such as reactor flow, need to be implemented within the reactor vessel. Despite its importance, the instrumentation is out of the scope of this work. Further information can be found in Reference [19].

### **4.2.2 Connected system components**

#### **4.2.2.1 Chemical and volume control system (CVCS)**

As discussed in Section 2.2.5, CVCS is a vital support system present in large PWRs. It functions to purify the RCS, increase or decrease the coolant boron concentration, and maintain the reactor coolant inventory. A continuous flow of reactor coolant is let down to the CVCS, where it is cooled, cleaned by filters and demineralizers, reheated, and pumped back into the primary system using a charging pump. The chemical shim is adjusted by adding more borated water or adding more demineralized water back into the primary. Reactor coolant inventory can be adjusted by mismatching the letdown flow and the reinjection flow. Reactor chemistry is controlled through the CVCS volume control tank.

As the functions of the CVCS are essential for continued long-term operation of the reactor, all iPWR designs require a similar support system, which requires a system external to the RPV connected to the primary system in the RPV. This system does not have safety-related functions, so a dedicated AC backup is not necessary. However, the system needs to be isolable from the RCS. This isolation function is safety-related.

The CVCS provides heat exchangers to cool the primary fluid to protect the demineralizers. Thus, some iPWR designs take advantage of this system to provide a means to remove decay heat after reactor shutdown, which is possible due to the lower thermal power generated by iPWRs. The CVCS heat exchangers in large PWRs are not sized for this decay heat removal function.

#### **4.2.2.2 Residual heat removal and auxiliary feedwater systems**

Large PWRs require to be cooled down after the reactor shut down to provide for system maintenance and refueling operations. Under normal operations, large PWRs cool down in two stages. Initially, the secondary system is employed to remove heat from the primary by dumping steam to the condenser via the turbine bypass system until system temperature no longer supports sufficient boiling. At this point, a forced-flow residual heat removal system (RHRS) removes reactor decay heat using a heat exchanger cooled by forced-flow safety-related component cooling water system (CCWS), see Section 2.2.7. The CCWS is cooled by the safety-related forced-flow plant service water system. The RHRS is not designed to operate at the temperature and pressure required at the start of plant cool down, then a two-step process is required.

In the event of LOCA, large PWRs employ a diverse auxiliary feedwater system (AFWS) using steam-driven, diesel-driven, or moto-driven (powered by a safety AC bus) feedwater pumps (see Section 2.2.6). These pumps draw water from a large condensate storage tank to provide water for continued steam generation. The steam is dumped into the atmosphere, allowing continued removal of decay heat from the primary. When insufficient steam is generated, the RHRS and related support systems, all powered by a safety AC bus, continue the plant cooldown to cold standby.

All iPWR designs plan to use the secondary system to initially remove decay heat under normal operating conditions. Then, some designs plan to use a non-safety-related forced-flow RHRS to assume the cooling down when steam is insufficient for heat removal during normal operations. However, different from large PWR designs, all iPWRs employ a passive decay heat removal system to remove the maximum core decay heat generation after a reactor trip. Heat is rejected to large plant water tanks capable of removing heat for 72 hours or more without refilling. Consequently, no diesel safety AC bus is required to support forced-flow RHRS, CCWS, or service water heat removal system in iPWRs. Water from a tanker truck can provide additional cooling water further than the initial 72 hours, or air cooling may be sufficient to further cooling.

#### **4.2.2.3 Emergency core cooling system and refueling water storage tank**

After a LOCA, large PWRs employ an emergency core cooling system (ECCS) to mitigate core damage (see Section 2.2.8). This system injects large amounts of cool, borated water into RCS. The ECCS also provides highly borated water to guarantee the reactor remains shut down following the cooldown associated with a main steam line rupture. This water source is the refueling water storage tank (RWST), which is located external to the containment, except

in the AP-1000 PWR design. Subsystems taking suction from this tank include high-pressure injection or charging pumps, intermediate-pressure injection pumps, and the low-pressure injection or RHRS. Besides, containment spray pumps take suction from the RWST to limit a containment pressure spike following a LOCA or a steam line rupture inside the containment (see Section 2.2.9). Some large PWRs employ cold leg accumulators that inject borated water into the reactor when pressure falls below the injection set point. These systems are safety-related and are backup-powered by the plant emergency diesel generators. Figure 2.11 [16] presents a typical large PWR ECCS.

Similar to the AP-1000, many iPWR designs have included the RWST inside the containment. The level of the RWST is well above the level of the top of the fuel. The iPWRs have eliminated large-break LOCAs by eliminating all large-bore piping. Small-break LOCAs are likely not to exceed the capacity of the CVCS charging pump. Additionally, the small-bore piping connected to an iPWR RPV is isolable as close as possible to the vessel, limiting the probability of a small-break LOCA. In case of a leak, ADS valves function to reduce pressure at a point where water from the RWST can be fed by gravity into the RPV to maintain the core covered. All ECCS cooling is performed by natural circulation. Thus, the various ECCS pumps do not require backup from emergency diesel generators in iPWRs.

Gravity-fed boron injection tanks are also used in many iPWRs. These tanks, located high inside the containment, ensure that the reactor remains subcritical following an accident. The tanks are a source of poison and provide an additional water source for emergency decay heat removal.

The iPWR containment designs are projected to be passively cooled to limit pressure spikes after an accident. In the NuScale design, the containment shell is designed to accept significantly higher pressure than a current large PWR design. Thus no containment spray is planned for the iPWRs, except the SMART reactor [19].

#### **4.2.2.4 External pool**

In the NuScale, the containment vessels sit in a shared open external tank referred to as the reactor pool. The NuScale containment conforms tightly to the reactor vessel without room for any additional water tank. Thus, the NuScale reactor pool provides the emergency heat sink function provided by internal RWST in other iPWRs. Additionally, the NuScale reactor pool provides an extra barrier to fission product release. The NuScale containment is kept under vacuum to enhance its heat transfer characteristics; thus, equipment is required to maintain the vacuum [19].

#### **4.2.2.5 Control room habitability equipment**

Large PWR designs require equipment to maintain the control room habitability after an accident or toxic gas release. The iPWR designs also have the same need. While large PWRs rely on safety-related AC backup-powered equipment for long-term functioning, the iPWRs rely on passive systems designed to work at least 72 hours, which requires the use of batteries and compressed air systems dedicated to this purpose.

#### **4.2.2.6 Diesel generators and electrical distribution**

Large PWRs require safety-related AC power backed up by an emergency diesel generator (EDG) to guarantee that the active safety-related equipment function when required. There

usually are two EDGs per large PWR onsite [19]. The EDGs are governed by plant technical specifications and have to be tested at least once a month. Every six months, each EDG must be shown to come up to speed and voltage and begin the loading sequence within 10 seconds of receiving a start signal. Although necessary to prove the safety basis of the plant, these tests can be harmful to the EDGs. Additionally, if one EDG is declared inoperable, the remaining EDG must be tested within 24 hours. Thus, in large PWRs, the EDGs are tested frequently, resulting in higher maintenance requirements.

In many iPWR designs, the diesel generators do not have a safety-related function; they become additional power supplies that enhance iPWR defense-in-depth by maintaining the availability of normal operating equipment that are not safety-related. These auxiliary diesel generators can be tested less frequently, and fast load testing can be relaxed such that the diesel generators can warm up for a few minutes before loading. Therefore, less maintenance is expected for the iPWR auxiliary diesel generators.

Large PWRs maintain EDG-backed up safety-related AC buses at 480 and 4160 V AC to operate active safety equipment. Additionally, safety-related power to operate instrumentation during and following an accident is required. This power is provided by battery-backed up 120 V DC and low voltage AC through an inverter. In iPWRs, there are no active safety-related equipment components; thus the high voltage safety-related buses are not required. However, power to reposition any iPWR safety-related valves is required. Thus, battery-backed up 120 V DC and low voltage AC through inverter are used to provide power for repositioning valves and powering instrumentation. Therefore, electrical distribution systems of large PWRs and iPWRs are similar, but the approach and amount of testing and maintenance differ.

## 4.3 Some Small Modular Reactors Today

The earliest concepts of small modular reactors (SMRs) emerged in the 1970s for merchant ship propulsion and industrial process heat applications. Nowadays, there are more than 50 designs with commercial involvement ranging from minor evolutions of operational reactors to fission-fusion hybrid designs [19]. Due to the significant number of designs, it is not easy to overview all projects that are being developed worldwide. As mentioned before, the interest of this work is to focus on PWRs; thus, only this type of reactors is discussed here. Additionally, the designs discussed here have an electrical output ranging from 27 MWe to 300 MWe. The description presented is a brief overview of the main features; only the description of the NuScale design includes more detailed information. Furthermore, as a means of comparison, the EPR (Evolutionary Power Reactor) description, which consists of a model capable of producing 1650 MWe, is also presented. For the EPR, the same information discussed for the NuScale design is included. Further information about the others designs can be found in references [7], and [19].

### 4.3.1 CAREM

CAREM (Modular Elements of Central Argentina) is an Argentinian design with a 27 MWe capacity (prototype) designed to supply energy to regions with small demands. It can also support seawater desalination processes to supply water to coastal sites. It has distinctive and characteristic features that simplify the reactor and also contribute to a higher level of safety: integrated primary cooling system, primary cooling by natural circulation, self-pressurization, and safety relying on passive features [19].

CAREM RPV contains the core, the SGs, the whole primary coolant, and the absorber rods drive mechanisms. The RPV diameter is 3.2 m, and overall length 11 m (see Figure 4.7 [19]).

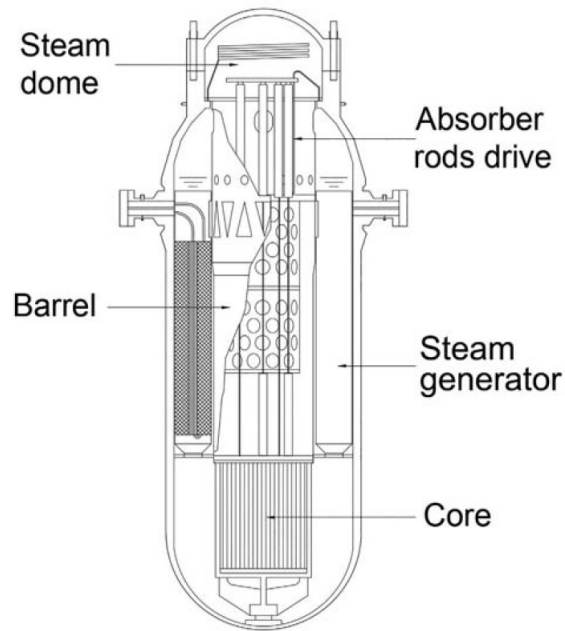


Figure 4.7: CAREM reactor pressure vessel and internals [19].

The core is composed of 61 hexagonal fuel assemblies with about 1.4 m of active length. Each fuel assembly has 108 fuel rods and 18 guide thimbles, and one instrumentation thimble. The fuel is 1.8% - 3.1% enriched  $\text{UO}_2$ . Core reactivity is controlled by  $\text{Gd}_2\text{O}_3$  used as burnable poison installed in specific fuel rods and by 25 movable elements that use as absorbent material Ag-In-Cd alloy. The coolant does not contain diluted boron for reactivity control. Each movable element consists of a cluster of rods linked by a structural element, where the cluster moves as a single unit. The movable elements fit into the guide thimbles. Besides used for reactivity control during normal operation, the movable elements are employed as a fast shutdown system. The core burnup is 24 GWd/ton (prototype), and the refueling cycle is 14 months. The designed operational life is 40 years.

The primary coolant flows over the shell side of 12 identical compact helical-coil tube SGs of the once-through type. The SGs are placed equally distant from each other along the inner surface of the RPV. The SGs transfer heat from the primary to the secondary circuit, producing dry steam at 4.7 MPa with at least 30 °C of superheating. The natural circulation in the primary circuit is induced by placing the steam generator above the core. The core inlet and outlet temperatures are 284 °C and 326 °C, respectively. The secondary system circulates upward within the tubes while the primary goes in a counterflow. For safety, the SGs are designed to withstand the primary pressure without pressure on the secondary side, and the live steam system is designed to withstand primary pressure up to isolation valves in case of an SG tube brake.

The self-pressurization of the RPV (steam dome) keeps the pressure very close to the saturation pressure at all operating conditions, including transients. The self-pressurization is achieved by balancing steam production and condensation in the vessel. The primary pressure operation is 12.25 MPa.

The safety systems of CAREM are based on passive features and must guarantee that there is no need for active actions to mitigate the accidents during a prolonged period. The

systems are duplicated to fulfill the redundancy criteria. The safety systems consist of two reactor protection systems, two shutdown systems, two passive residual heat removal systems (PRHRs), safety and depressurization valves, low-pressure injection system, and containment of pressure suppression type (pressure suppression pool) designed to withstand the pressure of 0.5 MPa.

Each shutdown system can maintain the core subcritical. The first shutdown system consists of the 25 movable elements with neutron-absorbing elements located over the core, which fall by gravity when needed. Internal hydraulic control rod drives avoid mechanical shaft crossing the RPV, thus eliminating any possibility of a LOCA as the whole device is located inside the pressure vessel. Nine out of 25 movable elements are fast shutdown systems, which are kept in the upper position during the normal operation. The second shutdown system is a gravity-assisted high-pressure injection of borated water from two tanks at high pressure located in the upper part of the containment, which actuates automatically when the first shutdown system fails is detected.

The PRHRs are heat exchangers that remove decay heat from the core by natural circulation. The heat exchangers are located in pools filled with cold water inside the containment building. The heat removed is transferred to the pools and then consequently transferred to the suppression pool of the containment. Only one out of two PRHRs guarantees the core decay heat removal during 36 hours in case of loss of heat sink or station blackout. Besides, two redundant diesel generators provide emergency supply for active cooling systems for an extended period.

The emergency injection system prevents core exposure in the case of LOCA. The system consists of two pressurized tanks with borated water connected to the RPV. When LOCA happens, the primary system is depressurized with the help of the PRHR to less than 2 MPa with water level over the top of the core. At this pressure, the low-pressure water injection system starts to inject water into the RPV. The integrity of the RPV against overpressure is guaranteed by safety relief valves that blow steam to the suppression pool. The primary steam, safety systems, the reactor coolant pressure boundary, and high-pressure components of the reactor auxiliary systems are enclosed in the primary containment (a cylindrical concrete structure with an embedded steel liner). This containment is of pressure suppression type having a dry and a wet well. The lower part of the wet well is filled with water that works as a condensation pool, and the upper part is a gas compression chamber. Provisions are considered for hydrogen control and reactor pressure vessel lower head cooling by the in-vessel corium retention.

The CAREM prototype construction began in 2014, and the first criticality of the prototype is scheduled for 2023 [7].

### 4.3.2 ACP-100

The ACP-100 is a Chinese design with a capacity of 125 MWe, designed for electricity generation, heating, steam production, and seawater desalination, which can be installed in remote areas with limited energy options or limited industrial infrastructure. ACP-100 is an iPWR with forced circulation of the primary coolant. Externally mounted RCPs drive the forced circulation. Four canned motor pumps are installed nozzle to nozzle to the RPV. The PZR is external to the RPV. The primary pressure operation is 15 MPa. The core inlet and outlet temperatures are 286.5 °C and 319.5 °C, respectively. The RPV diameter is 3.35 m, and overall length 10 m. Figure 4.8 [7] shows the ACP-100 reactor with other main equipment connected.



Figure 4.8: ACP-100 reactor with other main equipment connected [7].

The core is composed of 57 fuel assemblies with a total length of 2.15 m. Each fuel assembly has a square  $17 \times 17$  configuration. The fuel is 4.2% enriched  $\text{UO}_2$ . For reactivity control,  $\text{Gd}_2\text{O}_3$  is used as a burnable poison, and there are 20 control rods. Also, the coolant contains diluted boron. The refueling cycle is 24 months. The designed operational life is 60 years.

There are 16 once-through SGs, which are mounted within the RPV. The SGs produce steam at 4.5 MPa at a temperature over 290 °C. The main feedwater temperature is 140 °C.

The ACP-100 is designed with inherent and passive safety features. The safety system of ACP-100 consists mainly of the PRHRS, passive emergency core cooling system, passive containment air cooling system, and reactor ADS. Enhanced safety and physical security of ACP-100 are made possible by arranging the nuclear steam supply system underground. Severe accident mitigation is achieved by passive reactor cavity flooding preventing the RPV melt, passive hydrogen recombination system preventing containment hydrogen explosion, automatic pressure relief system, and RPV off-gas system to remove incondensable gases gathered at RPV head.

The PRHRS consists of one emergency cooler and associated valves, piping, and instrumentation. The emergency cooler is in the in-containment refueling water storage tank (IRWST), which is the heat sink for the emergency cooler. The system removes the decay heat from the core by natural circulation and provides cooling for seven days without operator intervention.

The emergency core cooling system consists of two coolant storage tanks (CSTs), two safety injection tanks (SITs), the IRWST, and associated injection lines. The ACP-100 has a safety-related DC power source to support accident mitigation for up to 72 hours and auxiliary power units to recharge the battery system for up to seven days. After the LOCA, the steam in containment is condensed continuously at the internal containment face resulting in heat conduction to the containment, which is cooled by the passive containment air cooling system.

The passive IRWST provides water for the emergency reactor core cooling system in the condition of LOCA and steam pipe rupture. The tank also absorbs the sprayed steam from the reactor cooling system during the reactor ADS operation. This tank also works as the heat sink of the PRHRS.

A demonstration plant is being constructed in Changjian Count, Hainan Province in China. A preliminary safety analysis report was completed in 2018, and initial site preparations and



manufacturing were begun in 2019 [19].

### 4.3.3 System-Integrated Modular Advanced Reactor (SMART)

The SMART is a South Korean design with a capacity of 107 MWe, designed for electricity generation, seawater desalination, heating, process heat for industries, and suitable for small or isolated grids. SMART is an iPWR where the RPV contains the reactor core, PZR, four canned motor RCPs, eight SGs, CRDMs, and reactor internals. The integrated arrangement of these components allows the removal of large-sized pipes connections between major components of the RCS, reducing the possibility of large-break LOCA. The large volume of the primary coolant provides large thermal inertia and a long response time, enhancing the resistance to systems transients and accidents. The large free volume in the top of the RPV located above the reactor water level is used as an in-vessel PZR, which can accommodate a wide range of pressure transients due to its large volume. The PZR keeps the primary pressure operation at 15 MPa due to the large PZR steam volume and a heater control without spray. Eight SGs are located equally spaced at the circumferential periphery inside the RPV and high above the core to allow natural circulation when necessary. The core inlet and outlet temperatures are 296 °C and 322 °C, respectively. The RPV diameter is 6.5 m, and overall length 18.5 m. Figure 4.9 [19] presents a scheme of the RPV.

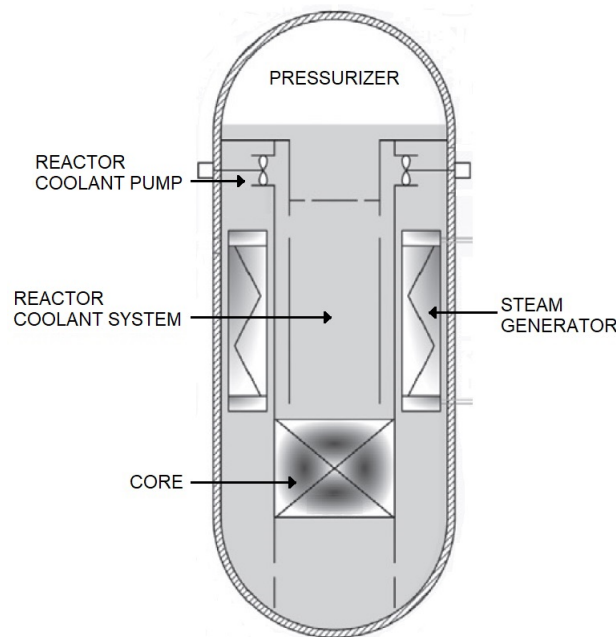


Figure 4.9: Simplified scheme of the SMART RPV [19].

The SMART core is composed of 57 fuel assemblies with a total length of 2 m. Each fuel assembly has a square  $17 \times 17$  configuration. The fuel is 5% enriched  $\text{UO}_2$ . For reactivity control, there are 25 control rods and soluble boron in the coolant. Besides, burnable poison is used to give flat radial and axial power profiles. The core burnup is approximately 54 GWd/ton, and the refueling cycle is 30 months. The designed operational life is 60 years.

There are eight identical once-through SGs with helical-coil tubes mounted within the RPV. The primary reactor coolant flows downward in the shell side of the SGs, while the secondary feedwater flows upward inside of the tube. The secondary feedwater evaporates in the SGs, producing steam at a 30 °C superheated condition with 5.8 MPa. In case of an abnormal

shutdown, the SGs can be used as the heat exchanger for the PRHRS, allowing an independent operation of this system from the hydraulic condition of the primary system.

SMART has four canned motor RCPs horizontally installed on the upper shell of the RPV. A canned motor pump does not require a pump seal which practically eliminates a small-break LOCA associated with pump seal failure. The four pumps produce forced circulation in the RCS, and due to this circulation, the core heat is delivered to the secondary system via SGs. The RCS and its supporting systems are designed with a sufficient core cooling margin for protecting the reactor core during all normal operations and anticipated operational occurrence.

The safety systems of the SMART include a mix of proven technologies and advanced design features. The systems consist of the reactor shutdown system, the PRHRS, the passive safety injection system (PSIS), the containment pressure and radioactive suppression system (CPRSS), PZR safety valves, ADS, and severe accident mitigation system. The reactor can be shut down under any circumstances by control rods insertion or boron injection. The reactor containment is resistant to any seismic activity and can withstand possible airplane crash incidents.

When the common decay heat removal mechanism using the secondary system is not operable, the PRHRS brings the reactor to a safe shutdown condition by natural circulation within 36 hours after the accident. Besides, it maintains the safe shutdown condition for additional 36 hours without operator corrective actions or aid of external AC power. The safety function of the PRHRS is maintained continuously for an extended period when the emergency cooldown tank (ECT) is refilled periodically by the PRHRS ECT refilling system. The PRHRS consists of four independent trains, and each train is constituted by one ECT, a PRHRS heat exchanger, and a PRHRS makeup tank.

The PSIS consists of four mechanically independent trains, and each train is constituted by one core makeup tank (CMT) and one safety injection tank (SIT) with related valves and instrumentation equipment. The PSIS provides emergency core cooling after postulated accidents. The emergency core cooling uses the CMTs and the SITs that keep the cooling inventory through the passive safety injection. The CMTs are full of borated water and provide makeup and boration functions to the RCS during the early stages of small-break LOCA or non-LOCA occurrences. The safety injection function of the PSIS is maintained for an extended period by periodically refilling the SITs.

The ADS consists of two trains, and each train is operated automatically when the water level of the CMTs reaches the designed setpoint level. The ADS lowers the RCS pressure so that gravity head injection from the SITs can be available at an early stage in LOCA. The ADS can be manually operated in the case of a total loss of the secondary heat removal accident. The ADS can depressurize the RCS below the operating pressure of a refilling system within at least 72 hours after LOCA, without operator or AC power aid.

The containment system is designed to secure the environment against primary coolant leakage and to contain radioactive fission products within the containment building. The CPRSS passively performs its safety function. The containment system is composed of the lower and upper containment areas, the IRWST, the CPRSS, and the CPRSS heat removal system. In the condition of a main steam line break or LOCA, part of the released energy is absorbed in the IRWST, and the remaining is removed to the environment by the CPRSS heat removal system. Fission products are scrubbed in the IRWST. Passive autocatalytic hydrogen recombiners are installed inside the low and upper containment areas to control combustible gas.

In 2016, Saudi Arabia agreed to pursue the development of SMART plants for the cogeneration of electricity and water. In January 2020, the standard design was approved [7].

### 4.3.4 KLT-40S

The KLT-40S is a Russian design developed for a floating nuclear power plant with a capacity of 35 MWe each module. It is designed to provide cogeneration capability for power and heat supply to remote areas without a centralized power supply. Besides, the floating power plant can be used for seawater desalination and for autonomous power supply for sea oil-production platforms. The design is based on the third-generation generation KLT-40 marine propulsion plant and is an advanced version of this reactor. The reactor can be manufactured in shipyards and delivered to the site fully assembled, tested, and ready to operate. There is no need to develop power transmission lines or the preparatory infrastructure required for land-based NPPs.

The KLT-40S design appears similar to a conventional PWR with a compact loop configuration and most primary components external to the RPV. The RPV accommodates the reactor core and internals. Thus, the RCs, PZR, and SGs are outside the RPV. The CRDMs are external and located above the reactor vessel lid. The length of the hot and cold leg pipes connecting the RPV with the SGs is kept very short to reduce the likelihood of large-break LOCA and due to space constraints. The primary circuit has four loop system with forced and natural circulation. The PZR uses gas as the working medium to keep the pressure in the primary. The primary operation pressure is 12.7 MPa, and core inlet and outlet temperatures are 280 °C and 316 °C, respectively. The RPV diameter is 2.0 m, and overall length 4.8 m. Figure 4.10 [19] presents a layout of the KLT-40S reactor.

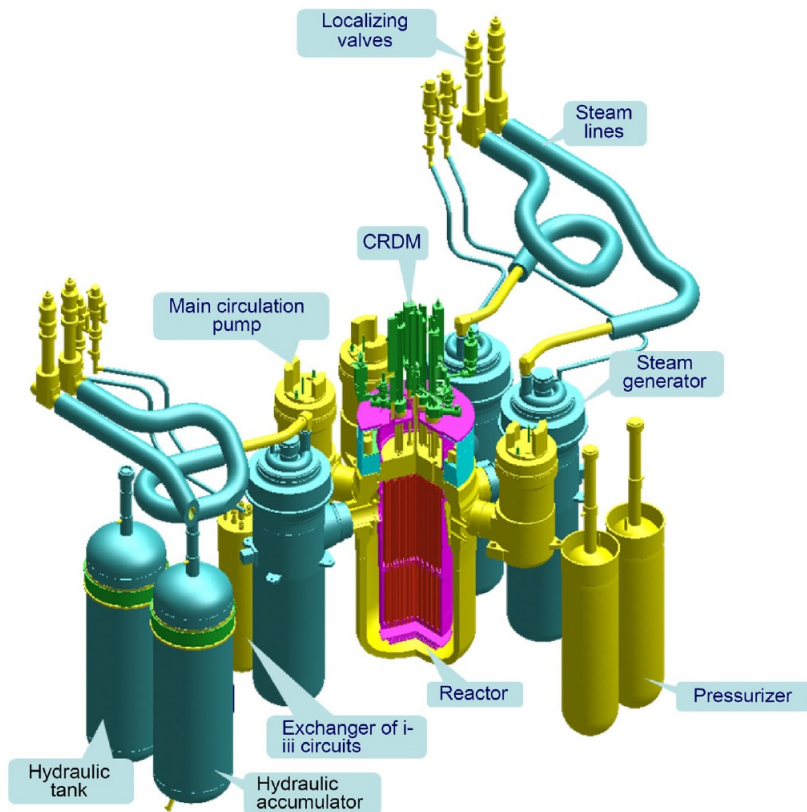


Figure 4.10: Layout of the KLT-40S reactor [19].

The core is composed of 121 fuel assemblies with a hexagonal cross-section. The number of fuel rods per fuel assembly can be 69, 72, and 75. The fuel is 18.6% enriched  $\text{UO}_2$ . For reactivity control, control rods and gadolinium as burnable poisons rods are used. There is

no diluted boron in the coolant. The core burnup is approximately 45.4 GWd/ton, and the refueling cycle is 30 to 36 months. The designed operational life is 40 years.

There are four once-through coiled SGs, one for each loop. After cooling the core, the coolant enters the SG, where it transfers its thermal energy to the fluid circulating in the secondary loop (secondary side of the SGs), and steam is produced at 290 °C with 3.82 MPa. The feedwater in the secondary side is injected with a temperature of 170 °C.

The safety aspects in the KLT-40S include the compact structure of the SG with short nozzles connecting the main equipment and primary pipelines with a smaller diameter, proven reactor emergency shutdown actuators based on different operation principles, relatively large coolant inventory, and high heat capacity of the primary resulting in larger thermal inertia of the system, external PZR operated with gas medium to guarantee slow primary pressure increase in transients, and active and passive system of reactor vessel cooling.

The decay heat removal system (DHRS) is intended to remove from the core the residual heat upon actuation of reactor emergency protection in case of abnormal operation, including accidents. The system includes two secondary passive cooling channels via SGs, one active secondary cooling channel via SGs, and one active cooling channel via the primary or via a third heat exchanger (independent circuit exchanging heat energy with ambient sea or lake). Passive cooling channels with water tanks and heat exchangers ensure reliable cooling to 24 hours.

The ECCS delivers water to the reactor core for core cooling in accidents associated with LOCA, makes up the primary coolant during process operation, and supplies coolant to the reactor at the failure of the shutdown system. The system includes a high-pressure ECCS subsystem with makeup, a high-pressure ECCS subsystem with hydraulic accumulators, and a low-pressure ECCS subsystem with recirculation pumps.

The containment of the KLT-40S is made of a steel shell designed to sustain mild pressurization. The reactor systems are positioned inside a reinforced reactor room whose bottom forms a steel-lined tank. This tank can be flooded with cooling water for decay heat removal and for shielding purposes.

The first floating power plant equipped with KLT-40S reactors was connected to the grid in December 2019 and entered full commercial operation in May 2020 [7].

### 4.3.5 SMR-160

The SMR-160 is a North American advanced PWR SMR design with a capacity of 160 MWe developed for electricity generation with optional cogeneration equipment such as hydrogen generation, heating, and seawater desalination. The SMR-160 is also configurable for sitting in water-scarce locations using an air-cooled condenser technology. The plant relies on both passive safety systems and natural circulation cooling for the primary circuit. The plant is greatly simplified relative to conventional plants to improve its fabricability, constructability, maintainability, and to reduce capital costs. The SMR-160 was designed with a philosophy driven by the criterion of achieving safety without relying on active systems or operator actions during design basis accidents.

The nuclear steam supply system (NSSS) includes the RCS that consists of the RPV and a SG in an offset configuration with an integrated PZR flanged to the top of the SG. The RPV and the SG are connected by a single connection that houses both the hot and cold legs in concentric ducts. The offset configuration permits easy access to the core without the need to move the RPV or SG during refueling. The PZR uses heaters and sprays to control the pressure. The primary operation pressure is 15.5 MPa, and core inlet and outlet temperatures

are 229 °C and 321 °C, respectively. Integrating the PZR with the SG eliminates significant primary piping. The large relative size of the PZR eliminates any need for PORVs. The RPV diameter is 3 m, and overall length 15 m. Figure 4.11 [19] presents the SMR-160 major components of the RCS.

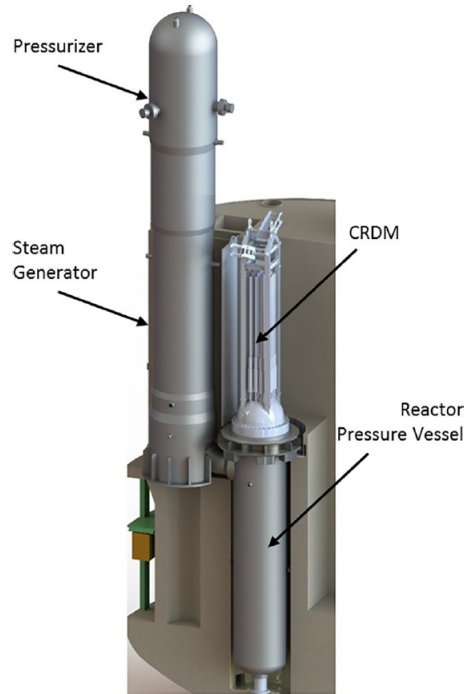


Figure 4.11: SMR-160 major components of the RCS [19].

The core comprises 57 fuel assemblies with the length of a standard light water reactor (approximately 3.7 m height). Each fuel assembly has a square  $17 \times 17$  configuration currently available from commercial suppliers. The fuel is 4.95% enriched  $\text{UO}_2$ . The long-term reactivity control is provided by burnable poisons integral to the fuel to optimize power distributions, cold shutdown margin, and hot excess reactivity. The short-term reactivity changes are performed by adjusting the control rod position and the boron concentration in the coolant. CRDMs and the control rod designs are based on existing technology. The CRDMs are located outside the RCS on the RPV upper head. The core burnup is approximately 45 GWd/ton, and the refueling cycle is 24 months. The designed operational life is 80 years.

There is only one vertically oriented once-through SG with the reactor coolant flowing inside the tubes. The SG is fed with sub-cooled feedwater to produce superheated steam at 3.4 MPa on the shell side. The SG has a large inventory of secondary water on the shell side, providing a substantial margin to avoid dry-out.

The SMR-160 safety basis incorporates a defense-in-depth approach with multiple and varied pathways for decay heat rejection. All safety systems are located inside the sturdy containment enclosure structure, which protects them from external hazards. All makeup water required for postulate LOCA is located inside the containment, making the containment isolable during LOCA, reducing the possible dose to the public and effects to the environment. Another large inventory of water is contained within a reservoir between the containment enclosure structure and the containment vessel, providing long-term postaccident handling and allowing the decay heat removal function to be transferred to air cooling for an unlimited period after a design basis accident.

The SMR-160 engineered safety features rely on passive and redundant safety systems that

also operate by natural circulation. The passive safety systems guarantee that safe shutdown can be maintained, and the decay heat removal occurs for an unlimited period without needing power, makeup water, or operator actions. When available, the operators can use active non-safety systems to mitigate events and prevent the use of the engineered safety features.

The passive core cooling system (PCCS) provides emergency core cooling and makeup water to the RCS during postulated accidents. The system employs passive means such as natural circulation for core cooling and compressed gas expansion and gravity injection for core makeup without using active components like pumps. The PCCS comprises four major subsystems: primary decay heat removal system (PDHR), secondary decay heat removal system (SDHR), ADS, and passive core makeup water system (PCMWS).

The PDHR directly cools the primary coolant by re-directing the reactor coolant through a heat exchanger rejecting the heat to a second loop full of water that rejects heat to the large annular reservoir around the containment (located between the enclosure and the containment vessel). The SDHR provides an alternative and distinct passive means to reject decay heat. The SDHR is a closed-loop system that relies on buoyancy-driven flow to route steam from the SG to a heat exchanger in the annular reservoir, where the steam condenses and rejects its latent heat. The condensate then returns to the shell side of the SG. The ADS safely lets down the RCS pressure to the sealed containment, allowing staged safety injection by the PCMWS, granting long-term recirculation within the containment vessel.

The containment system consists of a steel containment structure enclosed within a reinforced concrete containment structure, which provides shielding and protection from external events. The concrete containment structure walls are constructed of highly robust steel-concrete modules designed to resist an impact from a large commercial aircraft and other external potential hazards. Besides preventing the release of radioactive fission products to the environment, the containment system acts as a large passive heat exchanger. This system is partially embedded, with approximately half of the total height located below the grade, which maximizes the protection against external hazards and dampens seismic effect for critical components. The passive containment heat removal system passively cools the containment volume. During a postulated high-energy release, heat from the steam is rejected to the inner wall of the containment and then condensates while heat is transported to the water in the annular reservoir. The large heat transfer area and high heat conductivity of the metal containment wall result in almost instantaneous heat rejection to the annular reservoir, which then rejects heat to the environment. The large water inventory in the annular reservoir is enough to extract energy from the containment for over 3 months without replenishment, enabling the transition to air cooling, as previously mentioned.

In 2020, the preliminary design of the SMR-160 was completed. The Preliminary Safety Analysis Report is currently in development. Between 2026 to 2030, there is a targeted deployment of SMR-160 in Ukraine [19].

### 4.3.6 NuScale

The NuScale is also a North American design with a capacity of 60 MWe developed for electricity generation and non-electrical process heat applications. It is a small, modularized PWR composed of up to 12 modules installed in a single facility. Each module has a dedicated turbine and power conversion system that operates independently from the other modules. The NuScale adopts proven light-water reactor technology while eliminating the requirement for RCPs, large diameter-sized piping, and other components/systems included in large light water reactors. The plant operates efficiently at full-power conditions using natural circulation

in the core.

The NSSS contains the reactor core, helical-coil tube SG, and PZR, all included in the RPV. The NSSS is enclosed in a cylindrical containment vessel that sits in the reactor pool structure. The internal PZR keeps the RCS pressure constant during the reactor operation and transients. Heaters are turned on to increase the pressure, and sprays are used to reduce the pressure. The primary operation pressure is 12.8 MPa, and core inlet and outlet temperatures are 258 °C and 309 °C, respectively. The RPV diameter is 2.7 m, and overall length 17.7 m. Table 4.2 [7] presents some key reactor parameters of the NuScale. Figure 4.12 [19] presents a layout of the NuScale SMR and reactor module.

Table 4.2: Summary of key reactor parameters of the NuScale [7].

Key reactor parameter	Value
Core thermal output (MWth)	160
Electrical power output (MWe)	60
Primary pressure (MPa)	12.8
Core inlet temperature (°C)	258
Core outlet temperature (°C)	309
Core average temperature (°C)	284

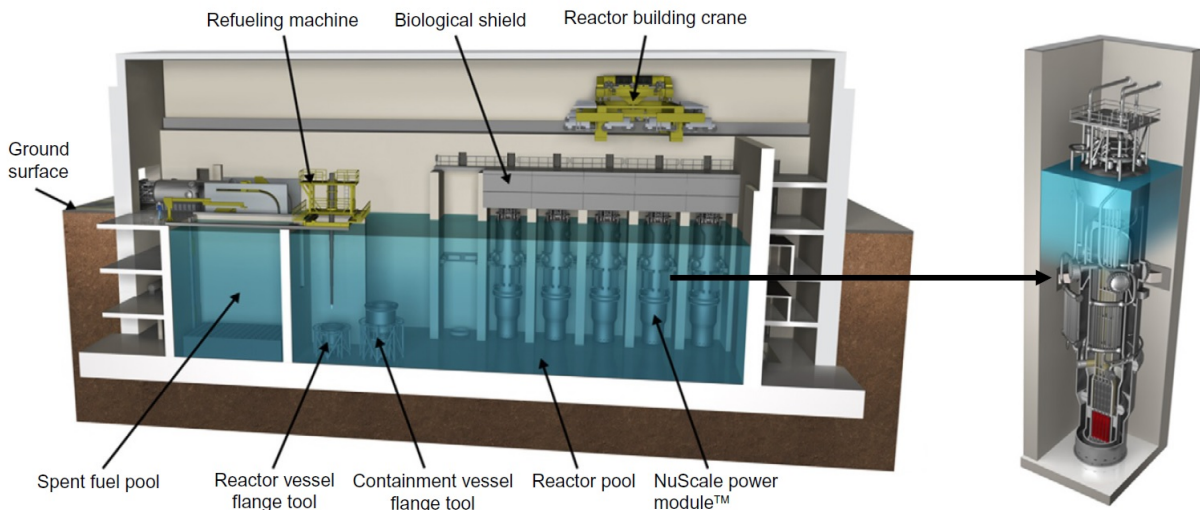


Figure 4.12: Cutaway view of NuScale SMR and reactor module [19].

The core comprises 37 fuel assemblies with a length half the height of a standard light water reactor (approximately 2 m height). Each fuel assembly has a square  $17 \times 17$  configuration and is supported by 24 guide tubes for the control rods and one central tube for instrumentation. The fuel is 4.95% enriched  $\text{UO}_2$ .  $\text{Gd}_2\text{O}_3$  mixed homogeneously in the fuel at specific rod locations is used as a burnable poison. Table 4.3 [20] presents a summary of some important NuScale reactor core design parameters. Reactivity control is achieved by using soluble boron in the primary coolant and 16 control rod assemblies. The control rods are organized in a shutdown group and a control group. The control group consists of four rods symmetrically located in the core that functions as a regulating group used during normal plant operation to control reactivity. The shutdown group comprises 12 rods that are used during shutdown and scram

events. Control rod length is 2 meters long and uses B<sub>4</sub>C and silver-indium-cadmium (Ag-In-Cd) alloy as absorber materials. Table 4.4 [20] presents a summary of some important NuScale reactor control rod assembly parameters. The core burnup is approximately 30 GWd/ton, and the refueling cycle is 24 months. The designed operational life is 60 years.

Table 4.3: Summary of some important NuScale reactor core design parameters [20].

Parameter	Value
Length of fuel assembly (m)	2.0
Number of fuel assemblies	37
Rods per fuel assemblies	264
Nominal UO <sub>2</sub> per assembly (kg)	249.24
Number of guides per assembly	24
Number of instrument tubes per assembly	1
Number of BP rods	Up to 32 per assembly
Gd <sub>2</sub> O <sub>3</sub> concentration	Up to 8%
Fissile enrichment	4.95%

Table 4.4: Summary of some important NuScale reactor control rod assembly parameters [20].

Parameter	Value
Control rod assembly mass (kg)	19.5
Control rod assembly total height (m)	2.0
Neutron absorber material	B <sub>4</sub> C and Ag-In-Cd
Number of absorbers per control rod assembly	24
Ag-In-Cd composition (weight percent)	80% Ag, 15% In, and 5% Cd

There are two intertwined helical-coil tube once-through SGs located inside the RPV, where heat from the primary coolant is transferred to the preheated feedwater circulating through the inside of the SG tubes. The fluid in the secondary side is heated and converted to steam at 4.3 MPa, which is further superheated to produce dry steam for the turbine generator.

The safety systems of the NuScale include integral primary system configuration, a containment vessel, passive heat removal systems, and severe accident mitigation mechanisms. The safety features included in the design are redundant and independent.

The ECCS contains two independent reactor recirculation valves and three independent reactor vent valves. In the condition of LOCA inside containment, the ECCS returns coolant from the containment vessel to the RPV, ensuring that the core remains covered with coolant and that the decay heat is removed. The ECCS provides additional decay heat removal in the unlikely situation of loss of feedwater flow together with the loss of both trains of the decay heat removal system (DHRS). The ECCS is also designed to remove heat and limit containment pressure via steam condensation, with heat being transferred to the inside surface of the containment vessel.

The DHRS provides secondary side reactor cooling in non-LOCA events when the normal feedwater is not available. It is a closed-loop, two-phase natural circulation system. There are two trains of decay heat removal equipment, each one attached to one SG loop. Each train has 100% capability of removing the decay heat load and cooling the primary coolant system.



Each train has a passive condenser immersed in the reactor pool. During normal operations, DHRS condensers are kept with sufficient water inventory for stable and effective operation.

The containment vessel contains the release of radioactivity following postulated accidents, protects the RPV from external hazards, and provides heat rejection to the reactor pool following the ECCS actuation. The containment vessel consists of a steel cylinder that houses the RPV, control rod drive mechanisms, and associated piping and components of the NSSS. This vessel is immersed in the reactor pool, which provides a passive heat sink for the containment heat removal in LOCA conditions.

In the following, some important parameters for the NuScale operation are summarized. The MTC, FTC, and boron worth coefficient are summarized in Table 4.5 [20].

Table 4.5: Summary of NuScale reactivity coefficients and boron worth coefficient [20].

Parameter	Range
Range of MTC (pcm/°C)	-9 to -58.5
Range of FTC (pcm/°C)	-2.93 to -3.73
Range of boron coefficient worth (pcm/ppm)	-7.6 to -13.7

The FTC presented in Table 4.5 [20] was calculated for a range of fuel temperatures by varying the time in the fuel cycle, coolant temperature, and power levels. The FTC values in this table represent the range of the FTC over this spectrum of parameters. As can be observed, the variation in the FTC is very small. On the other hand, the MTC has a greater variation than the FTC. The range presented here considers the MTC with the reactor at full power with an average moderator temperature at 284 °C. The boron worth coefficient range represents the maximum and minimum values of boron worth for all operational ranges. Figure 4.13 [20] shows how the boron concentration changes with the fuel burnup.

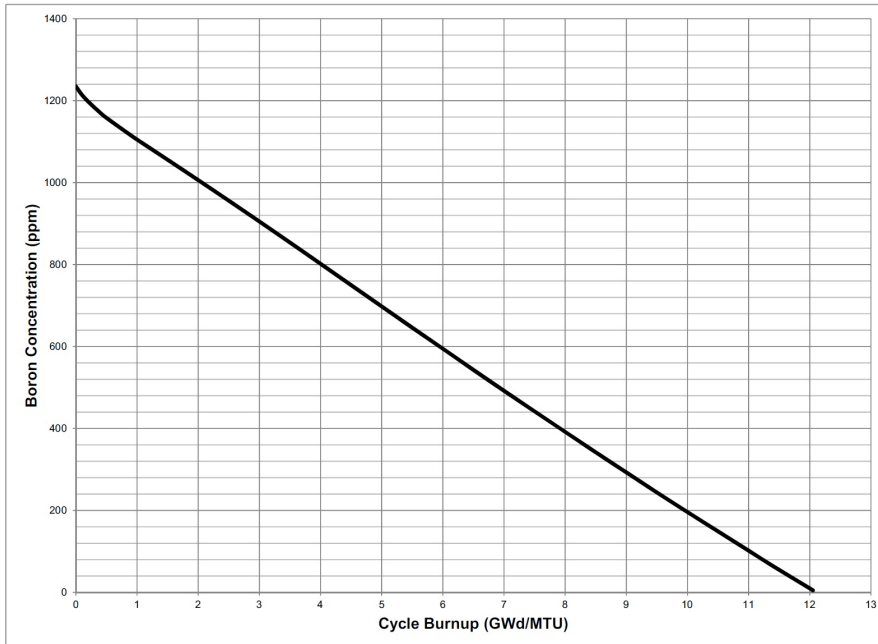


Figure 4.13: NuScale boron concentration variation with fuel cycle [20].

The total control rod worth and the xenon-135 worth at BOL and EOL are summarized in Table 4.6 [20].

Table 4.6: Summary of reactivity worths in NuScale [20].

Parameter	Value	
	BOL	EOL
Total control rod worth (pcm)	14414	15553
Xenon-135 worth (pcm)	2203	2515

The NuScale design certification is under regulatory review. The first commercial plant is targeted to be in operation in 2027 [7].

### 4.3.7 EPR

Differently from the designs presented previously, the Evolutionary Power Reactor (EPR) is a large PWR capable of producing 1650 MWe. The EPR is a French-German evolutionary third-generation design that combines and improves the best features of the latest reactors operating in France and Germany, being an evolutionary and innovative design with increased safety and performance levels [10].

The primary circuit consists of four loops, each containing an SG and an RCP and a PZR on one loop. The main components are designed to deliver high core power at a high steam pressure level for economic efficiency. The increased water inventory, large SGs and PZR, provides operating and safety margins. The RPV has a reduced number of welds which benefits safety and maintenance. The in-core instrumentation is mounted at the top of the vessel to reduce penetrations below the core. A heavy metallic reflector provides fuel savings and lower RPV fluence. The primary operation pressure is 15.5 MPa, and core inlet and outlet temperatures are 295 °C and 330 °C, respectively. The RPV diameter is 5.4 m and overall length 12.72 m. Table 4.7 [21] presents some key reactor parameters of the EPR. Figure 4.14 [21] presents a EPR cutaway.

Table 4.7: Summary of key reactor parameters of the EPR [21].

Key reactor parameter	Value
Core thermal output (MWth)	4590
Electrical power output (MWe)	1650
Primary pressure (MPa)	15.5
Core inlet temperature (°C)	295
Core outlet temperature (°C)	330
Core average temperature (°C)	312

The core comprises 241 fuel assemblies with a length of 4.2 m. Each fuel assembly has a square  $17 \times 17$  with 24 guide tubes for the control rods and instrumentations. The fuel is 4.95% enriched  $\text{UO}_2$ .  $\text{Gd}_2\text{O}_3$  mixed homogeneously in the fuel at specific rod locations is used as a burnable poison. Table 4.8 [21] presents a summary of some important EPR reactor core design parameters. Reactivity control is achieved by using soluble boron in the primary coolant and 89 control rod assemblies. Each control rod assembly contains 24 rods with annular absorbers attached to a spider assembly. The absorber rods are composed of stainless steel tubing containing annular silver-indium-cadmium (Ag-In-Cd) alloy as neutron

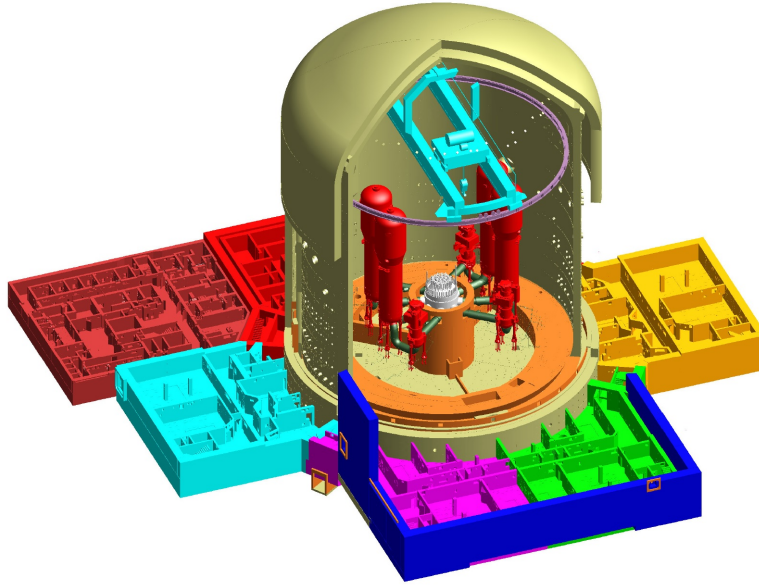


Figure 4.14: EPR cutaway [21].

absorber material. Table 4.9 [21] presents a summary of some important EPR reactor control rod assembly parameters. The core burnup is approximately 62 GWd/ton, and the refueling cycle ranges from 12 to 24 months. The designed operational life is 60 years.

Table 4.8: Summary of some EPR reactor core design parameters [21].

Parameter	Value
Length of fuel assembly (m)	4.2
Number of fuel assemblies	241
Rods per fuel assemblies	265
Nominal $\text{UO}_2$ per assembly (kg)	536
Number of guides per assembly	24
Number of instrument tubes per assembly	0 to 2
Number of BP rods	Up to 28 per assembly
$\text{Gd}_2\text{O}_3$ concentration	Up to 8%
Fissile enrichment	4.95%

The SGs are vertical shell and U-tube evaporators with integral moisture separating equipment. The reactor coolant circulates inside the tubes, transferring heat to the feedwater circulating on the shell side, where steam is generated and flows upward through moisture separators. The fluid in the secondary side is heated and converted to steam at 7.6 MPa.

The EPR safety divisions provide four times 100% redundancy, allowing preventive maintenance during operation and offering high reliability. The safety is reinforced by implementing an adequate level of redundancy, independency, diversity, and physical separation of the successive defense lines. A robust core melt mitigation is provided, including RCS depressurization system to eliminate high pressure, a core catcher located below and aside from the RPV pit to perform corium retention and cooling with passive flooding from the IRWST, dedicated heat removal system, and passive hydrogen catalytic recombiners. Active and passive safety systems are combined to make optimal use of their respective advantages. In the event of loss of off-site

Table 4.9: Summary of some important EPR reactor control rod assembly parameters [21].

Parameter	Value
Control rod assembly mass (kg)	61.82
Control rod assembly total height (m)	4.7
Neutron absorber material	Ag-In-Cd
Number of absorbers per control rod assembly	24
Ag-In-Cd composition (weight percent)	80% Ag, 15% In, and 5% Cd

power, emergency diesel generators can operate for three days (extendable), and backup diesel generators are available.

In the following, some important parameters for the EPR operation are summarized. The MTC, FTC, and boron worth coefficient are summarized in Table 4.10 [21].

Table 4.10: Summary of EPR reactivity coefficients and boron worth coefficient [21].

Parameter	Range
Range of MTC (pcm/°C)	5.22 to $-60.12$
Range of FTC (pcm/°C)	$-2.34$ to $-3.24$
Range of boron coefficient worth (pcm/ppm)	$-7.9$ to $-9.5$

As discussed, the FTC, MTC and, the boron worth depend on a variety of factors. Thus, the range presented in Table 4.10 [21] reflect this effect. As the fuel depletes, the boron concentration is decreased over the fuel cycle; this effect for the EPR is presented in Figure 4.15 [21].

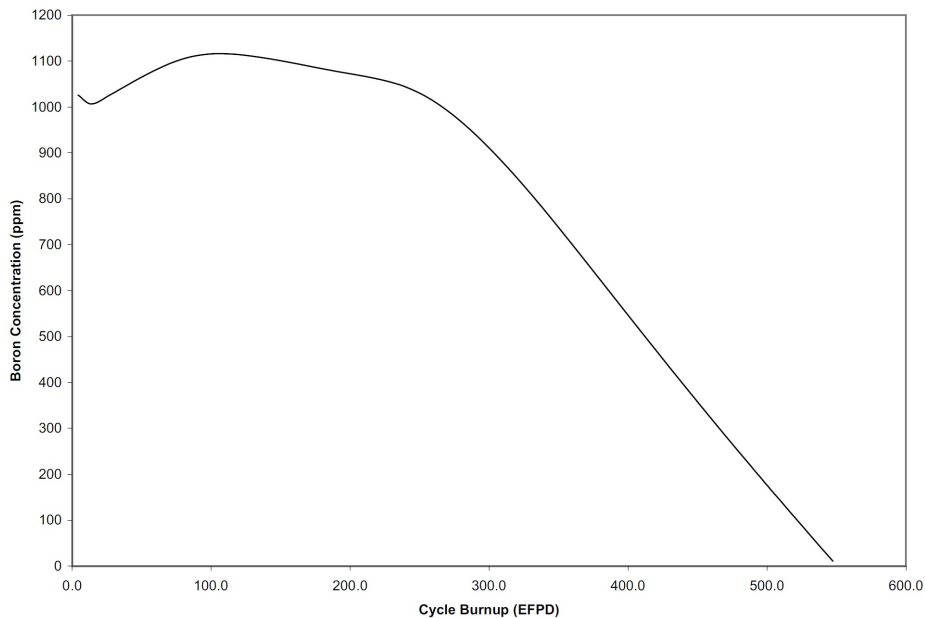


Figure 4.15: EPR boron concentration variation with fuel cycle [21].

The total control rod worths at BOL and EOL are summarized in Table 4.11 [21]. The xenon-135 worth was not specified in the consulted reference.

Table 4.11: Summary of reactivity worths in EPR [21].

Parameter	Value	
	BOL	EOL
Total control rod worth (pcm)	10942	11697
Xenon-135 worth (pcm)	Not specified	Not specified

Four different safety authorities have already licensed the EPR design, demonstrating that the design can meet a large variety of safety and regulatory requirements. Two EPRs have been in commercial operation in China since 2018.

# Chapter 5

## iPWR Simulator

The IAEA has established a program in nuclear reactor simulation computer programs to assist the Member States in educating and training. The aim is to provide insight and practice in the operation and behavior of nuclear power plants for a variety of advanced reactor types [22]. The simulators allow hands-on training for nuclear professionals engaged in teaching and training topics such as nuclear power plant design, technology, safety, simulation, and operations. The IAEA coordinates the supply and development of basic principles nuclear power plant simulators available for free to the Member States upon request. The IAEA also provides associated training material and sponsors training courses and workshops.

Recently, the participation of Member States in the IAEA program for the development of SMRs has increased, with a large number of designs under development for the several Member States. Most of the designs are light water cooled and moderated small iPWRs. Thus, the IAEA provides the integral water pressurized reactor simulator that is briefly described in this section. The main screen of the iPWR simulator is presented in Figure 5.1. Further information is available in References [8] and [22] and in Chapter 6.

### 5.1 Systems Simulated

The simulator has been designed for the primary and the balance of plant (BOP) behaviors. Thus, the following systems have been simulated: reactor core, reactor coolant system (RCS), main steam system (MSS), feedwater system (FWS), turbine system (TUR), generator system (GEN), condenser system (CNR), circulating water system (CWS), containment building system (CBS), automatic depressurization system (ADS), containment cooling system (CCS), gravity-driven water injection system (GIS), pressure injection system (PIS), passive decay heat removal system (PDHR), and protection and control system (PCS).

#### 5.1.1 Reactor core and reactor coolant system (RCS)

The design produces 150 MW<sub>th</sub> and 45 MW<sub>e</sub>. For coolant circulation, it is possible to select natural or forced circulation (both 424 kg/s), where four RCPs are employed. The stainless steel RPV has a volume of 80.78 m<sup>3</sup> and contains the reactor core, SG, and the PZR with 8.078 m<sup>3</sup>. The core inlet and outlet temperatures are 255 °C and 320 °C, respectively.

The PZR is integral to RPV and is separated from the main RPV volume by a baffle plate. It is designed to accommodate any volume changes and limit the pressure changes in the RCS.

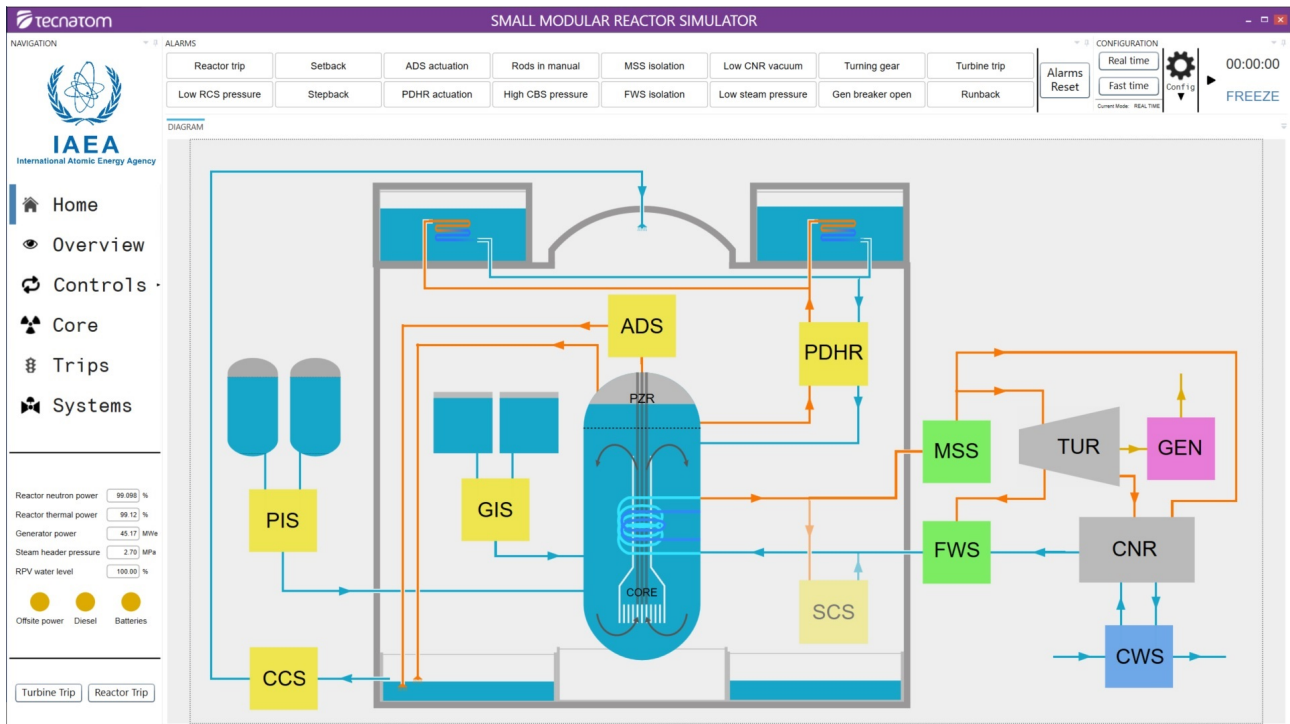


Figure 5.1: Main screen of the iPWR simulator.

The PZR keeps the primary at the operating pressure of 15.5 MPa. The PZR uses heaters and spray to maintain the reactor coolant pressure constant. The CVCS feeds the spray, and if it is not enough for reducing the pressure, there are two relief and two safety valves to prevent that RCS pressure exceeds the design value of 17.05 MPa. The PZR also has level control, which setpoint changes during operation to accommodate power transients, and it is controlled by the charge and discharge flow of the CVCS. The spray flow can avoid the relief valve opening when there is a load rejection of 10% with control rods in automatic. Each relief valve has a motorized valve in series to prevent LOCA through the relief valve if it fails open. Besides, there are three ADS valves designed to reduce pressure in the case of LOCA.

The core comprises 24 fuel assemblies, each of them having a square  $17 \times 17$  configuration. The heated length is 1.35 m, and the equivalent diameter is approximately 1.2 m. The fuel is 4.95% enriched  $\text{UO}_2$ . The reactivity control is made by control rods and boron diluted in the moderator. The control rods are divided into the control group and the shutdown group. There are eight control rods in the control group (divided into two banks with four rods each bank) and eight shutdown rods (only one bank). The rod worth is approximately 1042 pcm. Upon loss of power or scram, both groups are inserted in the core by gravity. For simplicity, there is no bank overlap.

The SG consists of two helical-coil tubes located inside the RPV at a suitable height above the core. The secondary water flows inside the tubes while the primary coolant flows through the shell side. The SG produces superheated steam at 2.7 MPa at full power.

The RCS has connections with safety systems: PIS and GIS, which flood the RPV at certain reactor pressure, and ADS, which reduces the RCS pressure in LOCA. RCS also has pressure and level instrumentations in PZR, used for PZR level and pressure control. Inside the RPV, there are also pressure and level instrumentations. Besides, there are flow transmitters in charge, letdown, and sprays lines and temperature transmitters at inlet and outlet reactor core and subcooling margin. Neutron power and variations in neutron power are also measured.

Additionally, PCS generates reactor trip when a certain setpoint is reached to prevent radioactivity release. The setpoints for reactor trip are low-pressure upper plenum (pressure lower than 11 MPa), low-level upper plenum (level lower than 5%), low flow downcomer, high core outlet temperature (temperature higher than 340 °C), high reactor neutron flux (flux higher than 120%), high SUR (SUR higher than 2 DPM), high-pressure upper plenum (pressure higher than 16.4 MPa), feedwater pumps trip, ADS actuation, seismic event, and manual scram. Figure 5.2 shows the RCS.

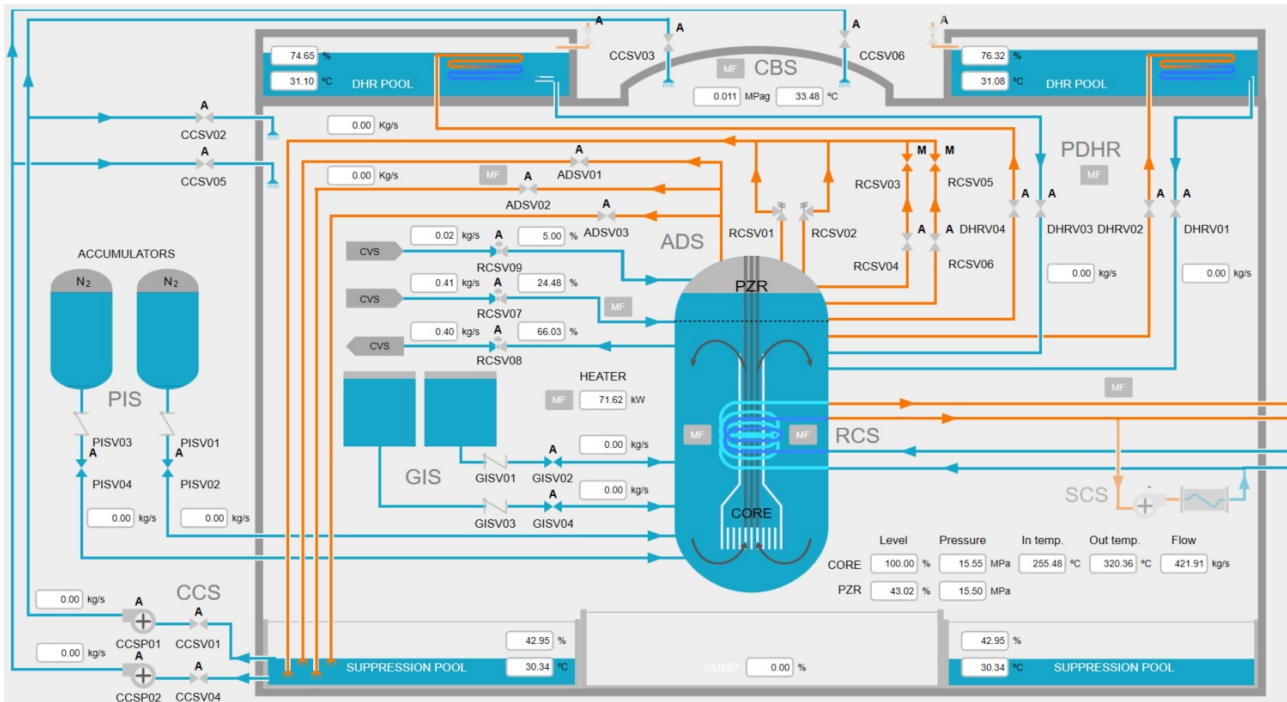


Figure 5.2: RCS, CBS, SCS, ADS, CCS, GIS, PDHR, and PIS.

### 5.1.2 Main steam system (MSS)

The MSS supplies steam from the SG to the turbine generator set in suitable quantities and adequate quality. There is just one SG with two helical-coil tubes located inside RPV at a suitable height above the core. Cold feedwater enters the secondary side tubes at the base of SG, and a superheated (around 30 °C) steam is collected from the top. The steam leaves the SG through an isolation valve on each steam line which closes by protection signal. At full power, the steam flow is 77 kg/s at 2.7 MPa.

The steam lines join in a manifold (steam header), and the steam passes through a main steam control valve and isolation valve into a one-stage pressure steam turbine. The PCS controls the position of these valves. The function of the isolation valves is to interrupt the steam flow to the turbine, and the function of the control valves is to regulate the steam flow to the turbine and regulate this flow during the turbine runup from 5 rpm to 3600 rpm, the synchronization speed.

The turbine bypass line enables the steam to pass straight from the SG to the condenser via a control valve and isolation valve. The bypass allows reactor cooling to be maintained in the event of a turbine trip, load rejection, and during startup or programmed shut down, controlling temperature excess in RCS or pressure excess in MSS depending on the main steam bypass



mode chosen. The PCS controls the position of these valves. The turbine bypass can absorb 100% power. Additionally, steam discharge allows steam to be dumped into the atmosphere via steam relief valves and safety valves, where the safety setpoint is higher than the relief setpoint. These valves open when the turbine bypass cannot absorb the steam produced by the reactor, so they have enough capacity to keep the reactor core cooled if the bypass is not available and a reactor trip has happened. The safety valves prevent the MSS pressure from exceeding the design value.

Turbine power is proportional to the turbine admission pressure, so a pressure transmitter is placed over the admission chamber to allow the turbine control calculation. Flow, pressure, and temperature transmitters are installed in each line and in the steam header. Besides, there are also flow and valve control position of the turbine line and turbine bypass line. Figure 5.3 shows the MSS.

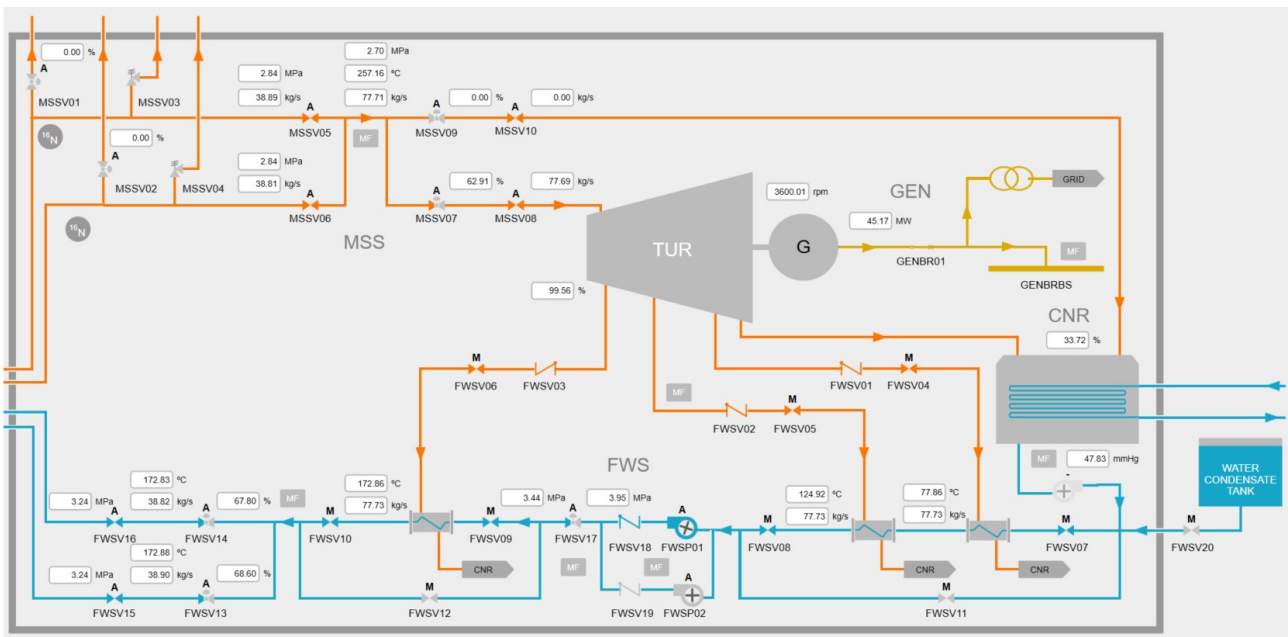


Figure 5.3: MSS, FWS, TUR, GEN, and CNR.

### 5.1.3 Feedwater system (FWS)

FWS provides the flow of treated and preheated water to the SG under necessary conditions, in an amount equivalent to that converted into steam inside the SG.

The condensate is extracted from the condenser by condensate pumps (not simulated) and preheated in three heat exchangers, which use steam extractions from the turbine to preheat the water. Preheating increases the efficiency of the plant.

The condensate is pumped back to the SG by two variable feedwater pumps (installed in parallel for redundancy), where each pump has 100% capacity. The trip of the feedwater pumps generates reactor scram. Feedwater pumps trip when there is low steam header pressure (less than 1 MPa) or low condenser level (10%). The feedwater flow is 77 kg/s and enters the SG via two lines (two helical-coil tubes) at approximately 173 °C. A feedwater control valve and an adjacent isolation valve control the feed into each helical-coil tube of the SG. The isolation valves close when feedwater pumps trip or when there is an injection signal. PCS calculates the position of the valves and the feedwater pumps speed demand. The control maintains the

equilibrium between the two helical-coil loops and takes into account the pressure difference between the main steam header and feedwater header with reheated condensate and the steam temperature.

There are valves at the inlet/outlet of the heat exchanger 1 and valves at the inlet/outlet of the heat exchanger 2 and 3 to isolate them. Besides, there is one valve per turbine extraction to isolate the feedwater exchangers in case of tube rupture inside the heat exchanger. The affected heat exchanger should be isolated, and the bypass valve opened. There is a bypass valve for the heat exchanger 1, while the heat exchangers 2 and 3 share the same bypass valve. Thus, the feedwater flow is not reheated and enters the SG cooler, this effect results in an increase in the neutron power due to the overcooling.

In case of turbine trip, feedwater pumps continue feeding the SG. FWS and MSS make core cooling during normal operation or by the PDHR in the loss of heat sink. There is a storage tank that adds water to the secondary side in case of loss of feedwater or main steam (opening a steam relief valve, for example). The tank can add water for 2 hours in case of opening the steam relief valve.

Regarding instrumentation, there are flow transmitters at the entrance of each line of the SG and temperature transmitters at the entrance/exit of each heat exchanger. Feedwater pumps can start or stop manually or automatically. When a feedwater pump stops, the other pump is automatically started if there is no malfunction activated. Figure 5.3 shows the FWS.

#### **5.1.4 Turbine system (TUR)**

The turbine provides mechanical power to the generator to satisfy the load demands of the grid, maintaining a frequency of 60 Hz. The generator produces 45 MWe at a speed of 3600 rpm.

The turbine consists of a one-stage pressure turbine. Steam is extracted from the turbine stage at three positions to preheat the feedwater to increase the efficiency of the plant. Once the steam has been expanded in the turbine, it is discharged into the condenser, where circulating water condenses it. PCS uses the first stage pressure transmitter to establish desired primary average temperature that controls the rod position when turbine leading mode is selected. The admission pressure is approximately proportional to the generated power (2.7 MPa at 100% power). PCS trips the turbine in case of low vacuum at CNR (pressure higher than 254 mmHg), reactor scram, reactor power less than 4%, manual turbine trip, low oil pressure (not simulated), and grid instabilities (not simulated). There are transmitters for turbine speed, turbine load demand, turbine load rate, and first-stage pressure. Figure 5.3 shows the TUR.

#### **5.1.5 Generator system (GEN)**

The generator converts the mechanical energy provided by the turbine into electricity. The GEN has a capacity of 45 MWe and a frequency of 60 Hz. The GEN is a self-exciting three-phase AC. The electrical energy is distributed to different consumption centers via a set-up transformer, and part is used for electricity supply at the plant itself. In case of loss of off-site power, diesel generators are started up to feed up the plant. In case of station blackout, just some plant components are fed up by batteries, such as the PCS.

The main generator is constituted by the shell, stator and rotor bearings, excitation (not simulated), and generator auxiliary systems (not simulated). When the generator is synchronized to the grid, the main breaker has to be closed. After a turbine trip, the main breaker

opens. There is a transmitter that measures the generator load (MWe). Figure 5.3 shows the GEN.

### 5.1.6 Condenser system (CNR)

The condenser consists of a shell and a set of tubes for the circulating water. The exhaust steam from the turbine enters the condenser shell side, and it is cooled and converted into condensate by the water flowing inside the tubes from the circulating water system. The condenser is the heat sink for the secondary circuit of the plant.

The condenser collects the flow from the turbine, the flow from the steam lines through the main steam bypass, and the flow from the drains of the heat exchanger chain. Condensate pumps extract condensate from the condenser. The condenser works under vacuum (47.83 mmHg) to keep the steam pressure of the water under the atmospheric pressure, improving the thermodynamic performance of the cycle. The condenser has pressure and level transmitters. Figure 5.3 shows the CNR.

### 5.1.7 Circulating water system (CWS)

The steam leaving the turbine is cooled in the condenser by the CWS. The CWS supplies to the condenser the amount of water needed to extract the maximum thermal load produced by the condensation of the steam from the turbine and to maintain the vacuum in the condenser.

The CWS has two different operating modes. The first one consists of taking and discharging water from and to the lake (open loop), and the second one recirculates water through the condenser tubes using a refrigeration tower (close loop). The system has two circulating pumps, each having a capacity of 50% of the total flow.

The cooling tower is a device that rejects heat to the atmosphere through the cooling of a water stream. It uses water evaporation to remove process heat and cool the working fluid to near the wet-bulb air temperature (the user can change this parameter). CWS is at atmospheric pressure while there is a vacuum in the condenser. In case of tube rupture, water flows into CNR from CWS. The shutdown of one or more CWS pumps generates a partial or total loss of vacuum in the condenser. The system has temperature transmitters at the entrance and exit of the condenser and a flow transmitter. Figure 5.4 shows the CWS.

### 5.1.8 Containment building system (CBS)

The containment building is an enclosure building that houses the reactor vessel, the cooling system, and part of the safety systems, among other systems. The containment is air containment (other SMR designs have a water containment).

The structure of the containment building consists of a cylindrical concrete structure with an embedded steel liner having a radius of 12 m, a height of 25.3 m, and a volume of 11445 m<sup>3</sup>. The primary containment is of pressure-suppression type with a dry well and a wet well. The dry well includes the volume that surrounds the reactor pressure vessel. A partition floor and a cylindrical wall separate the dry well from the wet well. The lower part of the wet well volume is filled with water that works as the condensation pool (576 m<sup>3</sup>), where PZR relief and safety valves and ADS valves discharge. The upper part is a gas chamber. CBS contains two pools at the upper part, which work as condensers for the PDHR.

Any water leaking from the RPV is collected within a cavity in the containment surrounding the lower section of the RPV, which floods over time, providing cooling for the RPV (sump).

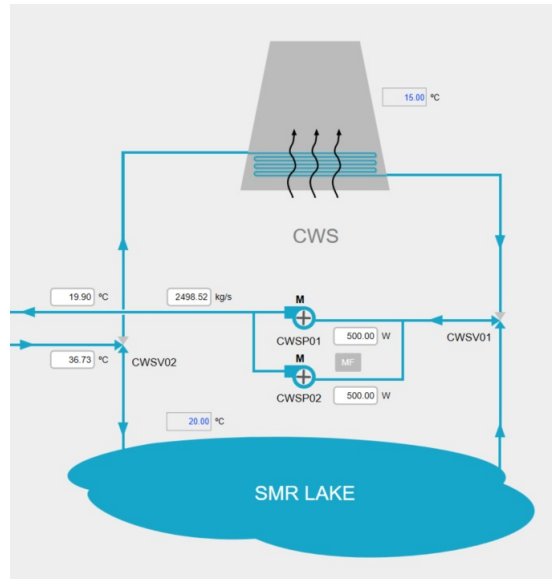


Figure 5.4: Circulating water system.

Any water that boils to steam within the containment is condensed on the steel liner of the containment. In case of the sump overflowing, the water goes to the suppression pool. A core spray system is used to reduce containment pressure and temperature, which is an active system with water being pumped from the containment suppression pool.

The CBS keeps within acceptable limits the leakage rates of radioactive materials to the environment, in normal operation and in any of the design basic accidents; it provides a radiation shielding of the reactor and the cooling system; it isolates the reactor cooling system and other safety systems from the external environment conditions, and; it provides the last barrier in the retention of radioactive products.

The containment isolation consists of a set of valves installed in the pipelines that pass through the containment building wall so that these lines can be isolated. These valves are designed to prevent the escape of radioactive fluids through the pipelines by isolating the containment building during an accident, especially the LOCA. The containment vacuum (0.011 MPa) is achieved by the use of the ventilation systems (not simulated).

The CBS has level and temperature instrumentations in each pool, suppression pool and decay heat removal (DHR) condensers (DHR pools). The air part of the CBS also has pressure and temperature transmitters. Figure 5.2 shows the CBS.

### 5.1.9 Automatic depressurization system (ADS)

The ADS is initiated by opening the three valves connected to the primary system, which release the steam into the suppression pool, where it condenses. ADS is a safety system together with GIS, CCS, PIS, and DHR.

The ADS lowers the reactor pressure by releasing steam to the suppression pool, where it condenses. The pressure reduction allows the PIS or GIS to supply water to the reactor to keep the core covered (in the case of LOCA, for example). The pressure relief valves provide redundancy, with each being able to provide 100% of the required pressure relief capacity. PCS calculates the ADS valve position, which opens one by one and needs about 5 minutes to open completely to avoid the core damage. ADS valves open if there is an ADS signal. An ADS signal is generated in case of low pressure upper plenum (pressure lower than 9 MPa), low level

vessel (level lower than 90%), high pressure upper plenum (pressure higher than 17.2 MPa), and high CBS pressure (pressure higher than 0.019 MPa). There are flow transmitters downstream ADS valves. Figure 5.2 shows the ADS.

### **5.1.10 Containment cooling system (CCS)**

CCS is a safety system that comes into operation automatically when the pressure is very high in the containment building (0.019 MPa). Borated water solution with 2500 ppm of boron from the CBS is sprayed into the containment building via spray nozzles.

CCS is an active system that pumps water from the containment suppression pool to the upper part via the spray nozzles. There are two independent trains, each train with a pump of 100% capacity. PCS calculates the pumps and discharge valves status demand that enters into operation when the containment pressure is higher than 0.019 MPa.

The CCS functions to reduce the pressure of the containment building to a value less than the design pressure in case of LOCA or steam line break or feedwater line break inside the containment, and; to reduce the concentration of iodine in the atmosphere of the containment building after an accident (not simulated). The instrumentation consists of one flow transmitter per train. Figure 5.2 shows the CCS.

### **5.1.11 Gravity driven water injection system (GIS)**

GIS is a passive water injection system. Once the pressure decreases in the reactor vessel, the system comes into operation by gravity. The system consists of two trains, where each train has one tank with borated water solution with 2500 ppm of boron connected to the reactor vessel.

The GIS injects water into the reactor vessel to reduce the pressure in the primary system and to ensure a shutdown margin. Each of the two tanks is connected to the reactor vessel above 20 m by one piping line with 2 valves. One valve is a check valve that opens when the pressure in the tank is higher than the reactor pressure, and the second one is a motorized valve that closes when the plant goes to shut down to avoid the tank discharge in the RCS when it is not required.

The line goes from the lower part of the tank to a position below the reactor core level. When the pressure in the primary system decreases to a specific level (pressure lower than 0.5 MPa), the check valves open automatically, and the borated water from the tank drains into the primary system by gravity. The GIS tanks and PIS tanks are designed to keep the core flooded under LOCA conditions for a long term. GIS has one flow transmitter per train. Figure 5.2 shows the GIS.

### **5.1.12 Pressure injection system (PIS)**

PIS is a passive injection system that comes into operation when the pressure in the reactor vessel is below 5 MPa. It consists of two trains with a borated water tank with 2500 ppm of boron concentration connected to the reactor vessel.

Once the ADS has depressurized the RCS up to 5 MPa, PIS passively injects borated water into the RPV. The storage tanks, one for each train, are pressurized to flood the RPV only when the system pressure drops below a specified pressure. This water injection keeps the water level within the RPV above the top of the core.

Each of the two tanks is connected to the RPV by one piping line with two valves, where one valve is a check valve, which opens when the pressure in the tank is greater than the RPV, and the second valve is a motorized valve, which closes when the plant goes to shut down to avoid the tank discharge in the RCS when it is not required. The PIS tanks and GIS tanks are designed to keep the core flooded under LOCA conditions for a long term. PIS has one flow transmitter per train. Figure 5.2 shows the PIS.

### 5.1.13 Passive decay heat removal system (PDHR)

The PDHR operates by condensing steam from the primary system in emergency condensers located in a pool inside the containment building and over the RPV to enable natural circulation. Two independent PDHR trains remove heat from the core by establishing natural circulation loops, where the decay heat removal pools work as the heat sinks.

In normal operation, FWS and MSS cool the reactor core. However, in case of losing them, PDHR is the system responsible for cooling the core. The RPV is connected to decay heat removal condensers within dedicated pools inside the containment. When the PDHR system is activated, the inlet and outlet valves open, and FWS and MSS are isolated. Water drains from the condenser tubes into the RPV and draws steam into the condensers, where heat from steam is transferred to the water pool, which establishes a natural circulation loop.

Each pool has a volume of 148.5 m<sup>3</sup>, which is enough to maintain the natural circulation for a minimum of 7 days and to take the reactor to a temperature lower than the temperature of zero load. If the decay heat removal pool does not adequately cool the tubes, there is not enough temperature difference in the tubes, and consequently, natural circulation does not occur.

Each train of the PDHR has sufficient capacity to remove decay heat after a shutdown from full power operations. The pools have a vent to lower pressure in case of overpressure transients (not simulated). PCS calculates the position of the valves, which open when there is a PDHR signal. PDHR has one flow transmitter per train. Figure 5.2 shows the PDHR.

The shutdown cooling system (SCS) is an active system (with pumps) that is used to take the plant to cold shutdown under normal operation (not simulated). Although not simulated, the Figure 5.2 shows the SCS.

### 5.1.14 Protection and control system (PCS)

The PCS function is to protect the three barriers between the fuel and the public: fuel cladding, reactor coolant, and containment. The PCS provides the changes required to keep the operating parameters. PCS includes the control loops necessary for controlling the reactor and a reactor protection system that trips the turbine or the reactor or causes stepbacks/setbacks when plant parameters exceed specific setpoints.

The PCS provides automatic protection against unsafe operation conditions during steady-state operation and power transients. It generates proper trip, interlock, and safety signals; it measures process parameters continuously during all operation modes, and; it keeps specific parameters and systems within their operating range.

The protection signals are reactor and turbine trip, reactor setback, reactor stepback, turbine runback, and safety signals (ADS and PDHR actuation signals).

The control system establishes and maintains the balance of power between the primary and secondary systems during steady-state plant operations. Additionally, it restricts transient operating conditions intending to prevent plant trip and reestablishing steady-state plant

operations. Moreover, it provides the operator with the necessary information by monitoring instrumentation to ensure understanding of the conditions of the process at each moment in time. The control systems are PZR pressure and level controls, feedwater control, turbine control, main steam bypass control, and rods control.

The PZR level is controlled by changing the charge and discharge flows of the CVCS. The setpoint changes during operation according to the average temperature of the RCS to accommodate eventual power transients. The PZR pressure control must maintain the RCS pressure constant at 15.5 MPa during the operation. The pressure is controlled by a bank of heaters, spray valve, and relief valves.

The feedwater control keeps an equilibrium between the two helical-coil loops of the SG and takes into account the pressure difference between the main steam header and the feedwater header with reheated condensate and the steam temperature.

The turbine control keeps the load required by regulating the steam flow to the turbine during power operation if the simulator is in turbine leading mode or keeps the steam pressure if the simulator is in reactor leading mode.

The main steam bypass control keeps the average temperature of the RCS or the steam pressure in MSS depending on the mode of operation (reactor leading or turbine leading mode).

The rods control moves the rods to keep the average temperature of the RCS in turbine leading mode. In reactor leading mode, it moves the rods to keep the reactor power demanded.

Each of the protection signals has an alarm associated, where the alarms belong to the PCS. Further information about the protection and control system can be found in Reference [22].

## 5.2 Systems Not Simulated

The following systems are out of the simulator scope or have a partial scope: shutdown cooling system, containment venting, generator auxiliaries, turbine auxiliaries, and off-site power, diesel and battery lights.

### 5.2.1 Shutdown cooling system (SCS)

The SCS is responsible for removing residual heat under normal operation. This system is an active system consisting of one pump and a heat exchanger cooled by the component cooling system.

### 5.2.2 Containment venting

Each DHR pool has a vent that vents to the atmosphere in case of the pool pressure reaches a determined setpoint.

### 5.2.3 Generator auxiliaries

Generator auxiliary systems such as oil and water and air cooling for the coils windings are not simulated. Additionally, to generate the required magnetic field to induce the electromotive force needed to generate electric power, shaft rotation and excitation are required. However, the excitation is also not simulated.

#### **5.2.4 Turbine auxiliaries**

Turbine auxiliaries such as low-pressure oil system for turbine bearing cooling and high-pressure oil system for electrohydraulic fluid are not simulated.

#### **5.2.5 Off-site power, diesel, and battery lights**

The simulation of off-site power, diesel, and battery lights is just logic for a good understanding of station blackout.



# Chapter 6

## Transients

As discussed in Section 3.6, transients are characterized by changes in operating parameters, temperature, and pressure in response to operator action or accident conditions. In this section, the transients described in Section 3.6 are simulated in the iPWR simulator, and the results are presented and discussed. Additionally to these transients, the steam generator tube failure is included in the discussions.

### 6.1 Power Maneuvering

As discussed in Section 3.6.1, the power maneuvering is a change in reactor power demand. This transient may occur when there is a variation in the power demand on the electric grid, for example. This transient may frequently occur in grids powered by different means of power generation (hybrid grids). As the technology develops, the use of hybrid grids increases, making the study of this transient even more important.

The transient analyzed here is the power change from 100% power to 50% power and then return the power to 100% as discussed in Section 3.6.1. The first step in the simulation is to load the initial condition. The initial condition selected is 100% power with natural circulation at BOL, which corresponds to the initial condition number 1 in the iPWR simulator. The steps for loading this condition are presented in Figure 6.1.

In this condition, the reactor operates at 100% power, generating 45 MWe with control rods in automatic with the tertiary circuit circulating water to and from the lake. During the entire transient, the control rods are maintained in automatic; thus, all the responses are performed automatically. The boron concentration in the RCS is kept constant. Before starting the transient, it is necessary to confirm that the reactor is in turbine leading control on the page Rods Position Control of the simulator (Figure 6.2(a)). Following, on the page Turbine Control of the simulator, the turbine load demand must be set at 22.5 MWe (equivalent to 50% power) with a turbine load rate of 2 MWe/min. After inserting these values, the Go button must be pressed, resulting in the transient start (Figure 6.2(b)). After the reactor and turbine reach 50% power with the parameters stabilized, the simulator is returned to 100% power by inserting 45 MWe in turbine load demand while the turbine load rate is kept the same.

The variations in nuclear and electric power are presented in Figures 6.3 and 6.4, respectively. From these graphs, one may observe that the nuclear power oscillates around approximately 50% following the electric power reduction, and, after some time, it stabilizes at 52%. Then, the nuclear power returns to approximately 98% due to the electric power increase.

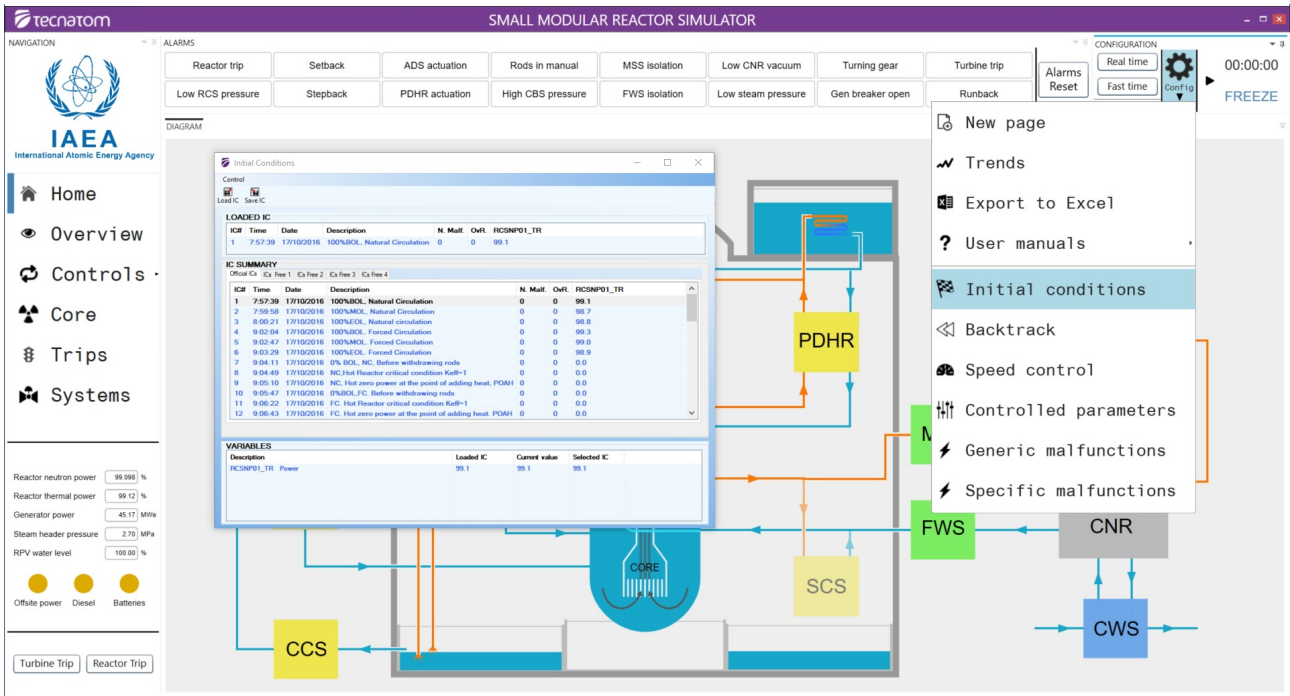
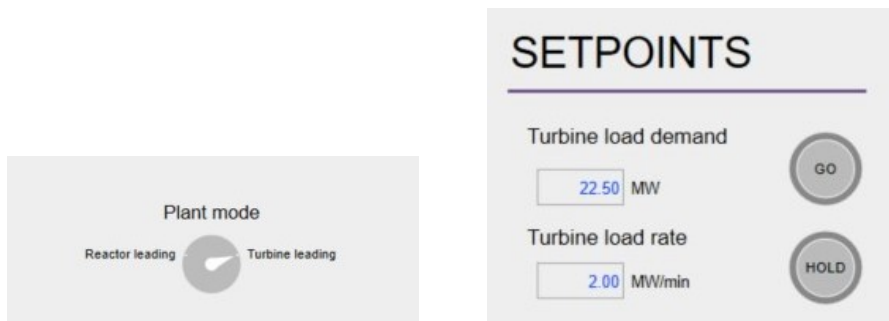


Figure 6.1: Steps to load initial condition number 1 in iPWR simulator.



(a) Plant operation mode in turbine leading.

(b) Turbine load demand and load rate.

Figure 6.2: Selecting turbine leading control, load demand and load rate.

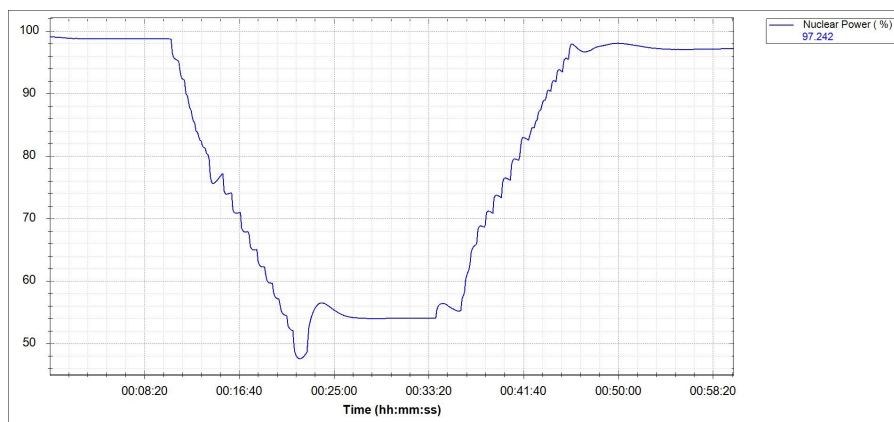


Figure 6.3: Nuclear power in power maneuvering transient.

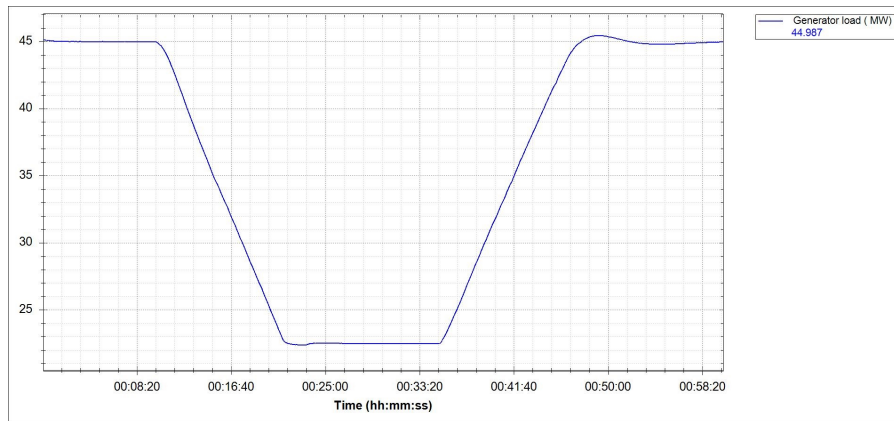


Figure 6.4: Electric power in power maneuvering transient.

As can be observed in Figure 6.5, with the power reduction in the turbine, less steam is required, resulting in a lower steam flow. Furthermore, as the power reduction was performed with a power rate of 2 MWe/min, the system was able to handle the transient without using the bypass flow to the condenser, resulting in a zero flow in the turbine bypass line. When the turbine power returned to 45 MWe, the flow to the turbine was restored to approximately its initial value.

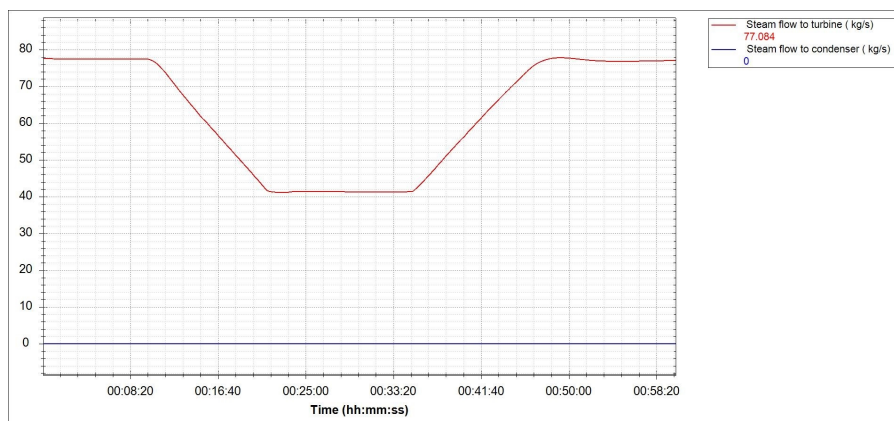


Figure 6.5: Steam flow to the turbine and to the condenser in power maneuvering transient.

Figures 6.6 and 6.7 show the steam flow from each helical-coil tube of the SG together with the respective feedwater flow. As can be observed, the control system keeps the balance between the steam flow and the feedwater flow to guarantee the same amount of steam generation and feedwater. The steam produced in each helical-coil tube of the SG is collected in the steam header and then directed to the turbine resulting in the steam flow presented in Figure 6.5.

As a consequence of the power reduction, the RCS average temperature also reduces because fewer fissions occur, and consequently, less heat is generated in the reactor core. On the other hand, increasing the power results in increasing RCS average temperature because more fissions occur and, consequently, more heat is generated in the core. These effects are shown in Figure 6.8, where the RCS average temperature and core inlet and core outlet temperatures are presented.

The decrease in RCS average temperature results in the contraction of the coolant. Due to this effect, the PZR level begins to lower, as shown in Figure 6.9. As a response to the decrease in the PZR level, the charge flow from the CVCS system increases while the discharge

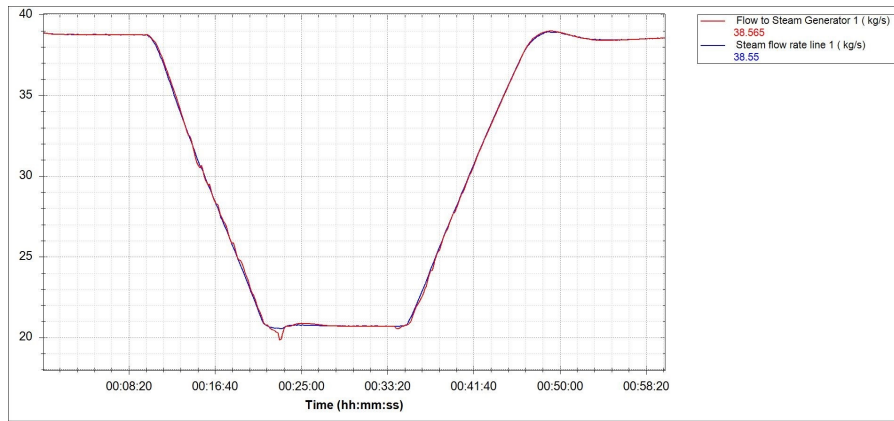


Figure 6.6: Steam and feedwater flow in helical-coil tube 1 of the SG in power maneuvering transient.

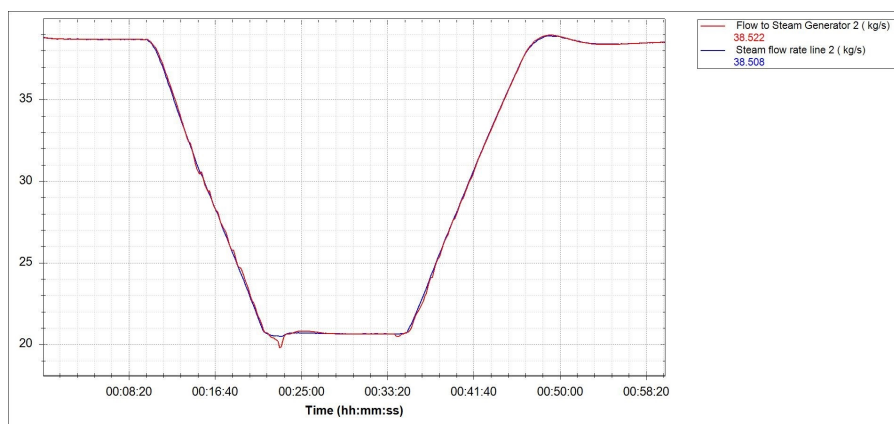


Figure 6.7: Steam and feedwater flow in helical-coil tube 2 of the SG in power maneuvering transient.

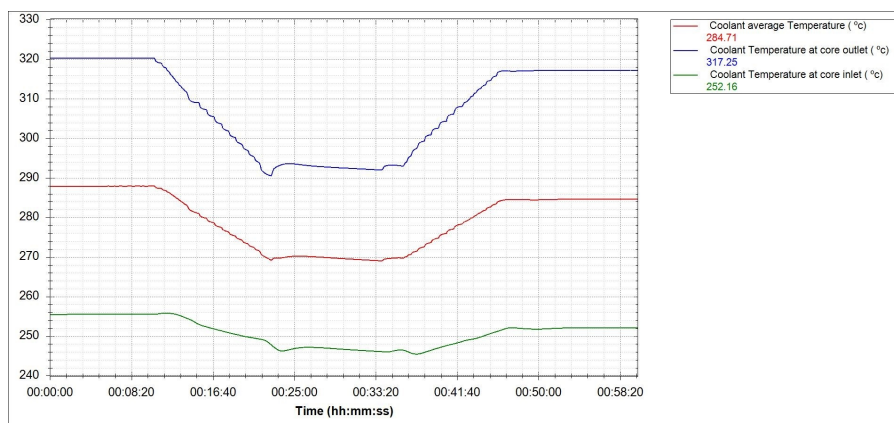


Figure 6.8: RCS average temperature and core inlet and core outlet temperatures in power maneuvering transient.

flow is maintained constant to restore the PZR level, as shown in Figure 6.10. However, the PZR level control depends on the RCS average temperature. Thus, reducing the RCS average temperature reduces the PZR level setpoint in the PZR level control system, as shown in Figure 6.9. During the power reduction, the PZR level is lower than the PZR level setpoint,

which results in an increase in the charge flow even though a reduction in the PZR level is being performed. Restoring the power to 100%, the coolant expands, which increases the PZR level. In response, the PZR level control system reduces the charge flow to zero. However, the PZR level continues to increase due to coolant expansion. The PZR level setpoint in the PZR level control system also increases because the operational PZR level at 100% power is higher than the PZR operational level at 50% power. During the transient, the PZR level is higher than the PZR level setpoint; thus, the charge flow is kept at zero even though an increase in the PZR level is being performed.

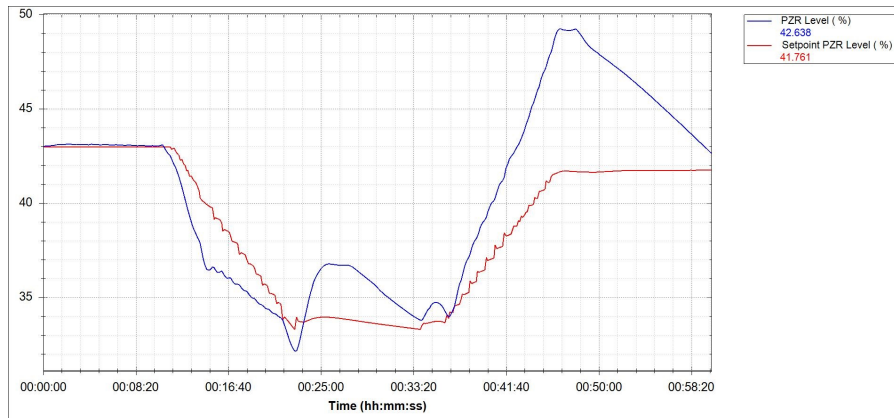


Figure 6.9: PZR level control setpoint and PZR level in power maneuvering transient.

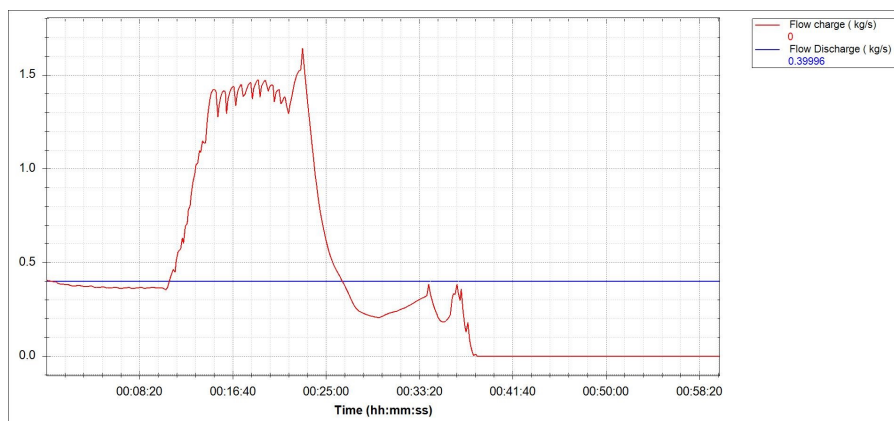


Figure 6.10: CVCS charge and discharge flows in power maneuvering transient.

The decrease in the RCS average temperature increases the moderator density. As the reactor has a negative MTC, the increase in moderator density during the power reduction inserts a positive reactivity in the core as presented in Figure 6.11. During the power reduction, the fuel temperature also reduces, which inserts a positive reactivity in the core because the FTC is also negative. This effect is presented in Figure 6.11. As mentioned before, the boron concentration is not changed during the entire transient; then control rods must be inserted to reduce the power and to compensate the positive reactivity inserted by the MTC and FTC, as shown in Figure 6.11. When power is increased, the opposite effect takes place. The MTC and FTC insert negative reactivity, and the control rods are withdrawn from the core to increase the power and to compensate for the MTC and FTC effects. The insertion of the control rod in the core results in a negative startup rate, while the withdrawal gives a positive startup rate. The startup rate is presented in Figure 6.12.

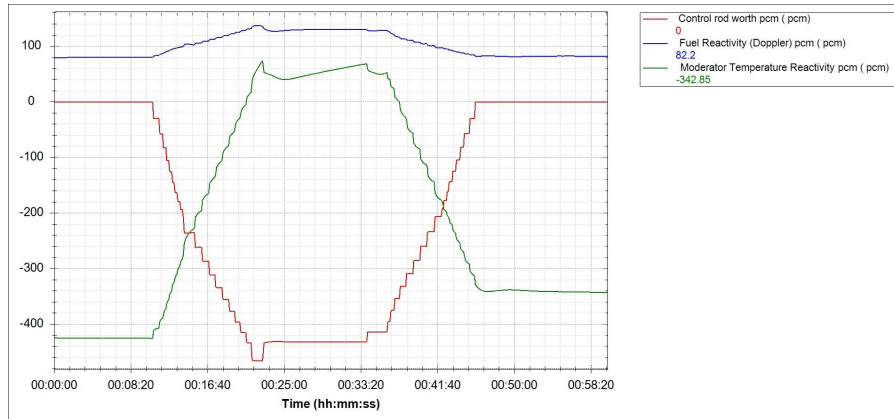


Figure 6.11: MTC, FTC, and control rods reactivities in power maneuvering transient.

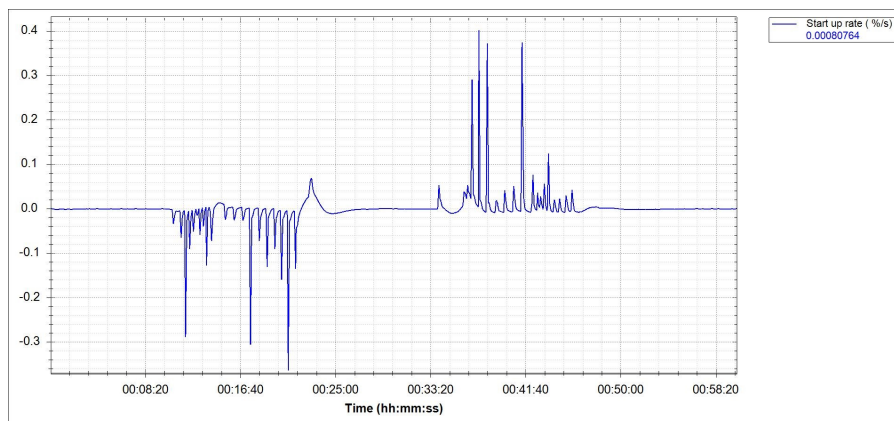


Figure 6.12: Startup rate during the transient in power maneuvering transient.

The xenon-135 and samarium-149 concentrations, previously in equilibrium, start to change when the power is reduced to 50%, which affects the core reactivity. The negative reactivity inserted by xenon-135 increases until it reaches a maximum after several hours. After the maximum, this negative reactivity begins to fall until its equilibrium value at 50% power, which is less negative than the negative reactivity at 100% power. Thus, the net effect of the reactivity inserted by the xenon-135 is positive. The control rods or the boron concentration must be used to compensate for this positive reactivity insertion. On the other hand, the negative reactivity inserted by the samarium-149 remains the same as 100% power. When the power is increased to 100%, the negative reactivity inserted by the xenon-135 decreases until reaching a minimum. After the minimum, this negative reactivity begins to rise until its equilibrium value corresponding to 100% power, which is more negative than the reactivity at 50% power. Thus, the net effect of the reactivity inserted by xenon-135 is negative, which must be compensated by the control rods or by the boron concentration. As previously, the samarium-149 negative reactivity also remains the same. Additionally to the xenon-135 and samarium-149, other fission products are generated and consumed during the transient, requiring adjustments in the core reactivity to compensate for the effects of these products. Due to the long time required (large power variation), the time for xenon-135 stabilization has not been waited. The xenon-135 reactivity is presented in Figure 6.13. In this graph, it is only possible to observe that the xenon-135 reactivity becomes more negative due to the power reduction, and, after the power increase, the xenon-135 reactivity slightly becomes less negative. Although the effect of samarium-149 is simulated, there is no option in the simulator to present the samarium-149

reactivity.

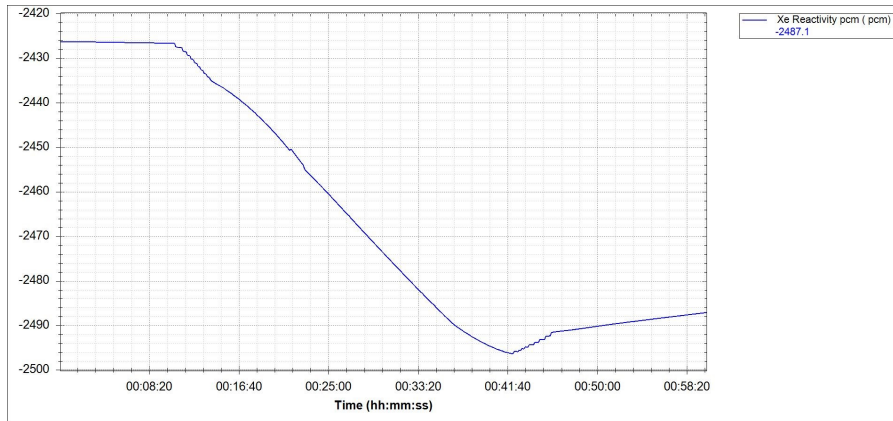


Figure 6.13: Xenon-135 reactivity in power maneuvering transient.

During the entire transient, the PZR pressure was kept approximately constant at the PZR operation pressure (15.5 MPa) by the PZR pressure control system, as shown in Figure 6.14.

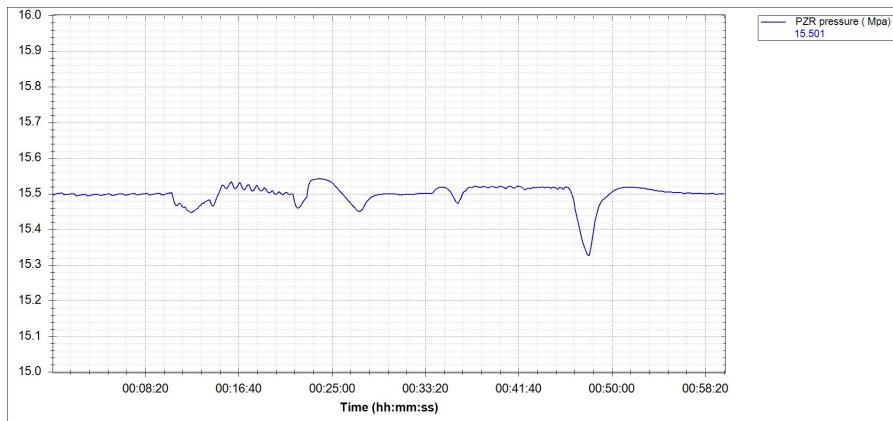


Figure 6.14: PZR pressure in power maneuvering transient.

In this transient, the entire control was performed automatically by the reactor control system, without intervention of the operator. The variation in the reactor power was performed only through the use of the control rods. During the power reduction to 50%, the control rods were inserted automatically in the core until the desired power was reached. As previously discussed, the insertion of the control rods in the core distorts the core neutronic flux, resulting in a non-uniform burning of the fuel. Thus, a possible action of the operator would be to increase the concentration of boron in the RCS, allowing the control rods to be automatically removed from the core by the reactor control system, thereby maintaining the reactor power and reducing the distortion in the neutronic flux caused by the control rods insertion. Boron dilution in the RCS would be required to return the reactor power to 100%.

## 6.2 Reactor Scram

As discussed in Section 3.6.2, in accident conditions or when reactor parameter limits are reached, the reactor responds by inserting all the control rods to mitigate or prevent adverse

effects. This sudden insertion of all control rods is known as a reactor scram. The results presented in this section refers to the manual scram from the reactor at full power.

The first step in the simulation consists of loading the initial condition. For this transient, the same initial condition loaded in Section 6.1 is used, 100% power at BOL with natural circulation. The next step consists of starting the transient. For this, the button Reactor Trip is pressed as highlighted in Figure 6.15.

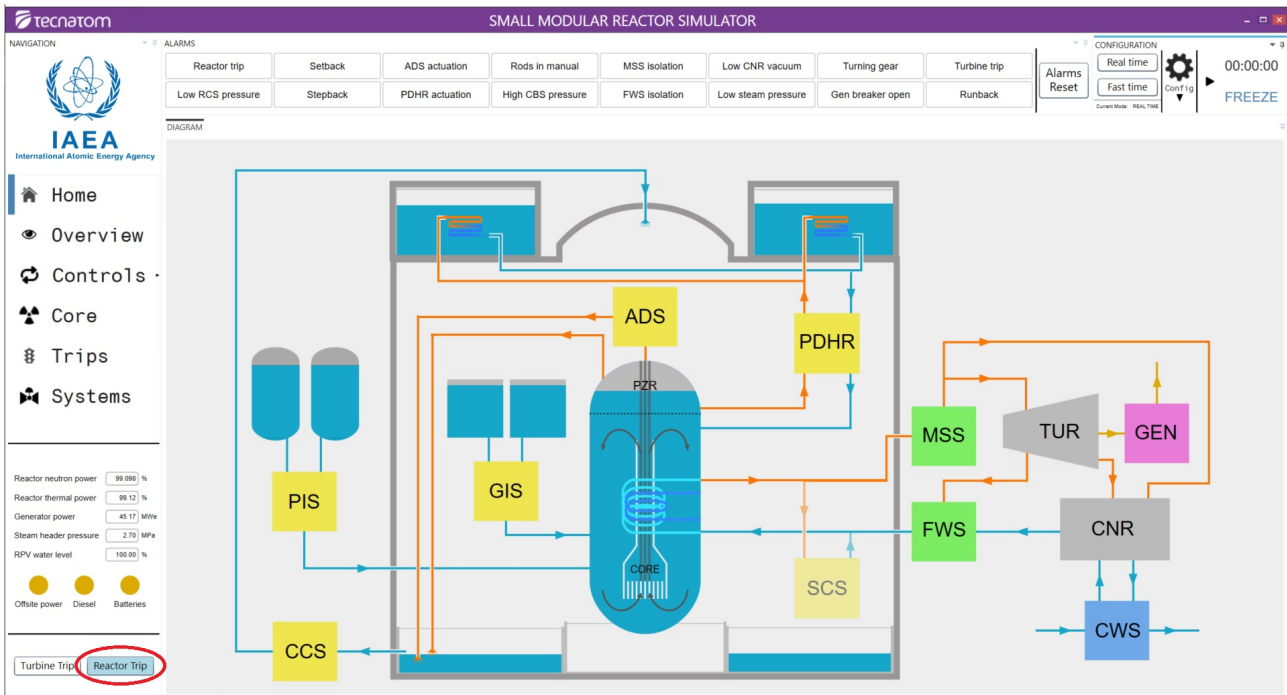


Figure 6.15: Starting the scram transient in the simulator.

After the scram, the control and shutdown rods are inserted in the core, resulting in a large negative reactivity insertion as shown in Figure 6.16. The insertion of this large negative reactivity rapidly decreases the nuclear power (neutron flux) and the thermal power, as shown in Figure 6.17. The large drop observed in the neutron flux is caused by the prompt neutrons that respond very fast to the negative reactivity insertion.

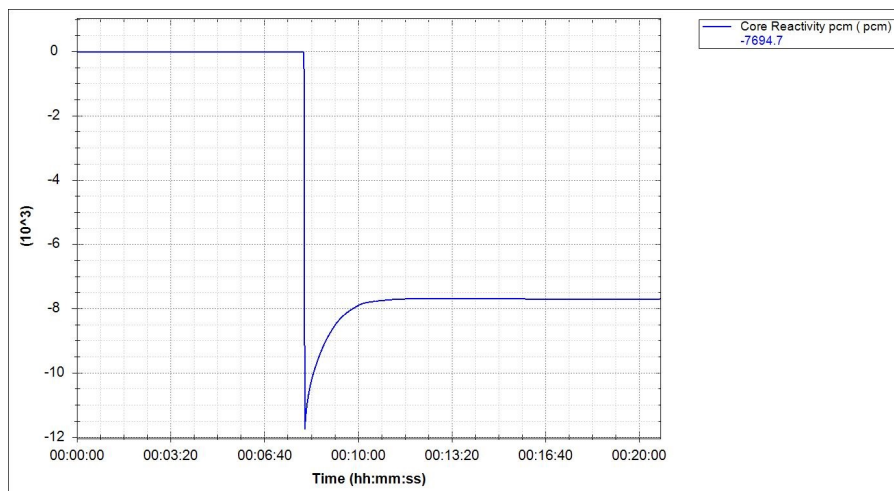


Figure 6.16: Core reactivity in reactor scram transient.



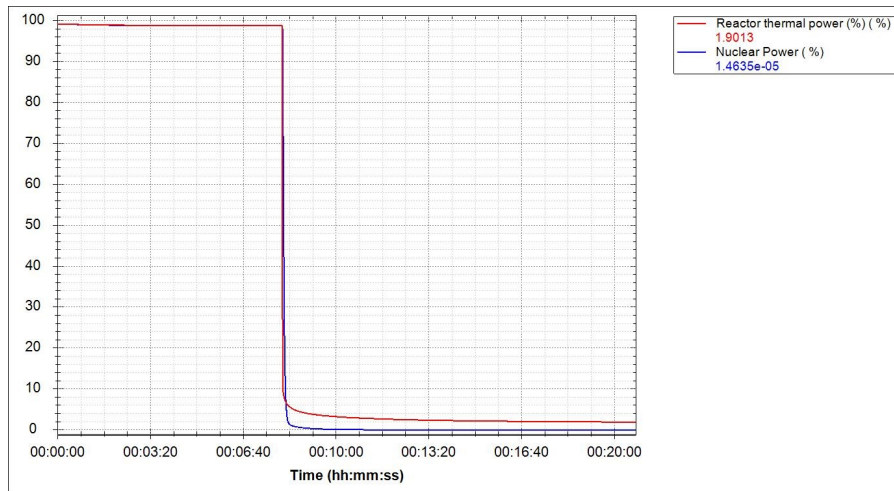


Figure 6.17: Nuclear and thermal powers in reactor scram transient.

As there is no longer heat production from fission, the moderator and fuel temperatures decrease, as shown in Figure 6.18. As the MTC and FTC are negatives, the decrease in moderator and fuel temperatures results in the insertion of positive reactivity in the core. This effect is presented in Figure 6.19. The effect of the positive reactivity inserted by the MTC and FTC can be observed by the increase in the core reactivity observed in Figure 6.16.

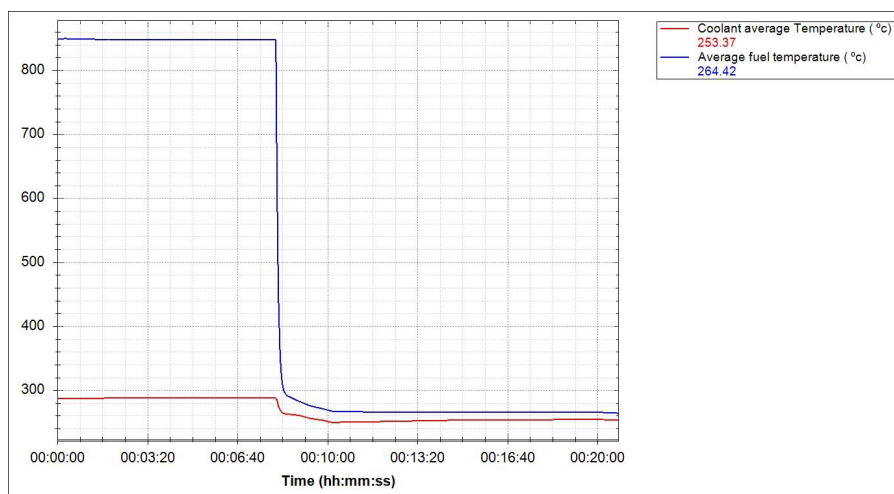


Figure 6.18: Moderator and fuel temperatures in reactor scram transient.

Despite the reduced number of fissions and the resulting loss of heat production after the scram, there still neutron and thermal sources in the core. The initial inventory of radioactive fission products and activated material continues to undergo radioactive decay for a long period. This effect can be observed in Figure 6.17, where the thermal power is not zero after the scram (the decay heat).

Additionally to the decay heat, neutrons continue to be generated from the inventory of delayed neutron precursors produced at full power. This results in a negative period of the power stabilized at approximately -80 seconds after the rapid drop of prompt neutron levels. To demonstrate this negative stable period, consider the two points presented in Figure 6.20, which are in the portion of the curve with the stable period of -80 seconds. The time interval between these points is 20 seconds. Using Equation 3.20 and the points in Figure 6.20, the

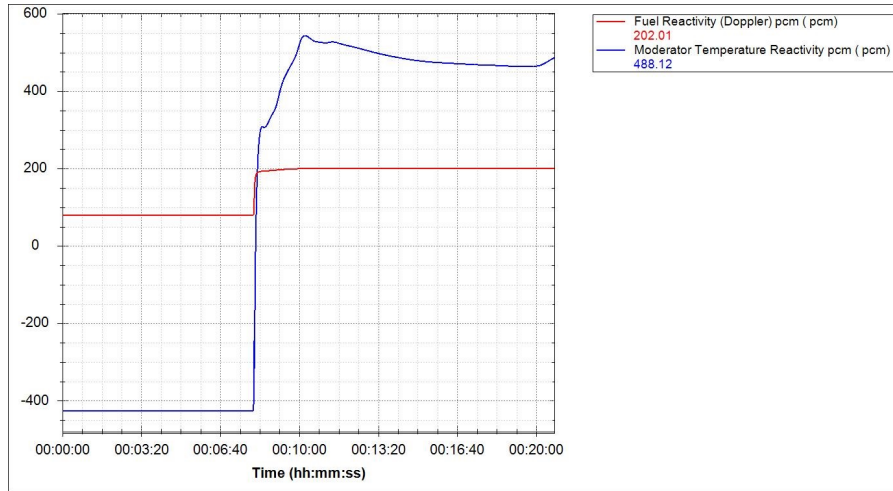


Figure 6.19: Moderator and fuel reactivities in reactor scram transient.

period results in:

$$P = P_0 e^{\frac{t}{\tau}} \Rightarrow \tau = \frac{t}{\ln\left(\frac{P}{P_0}\right)} = \frac{20 \text{ s}}{\ln\left(\frac{1.5817 \cdot 10^{-5} \%}{2.0275 \cdot 10^{-5} \%}\right)} = -80.55 \text{ s} \quad (6.1)$$

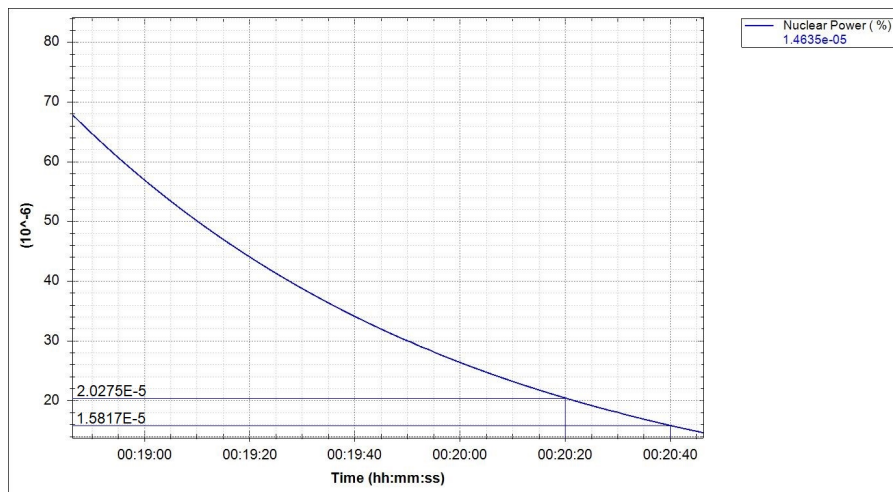


Figure 6.20: The -80 seconds stable period of the nuclear power in reactor scram transient.

After the scram, xenon-135 continues to be produced for several hours, inserting negative reactivity during this period. After the radioactive decay becomes the dominant term in xenon-135 production/loss, it decays for a few days resulting in the decrease of the negative reactivity inserted by xenon-135. As discussed in Section 6.1, the time required for the xenon-135 transient is too long; for that reason, only the increase in the negative reactivity of the xenon-135 after the scram is presented in Figure 6.21. Samarium-149 continues to be produced after the scram and then approaches the shutdown equilibrium concentration resulting in a stable negative reactivity insertion. Although simulated, it is not possible to present the negative reactivity inserted by the samarium-149 in the iPWR simulator.

As discussed, the scram is the sudden shutdown of the reactor to mitigate or prevent adverse effects in accident conditions or when reactor parameter limits are reached. The scram is performed automatically by the reactor protection system without the need for operator action,

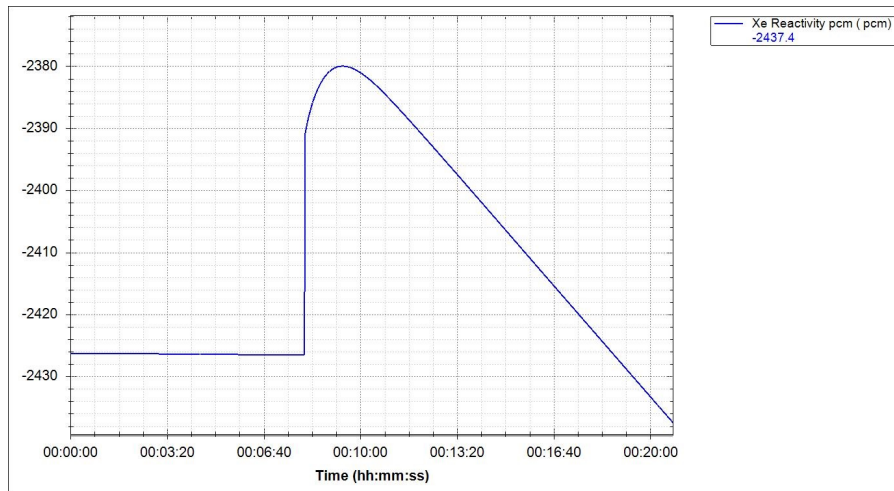


Figure 6.21: Increase in the negative reactivity inserted by xenon-135 after the scram in reactor scram transient.

unless in the case of manual scram. After the scram, the operator must guarantee that the reactor is adequately shut down and that the safety systems respond as expected. Due to the decay heat, the operator has to guarantee that the heat removal continues for a long period after the scram to avoid damage to the fuel and to the reactor core. Finally, the causes of the scram must be identified and corrected before restarting the reactor.

### 6.3 Loss of Coolant Flow

The loss of coolant flow transient was discussed in Section 3.6.3. It refers to a partial or complete loss of flow in the primary coolant loop during full power operation, which may be caused by a loss of one or more RCP due to electrical or mechanical failure in the pump motor, fault in the power supply to the pump motor or a pump motor trip caused by overcurrent or phase imbalance. Depending on the reactor design, the loss of RCPs does not require the immediate reactor shutdown. However, to continue the operation, the reactor power must be reduced to a level that depends on the number of lost RCPs.

In order to simulate this transient, a different initial condition is selected. As RCPs are required, the initial condition number 4, 100% BOL with forced circulation, is selected. In the iPWR simulator, when the loss of RCP is detected, the reactor control system automatically reduces the reactor power to 50% when one RCP is lost and to 30% when four RCPs are lost (reactor stepbacks). Thus, a failure in the reactor stepbacks is inserted to avoid the actuation of this system. The failure is inserted on the page Trips of the simulator by clicking in the malfunction button (MF) at Reactor Stepbacks and then activating the malfunction, as presented in Figure 6.22. The transient is started by stopping two out of four RCPs, which reduces the coolant flow from approximately 429 kg/s to approximately 269 kg/s. The idea was to reduce the flow from 100% to 50%, but stopping two RCPs reduces the flow to approximately 63%; however, the transient analysis is not affected. The RCPs are stopped by inserting an electric failure in RCPs number 2 and 4. The failure is inserted on the page Generic Malfunction of the simulator as presented in Figure 6.23.

After stopping the RCPs, the coolant flow is reduced as presented in Figure 6.24. By reducing the coolant flow, the coolant remains in the core for a longer time, which increases

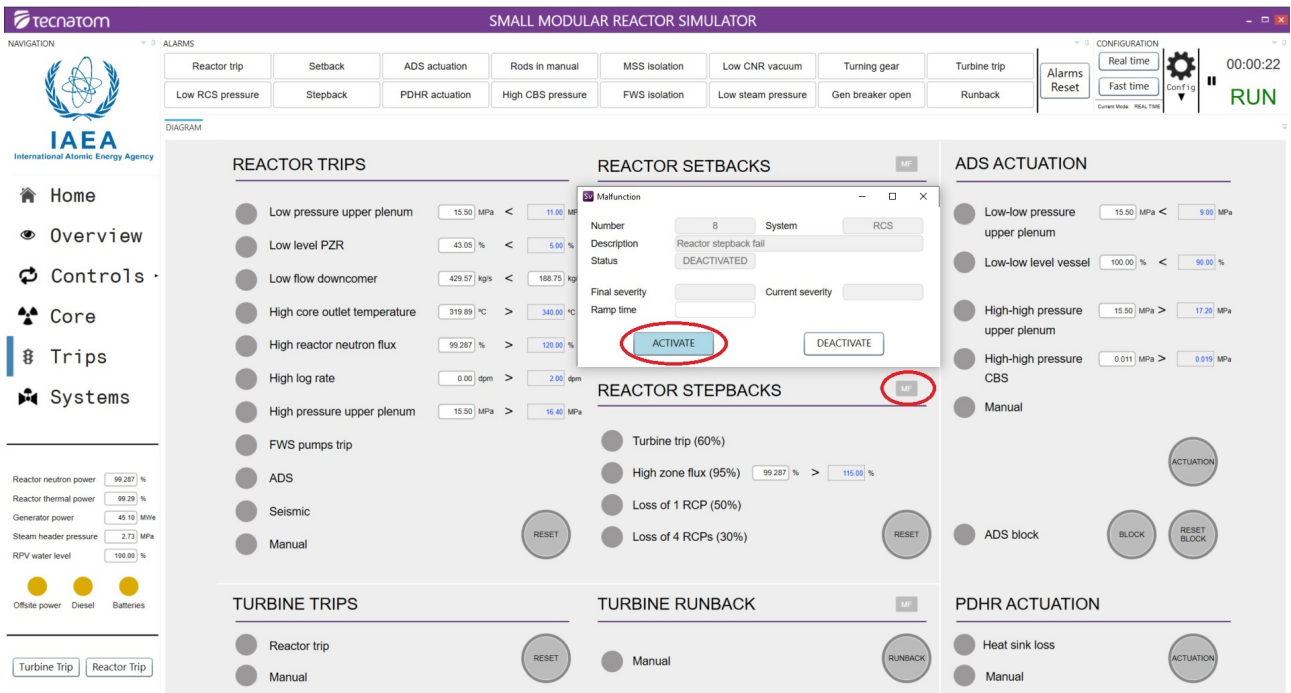


Figure 6.22: Inserting a failure in the reactor stepbacks.

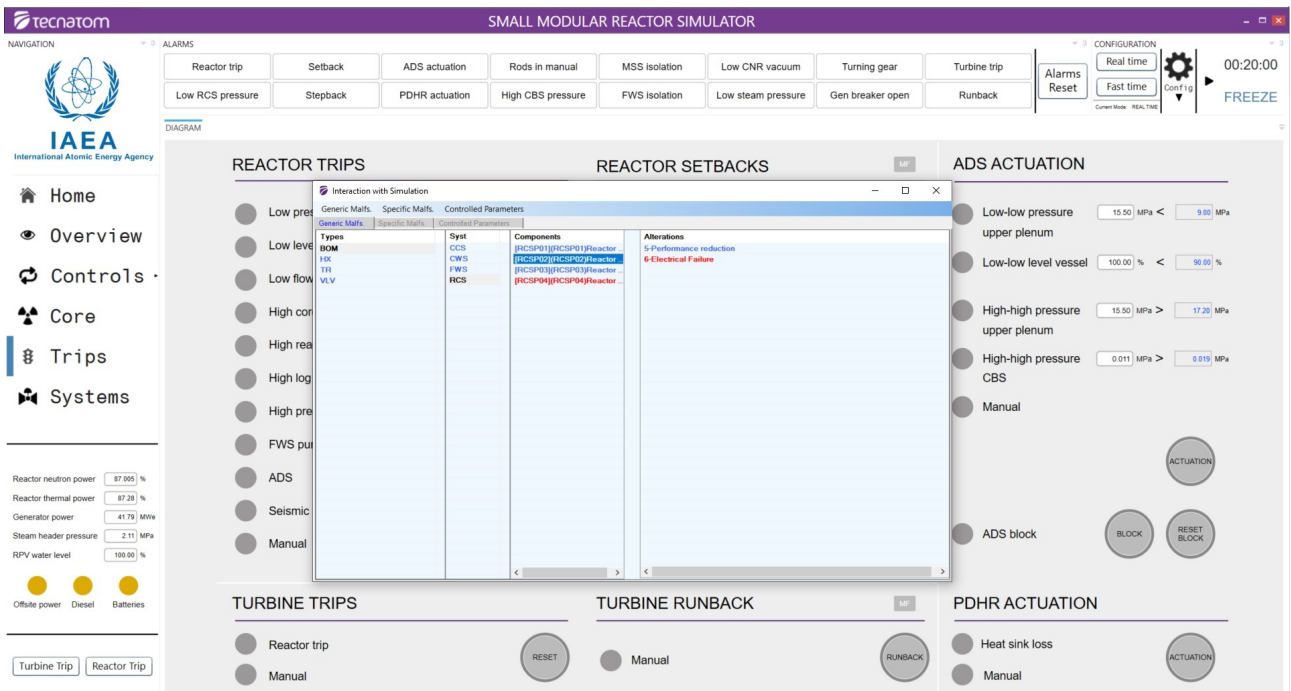


Figure 6.23: Generic Malfunction page showing the failed pumps.

the coolant temperature. This effect can be observed in Figure 6.25, where the average coolant temperature increases right after the reduction in the coolant flow.

The increase in the coolant temperature results in a negative reactivity insertion due to the negative MTC, resulting in a negative core reactivity as presented in Figure 6.26. The resulting negative reactivity inserted into the core decreases the reactor power, as presented in Figure 6.27. As the reactor power decreases, the fuel temperature also decreases, as shown in

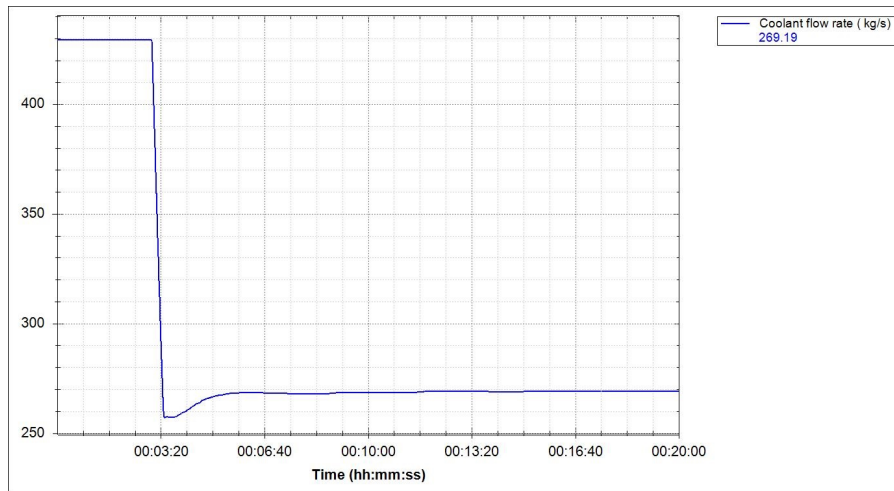


Figure 6.24: Coolant flow in the core in loss of coolant flow transient.

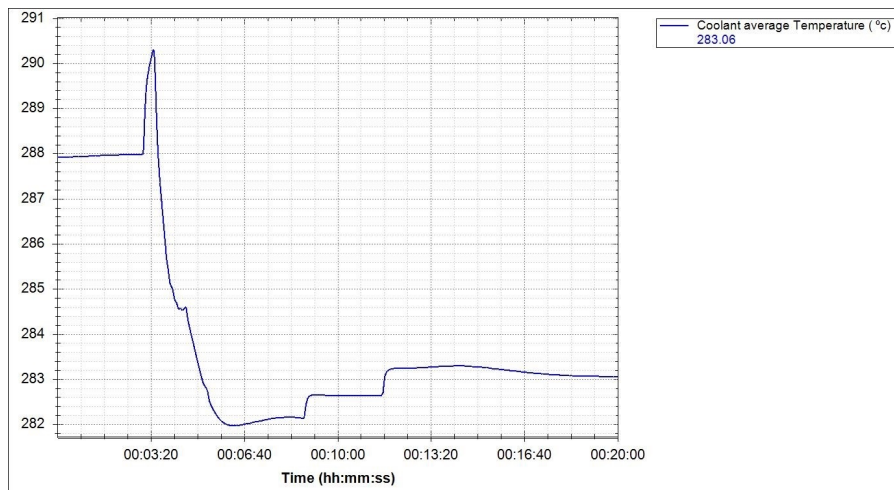


Figure 6.25: Average coolant temperature in loss of coolant flow transient.

Figure 6.28. The decrease in fuel temperature inserts a positive reactivity in the core due to the effect of FTC (Figure 6.26). After the transient, the reactor power reaches a stable condition at a power level lower than the full power level (approximately 87%) once the MTC and FTC balance each other.

In the following hours, the negative xenon-135 reactivity becomes more negative as xenon-135 concentration increases. After reaching the maximum negative value, the negative reactivity begins to lower until reaching the equilibrium level for the new reactor power, which is less negative than the level at 100% power (lower xenon-135 concentration). During the xenon-135 transient, the temperature is adjusted to counterbalance the xenon-135 reactivity. The effect of xenon-135 reactivity is presented in Figure 6.29, where, due to the long time required for the entire xenon-135 transient, only the increase in the xenon-135 negative reactivity is presented. The samarium-149 negative reactivity stabilizes at the same level.

As discussed, the loss of coolant flow is characterized by a complete loss or reduced RCS flow that can be caused by failures in RCPs. SMR designs that use natural circulation in the primary system are not susceptible to this transient. In the designs that use forced circulation, the reactor control system detects the failure and takes the required actions to minimize the transient effects. However, as demonstrated in the simulation, even though the reactor stepback

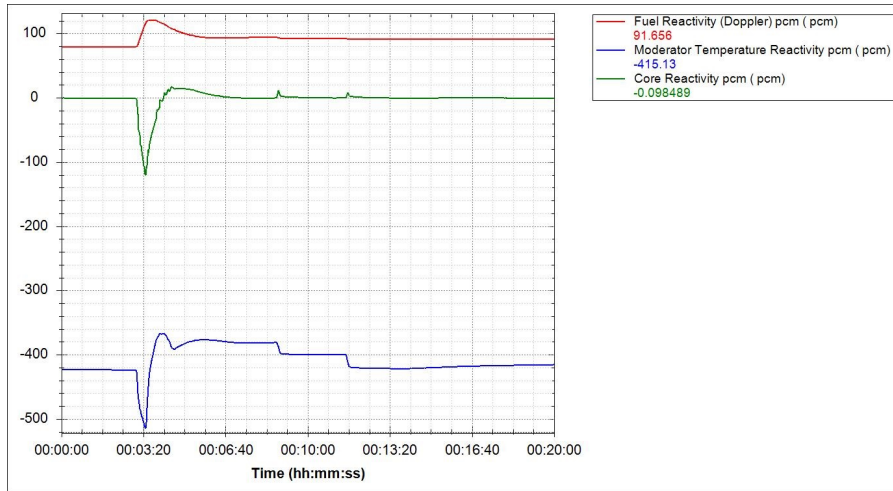


Figure 6.26: Core, MTC, and FTC reactivities in loss of coolant flow transient.

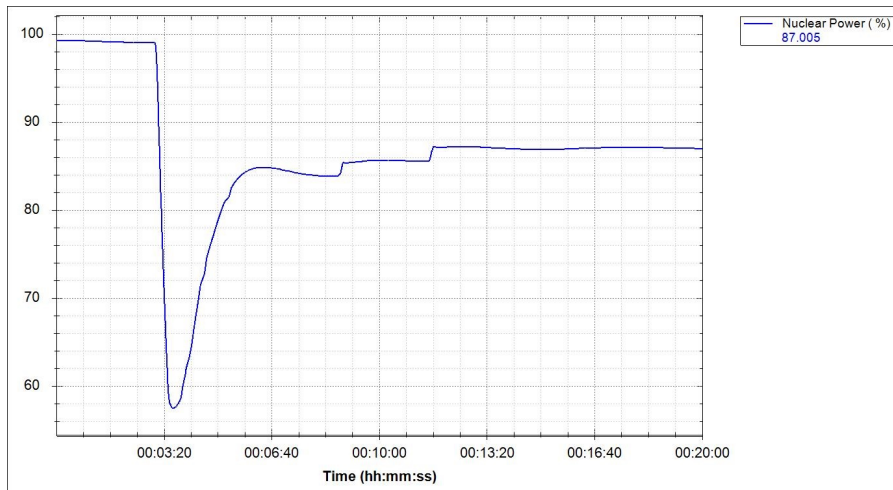


Figure 6.27: Nuclear power in loss of coolant flow transient.

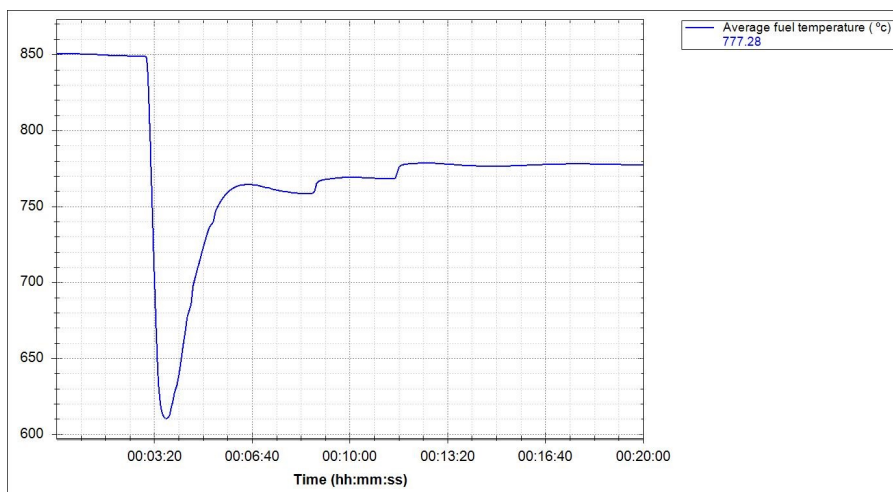


Figure 6.28: Average fuel temperature in loss of coolant flow transient.

response is defective, the reactor can handle the transient. After the loss of coolant flow, the operator must identify the causes of the failure and take the required measures to remedy the

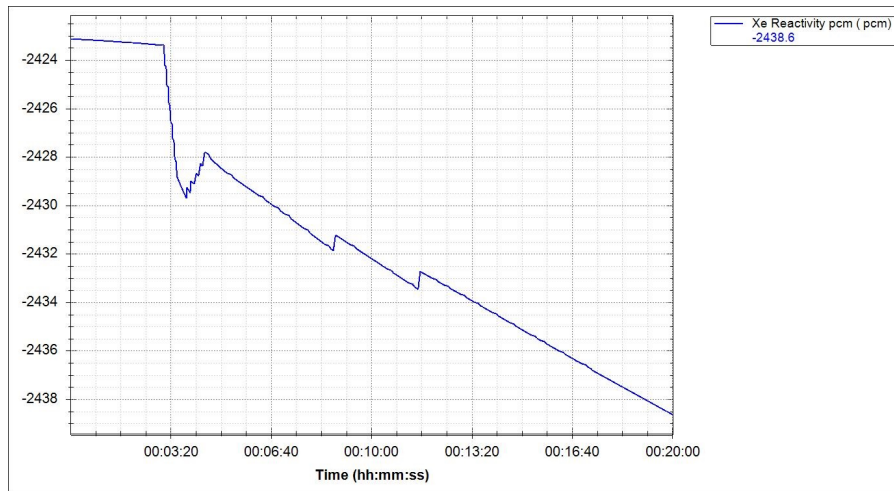


Figure 6.29: Xenon-135 negative reactivity in loss of coolant flow transient.

problem. When the reactor remains in operation, the operator must determine whether the reactor is in a safe condition (appropriate cooling) or whether it needs to be shut down. Besides, the operator must determine whether the correction of the failure can be performed with the reactor operating or not and how long it will be necessary to correct the problem.

## 6.4 Steam Generator Tube Failure (SGTF)

The SGTF can be caused by rapid propagation of a circumferential crack resulting in a double-ended rupture of the tube. In this event, the reactor coolant passes from the primary side of the SG to the secondary side, where steam is produced and travels through the main steam lines to the turbine. The pressure differential drives the flow between the RCS and the secondary side of the SG. The helical-coil tube design of the SG is different from the SG designs in conventional PWRs because the primary coolant is located on the shell side of the tubes. After tube failure, the primary coolant travels from the shell side of the SG into the tube through the break. Radionuclides present in the primary coolant are discharged through the failed tube into the atmosphere until the faulted SG is isolated by automatic closure of the main steam isolation valves (MSIVs). The protection system must maintain the radiological releases below the accepted limits and prevent the overflow of the SG secondary to avoid water entering the steam lines.

For this transient, the same initial condition loaded in Section 6.1 is used, 100% power at BOL with natural circulation. Next, a failure in the helical-coil tube 1 of the SG with 16% of severity is scheduled to start after 5 minutes of simulation. This malfunction is inserted in the iPWR simulator on page Specific Malfunction as presented in Figure 6.30. The entire transient occurs without operator intervention.

Immediately after the transient beginning, the high radiation alarm in main steam line 1 indicates a high radiation level in this line, as can be observed in the N-16 alarm in red located at the MSS part on the Systems page of the simulator and presented in Figure 6.31. Additionally, due to the loss of primary coolant to the secondary, the PZR level begins to lower, as can be observed in the PZR level curve in Figure 6.32. However, the pressure control system keeps the RCS pressure constant, as shown in Figure 6.33. Despite the failure, the heat removal is maintained in the core, which keeps the core inlet and outlet temperatures and the

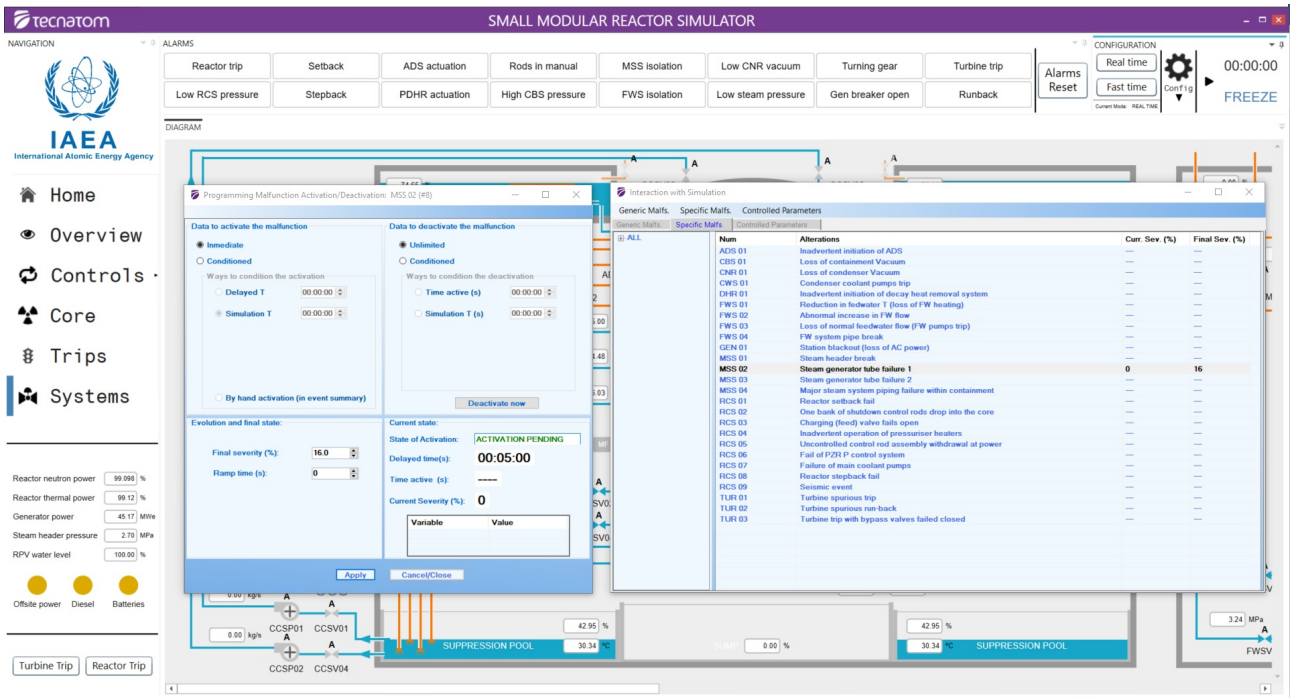


Figure 6.30: Inserting a SG tube failure with 16% severity.

average coolant temperature constant, as shown in Figure 6.34. As the RCS pressure and the average coolant temperature remain constant, the subcooling margin is maintained constant and positive, as presented in Figure 6.35, which avoids the formation of steam in the RCS.

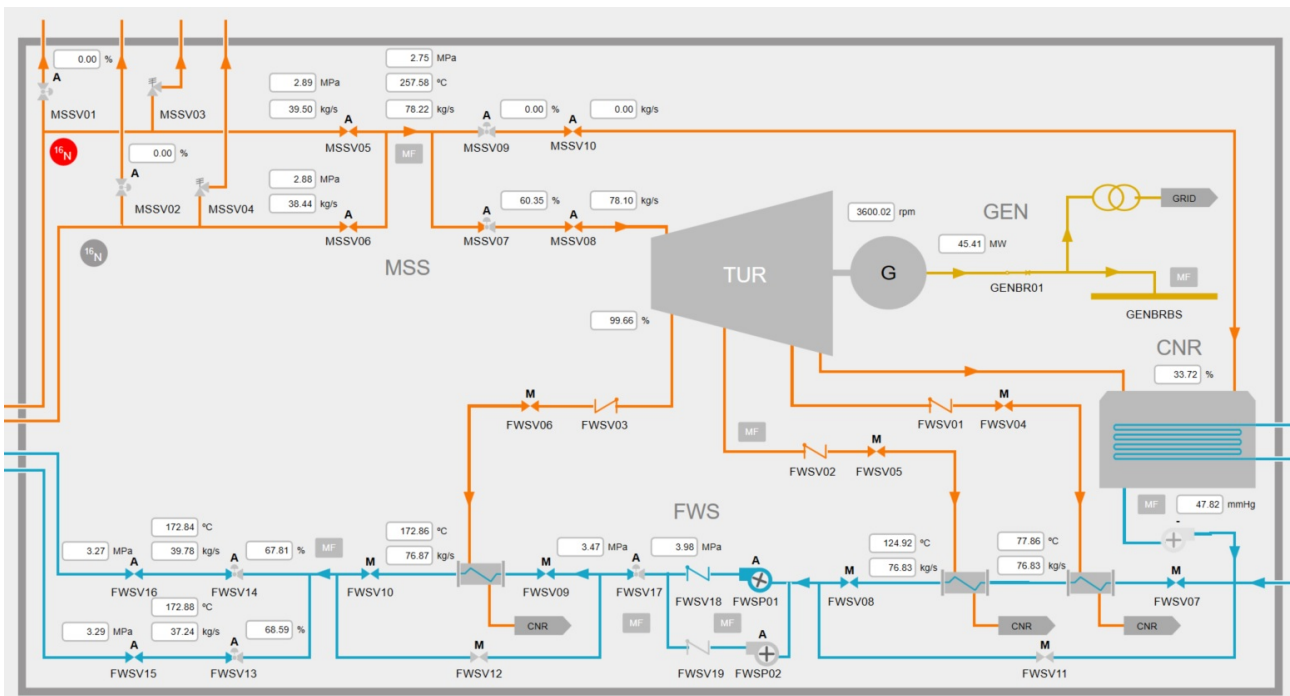


Figure 6.31: N-16 alarm indicating high radiation level in main steam line 1 in SGTF transient.

A decrease in the feedwater flow and a slight increase in the steam flow can be observed in the faulted helical-coil tube, as observed in the disbalance between the feedwater flow and the steam flow shown in Figure 6.36. In the non-faulted helical-coil tube, the steam flow and,





Figure 6.32: PZR level in SGTF transient.



Figure 6.33: PZR and RPV pressures in SGTF transient.

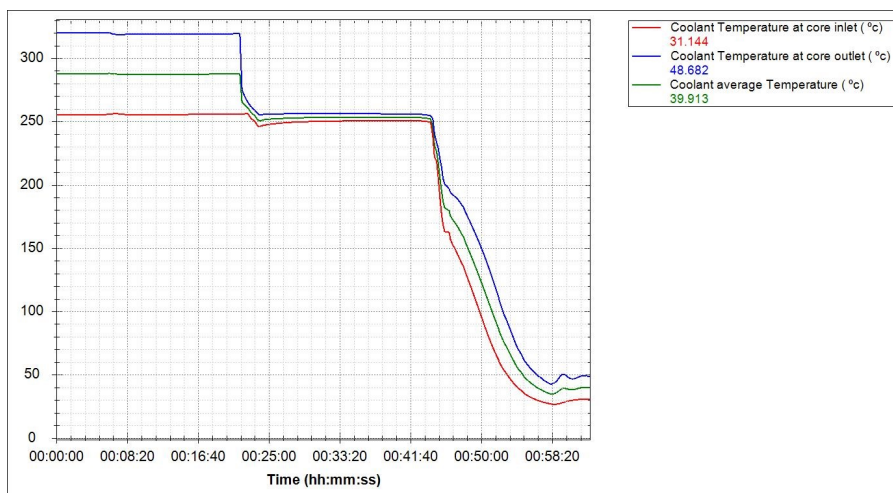


Figure 6.34: Core inlet and outlet temperatures and average coolant temperature in SGTF transient.

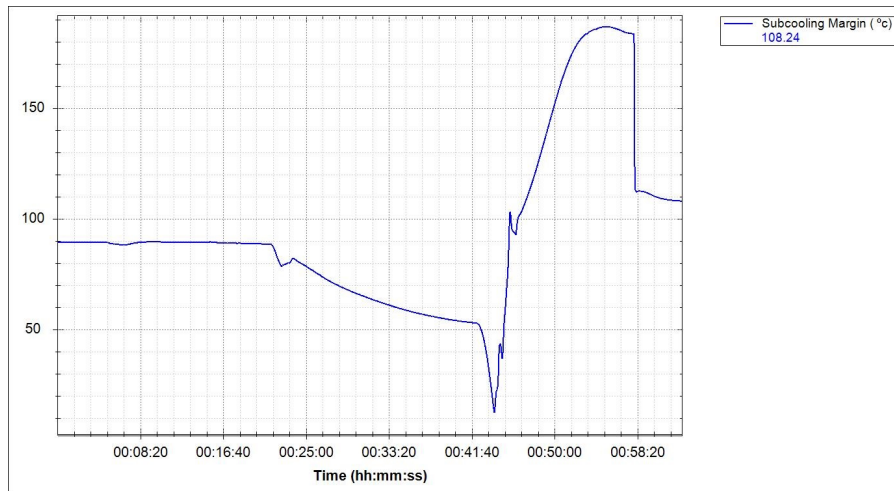


Figure 6.35: Subcooling margin in SGTF transient.

consequently, the feedwater flow are slightly decreased, compensating for the increased steam flow in the other coil. However, the steam flow and feedwater flow in this tube remain balanced, as shown in Figure 6.37. The increase in the pressure causes the disbalance in the flows observed in the faulted helical-coil tube once it is subjected to a slightly higher pressure, see Figure 6.38.

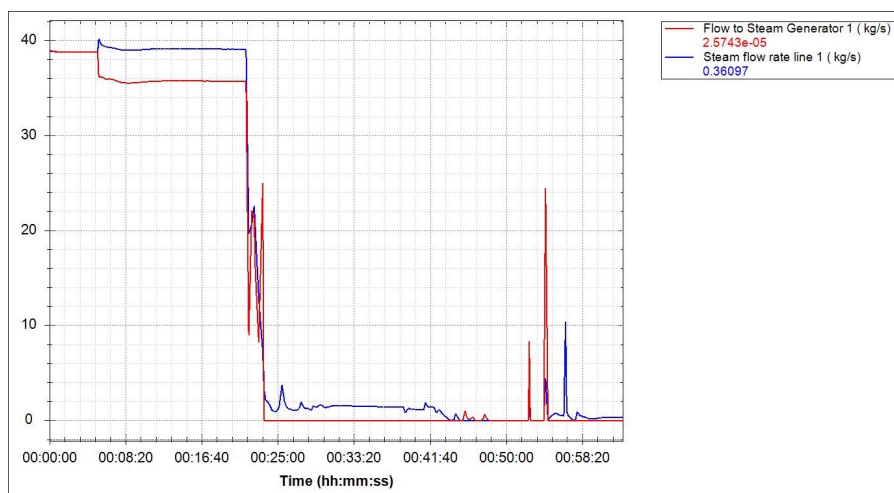


Figure 6.36: Steam flow and feedwater flow in the faulted helical-coil tube in SGTF transient.

After the beginning of the transient, the variables discussed previously stabilize except for the PZR level that continues to lower (Figure 6.32). In response, the PZR level control increases the CVCS charge flow while keeping the discharge flow constant, as observed in Figure 6.39.

The PZR level continues to lower, and when it is below 5%, it causes the reactor trip due to low level in the PZR. The reactor trip and its cause can be identified on the page Trips of the simulator, as shown in Figure 6.40. The red light indicates the cause of the trip. The reactor trip can also be observed in the Alarms part on this screen. After the trip, the PZR level continues to lower to 0%. The reactor trip causes the turbine to trip and, consequently, the opening of the generator breaker, which disconnects the generator from the grid. Both can be observed in Turbine Trips and in Alarms. The turbine trip closes the turbine control valves and directs the steam flow to the condenser, as shown by the decrease in the steam flow to the turbine and the increase in the steam flow to the condenser in Figure 6.41. The turbine trip

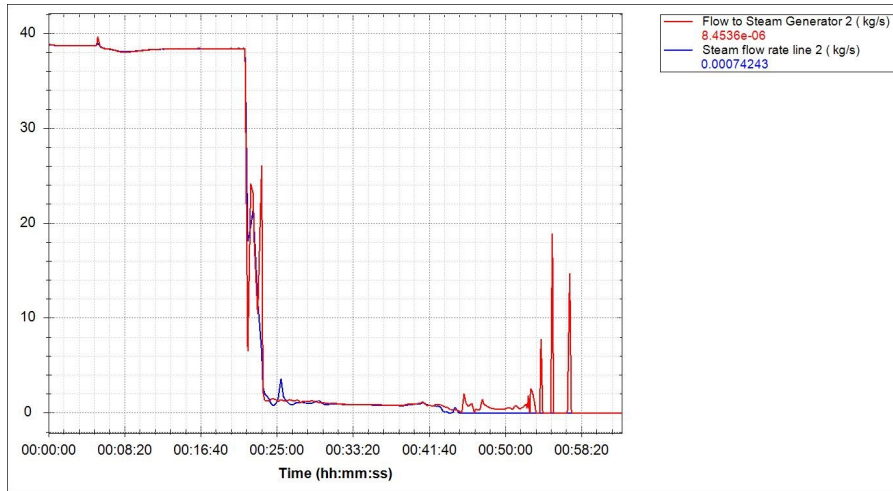


Figure 6.37: Steam flow and feedwater flow in the non-faulted helical-coil tube in SGTF transient.

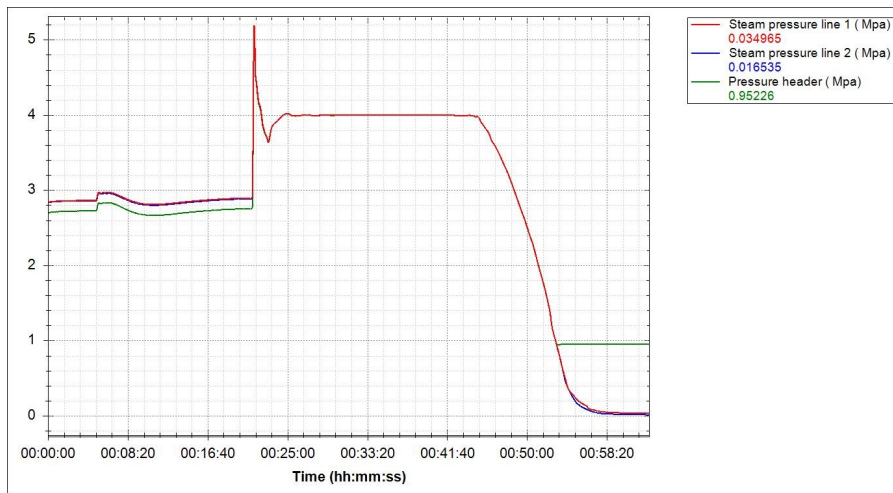


Figure 6.38: Steam pressure in the steam lines 1 and 2 and in the steam header in SGTF transient.



Figure 6.39: CVCS charge and discharge flow in SGTF transient.

also causes the increase in the pressure in the steam lines 1 and 2 and in the steam header (Figure 6.38).

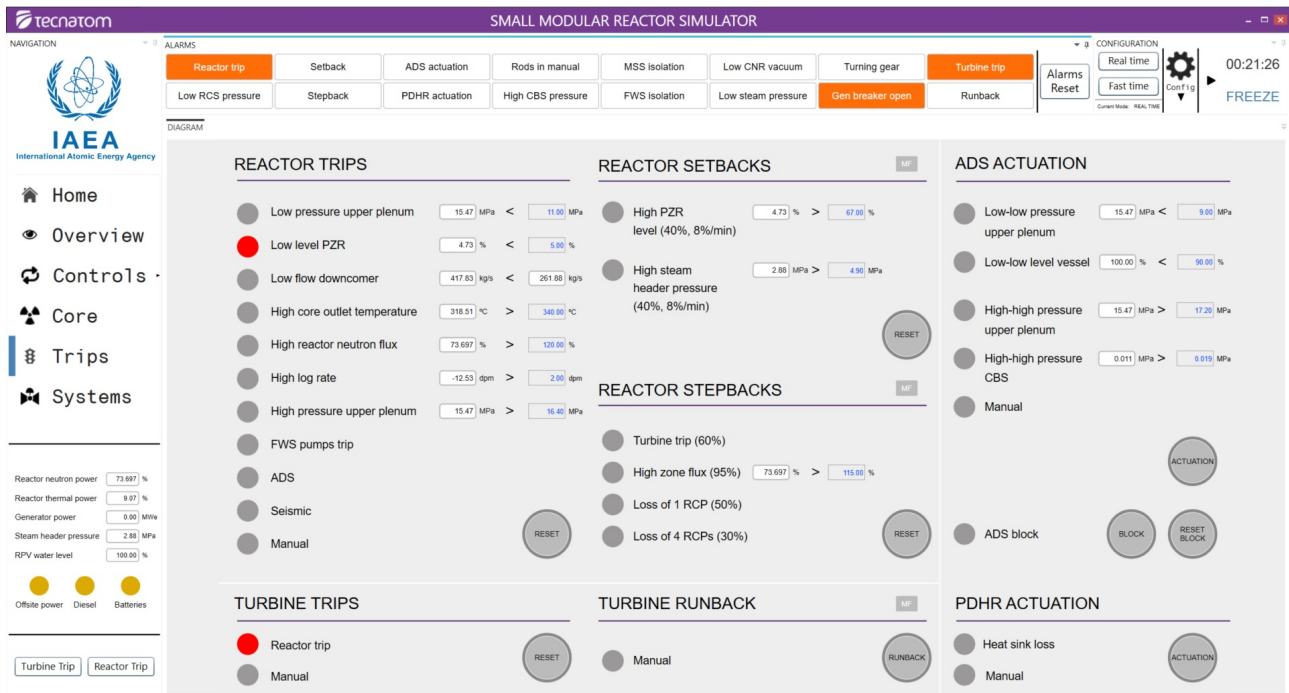


Figure 6.40: Trips page showing the reactor trip, the turbine trip, and the generator breaker opening in SGTF transient.

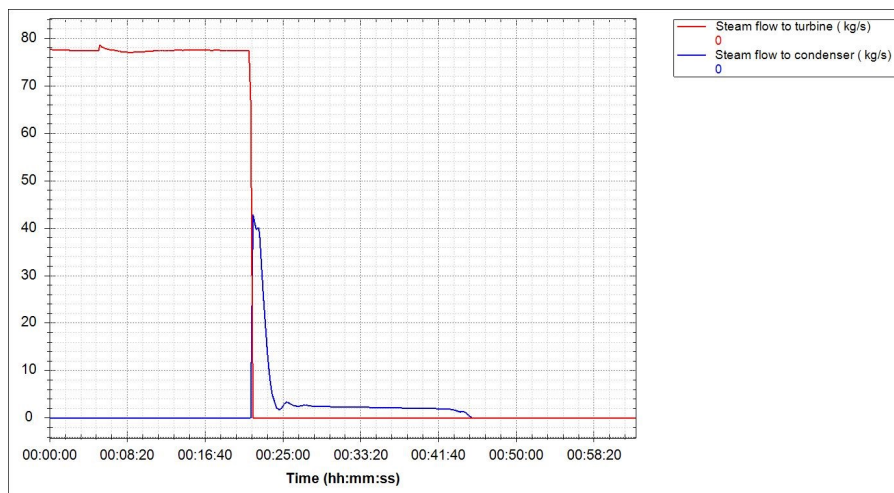


Figure 6.41: Steam flow to the turbine and to the condenser in SGTF transient.

As discussed in Section 6.2, the reactor trip causes the insertion of all control and shutdown rods in the core, resulting in the insertion of a large amount of negative reactivity (Figure 6.42). Following the trip, the moderator and fuel temperatures decrease, inserting a positive reactivity in the core due to the negative MTC and FTC. However, this positive reactivity is lower than the negative reactivity inserted by the rods. Thus, despite the reduction in the negative reactivity of the core, the overall result remains negative (Figure 6.42). This large negative reactivity insertion decreases the neutronic power and the thermal power, as observed in Figure 6.43.

Nevertheless, decay heat continues to be generated in the core; thus, the thermal power does not go to zero after the reactor trip.

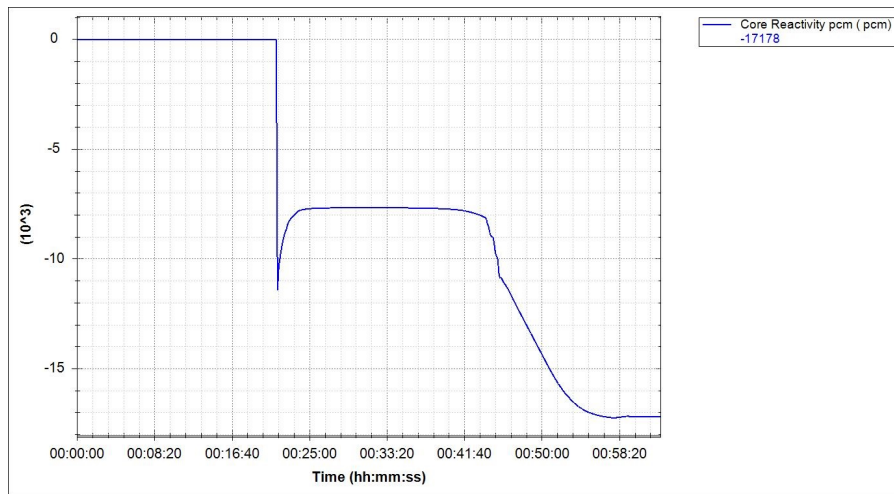


Figure 6.42: Core reactivity in SGTF transient.

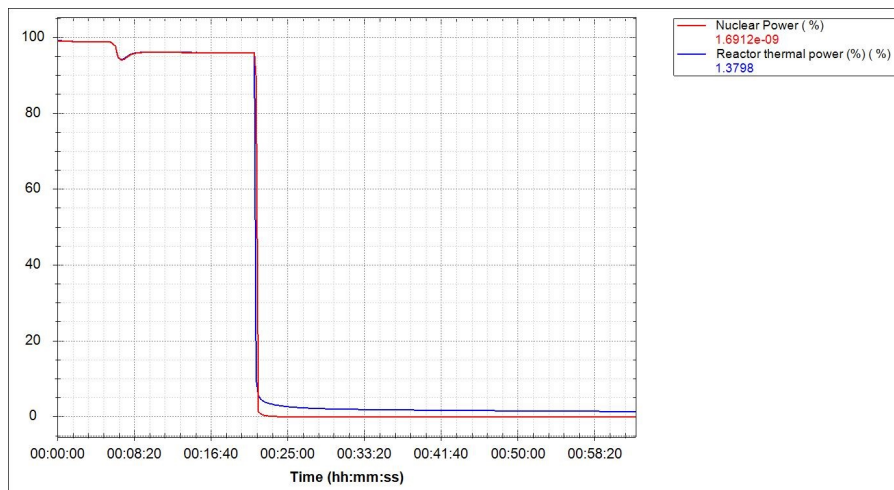


Figure 6.43: Nuclear power and thermal power in SGTF transient.

The decay heat requires heat removal to continue. Thus, the heat removal and the primary depressurization continue through the SG, as can be observed by the continued steam flow and feedwater flow from and to the SG in Figures 6.36 and 6.37, except for the feedwater flow to the faulted helical-coil tube that is zero because it is exposed to a higher pressure. Following the reactor trip, the RCS pressure continues to decrease (Figure 6.33). When the RCS pressure is lower than 9 MPa, the ADS system is actuated to reduce the RCS pressure allowing the actuation of the PIS and GIS systems. ADS actuation is verified by the opening of ADS valves and by the flow increase through these valves, as shown in Figure 6.44. Additionally, the ADS actuation causes the ADS actuation alarm and the increase in the suppression pool temperature, as shown in Figure 6.45. The ADS valves open sequentially with 5 minutes time delay.

At this point, the RCS depressurization and heat removal are being performed by the ADS, SG, and condenser. When the RCS pressure is lower than 5 MPa, the PIS begins to inject borated water into the RCS, as observed in Figure 6.46. The oscillations observed in this figure

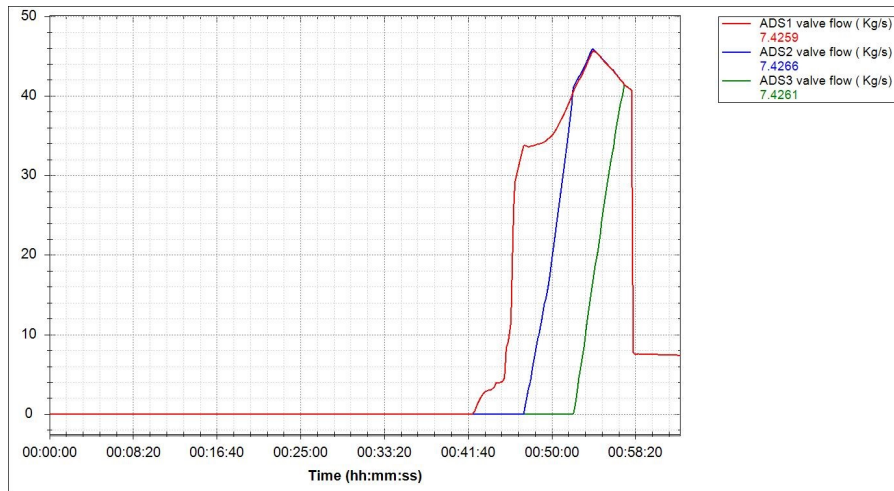


Figure 6.44: Flow through ADS valves in SGTF transient.

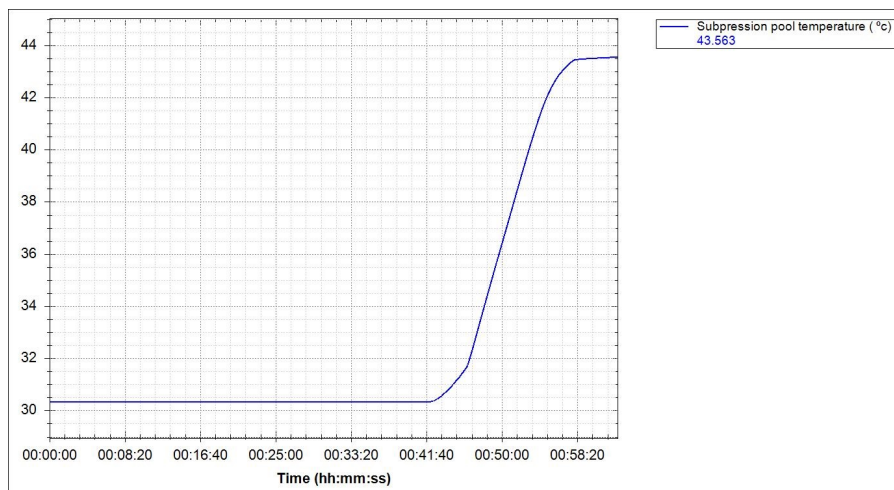


Figure 6.45: Increase in the suppression pool temperature due to the ADS actuation in SGTF transient.

are caused because the flow stops when the RCS pressure is higher than 5 MPa. Following the PIS actuation, the PZR level begins to increase (Figure 6.32) and the CVCS charge flow is decreased to zero when the PZR level is restored (Figure 6.39).

As the core is cooled and depressurized, the steam pressure in the steam header decreases because less steam is produced in the SG, as presented in Figure 6.38. When the steam header pressure is lower than 1 MPa, it causes the trip of the feedwater pump. The feedwater pump trip isolates the FWS, which actuates the PDHR due to the loss of the heat sink. PDHR operation can be observed by the increase in the flow of the PDHR and by the increase in the temperatures of the DHR pools, as shown in Figures 6.47 and 6.48. The PDHR actuation also activates the PDHR actuation alarm in the Alarm part of the simulator. The actuation of the PDHR system causes MSS isolation. The insulations of the FWS and MSS stop the feedwater and the steam flow (Figures 6.36 and 6.37), except for the steam flow in the faulted helical-coil tube.

The RCS depressurization continues, and when the pressure is lower than 0.5 MPa, the GIS begins to inject borated water into the system. The GIS actuation is confirmed by the GIS flow rising, as shown in Figure 6.49. The PIS and GIS inject borated water into the system,

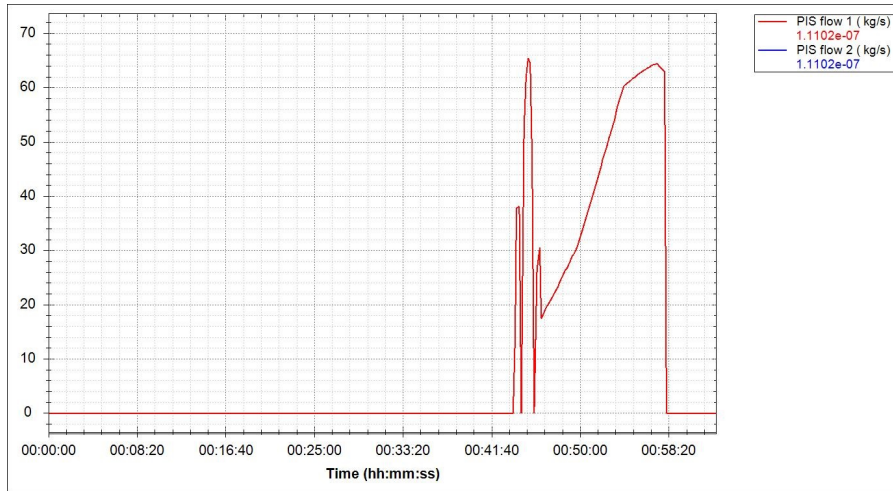


Figure 6.46: PIS flow into the RCS in SGTF transient.

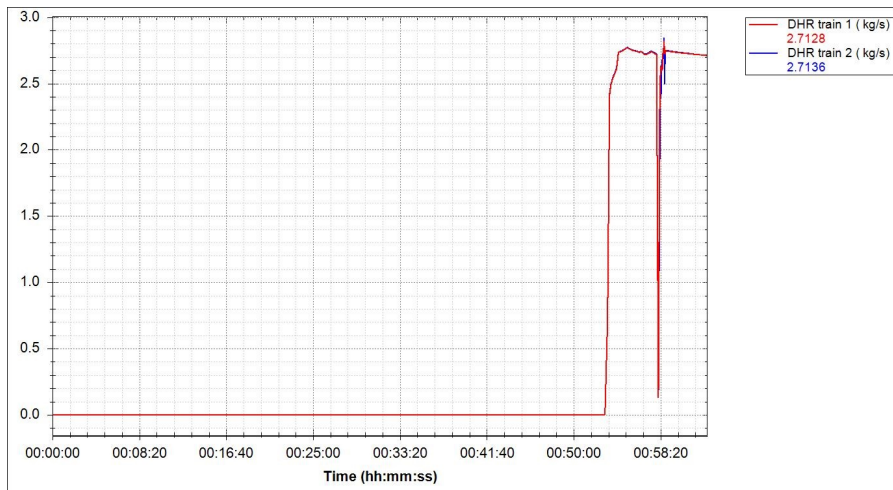


Figure 6.47: Flow in the PDHR in SGTF transient.

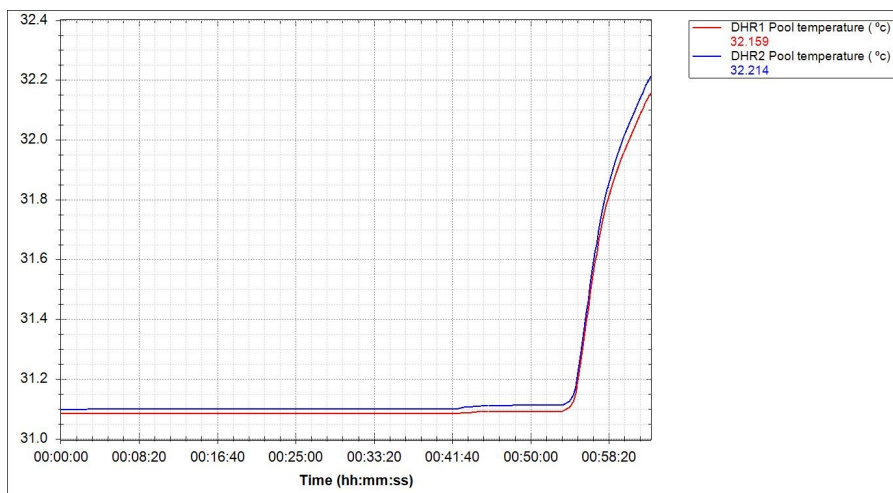


Figure 6.48: DHR pool temperatures in SGTF transient.

increasing the boron concentration in the RCS, as shown in Figure 6.50. The injection also restores the PZR level (Figure 6.32) and keeps the RPV level (Figure 6.51) almost complete

during the entire transient, avoiding the exposure of the fuel.

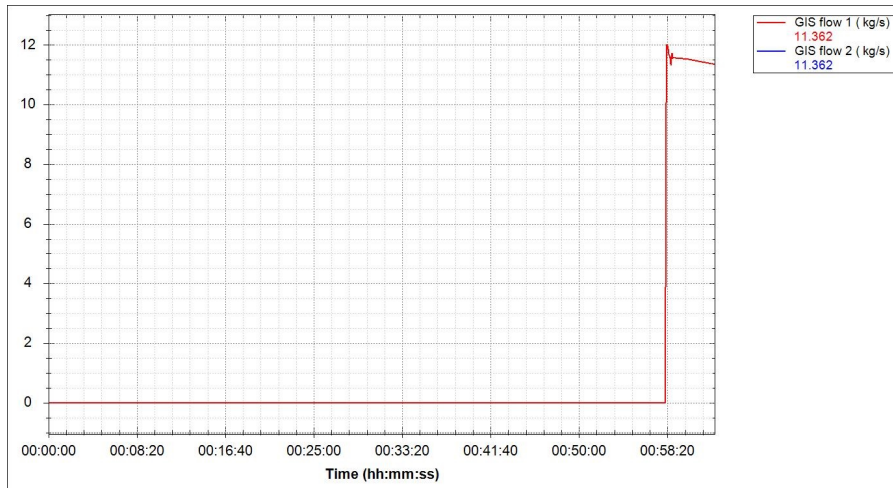


Figure 6.49: GIS flow in SGTF transient.

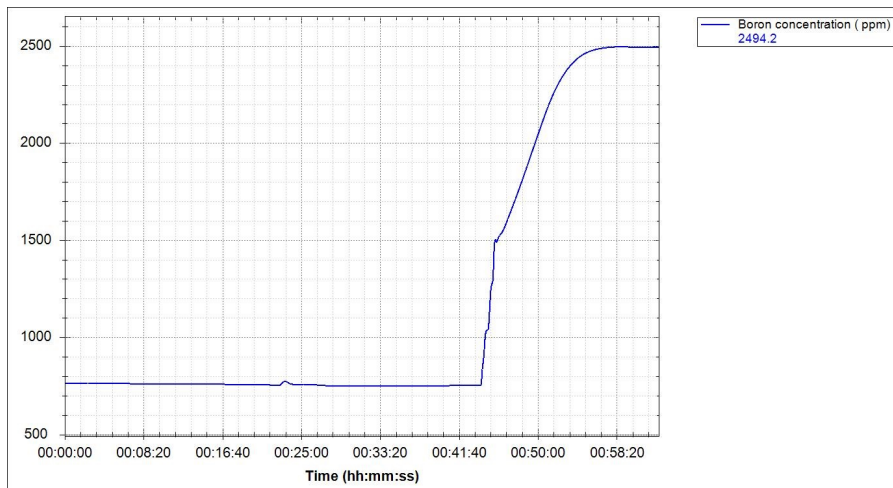


Figure 6.50: RCS boron concentration in SGTF transient.

As observed, the control and safety systems actuated to keep the reactor in a safe state. Not only the core remained covered during the entire transient (Figure 6.51), but also the coolant circulation was kept in the reactor core, as can be observed in Figure 6.52. From this graph, it can be seen that the RCS flow rate is non-zero during the entire transient. Additionally, the RCS and the average fuel temperatures remained stable or reduced as shown in Figures 6.34 and 6.53, and the RCS subcooling margin always remained positive (Figure 6.35).

The transient described in this section occurred without the action of the operator. However, it elapsed approximately 16 minutes from the transient beginning until the reactor trip, which is enough time for the operator to respond. The first step consists of identifying the SGTF. The flow in the break begins to reduce the PZR level while the CVCS tries unsuccessfully to restore the level, which continues decreasing. Radiation monitors located close to the steam lines detect the activity immediately after the break allowing the identification of the faulted helical-coil tube. Another indication that helps identify the failure is the mismatch between the feedwater flow and the steam flow. After identifying the SGTF, the operator acts to mitigate the failure. One crucial measure consists of isolating the faulted helical-coil tube to terminate



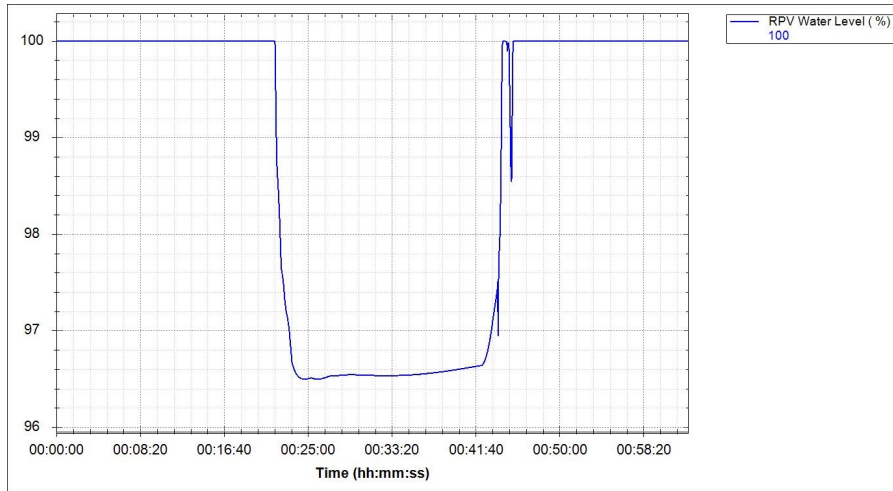


Figure 6.51: RPV level in SGTF transient.



Figure 6.52: RCS coolant flow rate in SGTF transient.



Figure 6.53: Fuel temperature in SGTF transient.

the radiological release. However, in the iPWR simulator, when the faulted helical-coil tube is isolated, it is pressurized by the RCS pressure, resulting in the opening of the relief and safety

valves located in the MSS lines. The relief valve opens at 5.3 MPa, and the safety valve opens at 5.7 MPa. The opening of these valves increases the loss of RCS inventory and, consequently, the scenario worsens. Thus, in the simulator, one option is to manually actuate the PDHR and block the ADS as soon as the failure is identified. The PDHR actuation isolates the FWS that trips the feedwater pumps and, consequently, the reactor. The RCS depressurization is performed only by the PDHR. When the RCS pressure reaches 5.3 MPa, the pressure for opening the MSS relief valve, the operator isolates the MSS stopping the radiological release. The RCS depressurization using only the PDHR takes longer. Therefore, another option is to actuate the ADS manually after actuating the PDHR. The depressurization occurs faster than in the previous case, but RCS inventory is lost to the suppression pool. Then, when the RCS pressure reaches 5.3 MPa, the MSS is isolated, and the ADS is disabled manually. The second option allows the MSS isolation faster than the first option, which reduces the radiological release.

# Chapter 7

## Conclusion

The climatic emergency is in evidence in the news worldwide, being recognized as one of the most significant challenges to the humanity and to the environment. Thus, the international community decided to limit the increase in the average global temperature to 1.5 °C above pre-industrial levels. To achieve this goal, activities that generate GHGs must be replaced by activities that reduce or even completely eliminate carbon emissions. Once the generation and use of energy account for approximately two-thirds of the total GHG emissions, they become an essential focus of the global response to climate change. Thus, options have been sought to replace energy generation with fossil fuels. Among the main options are nuclear power, hydropower, and renewable energy sources, such as solar and wind power. Currently, renewable energy sources generate energy intermittently, while hydropower causes considerable environmental consequences due to the necessity of dumping the water, changing the water flow, droughts, among others. Thus, nuclear energy appears as a reliable, steady, and clean source of energy.

Despite the great potential already demonstrated, nuclear weapons and nuclear accidents that occurred over time made nuclear energy to be viewed with considerable skepticism by politics and by the population. In addition, large NPPs are characterized by significant capital investment requirements and long construction times. These factors have hampered nuclear energy as an important tool for electricity generation, and this will remain so for the near future unless it goes through a drastic change from its current status. In that sense, those involved in the design and commercialization of NPPs seem to be alert to the demands of the market. From a financial perspective, financing and risk-sharing models, which can adapt to the needs of different markets, have been developed. In addition, the new reactor models have required less investment and reduced construction schedule. From a safety perspective, new advanced models have used the lessons learned from previous accidents to incorporate several technical developments that increase the safety of the new NPP designs. Among these technical developments, one may highlight the extensive use of passive safety systems, more efficient radiation containment systems, and the generation of less waste.

In the wake of cost reduction and increasing safety, the SMRs appeared. The term SMRs refers to reactors with modular manufacture and with power generation in the range between 25 MWe to 300 MWe. Historically, the development of SMRs started with integrated reactor designs. The significant advantage of this type of project is that most or all RCS components are enveloped. In this way, the integrated designs eliminate the piping between RCS components such as the hot and cold legs and the surge line, which connects the pressurizer to the hot leg. These changes practically eliminate the possibility of large-break LOCA occurrence, increasing

the safety of these designs. Economically speaking, the modularization of SMRs allows for a faster construction schedule and reduced costs. In addition, the modular approach allows for standardization and flexible applications: a small plant can be built using only a simple SMR, while a large plant can be built of multiple units. In that sense, SMRs can be used in markets that are equally accessible to traditional NPPs with large reactors or markets that are less suitable or even inaccessible to large reactors. Thus, SMRs can be used in places with well-developed electrical grids where they may even include large NPPs or in places less accessible to large NPPs, such as small islands, areas with limited access to water cooling, areas with technical limitations (small electrical grids) and areas with limited capital available.

Significant achievements have been observed in the development of SMR projects. In Russia, a floating unit with a generation capacity of 70 MWe, consisting of two SMRs of the KLT-40S design (35 MWe each), was connected to the electrical grid in December 2019, and in Argentina, a 27 MWe iPWR SMR (CAREM) is at an advanced level of construction. In addition, a large number of new SMR designs have recently been proposed. However, although these projects appear to be promising in the research and development phase, it is still unclear how they will progress towards demonstration and commercialization. In that sense, a successful SMR demonstration project is critical as a proof of concept before governments and utilities seriously consider the option.

In addition to safety features incorporated in the NPP advanced designs, the proper training of NPP personnel also effectively contributes to the safety of the facilities. In that sense, this work demonstrated the use of a PC-based simulator to study transients originated in normal operation conditions and in accident conditions of NPPs. The simulator used in the demonstration was the iPWR simulator (SMR), which is provided free of costs by the IAEA to the Member States through its education and training programs on learning about nuclear technologies using PC-based basic principle simulators. The iPWR simulator has proved to be a valuable tool to contribute to the understanding of fundamental concepts present in the behavior of NPPs and their reactors and also provided an excellent overview of how the various systems and components work together to generate power.

From the discussion presented in this work, the SMRs appear as an option when compared to large NPPs regarding cost reduction due to the modularization, mass production, and use of passive systems. Additionally, the flexibility of SMRs allows their use in remote areas and in other activities not related to power generation, such as desalination and hydrogen production. Thus, SMRs emerge as an important and affordable manner to generate energy with low carbon emission and with the capability to replace the fossil fuel power generation and consequently becoming an important tool to limit the global temperature increase to the desired levels.

# Bibliography

- [1] IAEA. *Climate Change and Nuclear Power 2020*. Viena: International Atomic Energy Agency, 2020. ISBN: 978-92-0-115120-9.
- [2] WNA. *Nuclear Power in the World Today*. <https://www.world-nuclear.org/information-library/current-and-future-generation/nuclear-power-in-the-world-today.aspx>. World Nuclear Association. Accessed: 2021-04-09 at 11:30h. 2021.
- [3] IAEA. “Nuclear Power and the Clean Energy Transition”. In: *IAEA Bulletin* (2020). ISSN: 0020-6067.
- [4] WNA. *Advanced Nuclear Power Reactors*. <https://www.world-nuclear.org/information-library/nuclear-fuel-cycle/nuclear-power-reactors/advanced-nuclear-power-reactors.aspx>. World Nuclear Association. Accessed: 2021-04-09 at 19:50h. 2020.
- [5] IAEA. *Power Reactor Information System*. <https://pris.iaea.org/PRIS/home.aspx>. International Atomic Energy Agency. Accessed: 2021-04-09 at 20:40h. 2021.
- [6] WNA. *Small Nuclear Power Reactors*. <https://www.world-nuclear.org/information-library/nuclear-fuel-cycle/nuclear-power-reactors/small-nuclear-power-reactors.aspx>. World Nuclear Association. Accessed: 2021-04-10 at 12:50h. 2021.
- [7] IAEA. *Advances in Small Modular Reactors Technology Developments: A Supplement to IAEA Advanced Reactors Information System (ARIS)*. Viena: International Atomic Energy Agency, 2020.
- [8] IAEA. *Nuclear Reactor for Education and Training*. <https://www.iaea.org/topics/nuclear-power-reactors/nuclear-reactor-simulators-for-education-and-training>. International Atomic Energy Agency. Accessed: 2021-05-27 at 09:50h. 2021.
- [9] WNA. *Nuclear Power Reactors*. <https://www.world-nuclear.org/information-library/nuclear-fuel-cycle/nuclear-power-reactors/nuclear-power-reactors.aspx>. World Nuclear Association. Accessed: 2021-04-10 at 17:00h. 2021.
- [10] IAEA. *Advanced Large Water Cooled Reactors: A Supplement to IAEA Advanced Reactors Information System (ARIS)*. Viena: International Atomic Energy Agency, 2020.
- [11] IAEA. *Simulators for Training Nuclear Power Plant Personnel*. Viena: International Atomic Energy Agency, 1993.

- [12] Paul Breeze. *Nuclear Power*. London: Academic Press, 2020. ISBN: 978-0-08-101043-3.
- [13] John R. Lamarsh and Anthony J. Baratta. *Introduction to Nuclear Engineering*. New Jersey: Prentice-Hall, 2001. ISBN: 0-201-82498-1.
- [14] Duke Energy. *How Energy Works: A Clean Energy Resource*. <https://www.duke-energy.com/energy-education/how-energy-works/nuclear-power>. Duke Energy. Accessed: 2021-04-12 at 10:40h. 2020.
- [15] WNA. *Nuclear Fuel and its Fabrication*. <https://www.world-nuclear.org/information-library/nuclear-fuel-cycle/conversion-enrichment-and-fabrication/fuel-fabrication.aspx>. World Nuclear Association. Accessed: 2021-04-12 at 13:20h. 2020.
- [16] NRC. *Reactor Concepts Manual*. Chattanooga: United States Nuclear Regulatory Commission, 2006.
- [17] IAEA. “Introduction to Water Cooled Reactor Theory with the Micro-Physics Simulator Lite Edition”. In: *Training Course Series 70* (2019). ISSN: 1018-5518.
- [18] Thomas W. Kerlin and Belle R. Upadhyaya. *Dynamics and Control of Nuclear Reactors*. London: Academic Press, 2019. ISBN: 978-0-12-815261-4.
- [19] Mario D. Carelli and Daniel T. Ingersoll. *Handbook of Small Modular Nuclear Reactors*. London: Woodhead Publishing, 2021. ISBN: 978-0-12-823917-9.
- [20] NRC. *Application Documents for the NuScale Design*. <https://www.nrc.gov/reactors/new-reactors/smr/nuscale/documents.html>. United States Nuclear Regulatory Commission. Accessed: 2021-04-07 at 14:30h. 2020.
- [21] NRC. *U.S. EPR Application Documents*. <https://www.nrc.gov/reactors/new-reactors/design-cert/epr/reports.html#fsar>. United States Nuclear Regulatory Commission. Accessed: 2021-05-01 at 19:35h. 2020.
- [22] IAEA. “Integral Pressurized Water Reactor Simulator Manual and Exercise Handbook”. In: *Training Course Series 65* (2017). ISSN: 1018-5518.